NOTICE: When government or other drawings, specifications or other data are used for any purpose other than in connection with a definitely related government procurement operation, the U. S. Government thereby incurs no responsibility, nor any obligation whatsoever; and the fact that the Government may have formulated, furnished, or in any way supplied the said drawings, specifications, or other data is not to be regarded by implication or otherwise as in any manner licensing the holder or any other person or corporation, or conveying any rights or permission to manufacture, use or sell any patented invention that may in any way be related thereto.

62-4-6

AIR FORCE INSTITUTE OF TECHNOLOGY

AIR UNIVERSITY
UNITED STATES AIR FORCE

SCHOOL OF ENGINEERING

WRIGHT-PATTERSON AIR FORCE BASE, OHIO

AF-WP-O-MAY 62 3,500

SAMPLING OF AIRBORNE RADIOACTIVE PARTICLES BY ELECTROSTATIC PRECIPITATION

Capt John W. Baker

GNE/Phys/62-2

SAMPLING OF AIRBORNE RADIOACTIVE PARTICLES BY ELECTROSTATIC PRECIPITATION

THESIS

Presented to the Faculty of the School of Engineering of

The Institute of Technology

Air University

in Partial Fulfillment of the

Requirements for the Degree of

Master of Science

By

John Wesley Baker, B.S. G.E.

Capt USAF

Graduate Nuclear Engineering

May 1962

Preface

I have attempted in this thesis to provide a complete and factual report of a study I conducted to determine the feasibility of using an electrostatic precipitator for fallout sample collection. A brief discussion of certain pertinent theory has been included to provide the reader with that basic knowledge necessary for an understanding of the subsequent presentations. I sincerely hope that the basic research conducted will ultimately lead to the development and production of an electrostatic precipitator that will allow a continuous fallout monitoring capability. The device envisioned would permit collection of an analyzable mass of sample in a short period of time on a compactible conducting plastic film that could be advanced through the collector as desired. This facility would provide a valuable adjunct to the present fallout monitoring programs.

I am indebted to my thesis adviser, Capt. Charles J. Bridgman, for not only introducing me to the initial concepts but also for spending many hours in helpful consultation as problems developed. I am also indebted to the many personnel at the WPAFB Aerial Reconnaissance Laboratory for their many helpful suggestions, for their assistance in obtaining needed supplies and equipment, and for providing the necessary laboratory and facilities. I would like to thank the Millipore Filter Corporation for providing samples of their filters that were used in the initial filtration concentration studies and for providing a very valuable bibliography and set of abstracts of related reports. I would like to express my thanks to A1/C Robert Mixon and the other personnel of the AFIT Physics Laboratory for their valuable assistance.

Finally, I would like to thank my wife for her patience, understanding, and encouragement and for constantly providing the quiet atmosphere necessary for study. Without her help, this study could not have been completed.

John W. Baker

Contents

Contents

List of Figures

List of Figures

List of Figures

List of Figures

List of Tables

Abstract

This thesis is a report of an experimental study that was conducted to design, build, and test an electrostatic precipitator to determine the feasibility of fallout sampling by electrostatic precipitation. A description of pertinent theory is provided, a detailed discussion of all parametric, experimental, and analytical studies is presented, and the resultant collector and collection facility, and collection and analysis technique is described.

Electrostatic precipitation of airborne particulates provides an improved method of radiological fallout sampling in that it provides a capability of qualitatively defining the nuclides present as well as quantitatively defining the gross radiative activity.

The results of an extended sample and analysis program portray the capabilities of this collection process. The conclusions resulting from this study are (1) electrostatic precipitation will provide a superior sample collection rate that might be increased even further by continued design studies, (2) removing collected particulates in a fluid bath would result in a selective solubility fractionation that would prevent an accurate concentration by filtration but would permit concentration by evaporation of the fluid, and (3) electrostatic collection on a thin compactible, conducting plastic film would provide an optimum collection technique since the film could be advanced through the collector at periodic intervals to allow a continuous sampling capability and all of the sample could be contained in a good thin-disc sample geometry. The samples collected during this study provided readily analyzable gamma scintillation spectra and an analysis of this spectra is presented.

SAMPLINC OF AIRBORNE RADIOACTIVE PARTICLES BY ELECIROSTATIC PRECIPITATION

I. Introduction

This thesis presents the results of a study that was conducted to determine the feasibility of using electrostatic precipitation as a means of collecting a representative sample of the airborne radiation. The thesis will describe the experimental and parametric studies conducted and the resultant collection system. Experimentally defined parameters and experimental failures will be presented as an aid to future studies. An extensive fallout collection and analysis program was conducted as a proof-test of the collection system and the results of this program will be presented as a portrayal of the capabilities and limitations of this collection system. Finally, a summary will be presented that will define the capabilities and limitations, the advantages and disadvantages, possible areas of improvement, and possible applications of this collection technique.

The thesis will consist of two main sections -- the equipment design section and the sample analysis section. The equipment design section will contain a brief analysis of the theory of radioactive decay and electrostatic collection, will describe the results of the experimental design efforts, and will provide a detailed description of the constructed equipment. The sample analysis section will include a definition of the sample collection technique, the results of the gamma analysis of each sample, and a nuclide determination based on gamma spectroscopy.

This thesis is based, in part, upon published theoretical studies. Parametric design experiments were performed to corroborate and optimize the theoretical values reported. The experimentation described in the equipment design section will be largely a chronological reporting of these efforts, the failures, and the final design values used. This reporting technique is used to provide maximum information for future research efforts. Complete data reporting is used in the sample analysis section to facilitate detailed interpretation of the analysis results.

The advent of the atomic era brought with it a new form of biological hazard -- radiological contaminants. While the radioactive products of natural decay have always been present, the contaminant resulting from artificial fission has increased the possible biologic hazard. The increased fallout resulting from nuclear detonations has prompted an extensive research effort to determine the radiological hazard on the surface of the earth and the rate of change of this radiation level through a knowledge of fallout mechanisms and the magnitude of the airborne contaminant burden (Ref 5, 7, 9, 12, 15, 17, 18, 19, 21, 24, 25, 26, 40, 41, 45). The effectiveness of this monitoring and research effort is dependent upon the availability of a collection system that will provide a timely, representative, and analyzable sample. This experimental study was an effort to improve upon presently available techniques.

II. Theory

General

An understanding of fallout sampling analysis techniques must assume a knowledge of the principles of radiation, an understanding of the airborne particulates, their size distribution and modes of formation, and an understanding of the requirements of an effective analysis program. A familiarity with the principles of electrostatic precipitation will also be required to understand the collection process described in this paper. A brief summary of the principles of radiation, particulate formation, and analysis techniques has been included to provide that basic knowledge required. A more thorough definition of the principles of electrostatic precipitation has been included to enable the reader to follow certain mathematical derivations and appreciate certain critical operating parameters.

Nuclear Radiation Theory

Nuclear radiation occurs as the result of nuclear decay of radioactive nuclides. Radioactive isotopes decay according to a fixed transmutation scheme with each step in the chain providing one or more types of radiant energy. An understanding of the properties of the various types of radiant energy, the theory of nuclear decay, and the specific transmutation schemes involved would permit a complete determination of the radiological intensity and types of nuclides present.

Beta particles are high speed electrons ejected from the nucleus in a nuclear decay process (Ref 38:13). Beta particles are born with an energy lying within an energy spectrum. These highly ionizing particles are short ranged and are stopped by thin shielding materials

and their intense ionization potential provides a means of radiation detection and permits a quantitative measurement of the radiological intensity but the fact that any given nuclide decay will produce particles having a broad spectrum of energies precludes a qualitative analysis capability. Gamma rays are a form of electromagnetic energy similar to X-rays but resulting from nuclear decay (Ref 38:20). Transmutation of any given nuclide will produce a group of specific gamma energies unique to that nuclide. This radiation has a much greater range than beta particles but is less highly ionizing and this lower ionization capability necessitates a greater sample activity for detection. The specific energies permit a qualitative analysis, however, through gamma energy measurement.

Detailed research has established the nuclear decay schemes for the many radioactive nuclides. This research has identified the most probable decay daughters, the types and energies of radiation emitted and the half-lives of the transmutations (Ref 1:163, 23:197-342, 13). Reference to this published data permits the analyst to identify the nuclides present through a detailed energy and decay rate study. Nuclear detection equipment is available that will discriminate between beta and gamma radiation. Relative ionization intensities permit the analyst to effectively screen beta radiation while measuring gamma rays or to use an ionization media for beta determinations that is insensitive to gamma radiation. Electronic circuitry converts the ionization energy into an electrical impulse proportional in amplitude to the intensity of the ionizing event. A typical radiological analysis might then include an integrated beta determination that will quantitatively define the radiation in counts per minute and a determination of gamma energies to qualitatively define the nuclides present.

Airborne Particulates

Now let us examine the particulates giving rise to this radiant energy. Radioactive fallout may be defined as those sirborne particulates, or aerosols, containing radiosctive isotopes or nuclides. The nuclides might be the result of a natural decsy of thorium and radium in the esrth's surface or they may be fission fragments and fission products from nuclear detonations and nuclear reactors. These nuclides might coalesce to psrticulste size or may adhere to dust particles present in the air (Ref 2, 7, 9, 12, 16, 17, 18, 19, 21, 24, 26, 41). Regardless of the mode of formstion, this thesis will assume that the agglomeration and adhesion processes will produce a homogeneous distribution of rsdioactive nuclides in a particulate sample. Furthermore, it is assumed that the radiological activity of a sample is directly proportional to its mass.

Extensive research has been conducted to define the modes of formation and the mechanics of transport of radioactive particles. Nstionwide and worldwide monitoring networks provide a continuous tabulation of radiologicsl contamination on the earth's surface (Ref 9, 41). Project "Ash Can" (Ref 9) provided a sampling of tropospheric and stratospheric contamination by high-altitude-balloon borne samplers. Project HASP, (Ref 7), the most recent and most extensive of the airborne sampling programs, employed high-altitude U-2 sircraft in a methodical meridional sampling of sir strata up to 70,000 feet to determine stratospheric concentrations and total burden of radioactive nuclides. Analysis of the HASP samples provided a definition of the trsnsport mechanisms and residence times of the sirborne particulates. While there is some disagreement between the findings of these sepsrate research efforts and continued resesrch will be needed to completely

define aerosol phenomena, there is a general agreement on the major contributing factors. The fireball from a nuclear detonation is believed to rise until it cools to a thermal equilibrium with its surroundings. The altitude achieved is dependent upon the yield of the weapon and the altitude of detonation. Scavenging of the solid fission fragments is accomplished by coalescence and by adhesion to earth debris in the event of a near-surface burst. The coarser scavenged particles fall to earth in the vicinity of the burst while the finer particulates disseminate into the troposphere and are carried by tropospheric air movements until they settle to earth after a residence time of approximately one month (Ref 7:vol 3 page 236). With a sufficiently large yield and a proper latitude and altitude of detonation, the fireball will penetrate the tropopause and come to thermal equilibrium in the stratosphere. Here the fission fragments will solidify and the fission products having gaseous precursors will decay to particulates. The cloud will be carried by stratospheric air movements with a minimum amount of lateral dispersion until gradual settling or vertical and lateral cloud movement injects it into the troposphere after an average stratospheric residence time of approximately eighteen months (Ref 7:vol 1 page 7). Turbulent action within the stratosphere could result in individual residence times of many months or even years. Analysis of normal non-radioactive stratospheric particulates reveals a preponderance of ammonium sulfate particles with radii in the range $0.10\mu < r < 1.0\mu$ (Ref 7:vol 5 page 133). Nucleate coalescence about these particles would substantiate the postulate that fission fragments are associated with particulates 0.1μ and larger.

Studies have been conducted that define the particle mass/size distribution, i.e., what percentage of the dust particles lie within a

given size range. A tabulation of these distributive percentages is presented in Table I. A knowledge of this mass/size distribution is required because the efficiency of any particulate collection process is size dependent. Correlations have been attempted that would define the type of radioactive contaminant present with a given particle size. While conclusive evidence is not available and published reports are contradictory, evidence would indicate that natural radioactive nuclides are associated with particulates 0.1μ (1×10^{-5} cm) and smaller (Ref 21) while fission fragments are associated with particulates 0.1μ and larger (Ref 7, 16, 17, 18). This could be explained by assuming that fission fragments from nuclear detonations are carried into the upper troposphere and stratosphere and gradually coalesce during the long slow fall back to the earth's surface. The natural decay of radium and thorium produces radon and thoron. These inert gases must then escape the earth's crust to be detected. These short lived isotopes might decay to their radioactive daughters at a low altitude and the shorter distance of fall would allow a shorter coalescence time with a resultant smaller particulate size.

Fallout Analysis Requirements

An effective fallout analysis program must provide an accurate and timely quantitative measure of the radiation intensity and a qualitative analysis of the nuclides present. The separate radioactive isotopes possess the same biological affinities as the stable isotopes of the elements. The biological hazard, therefore, is a function of not only the radiation intensity but the types of nuclides present.

The radioactive decay of a given nuclide takes place at a rate unique to that nuclide. Specific disintegrations, however, are random occurrences causing the frequency of energy emission to be defined by

Table I

Division of the Distribution Spectrum into Groups

Group	Particle Radius Range (μ)	Ave Radius (μ)	Dimensionless Mass $\frac{M}{c^1}$ (1)	Mass Fraction
1	0.1 - 0.15	0.125	.1762	.0881
2	0.15- 0.25	0.20	.2218	.1109
3	0.25- 0.35	0.30	.1461	.0731
4	0.35- 0.5	0.425	.1549	.0774
5	0.5 - 0.7	0.60	.1461	.0731
6	0.7 - 1.0	0.85	.1549	.0774
7	1.0 - 1.5	1.25	.1762	.0881
8	1.5 - 2.5	2.00	.2218	.1109
9	2.5 - 3.5	3.00	.1461	.0731
10	3.5 - 5.0	4.25	.1549	.0774
11	5.0 - 7.0	6.00	.1461	.0731
12	7.0 -10.0	8.50	.1549	.0774
			2.0000	1.0000

Source (Ref 26:63A)

(1) M = the mass of a particular group

$c^1 = r^3 \frac{dN}{d(\log r)}$ where N is the total concentration of aerosols per cm^3 from the smallest rsdius up to rsdius r.

statistical probability. Ionization is the result of an interaction between the radiant particle or ray and the atoms and molecules of the media through which the radiation travels. Ionization frequency is then also defined by a probability function determined by the ionization capability of the radiation and the atomic/molecular density of the media. Conversion of ionization energy to an electrical impulse and the portrayal of the amplitude of this electrical impulse is subject to statistical variation. The reliability of experimental results is subject to experimental error and must be corrected by statistical analysis. The relative effect of statistical variation is inversely proportional to the magnitude of the quantity being studied.

We see, then, that the sample must possess sufficient activity to permit a qualitative gamma analysis and minimize the effect of statistical variation. Assuming that the sample activity is directly related to the sample mass, this would mean that an effective collection program must retrieve the maximum percentage of the particulate from a maximum volume of air in the minimum amount of time.

Sample Collection Techniques

Fallout analysis requires the collection and concentration of airborne particulates. A typical collection procedure currently being used accomplishes this by passing air through a filter in a Staplex High-Volume Sampler (Ref 15:11, 41:192). Although essentially 100% of the airborne particulates are collected by this process, the impediment presented by the 0.3μ air filter restricts the air flow to 35 cubic feet per minute. If we define collector sensitivity to be the product of the collector efficiency times the air flow rate, we see that the mass of the sample collected during a given collection period is determined by this collector sensitivity. The Staplex High-Volume Sampler would have a sensitivity of

35 cfm X 100‰ = 35 cfm. A collection system having a greatly increased flow rate could provide a larger sample in a shorter period of time even though the collection efficiency were decreased. Ideally, a collector should possess an efficiency of 100‰ and an infinite flow rate. Practically, the collector sensitivity would be maximized by simultaneously maximizing these two parameters.

The electrostatic precipitator provides a means of greatly increasing collector sensitivity and sample collection rate. This collector presents a minimal impediment to air flow so the air flow rate is limited only by the size of the availahle blower system. With this theoretically unlimited air flow rate, we need only maximize the efficiency of collection for the given high flow to permit an optimum collector sensitivity and sample collection rate.

Electrostatic Precipitation

Electrostatic precipitation is accomplished by ionizing the dust particles in an ion field and subsequently collecting them on a charged plate by a coulombic force of attraction. In the precipitator designed for this thesis, the particulate bearing air flow enters the system through a corona field in the charging section (see Fig. 1). Here the aerosols become charged through the adsorption of corona ions. The magnitude of the adsorbed charge is dependent upon the current density in the corona field, the size of the particle, and the amount of time spent in the charging section. The air subsequently flows through a collection section composed of a stack of oppositely charged plates. The negatively charged particles are driven to the positive plate in a trajectory defined by the magnitude of the coulombic charge differential and the linear velocity of the air. Collection efficiency is maximized by maximizing the adsorbed charge and optimizing the parameters of the collection system. To understand the optimization procedures, we must first

understand the principles of electrostatic precipitation.

Particulate charging is accomplished by the adsorption of ions in a corona current field (Ref 32:318, 47:1187-1188). Corona current is an electron flow in a non-linear electrical field between a point source and a flat plate (Ref 27:148). While this phenomena is not completely understood, experimentation has shown that increasing the electrical potential between a point source and a plate will cause a current flow when a certain potential is reached. A further increase of potential will cause an increased current flow until the arcing potential is reached. The magnitude of the current is a function of the radius of curvature of the point source, the plate to point separation, and the separating media (Ref 35:97). Practically, the point source is approximated by a grid of tightly-strung very-fine wire placed opposite a solid plate. Electron density in the corona field is determined by the magnitude of the current between one wire and the opposing plate and the spacing between wires. The non-linearity of the electrical field is degraded by the adjoining wires and optimum current density is achieved by experimental design.

Particulate charging is accomplished by two charging mechanisms -- bombardment charging and diffusion charging (Ref 26:33). Bombardment charging results when an aerosol is struck by an ion whose motion is along the electrical field lines. Diffusion charging, on the other hand, results from the attachment of an ion which is in random motion due to thermal diffusion. Bombardment charging predominates for particles 0.3μ radius and larger while diffusion charging predominates for particles less than 0.1μ in radius. Both mechanisms have an appreciable influence in the intermediate range and the complete charging mechanism is a combination of these two effects. Differential equations describing the

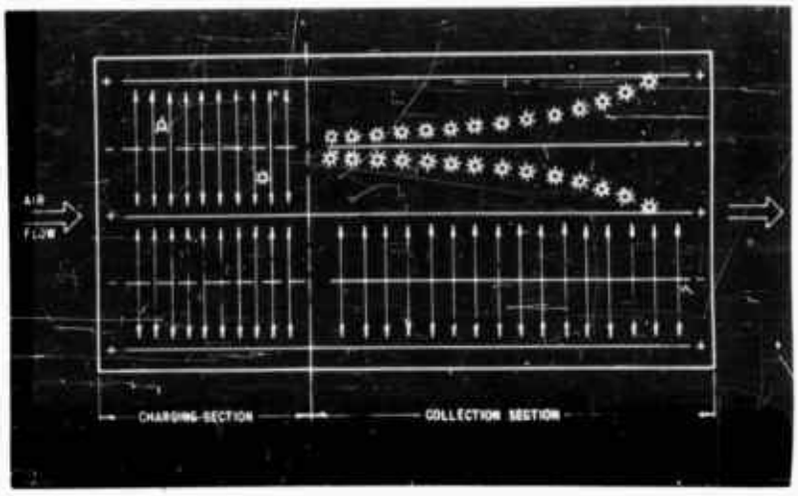

Fig. 1

Conceptual Drawing of an Electrostatic Precipitator

The particulate-bearing airflow is drawn into the inlet end at the left. The particulates adsorb an ion charge from the corona field in the charging section (I) and then are drawn to the positive collection plate in the collection section (II). The particulate-free airflow is exhausted at the right.

separate charging mechanisms have been developed (Ref 26:34-48) and will be briefly described below. The composite charging mechanism is deacribed by the summation of the separate differential equations. The summation results in a non-linear differential equation that cannot be solved by normal analytic means but a specific solution may be attained by graphical integration or numerical analysis solutions can be achieved by use of a digital computer.

An excellent description of aerosol size distribution, corona discharge phenomena and particulate charging mechanisms was presented in a thesis by Captain Donald L. Lamberson (Ref 26:34-43). The following derivations of the charging differential equations are a direct quotation from that paper. This long quotation is included here to insure an understanding of the principles involved and to credit the original theoretical derivation.

"Bombardment Charging. Particle charging by the ordered motion of ions in lines of force has received attention since 1923. The expression in use today is generally credited to Pauthenier, and a complete derivation and discussion of the expression is given by White (Ref 47:1187-1188). The problem is essentially one in electrostatics. An ion moves along a line of force until it strikes an aerosol particle. The charge transferred to the particle establishes a repulsive force so that the next ion which strikes the particle must overcome this Coulomb repulsion. Eventually, sufficient charge is acquired by the particle to nullify the electric field. Charging ceases and the particle is said to have received a saturation charge. White lists three assumptions necessary to solve the problem (Ref 47:1187):

1. The aerosol particles are spherical.
2. Particle diameter is much less than distance between particles.

3. In the immediate region surrounding a particle the ion concentration and electric field are uniform.

It is believed that assumptions (2) and (3) are valid for atmospheric aerosols and that (1) is a reasonable assumption (Ref 47:1187). The solution is obtained by considering the incident flux on the particle and the distortion of the lines of force. The differential equation describing this process is (Ref 11:306)

$$\frac{dq}{dt} = G\pi mnr^2E\left(1 - \frac{qe}{r^2EG}\right) \tag{8}$$

where q = particle charge (electrons)

t = time (sec)

m = mobility of negative ions $\left(\frac{cm}{sec}\left(\frac{statvolt}{cm}\right)^{-1}\right)$

r = particle radius (cm)

e = electric field $\left(\frac{statvolts}{cm}\right)$

$g = \left(1 + 2\left(\frac{K-1}{K+2}\right)\right)$

k = dielectric constant of aerosol

e = charge on electron (esu)

"This relation may be integrated by separation of the variables. The constant of integration is evaluated by assuming that q=0 when t=0. The resulting expression is

$$q = \left(1 + 2\left(\frac{K-1}{K+2}\right)\right)\frac{Er^2}{e}\left(\frac{emnt}{1 + emnt}\right) \text{ electrons} \tag{9}$$

clearly, as t becomes very large, q approaches a saturation charge q_o which is defined as follows:

$$q_o = \left(1 + 2\left(\frac{K-1}{K+1}\right)\right)\frac{Er^2}{e} \text{ electrons} \tag{10}$$

"The mean dielectric constant for aerosola waa found to be 4.0. (Note: This was done by aumming the dielectric constants for the individual organic and inorganic constituents found in an average dust sample. The average dust sample was determined by analyzing a large number of dust samples taken throughout the United States). The electronic charge is taken as 4.803×10^{-10} esu. It is desired to change the units of E to the more convenient $\frac{\text{volts}}{\text{cm}}$ by using the fact that 1 $\frac{\text{statvolt}}{\text{cm}}$ = 300 $\frac{\text{volt}}{\text{cm}}$. Substituting these values into Eq (10), one obtains

$$q_o = \frac{2Er^2}{(300)(4.803 \times 10^{-10})} = 1.387 \times 10^7 Er^2 \text{ electrons} \qquad (11)$$

where q_o is the saturation charge in electrons, E is the electric field in $\frac{\text{volts}}{\text{cm}}$ and r is the particle radius in cm. Thus the saturation charge varies directly as the field and the square of the radius.

"Time To Achieve Saturation Bombardment Charge. The particle charge as a function of time can be written

$$q = q_o \frac{1}{1 + \frac{1}{\sqrt{emnt}}} \text{ electrons} \qquad (12)$$

by substituting q_o into Eq (9) and dividing numerator and denominator by $\sqrt{emnt}$. The mobility (m), which is defined as the ion velocity between electrodes per unit electric field, of negative air ions at 1 atm pressure and room temperature is $1.78 \frac{\text{cm}}{\text{aec}}\left(\frac{\text{volts}}{\text{cm}}\right)^{-1}$, which in electrostatic units is $538 \frac{\text{cm}}{\text{sec}}\left(\frac{\text{statvolts}}{\text{cm}}\right)^{-1}$. Substituting this value and the electronic charge in Eq (12), one obtains

$$q = q_o \frac{1}{1 + \frac{1}{8.03 \times 10^{-7} nt}} \qquad (13)$$

Eq (13) can be solved for t as a function of q

$$t = \frac{1}{\left(\frac{q_o}{q} - 1\right)\left(8.03 \times 10^{-7}\right)} \text{ sec} \qquad (14)$$

where q_o is given by Eq (12) and where the ion density (n) must be determined independently.

"The ion density (n) is determined by the corona current, the area of corona discharge, and the velocity of the negative corona ions. The velocity is

$$w = mE = 1.78 \frac{\text{cm}}{\text{sec}} \left(\frac{\text{volt}}{\text{cm}}\right)^{-1} E\left(\frac{\text{volt}}{\text{cm}}\right) = 1.78\ E \frac{\text{cm}}{\text{sec}} \qquad (15)$$

for air at 1 atm and room temperature. Resorting to factor-label solution in a mixed system of units, one can obtain the ion density as follows:

$$n\left(\frac{\text{ions}}{\text{cm}^3}\right) = \frac{I(\text{amps})}{w\left(\frac{\text{cm}}{\text{sec}}\right) A(\text{cm}^2)} \frac{\left(\frac{\text{coulomb}}{\text{sec}}\right)}{(\text{amps})} \frac{\left(\frac{\text{ion}}{\text{sec}}\right)}{\left(1.602 \times 10^{-19} \frac{\text{coulomb}}{\text{sec}}\right)}$$

so that

$$n = \frac{I}{(1.78\ E) A (1.602 \times 10^{-19})} = 0.352 \times 10^{19} \frac{I}{EA} \frac{\text{ions}}{\text{cm}^3} \qquad (16)$$

where I is the corona current in ampheres, E is the effective field in $\frac{\text{volts}}{\text{cm}}$ and A is the area of the effective charging medium parallel to the electrodes. For wires between parallel plates this area is essentially the area of the plates.

"Once the ion density and saturation charge are known, the time for a particle to reach a specific charge q can be determined from Eq (14). Conversely, the charge acquired in a specific time could be computed from Eq (13). In order to show the fraction of charge received as a function of time, Eq (13) was plotted for an ion density of $10^9 \frac{\text{ions}}{\text{cm}^3}$, which is a

typical value. It was seen that with this ion density, charging is very nearly complete at 10^{-2} seconds.

"Maximizing Bombardment Charge. The design goal of the charging section of an electrostatic precipitator will be to achieve maximum charge in minimum time. It is now pertinent to discuss the manner of achieving this goal for the particles affected most by bombardment charging.

"For a given particle size Eq (11) shows that the saturation charge varies directly as the electric field. Therefore, the charging field should be as high as possible. The upper limit is the breakdown field, which will result in sparking. The time to achieve a given charge, according to Eq (14) varies inversely as the ion density. The ion density in turn varies directly as the corona current density and inversely as the field, where the current density is defined as the total corona current divided by the area through which it flows. Thus, for minimum time to acquire a given charge the current density must be maximum and the electric field minimum. However, the current density and field cannot be regarded separately as they are interdependent. It is better to say that minimum charging time is achieved when the current density to field ratio is maximum.

"Penney and Matick (Ref 35:97) have shown experimentally for wire-in-parallel-plate geometry that both the current and field are increased when either the applied voltage is increased or the cathode wire size is reduced with the restriction that the applied voltage must be equal to or greater than the corona onset potential and less than the sparking potential. In both cases the increase in current is greater than the increase in field, so that the current to field ratio increases. Therefore, one can say that an increase in applied voltage or a reduction in wire size both increase the saturation charge and reduce the time necessary to achieve it.

"In summation, to achieve maximum charge in minimum time for a given geometry the applied voltage should be as high as possible without sparking and current should be as great as can be sustained. The latter is achieved in negative corona by making the cathode geometry such that the surrounding field is as non-linear as possible. When the cathode is a wire, this means reducing the diameter.

"Diffusion Charging. As the particle size decreases below 0.3μ radius, the diffusion charging mechanism begins to be important. While bombardment charging is an electrostatic problem, diffusion charging is a problem in kinetic theory. The thermal motions of the ions cause a diffusion through the airstream molecules and result in collisions with aerosols (Ref 5:6). Theoretically, the charge acquired by diffusion is limitless although, as the Coulomb repulsion force increases, each additional ion will require more energy for attachment (Ref 5:6). White presents a solution to the problem by disregarding the external field (Ref 47:1188-1189). Penney, et al., have shown that the external field has a significant effect, but no analytical solution has been found to solve the resulting equations (Ref 52:318). The assumptions used by White to solve the problem are as follows (Ref 47:1188-1189):

1. The particles are spherical.
2. Particle diameter is much less than distance between particles.
3. In the immediate region surrounding a particle the ion concentration and electrical fields are uniform.
4. All ions which reach the particle are attached.

"The solution which results from kinetic theory is (Ref 46:1189)

$$\frac{dq}{dt} = \pi U n r^2 e^{\frac{e^2 q}{rkT}} \qquad (17)$$

where q = particle charge (electrons)

U = rms thermal velocity of ions $\left\{\frac{cm}{sec}\right\}$

n = ion density $\left\{\frac{ions}{cm^3}\right\}$

r = particle radius (cm)

e = electron charge (esu)

k = Boltzmann Constant

T = Temperature (°K)

"Equation (17) may be integrated and evaluated, if the particle is originally neutral, to yield

$$q = \frac{rkT}{e^2} \ln\left(1 + \frac{\pi Ue^2 rnt}{kT}\right) \qquad (18)$$

"For air at 30°C Hewitt (Ref 11:306) shows that Eq (17) and (18) evaluate to

$$\frac{dq}{dt} = 15.7 \times 10^4 \, nr^2 e^{-5.5\theta} \times 10^{-\theta} \frac{q}{t} \qquad (19)$$

and

$$q = 1.8 \times 10^5 r \ln(1 + 0.9\, rnt) \qquad (20)$$

"Thus the charge a specific particle receives by diffusion is dependent upon ion density and the time the kinetic forces are acting. However, one cannot use Eq (20) alone for particles between 0.1 and 0.3μ radius since bombardment charging is also occurring. Furthermore, it is not correct to add the charges given by Eq (20) and (11) for diffusion and bombardment charging because each equation was derived independently (Ref 11:303). Rather the differential equations (8) and (19) must be combined.

"Combined Diffusion and Bombardment Charging. The equation representing the effects of both diffusion and bombardment can be obtained by

combining Eq (8) and (19) to obtain

$$\frac{dq}{dt} = G(mnr^2E\left(1-\frac{qe}{r^2EG}\right)^2 + 15.7X10^4nr^2e^{-5.56x10^{-6}\frac{q}{r}} \quad (21)$$

"Substituting for G, m and e in electrostatic units and converting E from $\frac{\text{statvolts}}{\text{cm}}$ to $\frac{\text{volts}}{\text{cm}}$, one obtains

$$\frac{dq}{dt} = 11.16nr^2E\left(1-\frac{7.203X10^{-8}q}{Er^2}\right)^2 + 15.7X10^4nr^2e^{-5.56\ 10^{-6}\frac{q}{r}} \quad (22)$$

where q = particle charge (electrons)

n = ion density $\left(\frac{\text{ions}}{\text{cm}^3}\right)$

r = particle radius (cm)

E = electric field $\left(\frac{\text{volts}}{\text{cm}}\right)$

This expression can be simplified by grouping constants as follows:

$$\frac{dq}{dt} = A - Bq + Cq^2 + De^{-Jq} \quad (23)$$

where $A = 11.16nr^2E$

$$B = (2)(11.16nr^2E)\left(\frac{7.203X10^{-8}}{Er^2}\right) = 1.61X10^{-6}n$$

$$C = (11.16nr^2E)\left(\frac{7.203X10^{-8}}{Er^2}\right)^2 = 5.79X10^{-14}\frac{n}{r^2E}$$

$$D = 15.7X10^4nr^2$$

$$J = \frac{5.56X10^{-6}}{r}$$

"Equation (23) is a non-linear differential equation to which there is no analytic solution. The first three terms on the right side indicate the effect of bombardment charging while the last term accounts for diffusion charging. To obtain a solution to this equation it is necessary to use either computers or graphical integration" (Ref 26:34-43).

- - - - - - - - - End of Quote from Ref. 26 - - - - - - - - -

Collection of the charged particulate is permitted through the Coulombic force of attraction between the charged particle and the charged collection plates. The particulate in the collection field is acted upon by three forces:

(1) The perpendicular Coulombic force of attraction,

(2) The retarding force of the viscous media, and

(3) The tangential force of the air flow.

The Coulombic force of attraction is defined as

$$F = qeE \tag{24}$$

where q = the number of adsorbed electrons

e = the charge of the electron

E = the electric field between the collection plates.

Proper unit analysis will now define the attractive force as

$$F(\text{Dynes}) = 1.602 \times 10^{-12} qE \tag{25}$$

where E is in $\frac{\text{volts}}{\text{cm}}$. The motion of a spherical particle in a viscous medium is defined by Stoke's law to be

$$F = 6 \eta v_o r \tag{26}$$

where

F = the force of the particle in dynes

η = the viscosity of the medium in poise (1.8×10^{-4} poise at 75°F and 1 atmosphere of pressure (Ref 36:371)).

v_o = the terminal velocity of the particle in $\frac{\text{cm}}{\text{sec}}$, and r is the particle radius in cm.

It will be assumed that the terminal velocity is reached instantaneously upon interaction of the attractive force. Solving for v_o in the above equation, we find that

$$v_o = 4.73 \times 10^{-10} \frac{qe}{r}. \tag{27}$$

Stoke's law must be corrected by the Cunningham correction factor when particles less than 3μ diameter in an air medium are studied (Ref 36:1019). This correction factor has been determined (Ref 22:310) to be

$$C = 1 + \frac{9.42X10^{-6}}{r}(1.23 + 0.41e^{-0.934x10^{-5}r}) \qquad (28)$$

where r is the particle radius in cm and e is the exponential.
The product of Stoke's terminal velocity and the Cunningham correction factor will equal the drift velocity of the particle in the media

$$v_d = v_o C = \left(4.73X10^{-10}\frac{qE}{r}\right)\left(1 + \frac{9.42X10^{-6}}{r}(1.23+0.41e^{-0.934x10^{-5}r})\right) \qquad (29)$$

The distance between the plates in the collection section divided by the particle drift velocity will define the maximum amount of time required for a particle to drift to the collection plate, i.e., the collection time. The length of the collection section divided by the linear velocity of the air flow will define the transit time of a particle through the collection section. If collection time is less than the transit time, the particle will be collected. Since the charging equations show the adsorbed charge to be strongly dependent upon the particle radius, an analysis of the combined charging and collection equations will show that collection efficiency is directly proportional to particle size. We see from the collection equation that drift velocity is strongly dependent upon the amount of adsorbed charge and the potential existing between the potential plates. We see from the charging equations that the amount of adsorbed charge is most strongly dependent upon the intensity of the corona current. Optimum collection efficiency will be achieved by maximizing the adsorbed charge and collection potential consistent with equipment design limitations.

Corona Current. A corona current, or corona discharge, is produced when the electrical breakdown strength of a gas is overcome locally. This phenomena is described by Meek and Craggs (Ref 27:148) as "the transitory, faintly luminous and audible, glow discerned in a discharge gap at voltages below, though frequently near to, the sparking value." The essential requirements for corona discharge are

(1) the electrical breakdown strength of the gas must be overcome,

(2) the electrical breakdown must be local and not general, and

(3) the arcing potential of the gas must not be reached.

These requirements can be satisfied only in a non-linear field gradient since field linearity would result in a uniform electrical breakdown and arcing would occur. The degree of non-linearity defines the corona capability and a point-plane geometry having a linear field near the plane and a non-linear field near the point will provide the most effective field. Corona discharge can be classified as positive or negative corona on the basis of the polarity of the ions leaving the non-linear point. Cottrell (Ref 47:1186-1187) determined that negative corona is more stable and allows higher operating currents and voltages than positive corona. The above considerations define a charging geometry as a point source cathode opposite a plane anode with a charging potential greater than the electrical breakdown potential but less than the sparking potential.

A practical charging mechanism may be made by wrapping very fine wire around a conducting frame and placing this grid opposite a flat plate. Penney and Matick (Ref 35:7) have experimented with this wire-in-parallel-plate geometry and have shown that both the ionization current and field potential is increased when either the applied voltage is increased or the cathode wire diameter is decreased. These findings were corroborated in this thesis when an extensive experimental program was conducted in

which the grid wire diameter, the wire spacing on the grid, the grid to plate spacing, and the grid to plate potential were varied. The results of this parametric study defined the design of the charging section used in this thesis.

Summary

This chapter has been devoted to presenting that basic knowledge of nuclear radiation, airborne particulates, analysis requirements, and electrostatic precipitation theory that will be required to understand the subsequent description of experimental results. Much of the information presented in this chapter has been obtained from a theoretical study conducted by Captain D. L. Lamberson and references have been cited where appropriate.

We have seen that fallout analysis consists of a quantitative measurement of the radiation intensity through a determination of the beta and/or gamma energy intensity and a qualitative determination of the nuclide content through gamma ray analy is. Maximum sample activity is required to allow analysis of the weakly ionizing gamma radiation and minimize the effects of statistical variation. We have defined collection sensitivity as collector efficiency times the flow rate of air and have shown that the sample collection rate can be optimized by maximizing either or both of these parameters. The electrostatic precipitator has been shown to have a superior collection sensitivity by virtue of its increased flow rate capability. The collection efficiency of the electrostatic precipitator is directly proportional to the charge adsorbed by the aerosol and the potential between the plates in the collection section and inversely proportional to the plate separation distance and the linear air flow rate. The charge adsorbed on the particle is directly proportional to the ion density in the corona field, the length of time spent in the

corona field, and the particle radius. The desired maximum mass of sample may then be obtained by maximizing the air flow rate, the corona current, and the collection potential to provide a timely sample with adequate radiological activity.

III. Precipitator Design

General

This study was conducted to examine the feasibility of using an electrostatic precipitator to collect analyzable and representative samples of airborne radioactive contaminants. An electrostatic precipitator was designed and built to test this collection feasibility. The theoretical criteria presented in Chapter Two and the results of an earlier feasibility examination (Ref 39) were augmented by parametric studies to establish the initial precipitator design. Experience indicated the advisability of certain design changes which were subsequently incorporated into the test model.

This chapter will describe the electrostatic precipitator used in this study and will discuss the experimentation conducted in establishing the optimum design parameters. External factors that contributed to design decisions will be identified. The experimentation will be reported chronologically since initial results often influenced the studies of subsequent stages. Experimental failures will be noted to minimize the efforts of future design improvement experimentation. Finally, the resultant experimental model will be described in detail and critical values identified.

Contributing Factors

In addition to criteria established by theoretical design studies, certain practical construction considerations influenced the design development. The major external factors contributing to the experimental analysis and the design of the ultimate model were

(1) cost,

(2) reproducibility,

(3) the time required for design optimization, and

(4) the availability of materials and auxiliary equipment.

Of these four factors, the first three were considered in view of their effect on the utility of the ultimate working model but the fourth markedly influenced the experimental design.

Although cost and reproducibility were not prime considerations in the design of the experimental model, the possible future value as a practical collection device dictated their consideration in the developmental studies. The time required for experimental optimization of certain parameters was considered and when it was evident that the increase in efficiency would be negligible or unnecessary the optimization studies were terminated.

The availability of materials and auxiliary equipment was a major factor. Materials and fahricating facilities were available for the construction of the precipitator and the final design was influenced only by the cost of materials and ease of construction but the availability of the power supply, the fan and the ultrasonic cleaning facility defined several critical measurements. A power supply was available that would provide a maximum of 30,000 volts (30KV) and .035 amperes (35 ma). A fan was commercially available that would provide a regulated output at values ranging from 350 cubic feet per minute (350 cfm) to 3200 cfm and the inlet size of this fan influenced the cross-sectional dimension of the precipitator housing. An ultrasonic cleaning unit was commercially available that would accomplish the necessary collection plate cleaning. The size of the cleaning tank influenced the length of the collection plate and therefore the length of the precipitator. Air ducting was available in any desired size and the dimensions were chosen to provide an acceptable air flow head loss.

Design Criteria

This experimental model was designed to provide the maximum sample collection rate consistent with the limitations posed by the auxiliary equipment. The sample collection rate is dependent upon:

(1) the volume flow rate of air,

(2) the linear flow rate of air,

(3) the electric charge placed on the aerosol,

(4) the length of time the charged aerosol is in the collection section, and

(5) the time required for the particle to drift to the collection plate as determined by

  (a) the particle size and media viscosity and their influence on the Stokes-Cunningham terminal velocity,

  (b) the plate separation or drift distance,

  (c) the strength of the electrical field between the ground plate and the collection plate, and

  (d) the turbulence of the air stream.

This sample collection rate is influenced by a number of independent and interdependent parameters. The volume flow rate of air, for example, is a function of the linear flow rate and the cross-sectional area of the precipitator. The charge placed on the aerosol is a function of the charging current, the charging potential, and the amount of time spent in the charging environment. The fraction of the charged particles that are collected is a function of the amount of charge on the aerosol, the particle drift velocity, the linear air flow velocity, the plate separation distance, and the length of the collection section. Of these parameters, the maximum volume flow rate of air was fixed by the available fan, the cross-sectional area and linear flow rate were fixed by the

inlet dimensions of the fan, and the length of the collection plates was fixed by the dimensions of the ultrasonic cleaning tank. The variable parameters were then the charging current, the charging and collection potential, the length of the charging section, and the plate and grid-plate separation distance.

By definition, collector sensitivity is a function of the volume flow rate of air and the collector efficiency. With a fixed maximum volume flow rate of air dictated by the output of the available fan system, collector sensitivity could be maximized only by maximizing the collector efficiency. The charging and collection equations show that collector efficiency is most strongly dependent upon the ionization current in the charging section. A parametric study was conducted to establish the maximum ionization current. Optimum values for the remaining variable parameters were then chosen consistent with restrictions imposed by the established ionization current parameters.

Corona Current Parametric Study

In this experimental analysis, wire of a certain diameter was wrapped around a 6"x10 3/4"x1/8" flat aluminum frame. This wrapped grid was positioned in a plexiglass jig at measured distances from and parallel to a 6"x10 3/4"x1/8" flat aluminum plate (see Fig. 2). The grid was connected to the negative terminal of the power supply and the aluminum plate was connected to ground. The grid-plate potential was incrementally increased from 0 volts to 30 KV and the current was measured at each intermediate voltage setting. The grid-plate separation was varied from 10 cm to 2 cm in 0.5 cm increments and a set of voltage-current measurements were plotted for each position (see Fig. 3). This procedure was used for .001" Nichrome wire, .002" KOVAR wire, .0031" Nickel wire, .005" Nickel wire, and .005" "S" Tungsten wire. Corona current first occurred with a

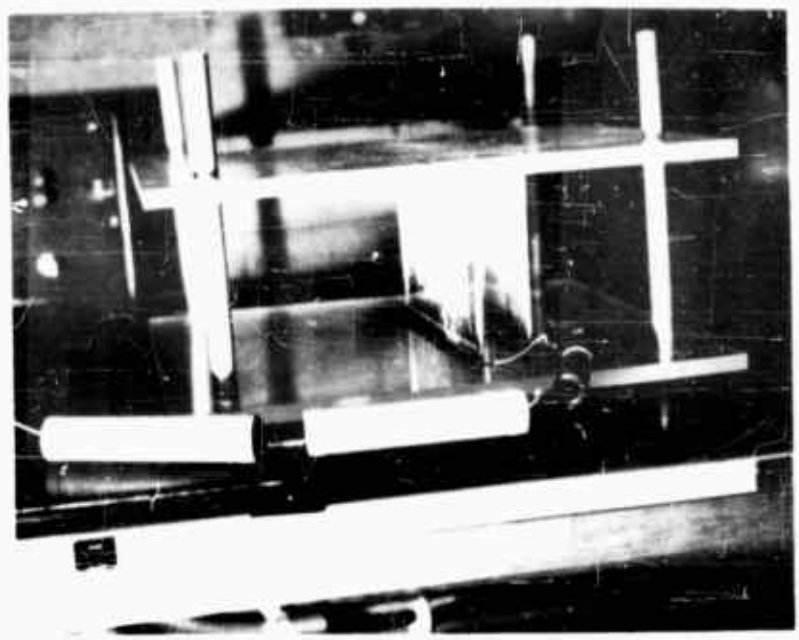

Fig. 2

Apparatus Used in Parametric Corona Study

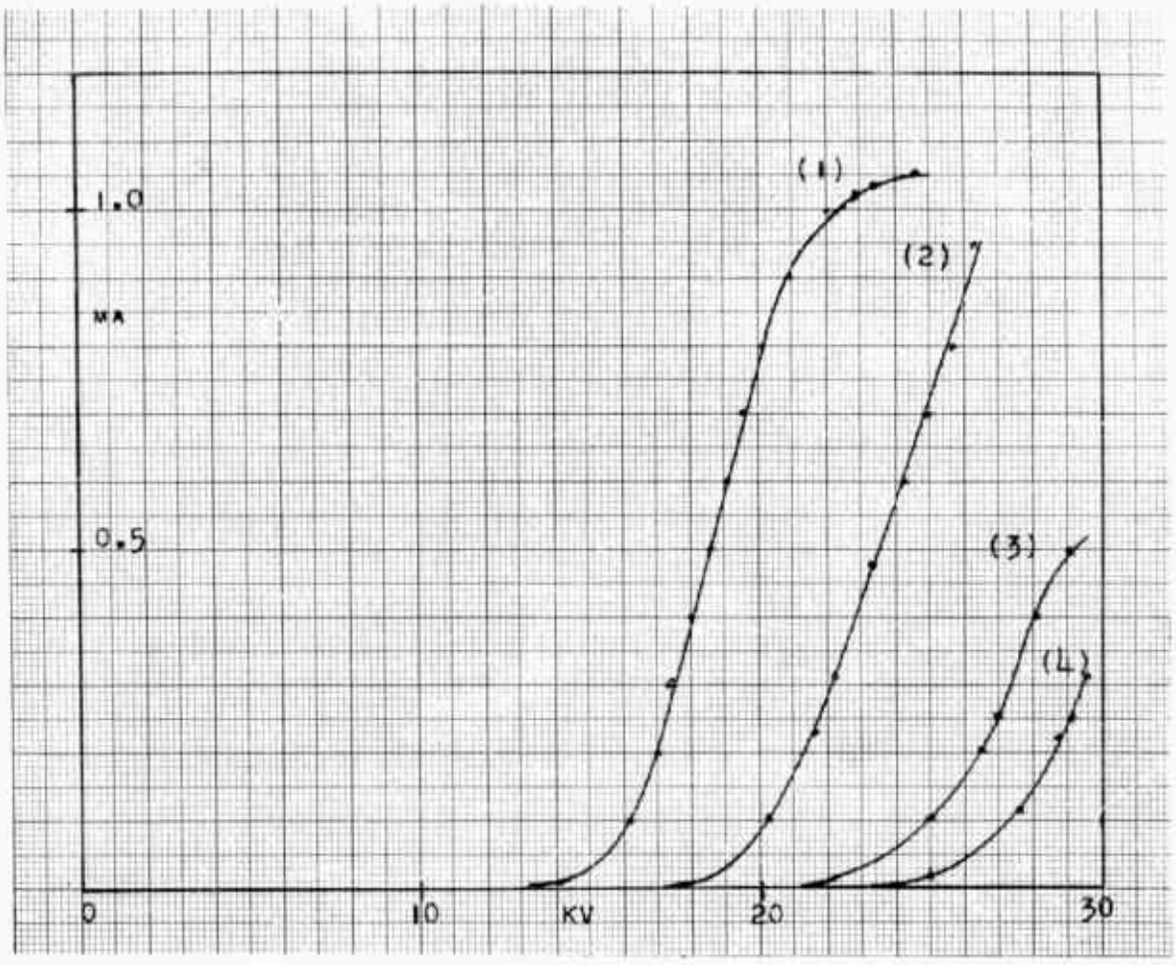

Fig. 3

Results of Parametric Corona Study

This portrayal shows a plot of corona current versus grid-plate potential for grid-plate separation distances of 2.0 cm, 2.5 cm, 3.0 cm, and 3.5 cm represented by curves 1, 2, 3, and 4 respectively for .005" "S" Tungsten wire.

grid-plate separation nf 4.0 cm and an ionization potential of 30KV. The onset of corona current occurred at lower ionization potentials with decreasing grid-plate separation. The magnitude of the corona current at a given ionization potential was increased with decreasing wire diameter but the tensile strength of the grid wire and the susceptibility to grid wire burnout defined a lowest practical diameter.

The available power supply was capable of supplying a maximum of 30KV/35ma. The parametric study was terminated when a grid-plate geometry was achieved that would permit a corona current of 1.3ma across a single grid-plate section with a potential difference of 23.2KV. This would provide a total corona current of 22ma across the seventeen grid-plate sections in the precipitator. A practical operating limit of 25KV was chosen to provide an equipment safety factor and an analysis of the charging equations showed that saturation charging of the available air flow would be achieved with the ionization current provided by this geometry. Additional parametric design might conceivably increase the voltage-current capability if such an increase is required and if a power supply is available that would provide the necessary voltage and current. A theoretical analysis (Ref 42) of an improved collection facility that employs a vastly increased air-flow rate indicates the need for this improved ionization capability.

Experimental evidence indicates that minor perturbations caused by scratches on the aluminum plates and frames or kinks or slack in the grid wires are extremely critical. Any deviation from a perfectly parallel grid-plate assembly establishes a source of arcing and precludes the formation of a corona current field. Evidence also indicates an increase in corona current and a decrease in arcing when air is forced through the corona section. It was also determined that arcing occurred in a plate-plate geometry at a lower potential than in a grid-plate geometry of the

same separation so the collection potential is limited to a lower value than that possible for the charging section.

Charging Section Design

The information gained in the corona current parametric study dictated the design of the precipitator charging section. The charging grid consisted of .005" "S" Tungsten wire wrapped on 0.25" centers around a 6"x10 1/4"x1/8" aluminum frame (see Fig. 2). Tungsten wire was chosen for its high temperature characteristics. The sides of the frame were 1/4" wide and all edges and corners were smoothly rounded. The perfectly flat polished aluminum plates had all corners and edges rounded. The grid-plate separation was 2 cm. An alternating series of 8 grids and 9 plates were placed horizontally in the inlet end of the electrostatic precipitator to form the charging section (see Fig. 4). The plates were connected to ground and the grids were connected through a current limiting resistor network to the negative terminal of the power supply. The current limiting action described below was provided by a 1 megohm-1 watt resistor bank in series with each grid. This resistor bank was designed to provide an optimum surge limitation while creating a minimum drop in the ionization potential. The resistors should ideally be high voltage resistors to preclude arcing across the resistor bank and should be physically as large as possible to permit maximum heat dissipation. The smaller resistors used in this experiment became hot, gradually changed resistance, and had to be replaced periodically. Since a network having enough resistance to satisfactorily quench transient surge currents would have resulted in excessive power dissipation and a prohibitive decrease in ionization potential, an additional variable current limiting network was provided by connecting a parallel bank of nine 200 watt light bulbs in series with the primary winding of the power supply transformer. A

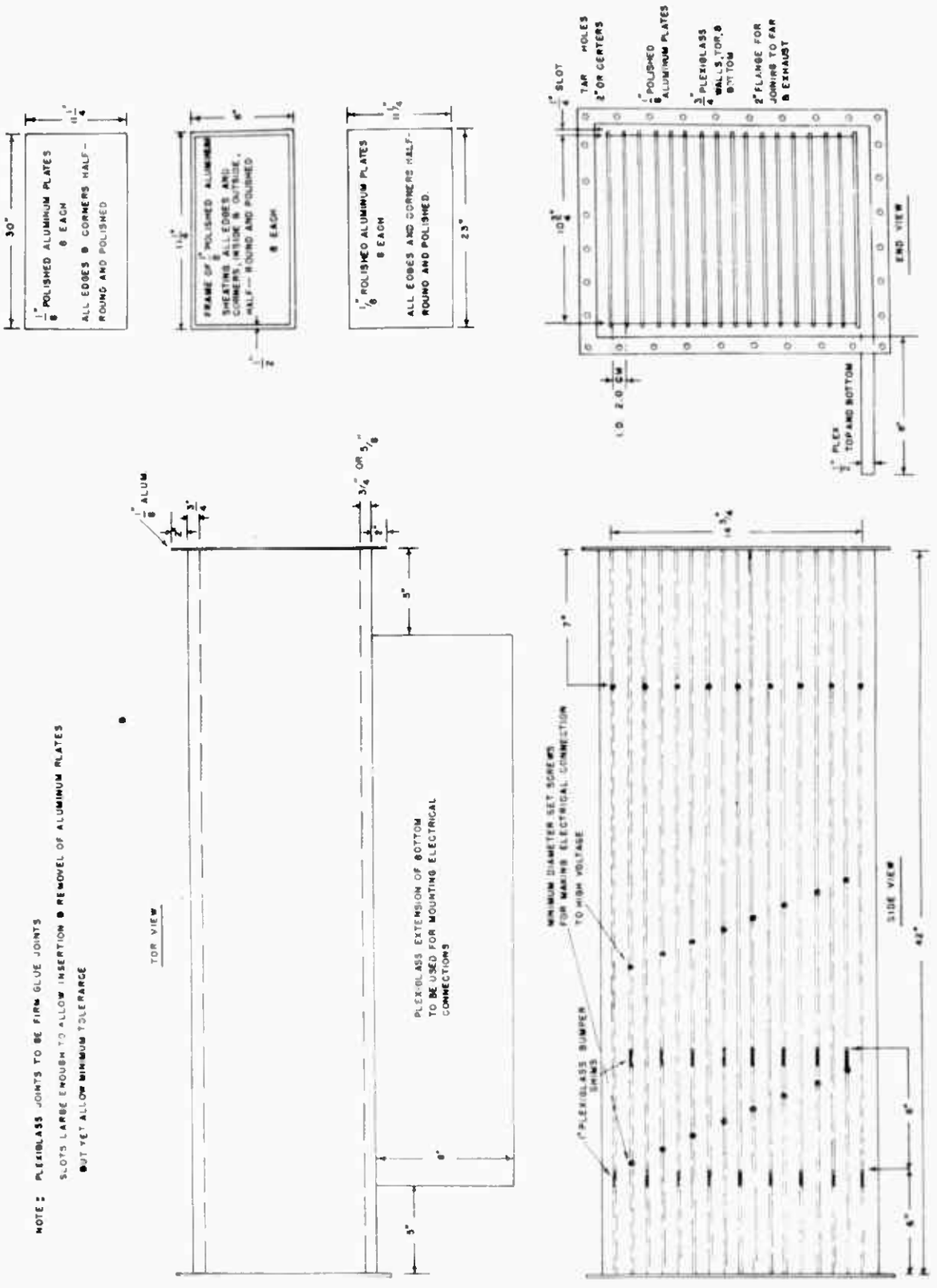

Working Drawing of Electrostatic Precipitator

Fig. 4

A current surge resulting from an arc in the charging section caused the light bulbs to glow brighter. This increased their resistance and caused a larger voltage to be dropped across the light bulb bank. This decreased the voltage across the primary transformer windings with a resultant decrease in the grid-plate potential. This decreased potential quenched the current surge before the over-current relay in the power supply was energized and the power supply shut off.

A maximum corona current was desired to provide a maximum charge on the aerosols. A standard current was desired to insure uniformity of collection conditions and protect the integrity of analysis results. A study was performed to determine the maximum allowable ionization current (see Fig. 5). The experimental model provided a total ionization current of 20ma at a charging potential of 23 KV. The ionization current was monitored during sample collections by observing the output current meter on the power supply and the charging and collection potentials were monitored with a Kilovoltmeter. Any attempt to operate at a higher current-voltage setting resulted in increased arcing that inevitably shut off the power supply. High humidity conditions resulting in condensation on the charging section walls necessitated a decrease in the current setting and excessive rain or snow caused prohibitive arcing that precluded collection.

Collection Section Design

The design parameters of the collection section were, for the most part, dictated by fixed or previously established parameters. The collection section consisted of a stack of seventeen horizontal aluminum plates. Nine of the plates were maintained at ground potential and formed the collection plate system. These were separated by eight plates maintained at a high negative potential to provide the high field force for Coulombic attraction (see Fig. 4). All plates were perfectly parallel

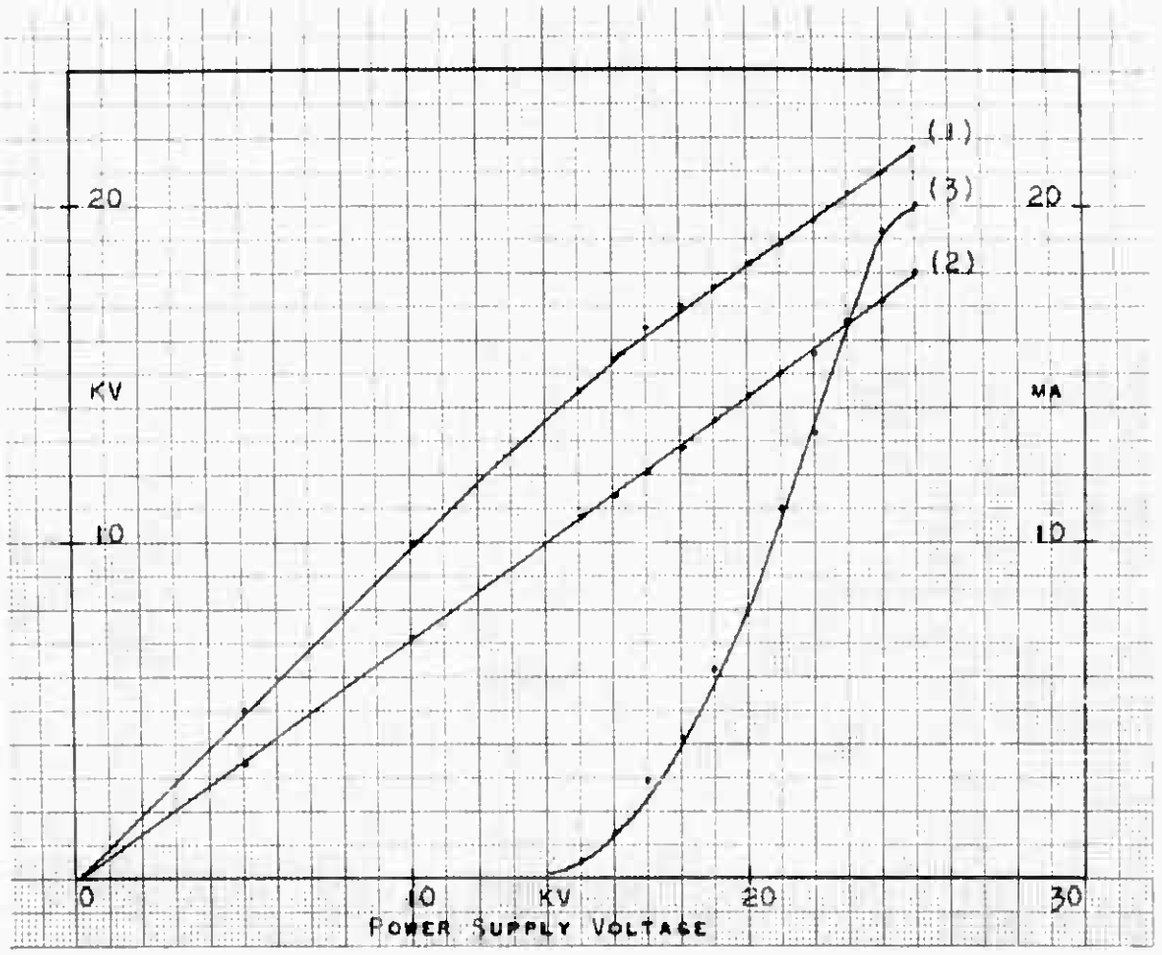

Power Supply Voltage

Fig. 5

A Plot of Ionization Potential (1), Collection Potential (2), and Corona Current (3) Versus Power Supply Voltage

and separated by a distance of 2cm. The ground, or collection, plates were an extension of the grounded plate in the charging section. Charged aerosols in the air flow were acted upon by the field force in the charging section and many were, in fact, collected while still in the charging section. A pronounced image of the grid net was reflected in the dust pattern immediately beneath the grid wires. The cross-sectional dimensions of the collection plates were dictated by the inlet dimensions of the available fan and the length of the ultrasonic cleaning tank. The collection plates could have been made in sections and a longer collection section provided but a solution of the collection equations using the maximum available linear flow rate, the charge achieved in the designed charging section, and a plate separation equal to the charging section grid-plate separation showed that the increased efficiency would be negligible. The collection potential was originally intended to be equal to the charging potential to provide a maximum collection potential with a simple electrical circuit. Experimentation showed, however, that arcing occurred in this plane-plane geometry with a plate separation of 2cm and a potential difference of 22KV. A voltage divider network was built using four high-wattage high-voltage resistors in series. This network was connected across the power supply and a tap-off between the third and fourth resistor provided a collection potential equal to three-fourths of the power supply output voltage.

The electrostatic precipitator housing was an open-ended box 14 11/16" x 10 3/4" x 42" inside dimension (see Fig. 4). The box was made of 3/4" plexiglass rigidly glued at all joints. The collection plates and charging grids slid into channels cut into the walls of the plexiglass frame with the charging grids and the negative collection section plates in-line. The decreased potential on the negative collection plates necessitated the installation of one-inch plexiglass insulating spacers between

them and the charging grids. Set screws tapped through the walls of the plexiglass frame provided electrical contact with the plates and grids. The grounded collection plates were removeable to permit removal of the collected aerosols. All plates were polished and all corners and edges were rounded and smoothed to prevent arcing.

An ILG Electric Ventilating Company Fan, Model BU 1350 was used in this experiment (see Fig. 6). This fan was powered by a 1 1/2 HP motor and a series of replaceable pulleys permitted air flows of 353 cfm, 706 cfm, 1059 cfm, 1412 cfm, 1765 cfm, 2118 cfm, 2471 cfm, 2824 cfm, and 3177 cfm, all $\pm$ 100 cfm. The series of volume flow rates were provided to experimentally examine the collector sensitivity at various volume flow rates.

Optimum collector sensitivity required a maximum volume flow rate of air and head loss in the collector was minimized by optimizing the plate and grid design. Airflow calculations were performed to insure a ducting head loss compatible with the fan design specifications. The ducting system brought air in from one side of the laboratory building and exhausted it out the other side to minimize air recirculation. The calculations showed that an 18" circular galvanized duct would present an acceptable head loss in this fifty foot ducting system.

The effect of air turbulence was not analyzed in this experiment. Efforts were expended, however, to maximize laminar flow in the collector by pulling air through the precipitator rather than pushing it. The effect of turbulent flow is believed to be negligible (Ref 39:67) since statistically as many particles are being driven toward the collection plate as are being carried away. This effect, however, was not experimentally verified. The effect of re-entrainment, i.e., the removal of particles already collected by the scouring action of the air flow,

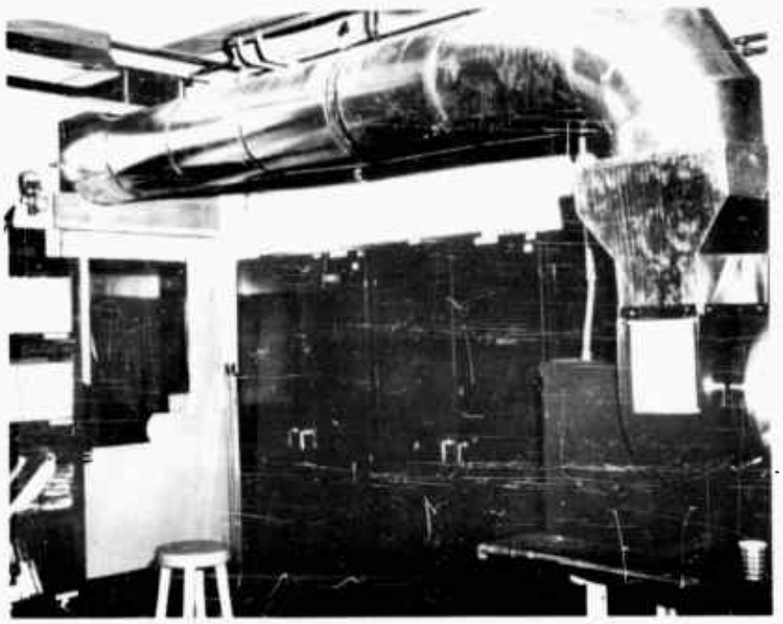

Fig. 6

A View of the Fan and Exhaust Ducting System

Airflow was pulled through the electrostatic precipitator by this fan and ducting system. A Gelman Thermal Anemometer visible in the upper left corner of the picture was connected to a probe mounted in the duct to provide a measure of the airflow rate.

was examined by mounting a Gelman Air Sampler between the exit end of the precipitator and the fan inlet (see Fig. 7). Repeated continuous samplings of four hour collection runs showed a negligible dust trace on a 2 micron Gelman Filter Paper. This post-collection sampling testifies to the collector efficiency and lack of particle re-entrainment.

The lethal voltages and currents associated with this experiment necessitated special precautionary measures. The collection plates and charging grids were positioned 6" in from the ends of the precipitator housing to insulate them from the connecting ducts. All electrical equipment was interconnected to earth ground. Prominent signs identifying the lethal voltages were displayed and the laboratory was locked except when the operator was present. The lethality of this equipment cannot be overemphasized.

The fan motor and power supply were electrically connected so that an unscheduled stoppage of any component or activation of the over-current/over-voltage relays in the power supply would turn off the electrical power to the entire system.

Collection Facility Design

The collection facility was designed to permit collection and subsequent concentration of the airborne particulates from a large volume of air. Precautions were taken to minimize recirculation of the air which would have diluted the aerosol burden. Instrumentation permitted a constant monitoring of ionization currents and potentials and air flow rates (see Figs. 6, 7).

The collection laboratory was on the ground floor of a two-story building. The air intake was from a 20' x 40' open courtyard in the center of the building and the air was exhausted through an external

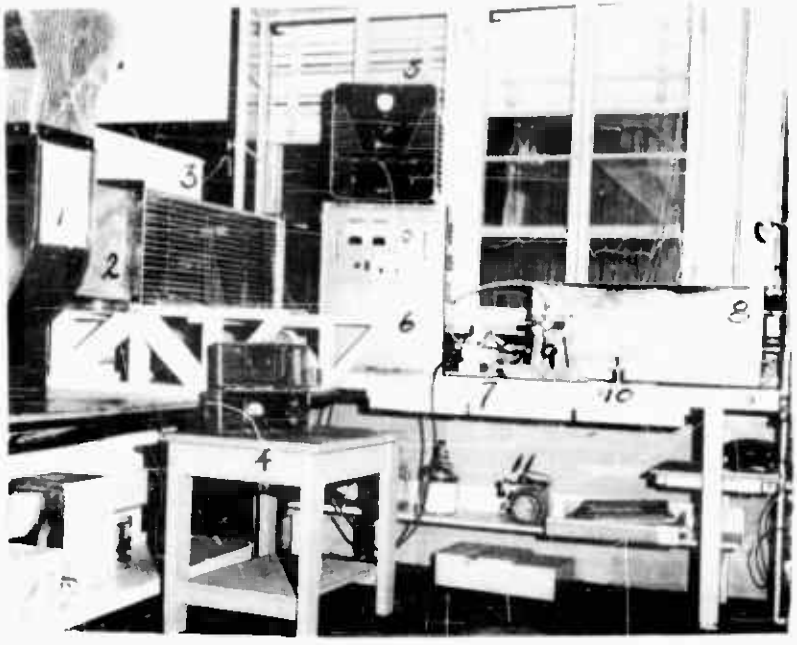

Fig. 7

An Overview of the Collection System

Air was drawn through the electrostatic precipitator (3) by the fan (1). A Gelman Air Sampler (11) mounted in the exhaust duct (2) provided a measure of the collection efficiency. The ionization and collection potentials provided by the power supply (6) were monitored with a kilovoltmeter (4). The collection plates were washed in an ultrasonic cleaning tank (8) that was powered by an ultrasonic generator (5). The cleaning fluid was pumped through a Millipore filter (9) by a small centrifugal pump (7). The collected filter samples were compressed and dryed in a 2"D x 1" press (10).

wall fifty feet away. It is believed that the chimney effect of the courtyard inlet did not detract from the sample validity and that the inlet-exit aeparation diatance effectively prevented recirculation dilution. The air entered the precipitator through a six-foot-long rectangular duct that projected through the laboratory wall to the outside courtyard (see Fig. 7). A 90° elbow was placed on the outside end of the duct to provide a rain/snow shield and a 1/2" wire screen covered the inlet end to keep out large objects. The exhaust air from the precipitator entered the centrifugal fan through a rectangular-circular transition joint. The air was exhausted vertically from the fan through a rectangular-circular transition joint to the 18" circular galvanized duct. The air flow was then carried through a 90° elbow and fifty foot of 18" galvanized ducting and exhausted through an outside wall. A 90° elbow on the exhaust end provided the aecond rain/snow shield. A Gelman thermal anemometer was mounted in the exhaust duct to provide a measurement of the air flow rate (see Fig. 6).

The precipitator housing waa bolted to the inlet and exhaust ducts through mounted flanges. The housing rested on a wooden support frame (see Fig. 7) and upon termination of a sample collection, the housing was disconnected from the duct line and pulled out to allow removal of the collection plates. Collection plate removal was accomplished by loosening the electrical set screws, inserting a hook into the drilled hole in the collection plate, and pulling the plates along their channel and out the exhauat end of the collector. The charging grids could be removed in a aimilar manner for grid wire repair.

Summary

This collection system was deaigned to provide the maximum sample collection rate consistent with limitations imposed by available

auxiliary equipment. The available air flow capacity, power supply, and plate cleaning facility established the major design limitations. Experimental design studies were conducted primarily to maximize the ionization current capacity and secondarily to optimize the remaining variable parameters consistent with values established by the ionization current requirements. Optimization studies were terminated when equipment capacities were achieved or possible efficiency increases did not warrant additional research time. Corollary design studies developed current limiting networks required for continued operation.

Air flow is drawn through an ionization current field produced by a stack of eight grids maintained at -23KV and 9 plates maintained at ground potential. With the maximum linear flow rate available, the aerosols achieve a saturation charge in the 6" charging section. The charged particles are carried by the air flow through a collection section containing a stack of nine grounded plates and eight plates maintained at a -18KV potential. The negatively charged particles are driven to the removeable ground plates by a Coulombic force of attraction. A Gelman Air Sampler mounted in the effluent stream verified the collection efficiencies predicted by the theoretical calculations. This collection efficiency, when multiplied by the volume air flow rate possible, would result in a large collection sensitivity and a large sample collection rate capability.

IV. Sample Collection Technique

General

This research study had two major objectives. The first was to design, build, and proof-test the electrostatic collection and secondary concentration process and the second was to use the proved collection process in an extended collection/analysis program to determine the local radioactive contamination. This chapter will discuss the procedural experimentation that was conducted to determine an optimum collection procedure and will describe the collection program finally adopted. The many procedural failurea will be described to assist future design improvement efforts.

Procedural Experimentation

The sample collection and concentration was accomplished in two steps. The airborne particulates were first removed from a measured volume of air by electrostatic collection on aluminum plates. The collected sample was then removed from the aluminum plates and concentrated to an analyzable geometry. The final sample should ideally contain all of the airborne contaminant from a measured volume of air and should be formed into a configuration amenable to gamma spectrographic analysis. Any deviation from this ideal sample should be defined so that the observed count rate might be corrected to a true count rate. The sample collection procedure should provide this defined sample in the shortest time possible and with a minimum expenditure of money and effort.

Initial studies clearly identified the practicability and efficiency of the electrostatic precipitator as a collection device. A Gelman Air Sampler was mounted downstream from the precipitator to test the particulate content of the air flow after precipitation (see Fig. 7). An

analysis of the filter papers subsequent to six sample collections revealed no vislble contaminant. The secondary concentration proved to be more difficult and a number of concentration techniques were tested in an attempt to optimlze the collectlon process. This optimlzation study accounted for a major portion of the research effort and the separate techniques examined will be discussed in detail.

Ultrasonic Cleaning

The original procedural concept envisioned a secondary concentration through the use of an ultrasonic water cleaning bath with subsequent filtration of the cleaning fluid. Despite the fact that experimentation ultimately disclosed a serious sample diminution through selective solubility and fractionation, valuable experience was gained during this developmental study and the techniques tested and results achieved will be reported.

The ultrasonic cleaning bath provided a slow but thorough method of removing the collected sample from the plates. Three plates were washed simultaneously for thirty minutes in ten gallons of distilled water and then rinsed with distilled water. A tissue swipe of the cleansed surface indicated that all of the sample had been removed. A small amount of detergent was added to the water bath to enhance the cleaning. Various commercial detergents were tested but common household low-sudsing detergents were found to be quite satisfactory and most available.

The collected particulates were to be removed from the water bath by pressure filtration. Initial planning called for filtration through a 25 mm Millipore fiiter since this would provide a sample that could be counted with a 1 1/2" x 1 1/2" NaI(Tl) scintillation crystal. Thls small scintillator would provide a good spectral resolution with a low background count rate. Initial filtration attempts quickly showed,

however, that this system would not provide an adequate filtration capability. The small filter papers immediately became packed and prevented fluid flow. A high pressure pump was installed and a 47 mm Millipore filter was tested but these filters also became clogged before an appreciable fraction of the fluid bath was passed. Finally, a 142 mm Millipore filter was tested (see Fig. 8) and an adequate filtration capability was achieved. Even this filtration system posed serious limitations, however, in that it was slow, expensive, and restricted essentially to particulates 0.22μ in diameter or larger. The resultant sample was presented on a series of filter discs 142 mm in diameter and had to be modified before it could be counted with the available 2" x 2" NaI(Tl) scintillation detectors.

Experimentation proved that repeated filtration was required. Filter papers with small diameter pores quickly became clogged and preliminary filtration through stages of coarser papers was required to successfully filter the bath. Since micron and sub-micron filter papers of this diameter are relatively expensive and filtration is a time consuming process, an optimum filtration schedule was required. The experimentally determined optimum sequence consisted of filtration through (1) a micropore glass prefilter, (2) a microfiber glass prefilter with a filter paper having a 3μ diameter pore size, (3) a 1.2μ filter paper, (4) a 0.8μ filter paper, (5) a 0.45μ filter paper, and (6) a 0.22μ filter paper. Usually more than one of the finer filter papers was required to successfully filter the entire ten gallon fluid bath. The separate filter papers were stacked to form a composite sample and this sample was baked to dryness. Two-inch-diameter discs were cut from this composite and the two-inch discs and all spare parts were stacked to form a 2"D x 1" cylinder. The cylinder was wrapped in a plastic

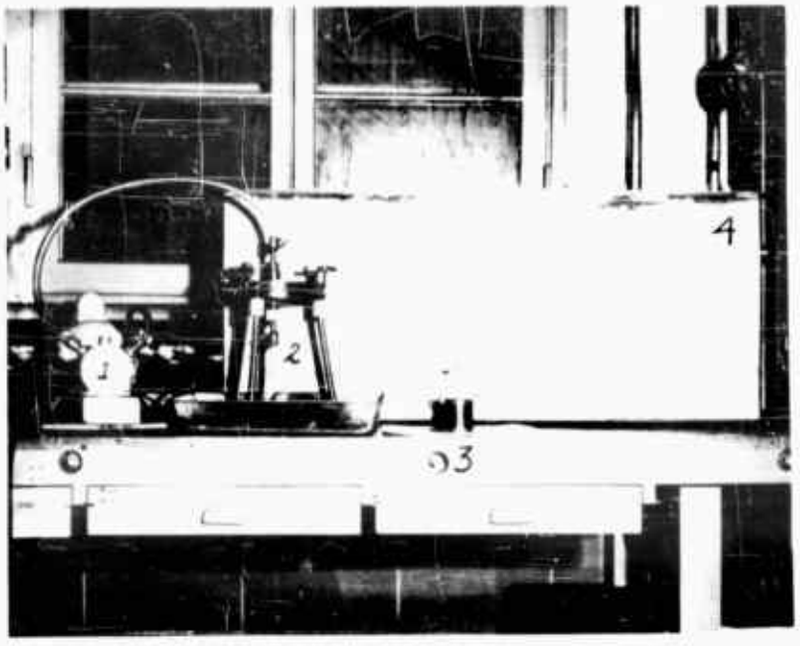

Fig. 8

The Ultrasonic Cleaning and Filtration System

The collection plates were immersed in water in the ultrasonic cleaning tank (4). R.F. energy provided by a generator was transformed into ultrasonic vibrations by a set of transducer crystals mounted in the base of the tank. The ultrasonic vibrations scoured the collected particulates from the plates. The particulate bearing cleaning fluid was pumped through a Millipore filter (2) by a centrifugal pump (1). The filter samples were compressed and dryed to the desired configuration in a 2"D x 1" press (3).

film and compressed in a 2"D x 1" cylindrical press (see Fig. 8) to the one-inch height and sealed with tape. This standard geometry formed the scintillation spectrometry aample. All sample handling and cutting was done over white paper to insure complete sample retention.

The filtrate remaining after the final 0.22μ filtration presented a very cloudy appearance. An analysis was conducted to attempt a correlation between particle size and activity and to determine the fraction of the activity that was lost in the discarded filtrate. A sample was collected for twelve hours, washed, and carefully filtered in accordance with the above filter aequence. The fluid was filtered through the 0.22μ filter paper three times to insure collection of all particulates 0.22μ in diameter or larger. The separate-pore-size-filter samples were counted individually and as a composite. The particle-size/activity correlation was suspect because micropore filters adsorb a portion of the particles smaller than the pore diameter through electrostatic adsorption (Ref 30:2). The filtrate was boiled to dryness and the filtrate residue was analyzed for gamma activity. The filtrate residue was found to have an integral count rate nearly equal to that of the composite filter sample and one of the spectral peaks showed a marked increase in relative amplitude.

A second sample was taken to test the validity of this filtrate residue activity determination. A modification of the collection/ concentration technique was employed, however, to test the possible contribution of ultrasonic vibration to the sample diminution. The aluminum collection plates were washed by hand uaing a small tissue swab. The wash water was carefully filtered as before and the separate-pore-size-filter samples were again counted individually and collectively. The particle-size/activity correlation achieved during this test differed

markedly from that in the previous examination. This variance indicates that either the filtration process does not provide an accurate particle size definition or that there is no standard correlation between particle size and activity. The many experiments referenced in Chapter Two would indicate the credibility of the particle-size/activity correlation and indicate that the variance noted in this analysis is due to the electrostatic adsorption phenomena associated with microfiber filters. The filtrate from this analysis was evaporated to dryness as before and the residue analyzed. This residue exhibited an even greater gamma activity and proved that the fractionation was not due to the ultrasonic vibration. Instead, it is postulated that the high filtrate activity is due to a selective solubility of the sample constituents in the cleaning solution.

The ultrasonic cleaning and subsequent filtration not only caused experimental difficulties but also presents disadvantages as a standard collection technique. The ultrasonic cleaning, filtration, and subsequent sample preparation is expensive and time consuming. An undefined portion of the sample is lost in the washing and filtration process and the collection capabilities of the electrostatic collection process is not fully exploited. An adequate sample is retained for a qualitative analysis but the accuracy of the quantitative determination is suspect. These limitations would preclude the adoption of this process as an acceptable concentration technique.

Collection on Foil

Primary electrostatic precipitation on a thin foil would present several obvious advantages. The foil could be compressed into an acceptable sample geometry without benefit of an expensive, time consuming, and sample diminuting secondary concentration. Collection devices could

be designed wherein the foil could be periodically or continuously advanced through the collector and permit extensive monitoring of upper air strata or continuous monitoring of radiological contaminants on the surface of the earth. Such a collection device would incorporate the increased collection capabilities of the electrostatic precipitator into the dynamic monitoring system desired in airborne monitoring programs and radiological defense programs in civil defense and reactor facilities.

A compaction test was conducted to determine whether a plastic foil large enough to cover the collection surface might be formed into an acceptable sample configuration. A forty square foot sample of a household plastic foil, Handy Wrap, was compressed in a 2"D x 1" press and heated to 154°C. The foil was baked and compressed into a solid hard plastic cylinder 2"D x 3/4". This would form a very adequate and accurately reproduceable sample geometry with negligible self-absorption characteristics. A similar area of household aluminum foil would theoretically occupy an acceptable volume and could be compacted into a satisfactory geometry but compaction would be much more difficult and this compaction was not attempted. The self-absorption of an aluminum geometry would not be negligible but could be experimentally determined and a compensation factor calculated. The compaction and adsorption characteristics of a thin plastic foil would provide the superior media, however, if collection could be satisfactorily accomplished.

A single thickness of Handy Wrap was placed over the aluminum collection plates and taped in place with Scotch Brand Filament Tape No. 880. The plastic foil did not disintegrate in the air stream and relatively little arcing was encountered but a six-hour collection provided a sample that had less than 5‰ of the activity of a sample collected directly on the aluminum plates. The Gelman Air Sampler mounted down-

stream from the collection showed that a large portion of the aerosols had gone through the precipitator. It is believed that the plastic foil provided a dielectric that either perturbated the electrostatic collection field or prevented the neutralization of charge on the collected particles. If the adsorbed charge was not allowed to leak off the collected particles, the collection plates would develop a negative charge and inhibit collection of the negatively charged aerosols.

A second attempt at foil collection was made. This time the foil was tightly wrapped around the aluminum plates and sealed to itself by heating to form a tight envelope. This plastic envelope was sprayed with an anti-static compound in an attempt to form a conducting surface. The sample collected on this foil exhibited approximately 5‰ as much activity as a sample collected on bare aluminum. Sufficient activity was present to permit a qualitative spectral analysis but an acceptable quantitative determination was not possible.

Practical collection requirements would define the obvious advantages of a foil as a collecting surface. Compaction and self-absorption characteristics would identify a plastic as a superior foil material. Experimental studies, however, point out the requirement for a conducting rather than a dielectric media and the success of this possibly superior technique is dependent upon the availability of such a thin conducting plastic foil. Such a material was not found or tested during the course of this study. An aluminized mylar film was considered but this material was not available for test during the time period of this analysis.

Alternate Concentration Techniques

Several alternate concentration techniques were examined in an attempt to circumvent the cleaning and filtration requirement. An attempt was made to dry-wipe or scrape the collected particulates from the plates.

The collected dusts were found to form a tightly bound film that defied complete removal. That portion that was removed formed a very light dust that was easily lost. Evaporation of the ten-gallon ultrasonic-bath solution was considered but rejected because of the time and effort required and the problems involved in accurately reclaiming the reaidue. An attempt was made to install partitions in the cleaning tank to minimize the volume of cleaning aolution required but the ultrasonic vibrations disrupted all attempts at mastic bonding and the presence of the transducer crystals in the bottom of the ultrasonic tank prohibited the application of heat neceasary for welding or soldering. The plates were satisfactorily washed by hand and the resultant one gallon of wash water evaporated in one sample collection but this technique was time consuming and presented difficulties in the accurate reclamation of the residual sample.

One set of collection plates were washed by hand with isopropyl alcohol to examine the selective solubility phenomena. The plates were satisfactorily cleaned with approximately one-half gallon of alcohol and the solution was filtered and analyzed as in the previous water samples. The filtrate was evaporated to dryness in a relatively short time and the filtrate residue was examined for gamma activity. This sample also exhibited gamma activity in the filtrate residue but to a lesser degree than the residue from the water-bath filtrate. The residue from the water-bath filtrate exhibited an activity roughly equal to that of the composite filter sample while the residue from the alcohol filtrate exhibited less than 5‰ of the total activity.

The relatively short evaporation time required for a volatile cleaning fluid would indicate a superior concentration technique. Since alcohol evaporates at a relatively low temperature, a plastic film inter-

liner could be used in the container and the alcohol evaporated in a water bath. The residual sample would then be contained within the plastic interliner. The plastic interliner might then be baked and compressed into a flat and accurately reproduceable sample geometry that would provide an excellent geometry factor.

Summary

An analysis of the downstream air flow substantiated the theoretical practicality and efficiency of the electrostatic precipitator as a fallout collection device. The time, effort, and cost considerations and the selective solubility of the sample constituents precludes adoption of the ultrasonic water bath cleaning and fluid filtration as a secondary concentration process. Sample collection on a thin plastic film would present several advantages and would permit a truly superior collection technique if such a thin conducting film were available. In the absence of such a film, the plates may be washed by hand in a volatile alcohol and the sample reclaimed by evaporation in a plastic-lined container. Ultrasonic cleaning in an alcohol bath could be used but a smaller cleaning tank should be employed to minimize the volume of cleaning solvent required. The solvent could be reclaimed through distillation recovery but even without this recovery the alcohol process would be less expensive than the filtration technique.

V. Sample Analysis Techniques

General

A complete identification of radiological contamination requires a quantitative definition of the radiation intensity and a qualitative determination of the nuclides preaent. There are a number of analytical techniques available that will provide portions of this information. Beta analysis provides a relatively quick and easy determination of the gross radiation intensity and requires a comparitively small sample. Certain isotopes decay by beta emiasion alone and require beta analysis for intensity determination. This analysis technique, however, provides only limited knowledge of the types of nuclides present. Radiochemistry allows an exact qualitative determination but only a limited knowledge of the gross radiative intensities. Gamma ray spectroscopy provides the best single analytical technique with both a qualitative and quantitative capability but requires an adequate sample concentration. The electrostatic precipitation sample collection technique was designed to provide this sample concentration. The sample collection and analysis program was conducted to test the feasibility of this collection process as well as to analyze the local fallout and gamma ray spectroscopy was chosen as the analytical technique.

Gamma spectroacopy consists of the detection and portrayal of the gamma rays emitted by a radioactive sample and an analysis of the resultant spectrum to identify the gamma energies unique to a specific nuclide. Detection ia accomplished through the use of a scintillation crystal, a photomultiplier tube and an electronic pulse height analyzer. The resultant spectrum is a plot of cumulative counts versus gamma energy.

The gamma photon gives up its energy in the scintillation crystal. This ionization produces a flash of light proportional to the energy of the incident photon. The light flash is converted to an electron pulse in a photomultiplier tube and the output of the photomultiplier tube is an electronic pulse proportional in amplitude to the energy of the incident photon. This pulse is fed into the appropriate differential energy channel of a multichannel analyzer where it is stored in memory. The final result is a tabulation of the cumulative number of photons having energies that fall within the separate differential energy widths. Since the separate nuclides emit gamma photons with energies unique to that nuclide, an examination of the spectrum of a composite sample will allow the analyst to identify the separate energy peaks and thus identify the isotopes present.

Detection System Design

A single radioactive isotope may have two or more gamma energies associated with it. Separate isotopes may emit gamma photons with nearly equal energies. A composite sample containing a number of isotopes will therefore present a rather complex spectra. The resolution of the system, i.e., the width and sharpness of the energy peaks, will determine the ability of the analyst to differentiate between peaks. The efficiency of the detection system will influence the amplitude of the peaks and will determine whether they are portrayed as recognizable peaks.

In theory, a photon with a given energy should always result in an electronic pulse of the same amplitude and be stored in the same memory bank of the multichannel analyzer. In practice, a spread of pulse sizes is experienced (Ref 31:86) and a monoenergetic peak is not obtained. Perfect resolution is dependent upon deposition of the entire photon

energy, a perfect correlation between ionization energy and light emission within the scintillator, utilization of all the emitted light pulse, a perfectly standard photoelectric transformation within the photocathode, a standard electron multiplication within the photomultiplier, and uniform amplification and registry of the pulse within the multichannel analyzer circuitry. The actual spectral resolution is determined by the efficiency of the individual components and the overall efficiency of the assembled system.

The ratio of incident photon energy to the emitted light energy is a function of the size, type, purity, and geometry of the scintillation crystal. A large scintillation crystal will absorb a larger fraction of the incident photon energy but will also provide a higher background count rate. The NaI(Tl) scintillation crystal is hygroscopic and develops a yellowish discoloration if not properly sealed against moisture. The discoloration degrades the incident-energy/emitted-light ratio. The size, shape, and activity of the sample will dictate the crystal requirements but a clear crystal that is as large as the background count rate will permit will generally give the best results (Ref 10:87).

Maximum utilization of the emitted light pulse is assured by minimizing the self-absorption within the crystal, by providing a good reflecting surface around the crystal, by providing a good optical bond between the crystal and the photomultiplier tube, and by excluding all external light from the crystal-tube combination. The photoemission ratio and electron multiplication is a function of the photomultiplier tube design and construction and can be maximized only by choice of tubes. Electronic noise is minimized by circuit construction and shielding and signal transmission is enhanced by installing a cathode follower between the photomultiplier tube and the linear amplifier stage of the analyzer.

The detection system to be used in this analysis program waa designed in conformance with the above criteria. The building containing the counting equipment also contained a 2 MEV Van de Graaff generator and a number of radiation standards. The detection facility was built in a room as far from the source of this background radiation as possible. Despite these precautions, operation of the Van de Graaff generator produced a relatively high low-energy gamma background count rate. The sample count rate in the similar low-energy region was, however, approximately two orders of magnitude larger so counting operations could be continued even while the Van de Graaff generator was running. A White cathode follower circuit was built and installed to minimize the excessive line loss in the long cabling running to the Radiation Instruments Development Laboratory 256 channel analyzer. A number of NaI(Tl) scintillation crystal/photomultiplier tube combinations were tested for spectral resolution. A series of 1 1/2" x 1 1/2" crystals were examined in attempt to minimize hackground considerations but the resolution of the available crystals was poor. It later became apparent that these crystals would have been too small for the sample geometry anyway. An analysis of the single 5" x 5" NaI(Tl) crystal available revealed a prohibitively poor resolution. Analysis of a series of 2" x 2" NaI(Tl) crystals with Dumont 6292 photomultiplier tubes provided a useable combination with a resolution of 8.7‰. Price (Ref 38:199) defines resolution as $w_{1/2} = \frac{\Delta h_{1/2}}{h_{max}} \times 100‰$ where h_{max} is the pulse height corresponding to the maximum in the curve while $\Delta h_{1/2}$ is the pulse-height interval between the points at which one-half of the maximum value occurs. He defines 10‰ as an acceptable resolution for a $Na^{T}(Tl)$ crystal and states that a resolution of 6‰ is considered nearly perfect.

The lower discriminator of the multichannel analyzer (see Fig. 9) was aet at 260 so that zero energy was portrayed in analyzer channel No. 2. This was done to insure registry of all low-energy gamma-energy pulses. The upper discriminator was set at its maximum value to pass all pulses. The normal gain setting of the linear amplifier was set on the basis of information gained from 1000 minute counts of the sample. The amplifier gain was set so that the highest energy gamma observed appeared near the end ot the spectra. This was done to spread the spectra out as much as possible while insuring portrayal of all gamma peaks to provide maximum separation between energy peaks. With this gain setting, channel No. 256 would represent approximately 2.2 MEV. Special studies were conducted with amplifier gain settings of two and four times the normal setting to expand the spectra and allow detailed examination of the low-energy end of the spectra.

Shielding Geometry Design

A shielding geometry was required that would minimize the count rate due to natural background radiation, provide easy access to the crystal face, and provide a fixed sample holder for counting geometry reproducability. A number of shielding geometries were built and tested in an attempt to devise an optimum geometry. An optimum geometry (Ref 10:11-23) would reduce the background radiation level to a point where corrections to the data will be small for the normal low intensity samples. The walls should be as thick as possible commensurate with the availability of shielding materials. The chamber should be as large as possible to minimize the solid angle subte ded by Compton backscatter. X-ray peaks resulting from interactions with the shielding materials may be minimized by a series of interliners that have a high cross-section for the absorption of the fluorescent radiation from the preceding liner.

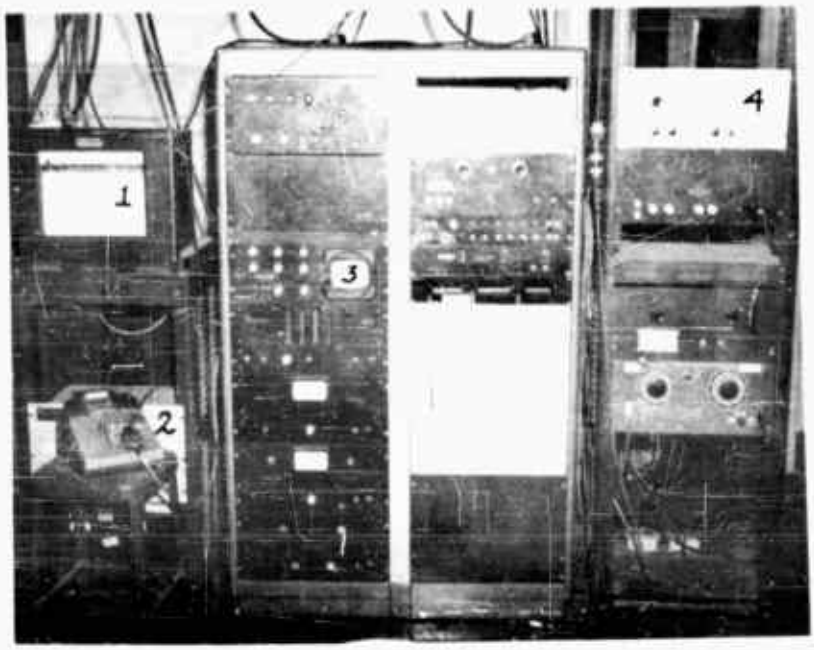

Fig. 9

The RIDL 256 Channel Analyzer

The signal from the detection system is fed into the linear amplifier (4). Data presentation is provided by a Brown Recorder (1), a computer tape (2), and an oscilloscope (3).

One arrangement is to line the Pb shield with 0.030" to 0.060" of Cd and 0.005" of Cu in that order. The interliners were tested in a Pb shield with 4" walls and an internal measurement of 8" x 8" x 14" and in a 10"D x 16" cylindrical Pb shield that had 2" walls but the decrease in background did not warrant the additional effort that would have been required for sample installation. The adopted shield geometry (see Fig. 10) consisted of a cubical Pb shield with 4" walls, base, and top and a 12" x 12" x 14" internal cavity that housed a cylindrical Pb shield (see Fig. 11). The cylindrical shield contained a sample rack that permitted counting geometry reproducability. This shield admitted an average background of approximately 65 cpm. A hole in the front wall of the external cubical shield and a swinging door in the internal cylindrical shield permitted access to the crystal face. The external access was sealed with four inches of lead during counting operations.

Calibration Techniques

A calibration of the detection and analysis system was required that would define a correlation between analyzer channel number and gamma energy and between the observed count rate and actual sample gamma activity. The multichannel analyzer circuitry did not possess linearity across its entire spectral response and was subject to drift during the course of an extended counting program. The cylindrical sample presented a unique geometry factor not readily amenable to mathematical calculation and determinable only through an experimental analysis.

A set of small, disc, gamma spectrometer sources produced by Tracerlab Inc. was available in the laboratory. A composite standard was required that would provide identifiable peaks at intermittent points throughout the entire energy spectra of the aerosol sample. A set of

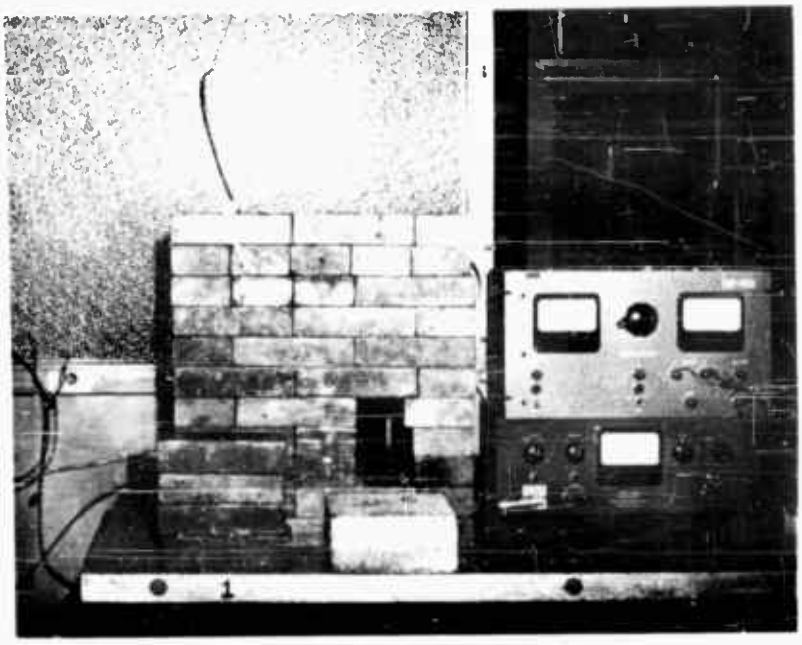

Fig. 10

Detection Facility

The cubical Pb shield portrayed here has 4" thick walls, base, and top and a 12" x 12" x 14" internal cavity. Access to the internal cylindrical shield is provided through a port in the lower right corner of the external shield. This port is closed during counting operations by four lead bricks (1). The scintillation crystal and photomultiplier tube is fixed in position above a sample rack in the internal cylindrical shield. The power supplies provide dynode potentials for the photomultiplier tube and power for the White Cathode Follower (2).

Fig. 11

Cylindrical Detection Shield

This detection shield is identical to the internal shield used in this study except that the door was hung from the left side.

four standard sources -- Co^{60}, Cs^{137}, Ba^{133}, and Na^{22} -- was chosen that would provide this spectral response. The sources were counted separately, their spectra was plotted on four-cycle-semi-log paper, and their respective photopeaks identified (see pages 84-87 Appendix A) from energy values presented in the Scintillation Spectrometry Gamma-Ray Spectrum Catalogue (Ref 10). A composite sample was then formed by stacking these disc sources on a sample holder with the most active source on the bottom and the sample was taped in place. The composite sample was counted, the spectrum plotted, and the photopeaks identified (see page 83 Appendix A) to provide a spectral standard for future analyzer-channel-number/gamma-energy correlations. A calibration count of this composite standard was taken before and after all subsequent sample analyses to provide a spectral calibration and identify any analyzer drift.

A correlation was required between the observed count rate and the actual sample disintegration activity. A knowledge of the sample activity could be related to the activity present in the atmosphere through a knowledge of the volume of air sampled. While the total absolute counting efficiency for a given size NaI(Tl) scintillation crystal is known for a point source located on the axis of and at a known distance from the face of the crystal (Ref 10:app. 1), no such calibration factor is available for a cylindrical geometry. An experimentally determined calibration factor was obtained (see Appendix B) by homogeneously distributing a measured activity of Co^{60} throughout a cylindrical configuration of the same size and composition as the collected particulate samples. An identical volume of the same Co^{60} solution was deposited as a point source on a polystyrene film in a source holder. Comparitive determinations were made between the measured activity of the cylindrical

source and the point source and this determination, in conjunction with the reported absolute counting efficiency of the point source (Ref 10: app. 1) provided a measure of the overall absolute counting efficiency of the cylindrical sample. Subsequent samples were prepared as nearly as possible to this standard dimenaion to preserve the accuracy of this correlation factor.

Sample Analysis Techniques

A valid sampling and analysis program would require that the sample collections and sample analyses be conducted at regularly scheduled intervals and that external parameters be maintained constant to insure integrity of the analytical results. The frequency of the collection and inspection intervals should be determined by the observed time rate of change of the sample activity. The external collection and analysis parameters, i.e., collection times, potentials, and air flow rates and analysis amplification and length of count, should be established to provide a clearly analyzable and statistically reliable analysis spectra. Any deviation from this established schedule should be noted in the analytical evaluation.

The analysis program in this study was used to test the separate collection techniques and proof-test the completed system and was conducted concurrently with the developmental study. Collection and analysis intervals were determined largely by developmental progress and external parameters were varied as the experimental technique was developed. The samples studied during this developmental stage provided clear spectra for qualitative analysis and reflect the effect of improvements and are retained for this purpose.

The initial analysis program called for a sample to be collected at the start of every week and a primary count taken immediately after col-

lection. All samplea were to be counted weekly at the end of the week. Samples were to be collected for aix hours and counted for ten minutea and each counting aesaion was to contain a ten minute initial and final background count and a ten minute spectral calibration count. The net results of each count was to be plotted on five-cycle-semi-log paper, K-E No. 359-91LG, and an analyzer-channel/gamma-energy correlation noted from the standard calibration count. The net integral count rate from the primary count was to be divided by the measured volume of air sampled to provide a measure of the atmospheric activity in disintegrations per minute per cubic meter of air. The cumulative spectra from each sample were to be studied by spectral and decay rate analysis to identify the sample nuclide content.

Deviations from this eatablished program occurred during the developmental phase and during periods of inclement weather. Rain and snowfall caused excessive arcing in the charging section and precluded collection. Changes in this program were also made based upon additional experience in analytical technique. The ten-minute count did not permit spectral resolution of the low-count-rate gamma energies and a one hundred minute counting period was chosen. This resulted in an excessive counting time aa samples were accumulated and, since the observed decay rates did not warrant this counting frequency, the individual samples were counted less frequently. Experience showed that a linear amplifier coarse gain setting of 1/4 and a fine gain setting of 100 provided the best spectral portrayal. Spectral studies were made intermittently at a gain setting of 1/2 and 1 to expand the spectra by a factor of two and four respectively and permit a more detailed inspection of the low energy spectra. The lower discriminator of the multi-channel analyzer was set to make a zero gamma energy correspond to channel number

two to insure that the lowest energies were recorded. The upper discriminator was set at its maximum value to preclude discrimination against the highest energies. The energies of the separate spectral peaks were defined by the channel/energy calibration and the nuclides corresponding to these separate gamma energies identified through comparison with established nuclide spectral tabulations (Ref 10).

Reference to the decay scheme of the natural radioactive decay series will show that the effective half-lives of these decay products is less than twelve hours (Ref 20:206-209, 2:23, 27). This would mean that the spectra observed in this analysis would be due to the long-lived decay products of nuclear fission. A percentile tabulation of significant fission products (Ref 1, 3, 4, 7, 10, 14, 23) along with an analysis of their separate decay schemes (Ref 13, 23) provided a possible listing of isotopes that might be present. A knowledge of the time schedule of past nuclear detonations provided an aid in the decay scheme analysis by identifying the length of time the fission products have been decaying.

Summary

An extended collection and analysis program was conducted to proof-test the electrostatic collection technique and provide an analyais of the local airborne radiological contamination. Scintillation spectrometry was chosen as the best analytical technique since it combines a qualitative and semi-quantitative analysis capability. Beta analysis would provide a valuable corollary to this type of analysis but the sample configuration did not readily lend itself to beta determination. Successful scintillation spectroscopy is dependent upon an adequate sample activity and detection efficiency and a good spectral resolution. The electrostatic collection technique provided a readily analyzable sample in a reasonable collection period. Detection and analysis design con-

sideration were identified and experimental studies were described. Analyzer-channel-number/gamma-energy calibration and count-rate/sample-activity correlation techniques were described. The data obtained from the extended monitoring program permitted a good qualitative study of the local atmospheric nuclide content and provided a reasonably accurate quantitative definition of the gross fallout count rate. The results of the analysis program clearly points out the potentialities of the electrostatic precipitator as a fallout sample collection technique.

VI. Conclusions

General

The purpose of this thesis has been to discuss the feasibility of electrostatic precipitation as a radioactive fallout sample collection technique. The findings reported in this thesis are the result of a feasibility study that included:

1. a parametric study of theoretical design parameters,
2. design and construction of an experimental model,
3. an experimental determination of an optimum collection and secondary concentration technique, and
4. a gamma spectrographic analysis of the collected samples as a proof-test of the collection technique.

The experimental evidence would indicate that electrostatic precipitation would provide an excellent fallout sampling technique. A summary of the experimental collection results will show that this system will provide a sample having sufficient activity to permit a qualitative nuclide determination as well as a gross quantitative radioactivity determination and that this sample may be accumulated within a practical collection period. A summary of the results of the sample analysis program will provide a proof-test of the capabilities of this collection technique.

Experimental Collection Results

The goal of this study has been to provide a collection system that will provide a sample having sufficient activity to permit a qualitative nuclide determination as well as a gross quantitative radioactivity determination and that will accumulate the necessary sample mass within

a practical collection period. An electrostatic collection system was designed and built using experimentally optimized parameters defined by previous theoretical studies. This system was designed to provide a large collection sensitivity -- the product of collector efficiency times the volume flow rate of air. The minimal impedance to air flow presented by the electrostatic precipitator predicted a possible large increase in collector efficiency over air filter models despite a possible decrease in collector efficiency. Efficiency studies employing a Gelman Air Sampler in the effluent air stream verified the theoretically predicted high efficiencies when collection was accomplished with an air flow rate of 50 m^3/minute, a charging potential of 21KV, a collection potential of 17KV, and an ionization current of 20ma. The net result was a collector sensitivity of essentially 50 m^3/minute. This represents a vast improvement over the air filter collection techniques and permits a much larger sample collection rate capability. A contemporary theoretical study (Ref 42) would indicate that the parameters of this experimental model might be refined and extended to permit an even greater capability.

Since electrostatic collection requires a large collection area, a secondary concentration was required to transform the collected sample into an analyzable geometry. Although a selective solubility fractionation phenomenon created a serious loss of sample that destroyed the validity of any quantitative determination and prohibited the use of the originally envisioned ultrasonic cleaning and subsequent filtration as a sample concentration technique, concentration methods were found that would protect the quantitative validity of the collected sample and provide a readily analyzable sample geometry. The use of a plastic film as a collection surface was studied in an attempt to preclude the secondary

concentration requirement. Compaction studies indicated the desirability of this material but satisfactory collection was not achieved. It is believed that the dielectric properties of this material prohibited neutralization of the collected charges and that a conducting material having the same compaction properties might provide an optimum collecting surface. In the absence of this collection material, it is suggested that the aluminum collection plates be washed clean with a minimum amount of volatile alcohol and this particulate bearing fluid be evaporated to dryness in a plastic bag in a water bath. The plastic bag containing the collected sample could then be compacted to a flat disc/cylinder and counted as a disc sample. The high collection sensitivity and measured air flow of the electrostatic precipitator coupled with this quantitatively reliable concentration technique would provide a readily analyzable sample that would permit a qualitative and quantitative analysis of the airborne radiological burden in a minimum time.

Sample Analysis Results

An extended sample collection and analysis program was conducted concurrently with the experimental development. This program was designed to provide a proof-test of the collection technique as well as an analysis of the local fallout rate. The collected samples provided readily analyzable gamma spectra and a qualitative nuclide determination was possible with all secondary concentration methods. The selective solubility fractionation phenomenon associated with ultrasonic cleaning and filtration was discovered late in the experimental phase of the study and precluded a reliable quantitative analysis of the accumulated data. This discovery also negated a proposed secondary study -- a correlation study of fallout rate as a function of time, meteorological conditions, and seasonal variation.

The results of the qualitative analysis tabulated below portray the capabilities of this collection and analysis technique. While only the qualitative results are shown because of the known error in quantitative data, integral count ratea of each sample were available that could have been related to disintegrations per minute per cubic meter of air through the known total absolute counting rate efficiency (see Appendix B) and known volume of air sampled. This data would indicate an ability to identify radioactive nuclides with rather small airborne concentrations.

Spectral Energy in MEV	Relative Number of Counts per Minute	Nuclide
0.130	250	Ce^{144}
0.199	150	Backscatter
0.233	120	Na^{85}
0.492	120	$Ru^{108}Rh^{108}$
0.568	60	Ba^{140}
0.729	160	Zr^{95}
1.17	8	Co^{60}
1.51	6	Unknown
1.89	4	Y^{88}
2.32	1	Unknown
2.77	0.5	Y^{88}

Summary

This study has shown not only the feasibility of this collection technique but alao the capabilities of this system and its value as an adjunct to the present arsenal of fallout analysis equipment. The improved collection rate capability would not only provide a qualitative as well as a quantitative analysia capability but would also

permit collection and analysis of a fallout sample within a shorter period of time. A contemporary theoretical parametric study (Ref 42) would indicate even greater capabilities with higher air flow rates with possible applications as an airborne sampling device. Development of the thin compactible plastic film as a collection surface would permit periodic or continuous movement of the collection surface through the collector and provide a capability for collecting any desired number of samples at separate altitudes or a continuous monitor of civil defense or reactor facilities. It is highly recommended that this developmental study be continued and that this system be adopted as a fallout sampling technique.

VII. Recommendations for Future Actions

The true value of a fallout sampling device lies in its ability to accumulate particulate samples at the desired rate under all meteorological conditions and in any desired collection environment. The sample should be collected with a minimum of effort and expense and a continuous or intermittent monitoring capability should be provided. In view of the above considerations, the following recommendations of areas for future study are submitted.

1. The experimental optimization of corona currents should be continued. This increased ionization capability achieves increased importance as increased air flow rates are considered.
2. The possibility of collection on a compactible foil should be thoroughly studied. If such a foil is found, it should be incorporated into a dynamic collection system that would allow a periodic advance of the collecting surface through the collection section. This would permit the continuous or periodic monitoring capability desired by sampling networks on the surface of the earth and by upper air sampling systems.
3. A system should be devised to prevent intake and/or condensation of moisture within the charging and collection sections. This moisture seriously detracts from the collection capabilities in that it precludes collection during inclement weather.
4. A study of corona currents in near-vacuum conditions should be made. This parameter might have serious implications in the utilization of this technique in upper air studies.
5. The effect of turbulence on precipitator efficiencies should be experimentally verified. While theoretical studies would

tend to discount the effects of this phenomena (Ref 39), the validity of quantitative determinations would demand verification of all suspected collection criteria.

Bibliography

1. Bolles, R. C., and N. E. Ballou. "Calculated Activities and Abundances of U^{235} Fission Products." Nuclear Science and Engineering, 5:156-185 (1959).

2. Bridgman, C. J. Airborne Radioactivity. M. S. Thesis, North Carolina State College, 1958.

3. DeBolt, H. E. "How Radiation Monitor Guards Nuclear Navy." Electronics, 33:43-45 (January 22, 1960).

4. Diamond, H., et al. "Heavy Isotope Abundance in Mike Thermonuclear Device." Physical Review, Volume 119, 14:2000-2004 (September 15, 1960).

5. D, Giovanni, H. J., et al. Feasibility Study of an Electrostatic Stratospheric Dust Sampler. Report No. NYO 2367. Mt. Vernon, New York: Del Electronics Corporation, December 15, 1958.

6. Fields, P. R., et al. "Transplutonium Elements in Thermonuclear Test Debris." Physical Review, Volume 102, 1:180-182 (April 1, 1956).

7. Friend, J. P., et al. The High Altitude Sampling Program. 5 volumes. Report No. DASA 1300. Prepared for Defense Atomic Support Agency, Washington 25, D.C. by Isotopes, Inc., Westwood, New Jersey, August 31, 1961.

8. Ghiorse, A., et al. "New Elements Einsteinium and Fermium, Atomic Numbers 99 and 100." Physical Review, Volume 99, 3:1048-1049 (August 1, 1955).

9. Hardy, E. P. Jr., et al. Fallout Program Quarterly Summary Report, June 1 through Sept 1, 1960. Report No. HASL 95. New York: Analytical Division, Health and Safety Laboratory, United States Atomic Energy Division, October 1, 1960.

10. Heath, R. L. Scintillation Spectrometry Gamma-Ray Spectrum Catalogue. Idaho Falls, Idaho: Phillips Petroleum Co., Atomic Energy Division, July 1957.

11. Hewitt, G. W. "The Charging of Small Particulates for Electrostatic Precipitation." Transactions: American Institute of Electrical Engineers, Communications and Electronics - Part 1, 76: 300-306 (July 1957).

12. Holland, J. Z. Stratospheric Radioactivity, Data Obtained By Balloon Sampling. Report No. TID 5555. Wash. 25, D.C.: Environmental Sciences Branch, Division of Biology and Medicine, U.S. A.E.C., May, 1959.

13. Hollander, et al. "Tables of Isotopes." Reviews of Modern Physics, Volume 25, 2:469-651 (April 1953).

14. Huizenga, J. R., and H. Diamond. "Spontaneous Fission Half-Lives of Cf^{254} and Cm^{250}." Physical Review, Volume 107, 4:1087-1090 (August 15, 1957).

15. Jordan, H. S. Radiation Measurement of the Effluent From The KIWI-A Series of Reactors. Report No. TID 4500. Washington 25, D.C.: Los Alamos Scientific Laboratory of the University of California, June 29, 1961.

16. Junge, C. E. "Atmospheric Chemistry." Advances in Geophysics, 4. New York: Academic Press Inc., 1958.

17. -----. "Natural Aerosols and Nuclear Debris Studies - Progress Report 1." GRD Research Notes 8. Report No. AFCRC - TN - 58 - 692. Bedford, Mass: Air Force Cambridge Research Center, September 1958.

18. -----. "Natural Aerosols and Nuclear Debris Studies - Progress Report II. "GRD Research Notes 24. Report No. AFCRC - TN - 59 - 627. Bedford, Mass: Air Force Cambridge Research Center, November 1959.

19. Kalkstein, M. I., et al. Natural Aerosols and Nuclear Debris Studies, Progress Report No. 2, Report of Progress on Air Force Project 7690 and Atomic Energy Commission Contract AT (49-7)-1431. Report No. AFCRC-TN-59-627. Bedford, Mass. November, 1959.

20. Kaplan, Irving. Nuclear Physics (4th printing). Reading, Mass: Addison-Wesley Publishing Co. Inc., July, 1958.

21. Kawaski, K., and K. Kato. "Size Distribution of Radioactivity of the Natural Radioactive Dust." Journal of the Physical Society of Japan, 14:234-235 (1959).

22. Kennard, E. H. Kinetic Theory of Gases. New York: McGraw-Hill Book Co. Inc., 1938.

23. Kinsman, Simon. Radiological Health Handbook. Cincinnati, Ohio: U.S. Department of Health, Education and Welfare, Public Health Service, Bureau of State Services, Division of Sanitary Engineering Services, Robert A. Taft Sanitary Engineering Center, January, 1957.

24. Klement, Alfred W. Jr. Radioactive Fallout From Nuclear Detonation of February and April 1960. Report No. TID 6235. Washington 25, D.C.: Fallout Studies Branch, Division of Biology and Medicine, U.S. Atomic Energy Commission, 1961.

25. -----. Review of Potential Radionuclides Produced in Weapons Detonations. Report No. WASH 1024. Washington 25, D.C.: Division of Biology and Medicine, U.S. Atomic Energy Commission, July 30, 1959.

26. Lamberson, D. L. A Study of the Electrostatic Precipitation of Radioactive Aerosols. M. S. Thesis, Air Force Institute of Technology, 1961.

27. Meek, J. M., and J. D. Craggs. Electrical Breakdown of Gases. Oxford Clarendon Press, 1953.

28. Miller, W. F. and W. J. Snow. "Design Calculations for NaI Systems." Review of Scientific Instruments, 34:905-907 (August 1960).

29. -----. "Energy Loss Spectra for Gamma Rays in NaI." Review of Scientific Instruments, 31:39-45 (January, 1960).

30. Millipore Filter Corporation. Detection and Analysis of Contamination. Bedford, Mass.: Millipore Filter Corporation, N.D.

31. Mott, W. E. "Scintillation and Cerenkov Counters." Encyclopedia of Physics, Volume XLV, Nuclear Instrumentation II. Berlin-Gottingen-Heidelberg: 1958.

32. Murphy, H. T., et al. "A Theoretical Analysis of the Effects of an Electrical Field on the Charging of Fine Particulates." Transactions: American Institute of Electrical Engineers, Communications and Electronics - Part 1, 78:318-325 (September 1959).

33. Okada, Minoru. "Gamma Spectra of Short-Lived Nuclides." Nucleonics 19:79-81 (September 1961).

34. Peele, R. W., and T. A. Love. "Method for Detecting Non-Proportionality of Response for Gamma Ray Scintillators." Review of Scientific Instruments, 31:205-206 (February 1960).

35. Penney, G. W., and R. E. Matick. "Potential in D.C. Corona Fields." Transactions: American Institute of Electrical Engineers, Communications and Electronics - Part 1, 79:91-99 (May 1960).

36. Perry, John H. (Editor). Chemical Engineers' Handbook (Third Edition). New York: McGraw-Hill Book Co., Inc., 1950.

37. Pope, Alan. Wind-Tunnel Testing (Second Edition). New York: John Wile and Sons, Inc., 1954. (Pages 80-90).

38. Price, William J. Nuclear Radiation Detection. New York: McGraw-Hill Book Co. Inc., 1958.

39. Rose, H. E., and A. H. Wood. An Introduction to Electrostatic Precipitation in Theory and Practice. London: Constable and Co. Ltd., 1956.

40. Rubenstein, M. J. The Determination of Airborne Radioactivity. M. S. Thesis, Air Force Institute of Technology, 1961.

41. Setter, L. R., et al. "Air-Borne Particulate Beta Radioactivity Measurements of the National Air Sampling Network - 1953 - 1959. American Industrial Hygiene Association Journal, Volume 22, 3:192-200 (June 1961).

42. Stuart, R. S. The Analysis, Optimization, and Design of an Airborne Radiation Sampling Electrostatic Precipitator. M. S. Thesis, Air Force Institute of Technology, 1962.

43. Voress, H. E., et al. Radioactive Fallout, Bibliography of Selected Atomic Energy Commission Reports. Report No. TID 3087. Washington 25, D. C.: Office of Technical Information Services, 1960.

44. Vuorinen, Antti P. U. "Effective Background Shield for Low Activity Measurements." Review of Scientific Instruments, 31:573-574 (May 1960).

45. Western Precipitation Corporation. Conceptual Study of Possible Collecting Systems for Use in Stratospheric Sampling. Report No. TID 5971. Los Angeles, Calif.: Western Precipitation Corp., 1961.

46. White, H. J. "Modern Electrical Precipitation." Industrial and Engineering Chemistry, 47:932-939 (May 1955).

47. -----. "Particle Charging in Electrostatic Precipitation." Transactions: American Institute of Electrical Engineers - Part II, 70:1186-1191 (1951).

Appendix A

Data Analysis

This appendix presents a detailed reporting of the sample analysis program. The sample analysis program was conducted concurrently with the colleetion development study. Developmental changes in the collection and analysis techniques are reflected in the sample analysis results and a chronological tabulation of key developmental changes will be required before a valid interpretation of the analytical results is possible. The chronological key will be followed by a complete study of the individual samples and finally by the author's interpretation of the analytical results.

Chronological Key

1 July 61 - 30 Nov 61: Design and construction of electrostatic precipitator and collection facility.

30 Nov 61 - 15 Dec 61: Experimental development of ultrasonic cleaning and fluid filtration concentration technique. Sample No. 1 was discarded because of a four-day separation between collection and concentration with a possihle loss of sample.

15 Dec 61 - 2 Feb 62: Experimental development of analysis facility conducted concurrently with periodic collection program. Calibration standard was prepared, the cylindrical geometry factor was determined and the optimum linear amplifier gain settings and analyzer discriminator settings were established. Experience showed that 100 minute counts were desired for clear spectral portrayal. Sample analysis results obtained prior to this date are not plotted because of variation in

abscissa scale and lack of sufficient detail portrayal provided by originally scheduled 10 minute sample counts.

2 Feb 62 - 12 Mar 62: A concurrent sampling and analysis. The selective solubility fractionation phenomenon was discovered on 26 Feb 62. This discovery defined an error in the quantitative integral count results and precluded an interpretation of the sample activity as a function of time, seasonal changes and meteorological variations. The cylindrical geometry factor is not applied to the integral count results since a quantitative analysis is not possible and the unmodified count rate results show a more valid picture of the observed count rates. Alternate concentration techniques were studied during this period and the results of the individual techniques are portrayed in the sample analysis results.

Data Analysis

The following tabulation is a result of an analysis of the accumulated data. The tabulated values of spectral energy peaks represent an average value of corresponding peaks in the sample spectra. The tabulated value of cpm is intended to portray only relative amplitudes of spectral peaks, i.e., relative nuclide activities, and is not intended to portray an actual evaluation of the specific nuclide activity. The final column represents the author's interpretation of the nuclides responsible for the separate gamma energies. This analysis is based on reported values of nuclide decay gamma energies (Ref 1, 10, 13). Those spectral peaks above 1.51 MEV provided poor resolution because of the low count rate.

Spectral Energy in MEV	Relative Number of Counts per Minute	Nuclide
0.130	250	Ce^{144}
0.199	150	Backscatter
0.233	120	Nb^{95}
0.492	120	$Ru^{106}Rh^{106}$
0.568	60	Ba^{140}
0.729	160	Zr^{95}
1.17	8	Co^{60}
1.51	6	Unknown
1.89	4	Y^{88}
2.32	1	Unknown
2.77	0.5	Y^{88}

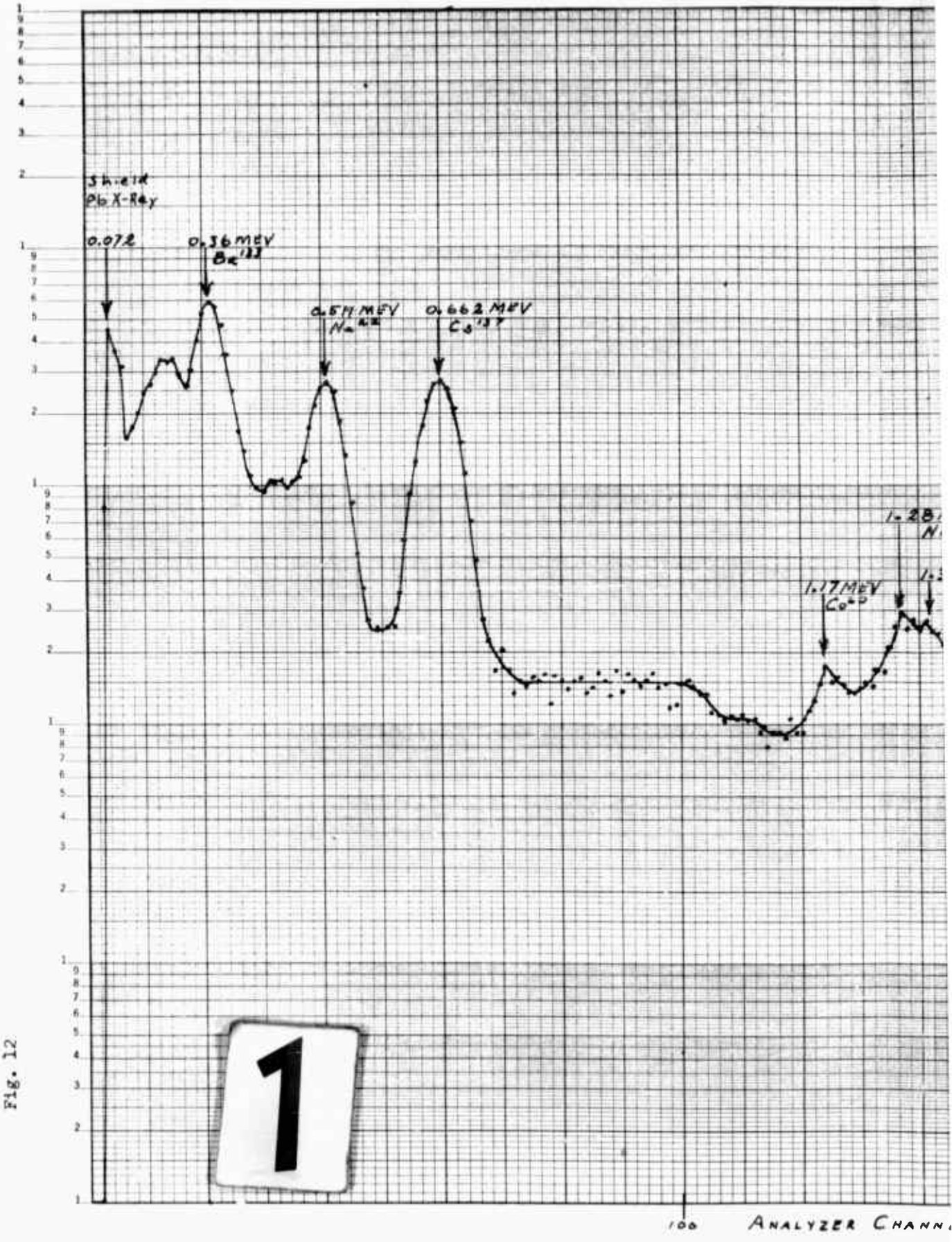
Sh. elt
Pb X-Ray
0.072
0.36 MEV
Ba 133
0.511 MEV
Na 22
0.662 MEV
Cs 137
1.17 MEV
Co 60
1.33
100
ANALYZER CHANN

Fig. 12

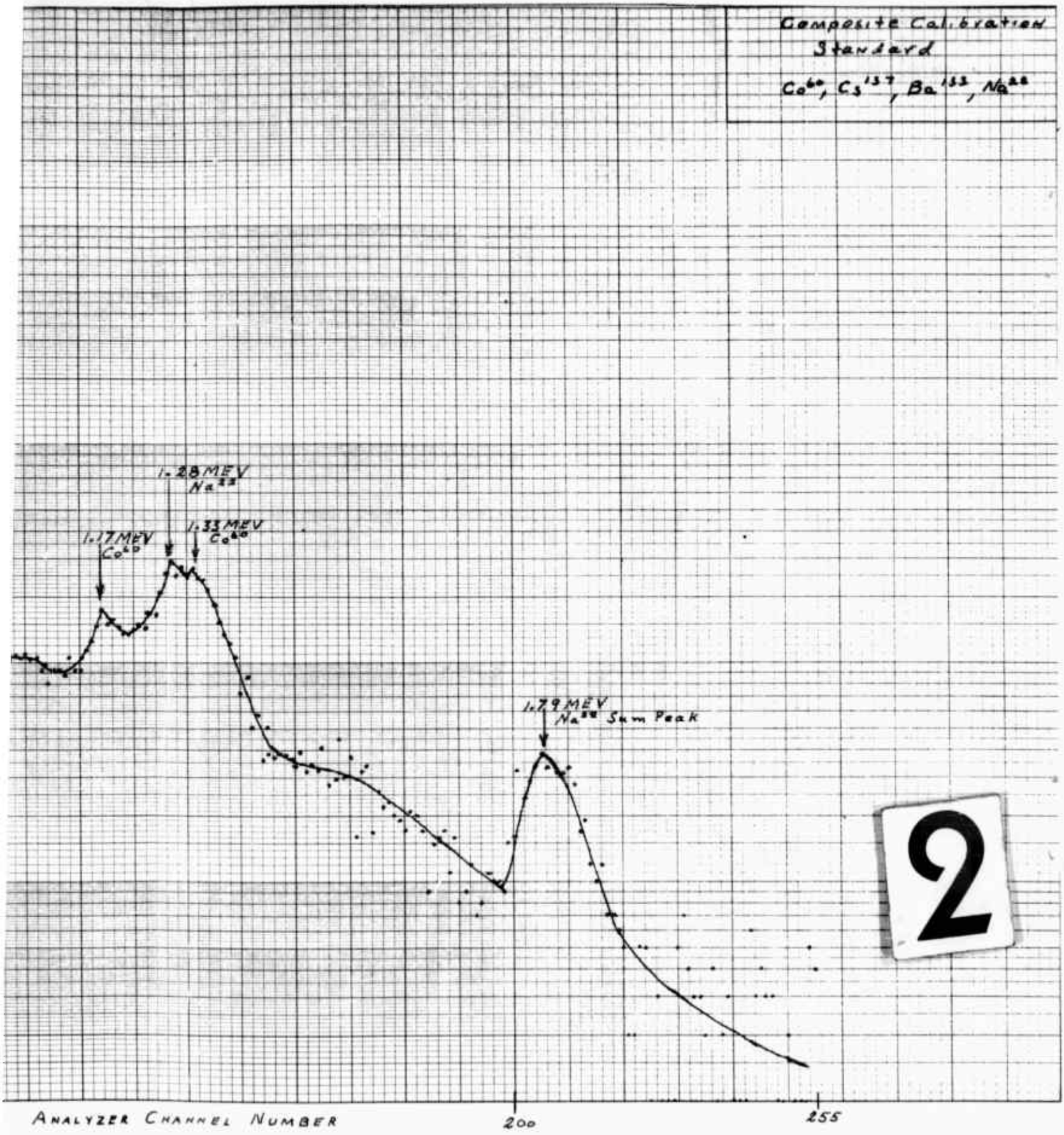
Composite Calibration Standard
Co^{60}, Cs^{137}, Ba^{133}, Na^{22}
1.28 MEV Na^{22}
1.33 MEV Co^{60}
1.17 MEV Co^{60}
1.79 MEV Na^{22} Sum Peak
2
Analyzer Channel Number
200
255

Fig. 12

Calibration Standard
Gain = 1/4

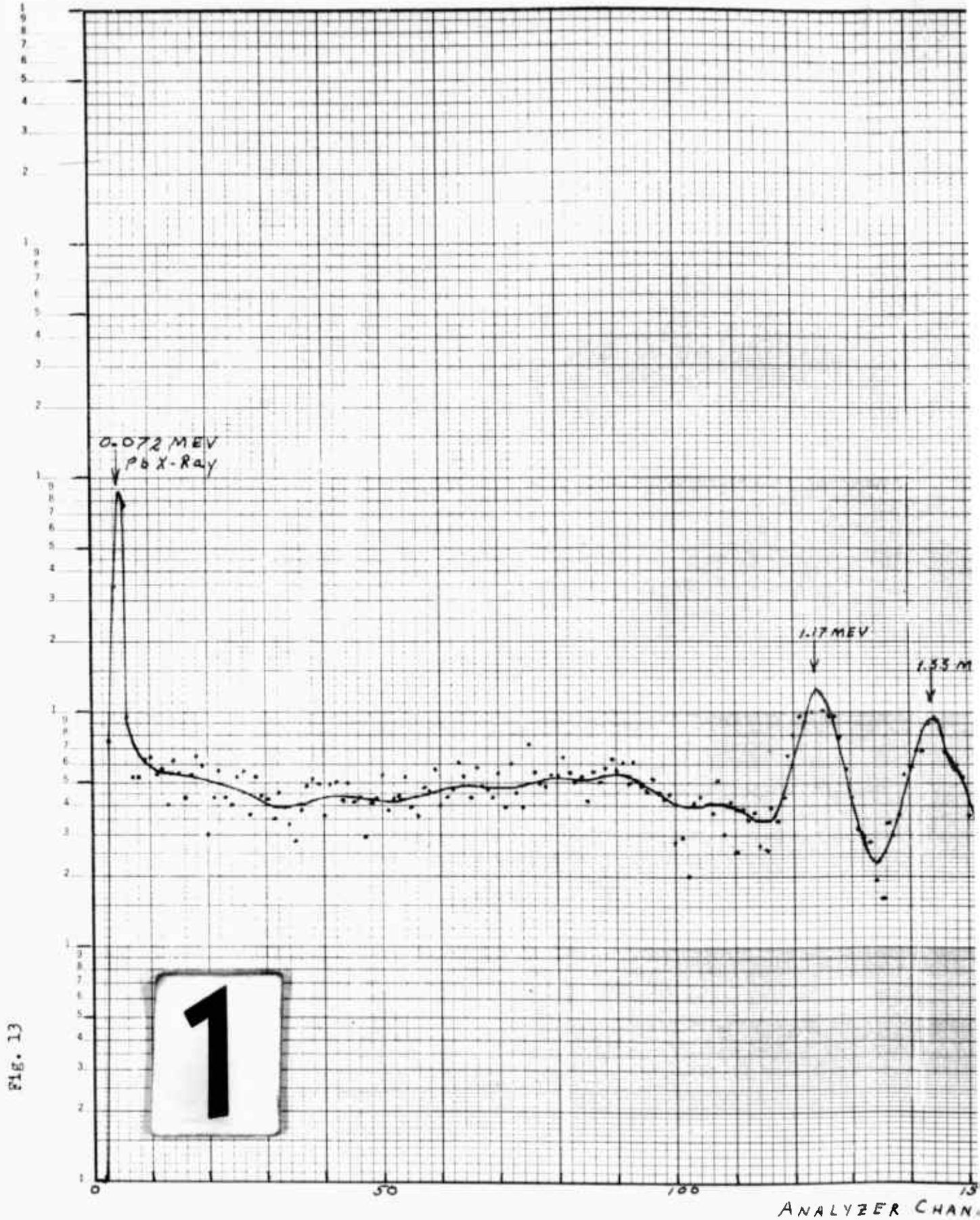

Fig. 13

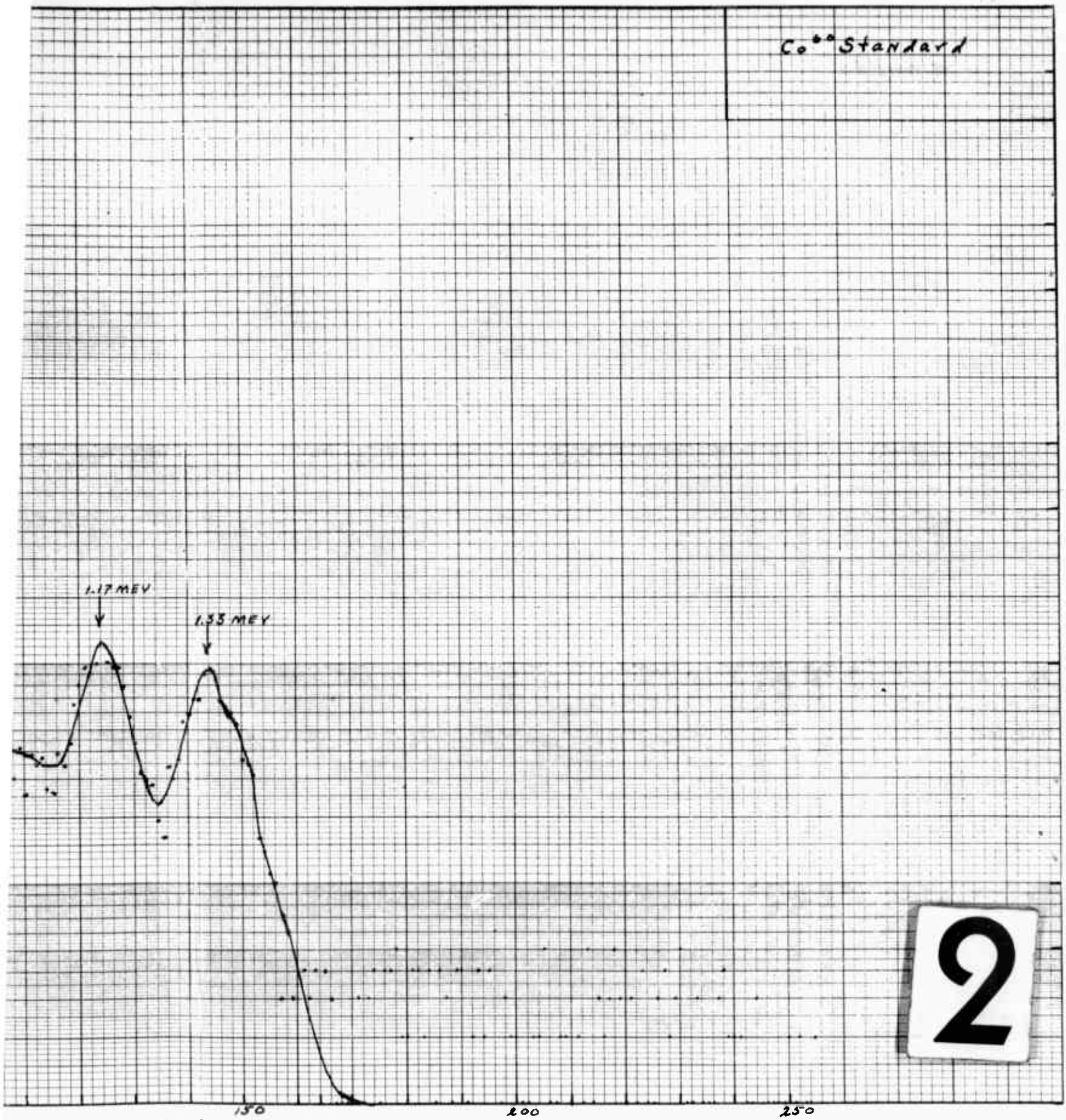
Co⁶⁰ Standard
1.17 MEV
1.33 MEV
150
200
250
ANALYZER CHANNEL NUMBER

2

Fig. 13

Co^{60} Standard

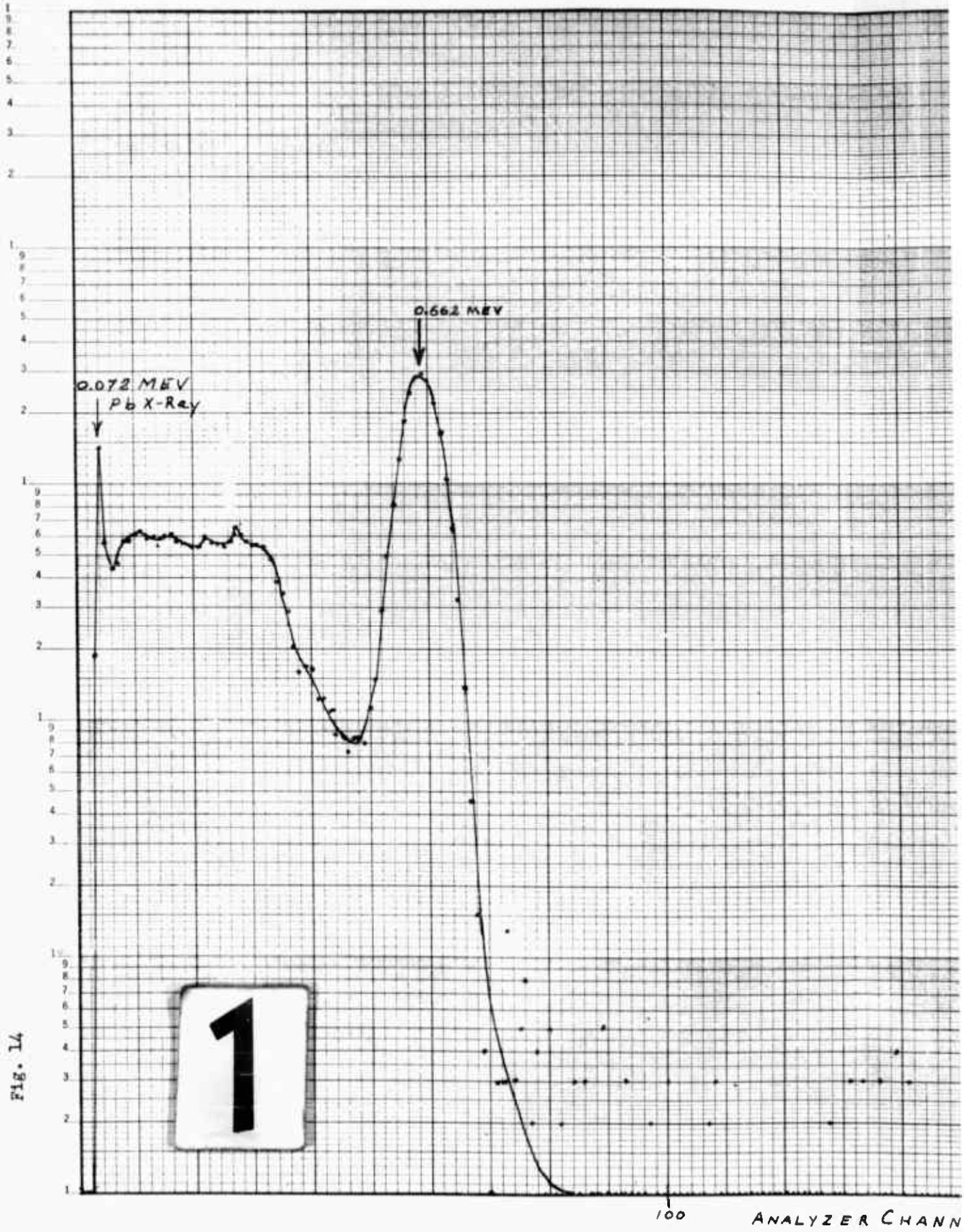

Fig. 14

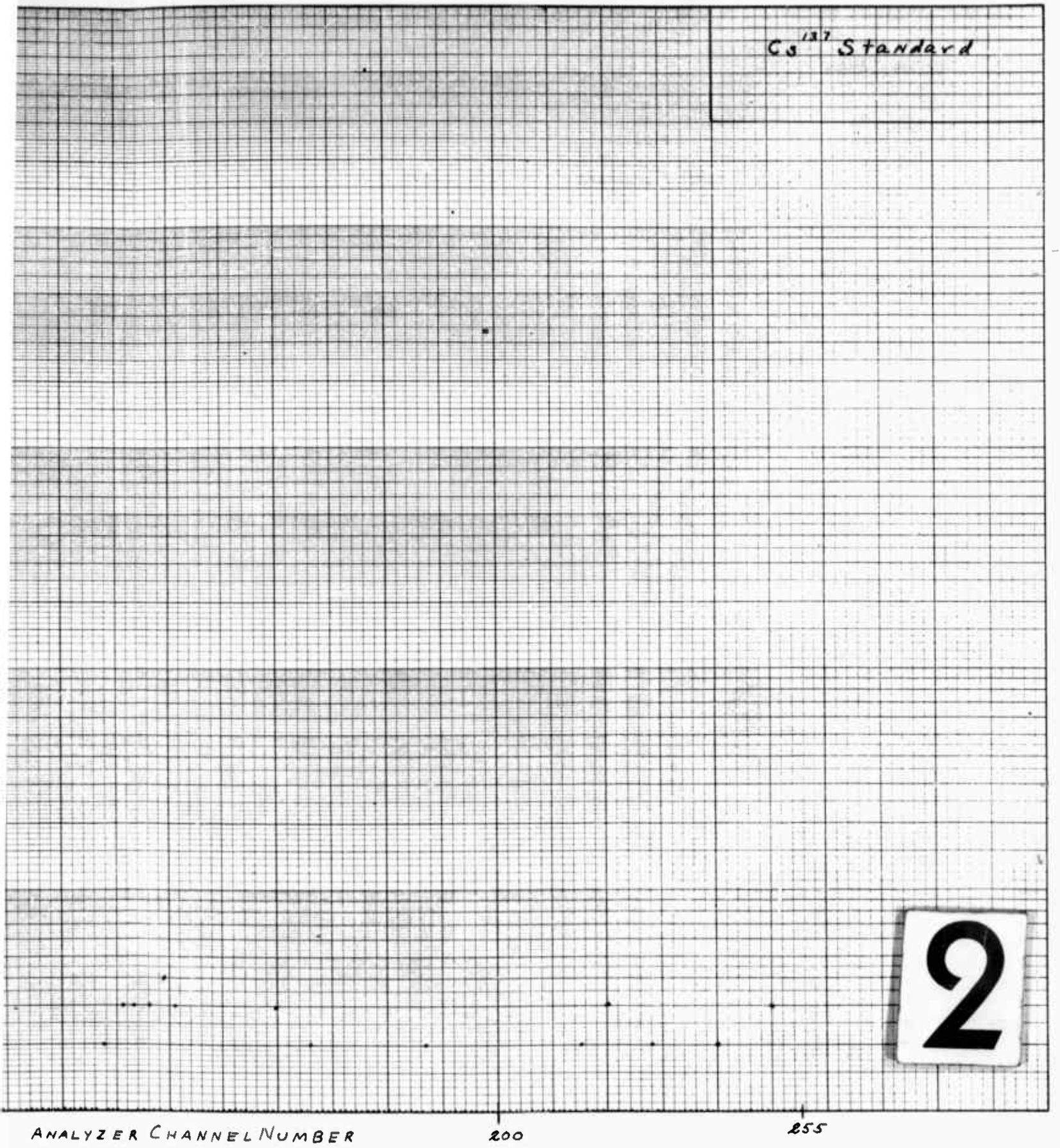
Cs^{137} Standard
2
ANALYZER CHANNEL NUMBER
200
255

Fig. 14

Cs^{137} Standard

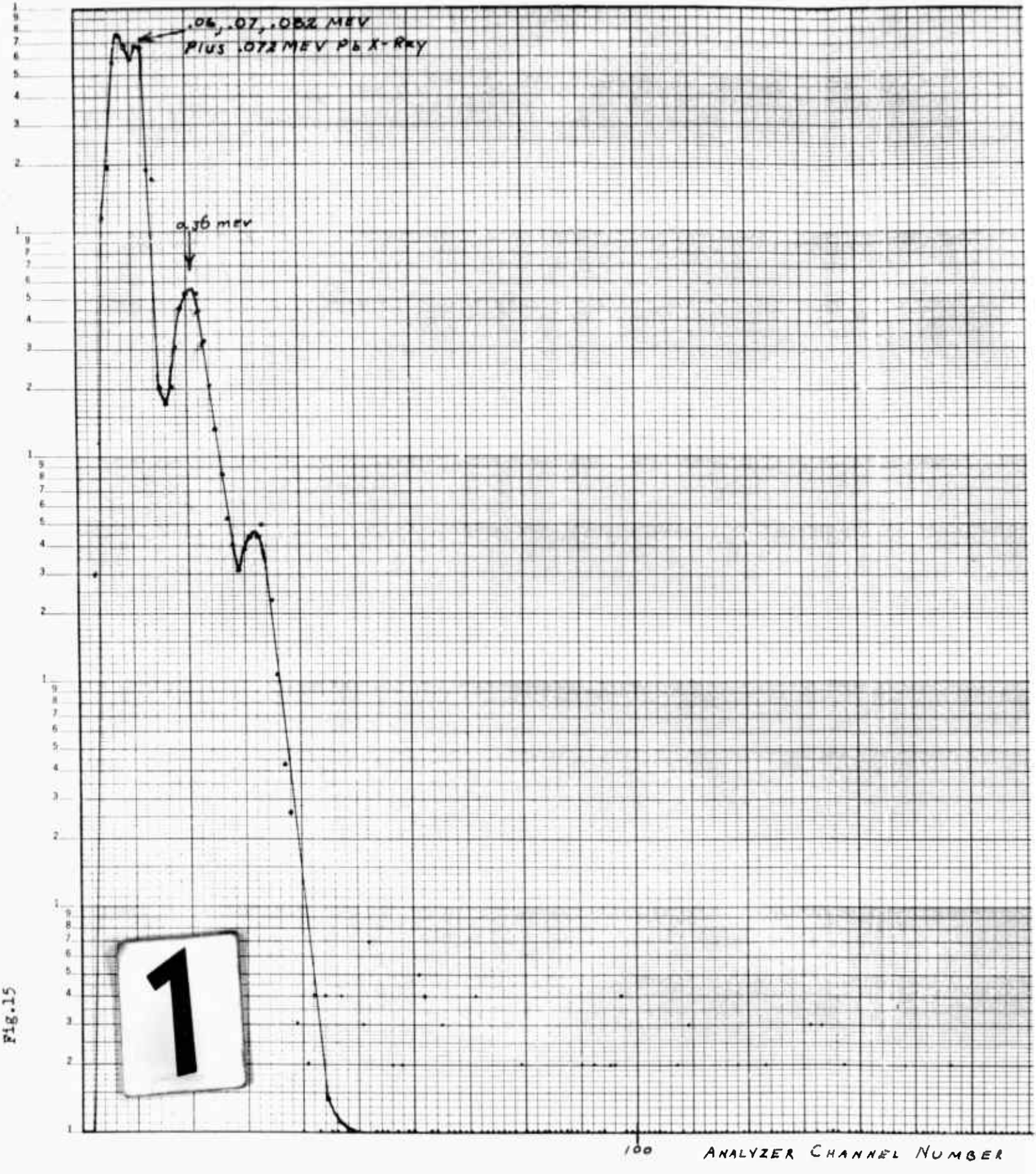
.06, .07, .082 MEV
PLUS .072 MEV Pb X-RAY
0.36 MEV
100
ANALYZER CHANNEL NUMBER

Fig.15

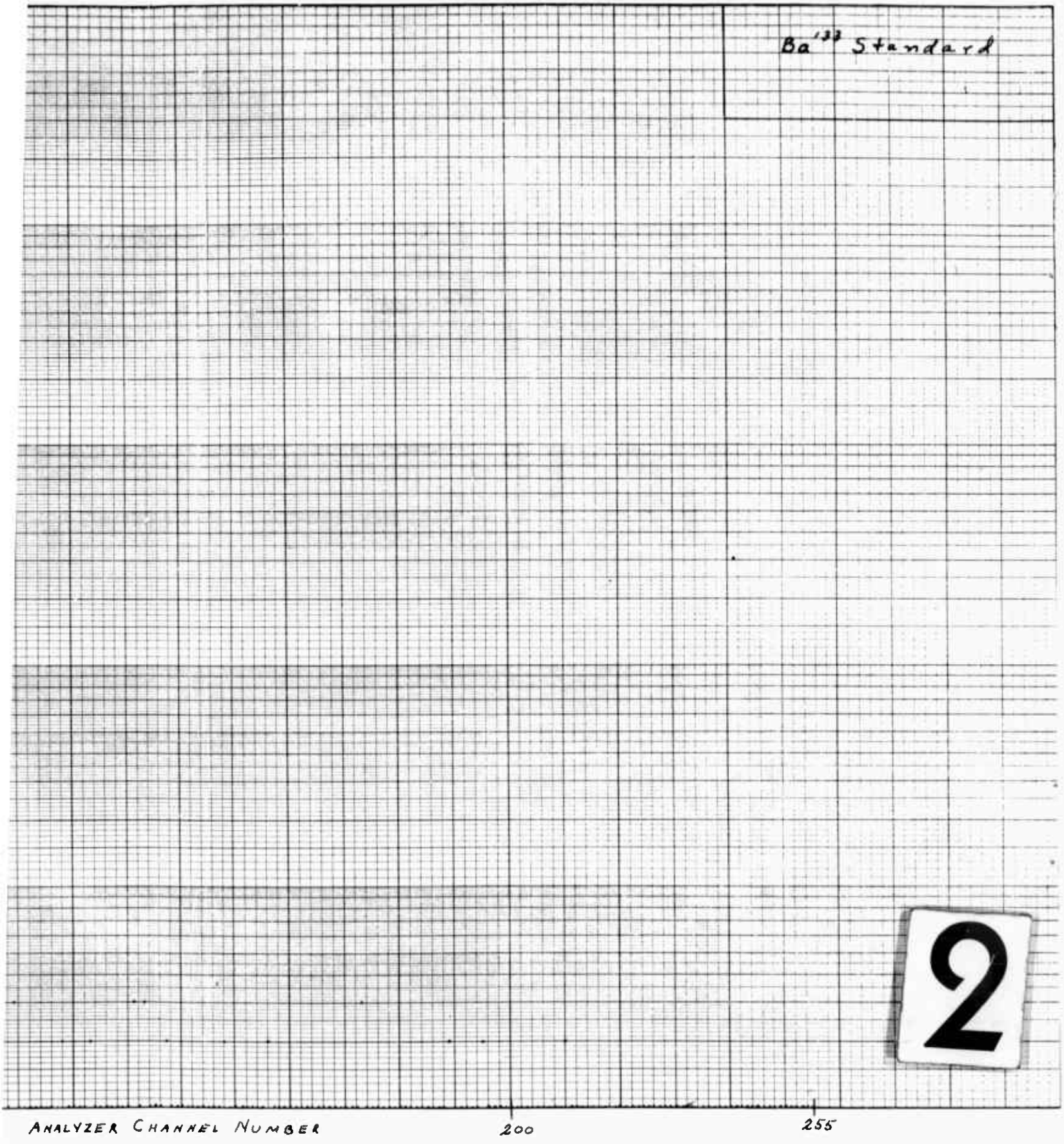
Ba^{133} Standard
2
ANALYZER CHANNEL NUMBER
200
255

Fig. 15

Ba^{133} Standard

Fig. 16

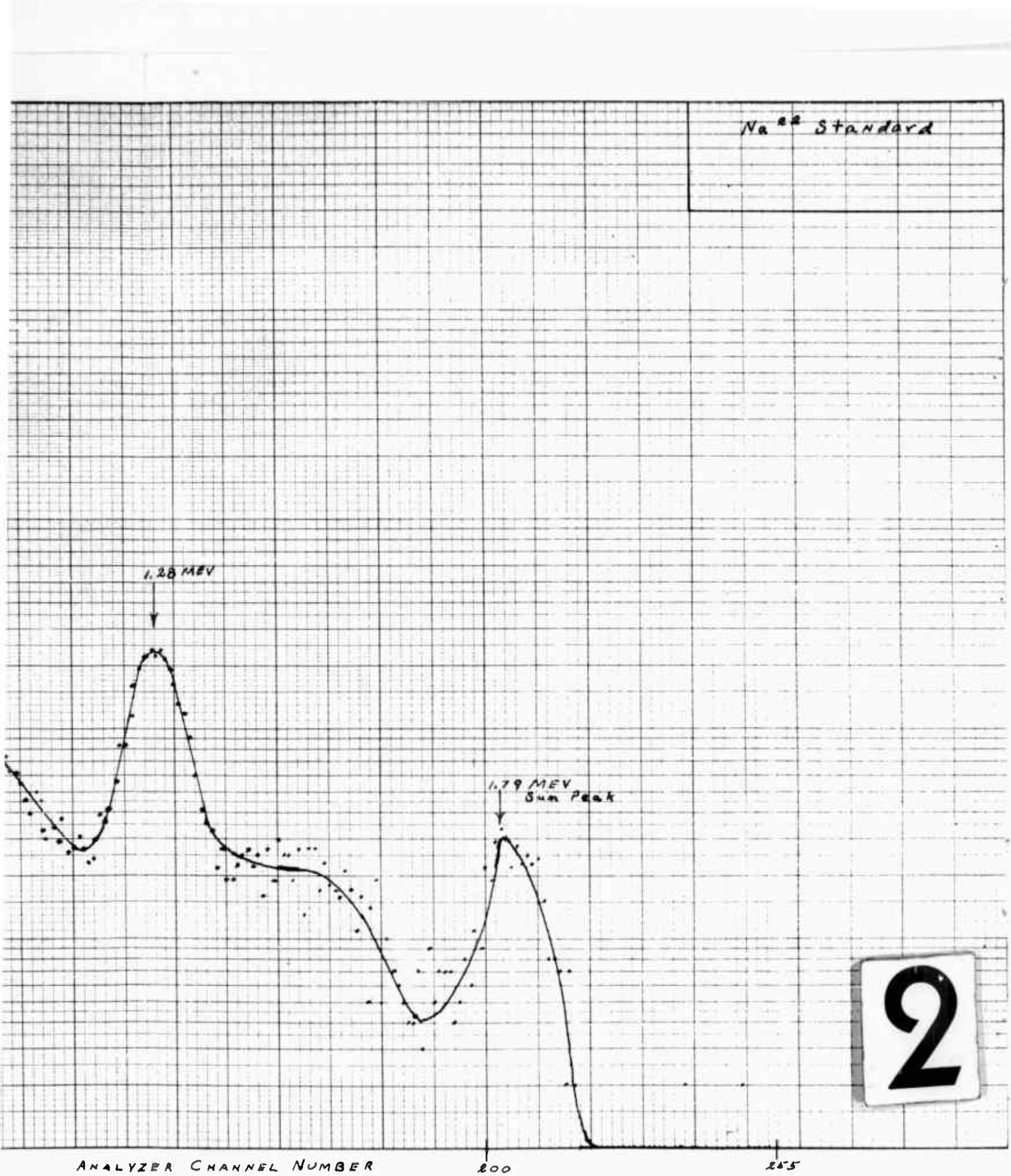
Na 22 Standard
1.28 MEV
1.79 MEV
Sum Peak
2
ANALYZER CHANNEL NUMBER
200
255

Fig. 16

Na^{22} Standard

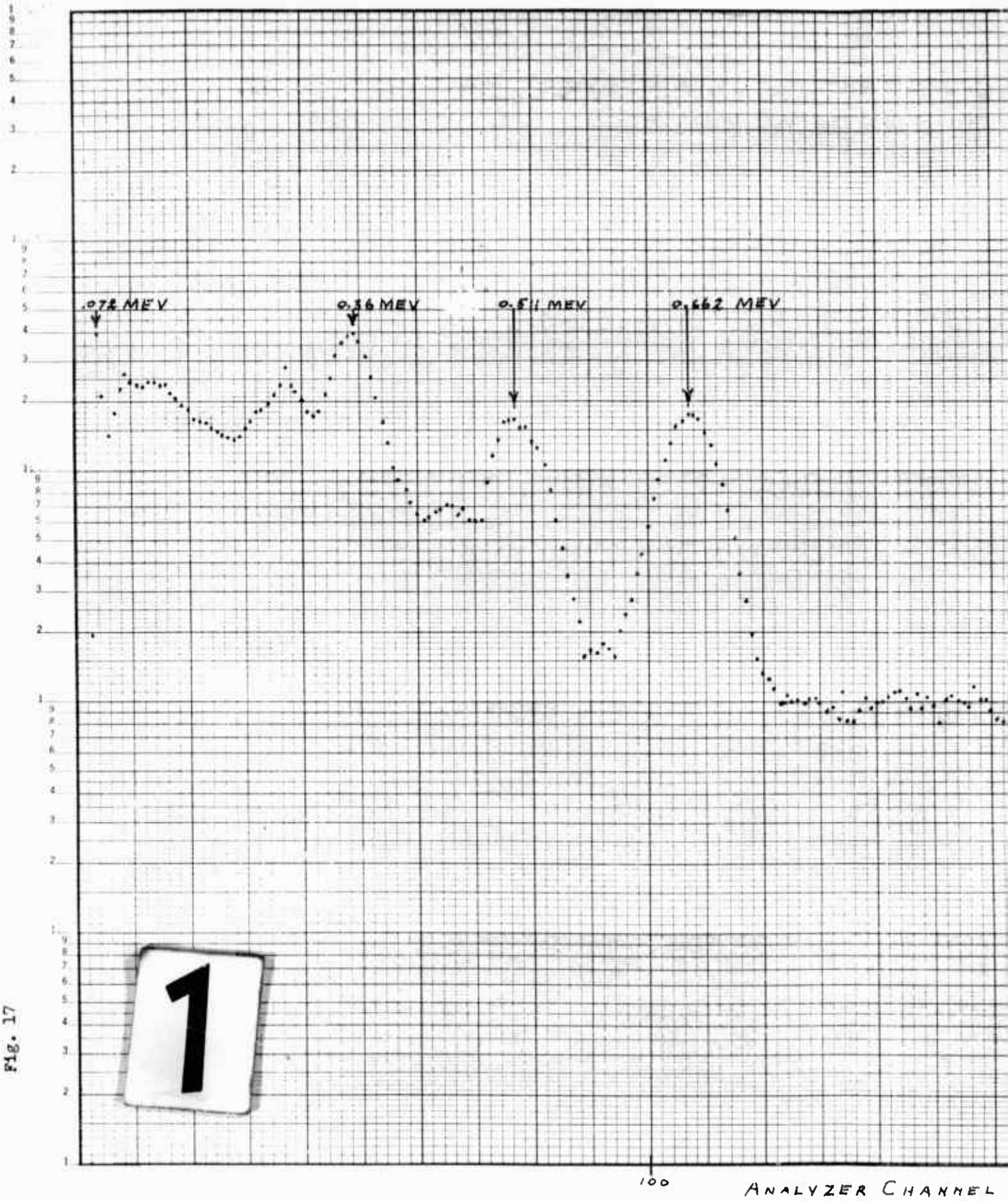

Fig. 17

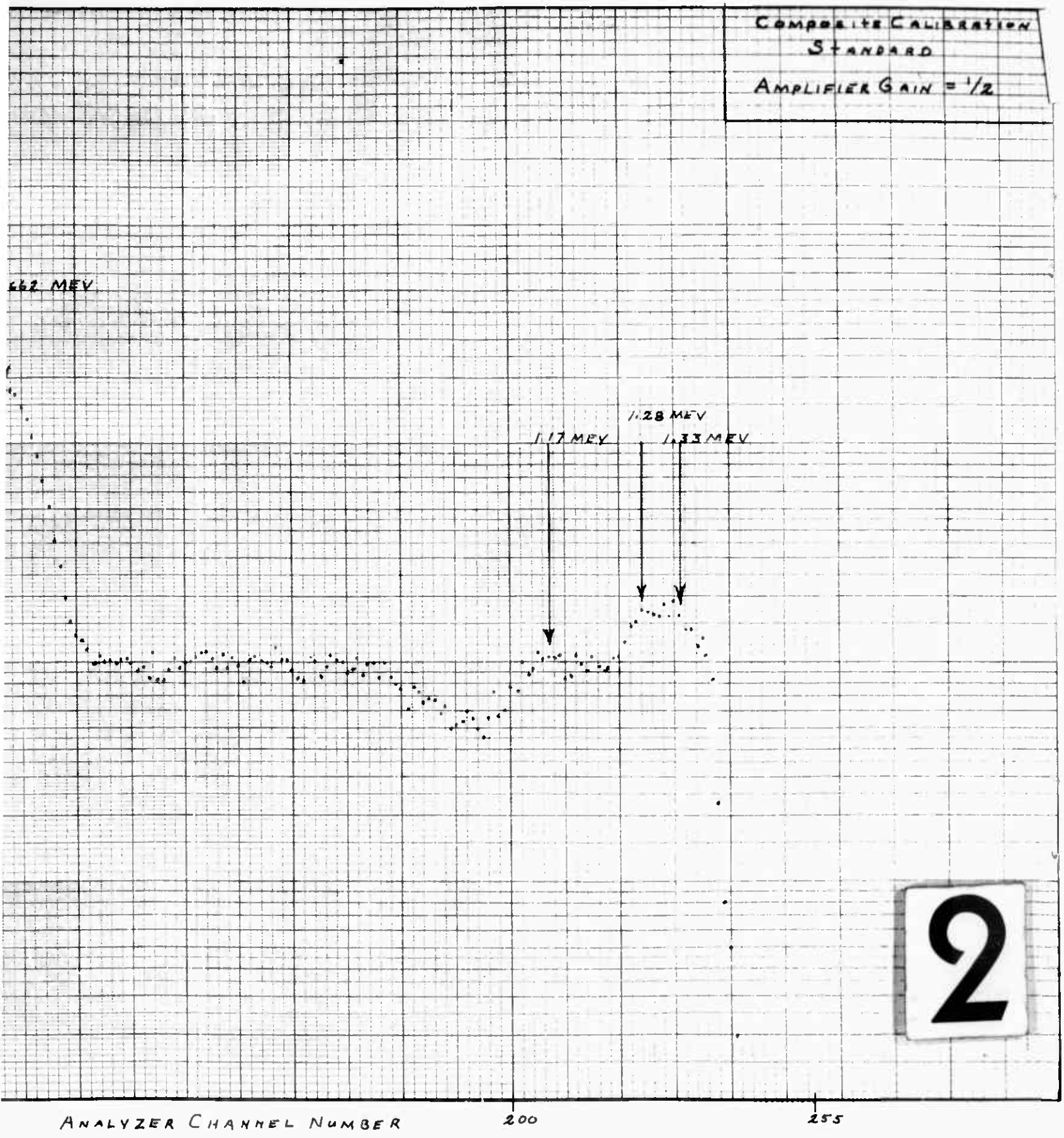
COMPOSITE CALIBRATION
STANDARD
AMPLIFIER GAIN = 1/2
.662 MEV
1.17 MEV
1.28 MEV
1.33 MEV
2
ANALYZER CHANNEL NUMBER
200
255

Fig. 17

Composite Calibration Standard
Gain = 1/2

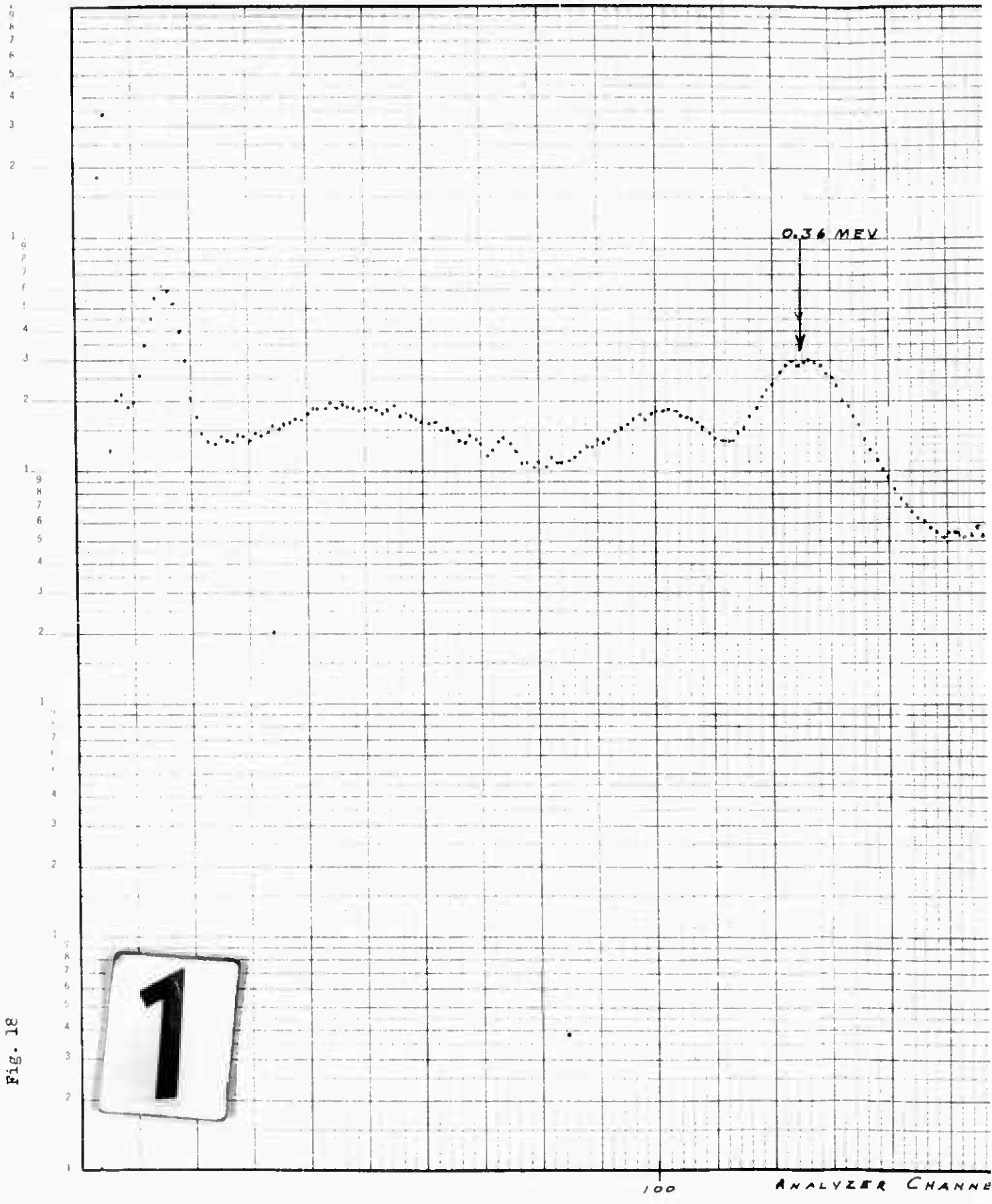

Fig. 18

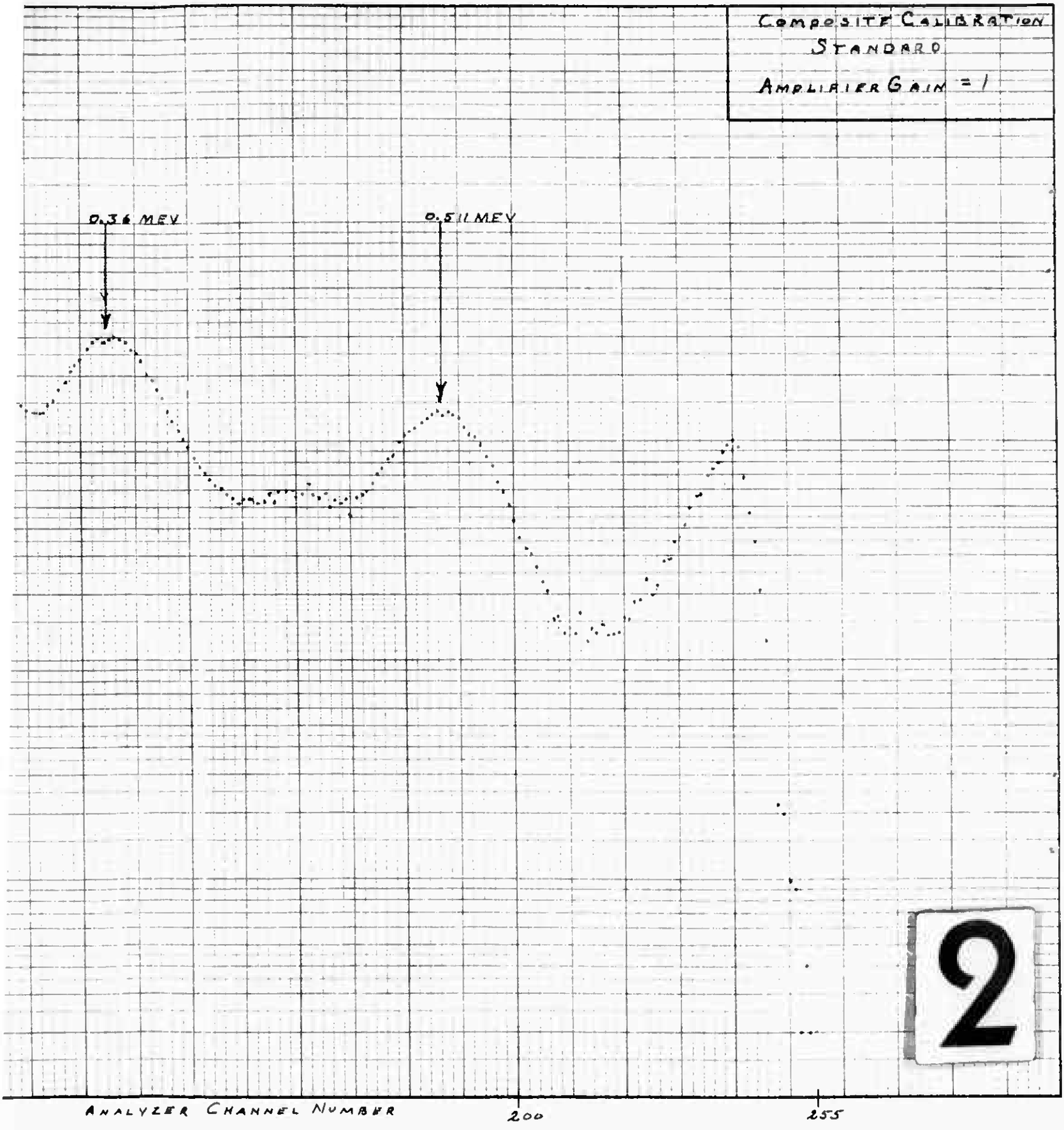
COMPOSITE CALIBRATION
STANDARD
AMPLIFIER GAIN = 1
0.36 MEV
0.511 MEV
2
ANALYZER CHANNEL NUMBER
200
255

Fig. 18

Composite Calibration Standard
Gain = 1

Sample No. 1

Collection Data:

Sample Collected 1348-1648/7Dec 61
Weather: Clear; Temp=35°F.

Charging Potential	23.0KV
Collection Potential	18.1KV
Ionization Current	20.0ma
Volume flow rate of air	49.5 m^3/minute
Collection time	188 minutes
Total air sampled	9,266 m^3

No discoloration of Gelman Air Sampler filter in effluent air stream. The collected sample was left in the electrostatic precipitator while filtration techniques were tested. The collection plates were cleaned in an ultrasonic water bath on 14 Dec 61. The filtered sample was analyzed as an analysis exercise but the length of time between collection and concentration caused some doubt as to the sample validity and the sample was discarded.

GNE/Phys/62-2

Sample No. 2

Collection Data:

Sample collected 0755-1155/15 Dec 61.
Weather: Partly overcast; Temp=20°F; Wind=3 knots SW.

Charging potential	22.8KV
Collection potential	18.2KV
Ionization current	20.0ma
Volume flow rate of air	44.5 m^3/minute
Collection time	240 minutes
Total air sampled	10,690 m^3

No discoloration of Gelman Air Sampler filter in the effluent air stream.

Analysis Data:

This sample was counted repeatedly during the development of the analysis facility. The dissimilarity of the equipment settings, the counting times, and the counting geometry configuration would destroy the validity of the sample results and the results are not portrayed.

GNE/Phys/62-2

Sample No. 3

Collection Data:

Sample collected 0816-1249/26 Dec 61
Weather: Partly cloudy; Temp=25°F; Wind=18 knots from S.W.

Charging potential	21.8KV
Collection potential	17.9KV
Ionization current	20.0ma
Volume flow rate of air	49.5m^3/minute
Collection time	273 minutes
Total air sampled	13,513 m^3

Slight discoloration of Gelman Air Sampler filter in effluent air stream.
Collection plates cleaned in ultrasonic water bath and cleaning fluid filtered through successive filtration to 0.45μ.

Analysis Data:

Date	Integral Count Rate* Counts/min/m^3 of Air	Counting Time	Remarks
26/12/61	0.391	100 min	Amp gain=1/4:85**
27/12/61	0.420	100 min	Amp gain=1/4:85
3/ 1/62	0.255	10 min	Amp gain=1/4:85
3/ 1/62	0.472	10 min	Amp gain=1/2:85
3/ 1/62	0.126	10 min	Amp gain=1/8:85
3/ 1/62	0.244	10 min	Amp gain=1/4:85
26/ 1/62	0.283	10 min	Amp gain=1/4:85
2/ 2/62	0.247	100 min	Amp gain=1/4:100***
9/ 2/62	0.246	100 min	Amp gain=1/4:100
17/ 2/62	0.210	100 min	Amp gain=1/4:100
22/ 2/62	0.190	100 min	Amp gain=1/4:100

* A subsequent discovery of selective solubility fractionation phenomenon would indicate that this count rate is too low.

** This defines a Linear Amplifier goarse gain setting of 1/4 and a fine gain setting of 85. This establishes the energy correlation of the abscissa.

***On 2 Feb 62 a standard amplifier gain setting of 1/4:100, a lower discriminator setting of 260, and a standard counting time of 100 minutes was adopted. Analyses prior to this date are not plotted since an abscissa energy correlation is not presented and shorter counting timea would reflect an erroneous deviation in peak amplitudes. These remarks apply to the subsequent analysis presentations.

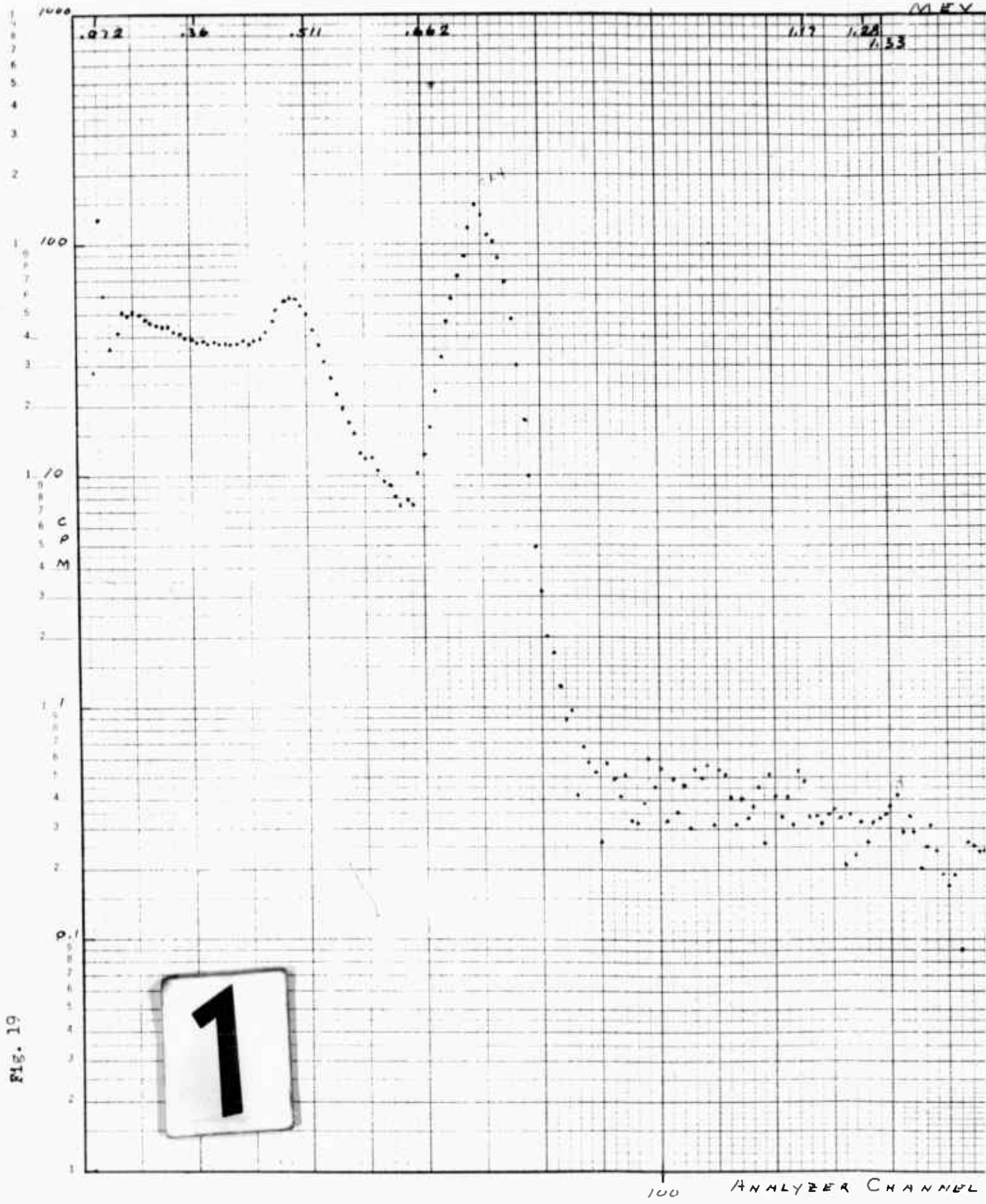
MEV
.022
.36
.511
.662
1.17
1.28
1.33
1000
100
10
1
0.1
CPM
100
ANALYZER CHANNEL

Fig. 19

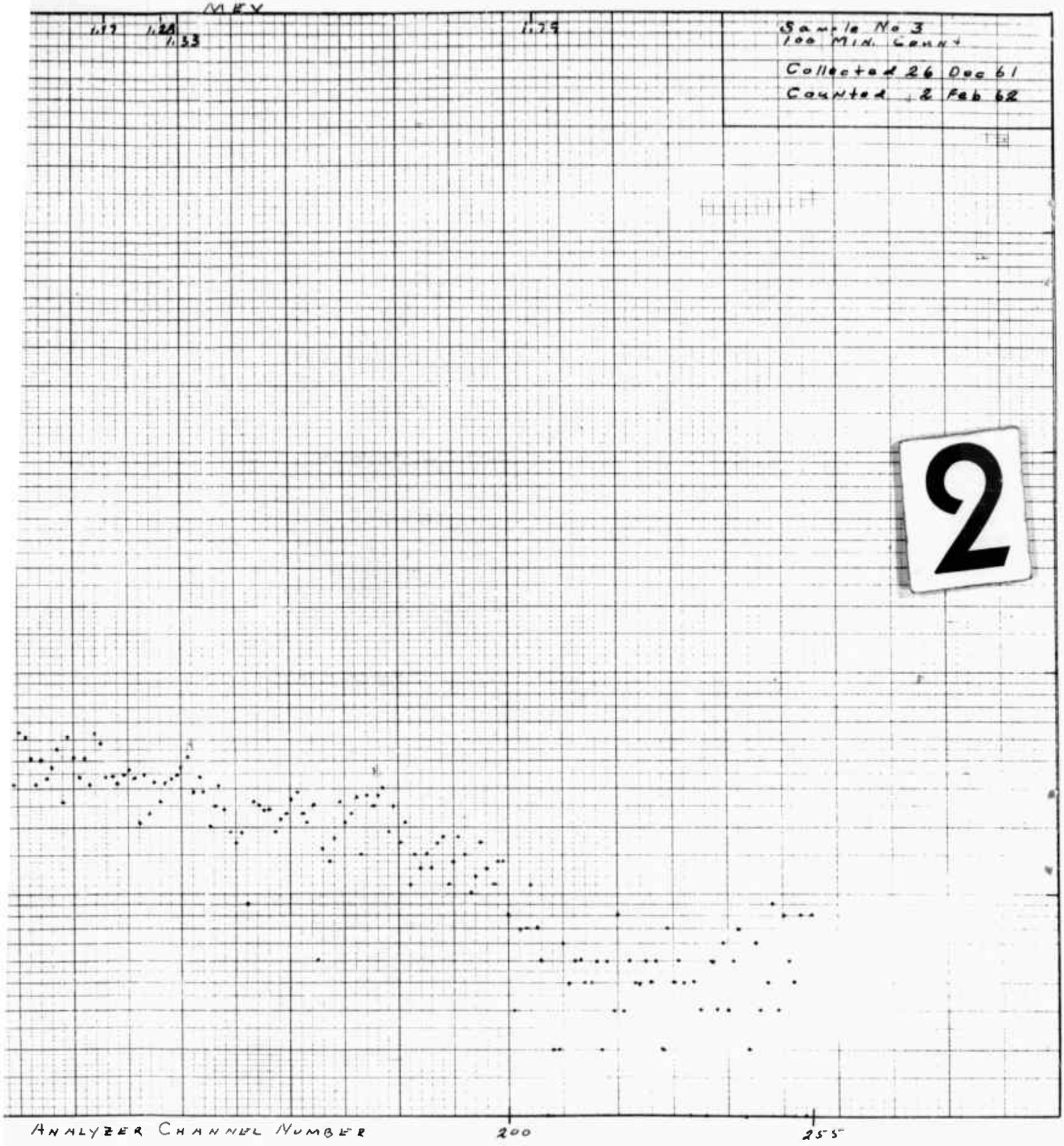
MEV
1.17
1.28
1.33
1.77
Sample No 3
100 MIN. Count
Collected 26 Dec 61
Counted 2 Feb 62
2
ANALYZER CHANNEL NUMBER
200
255

Fig. 19

Sample No. 3
100 Min Count
Collected 26 Dec 61
Counted 2 Feb 62

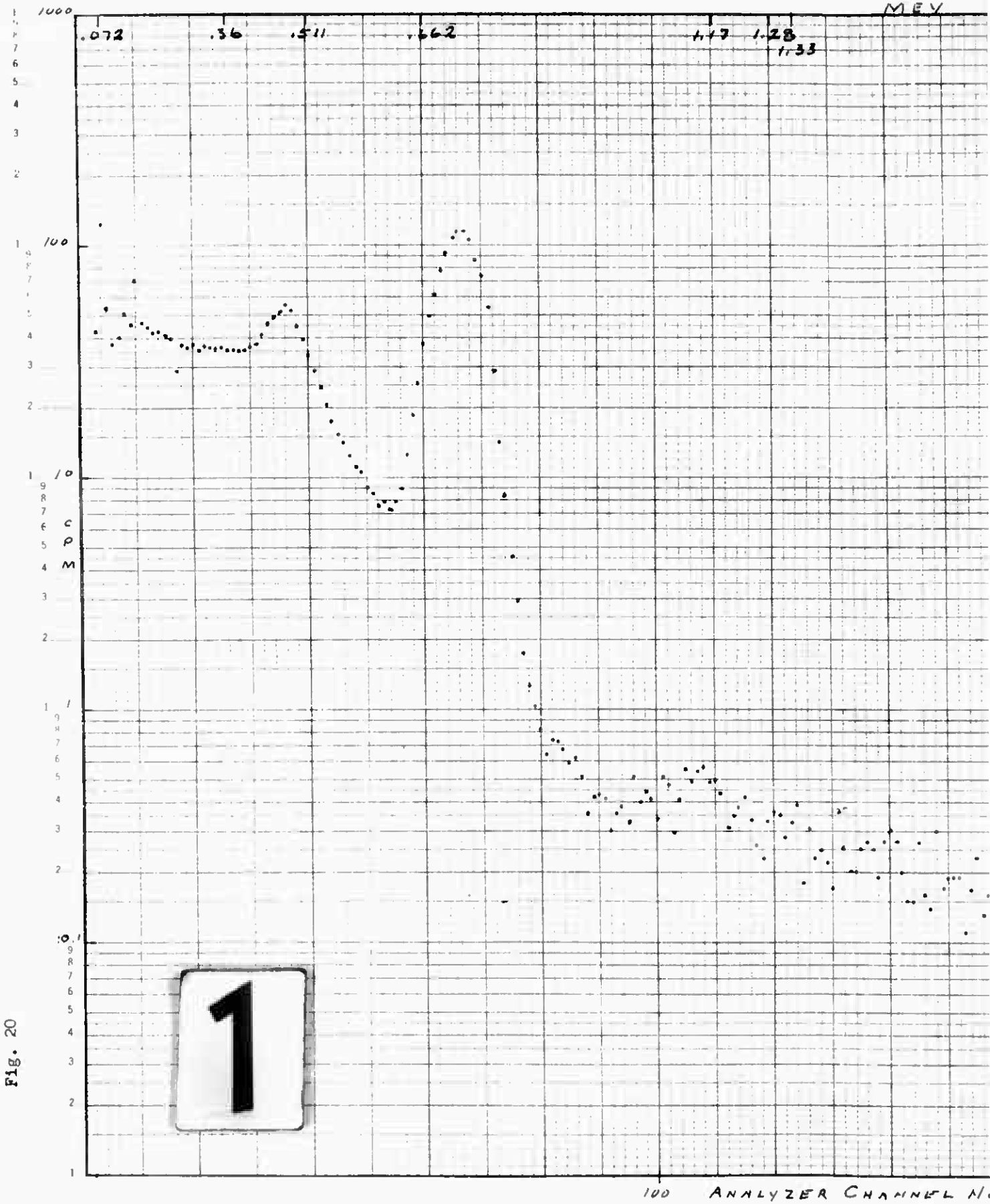
MEV
.072
.36
.511
.662
1.17
1.28
1.33
1000
100
10
1
CPM
100
ANALYZER CHANNEL N

Fig. 20

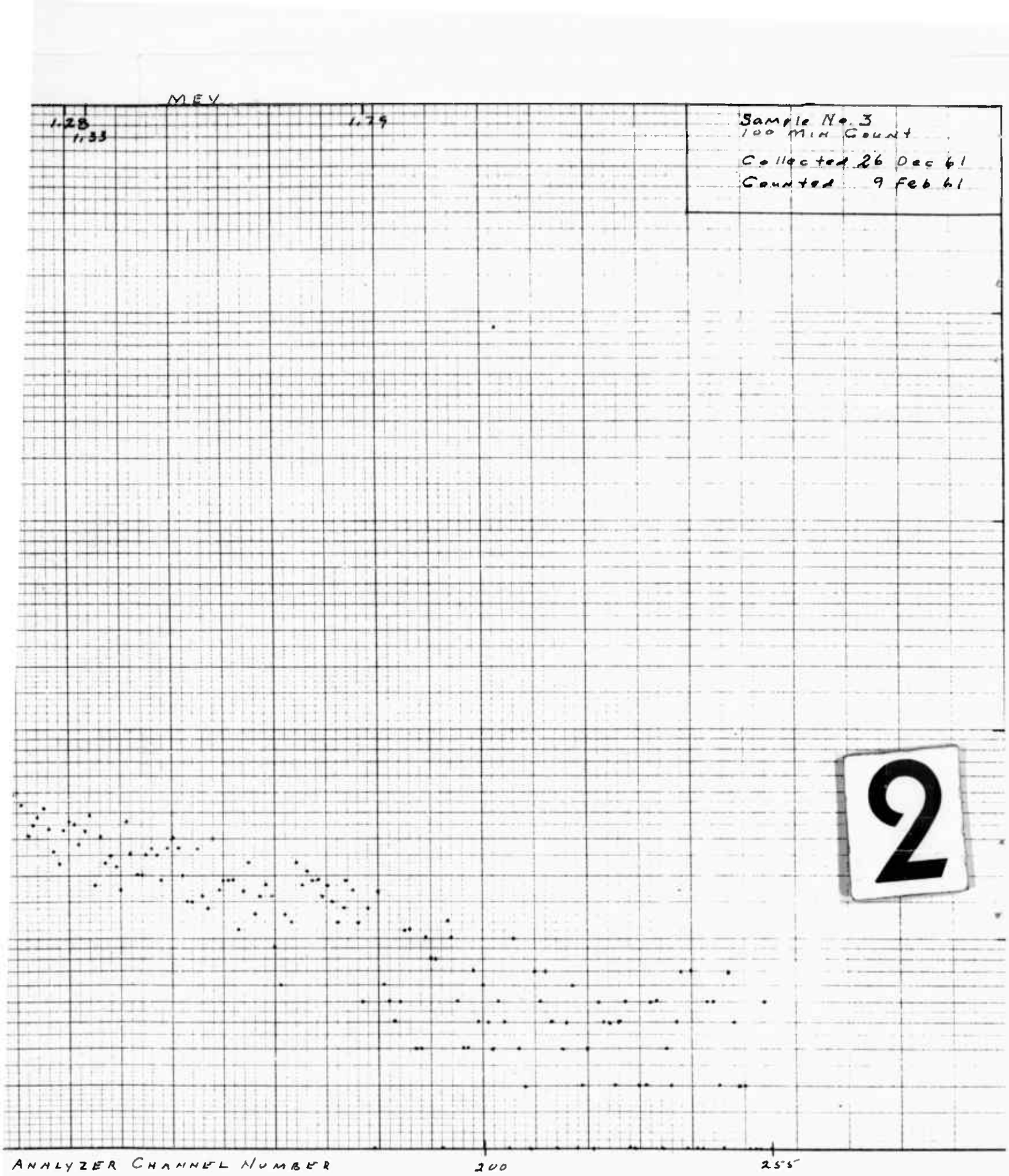
MEV
1.28
1.33
1.79
Sample No. 3
100 MIN Count
Collected 26 Dec 61
Counted 9 Feb 61
2
ANALYZER CHANNEL NUMBER
200
255

Fig. 20

Sample No. 3
100 Min Count
Collected 26 Dec 61
Counted 9 Feb 62

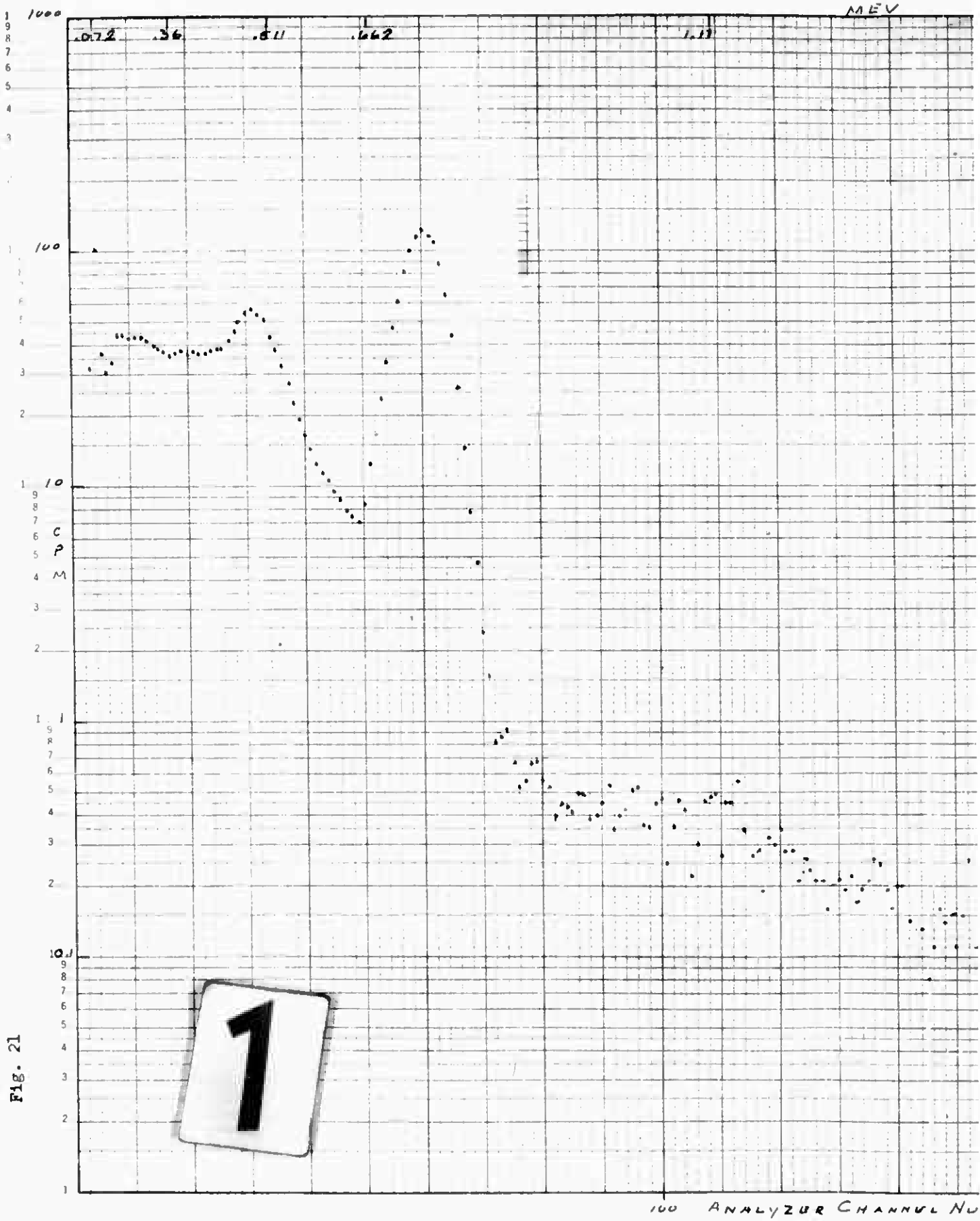
MEV
.072
.36
.511
.662
1.17
1000
100
10
1
CPM
100
ANALYZER CHANNEL NU

Fig. 21

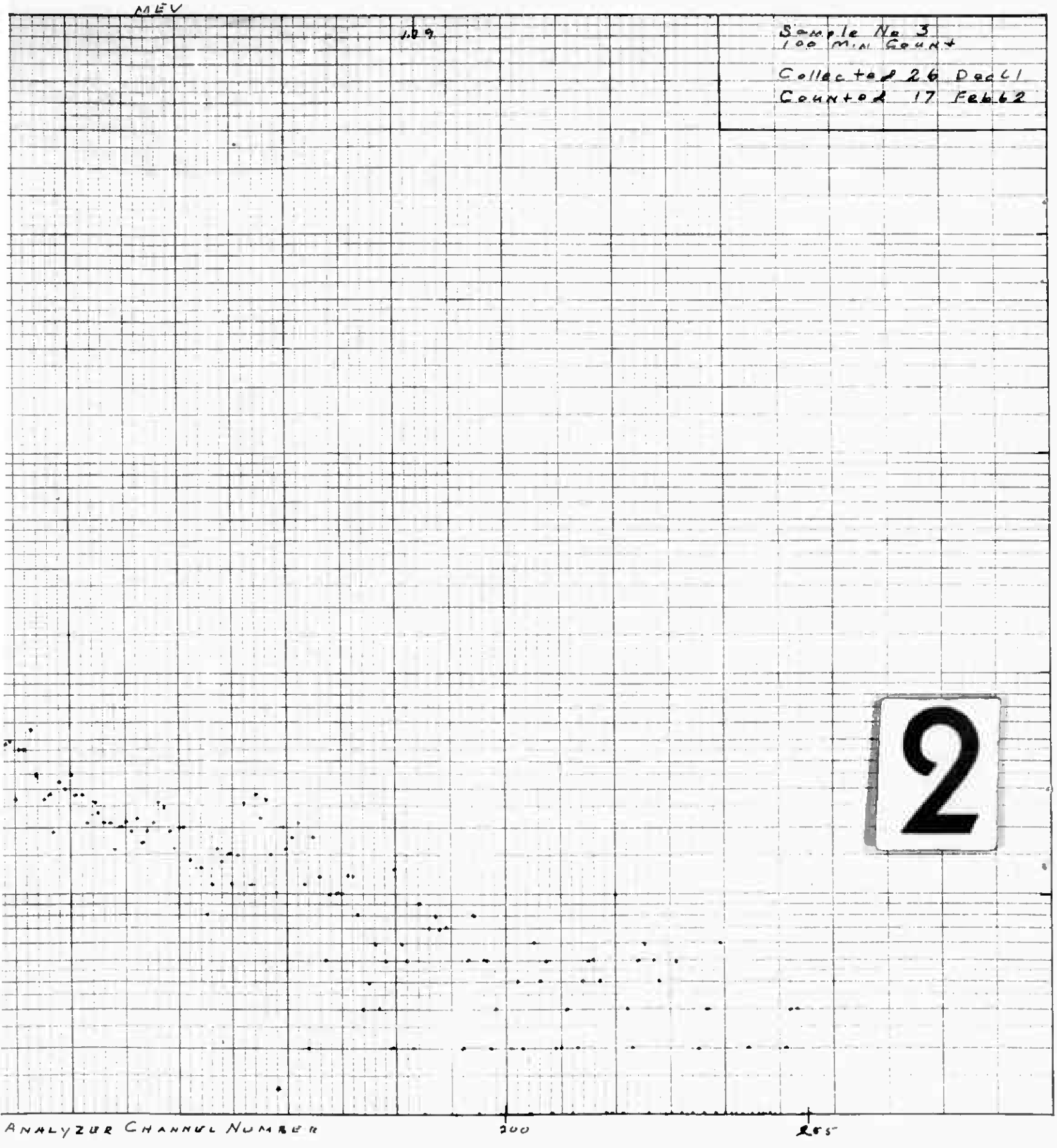
MEV
1.09
Sample No 3
100 MIN Count
Collected 26 Dec 61
Counted 17 Feb 62
2
ANALYZER CHANNEL NUMBER
200
255

Fig. 21

Sample No. 3
100 Min Count
Collected 26 Dec 61
Counted 17 Feb 62

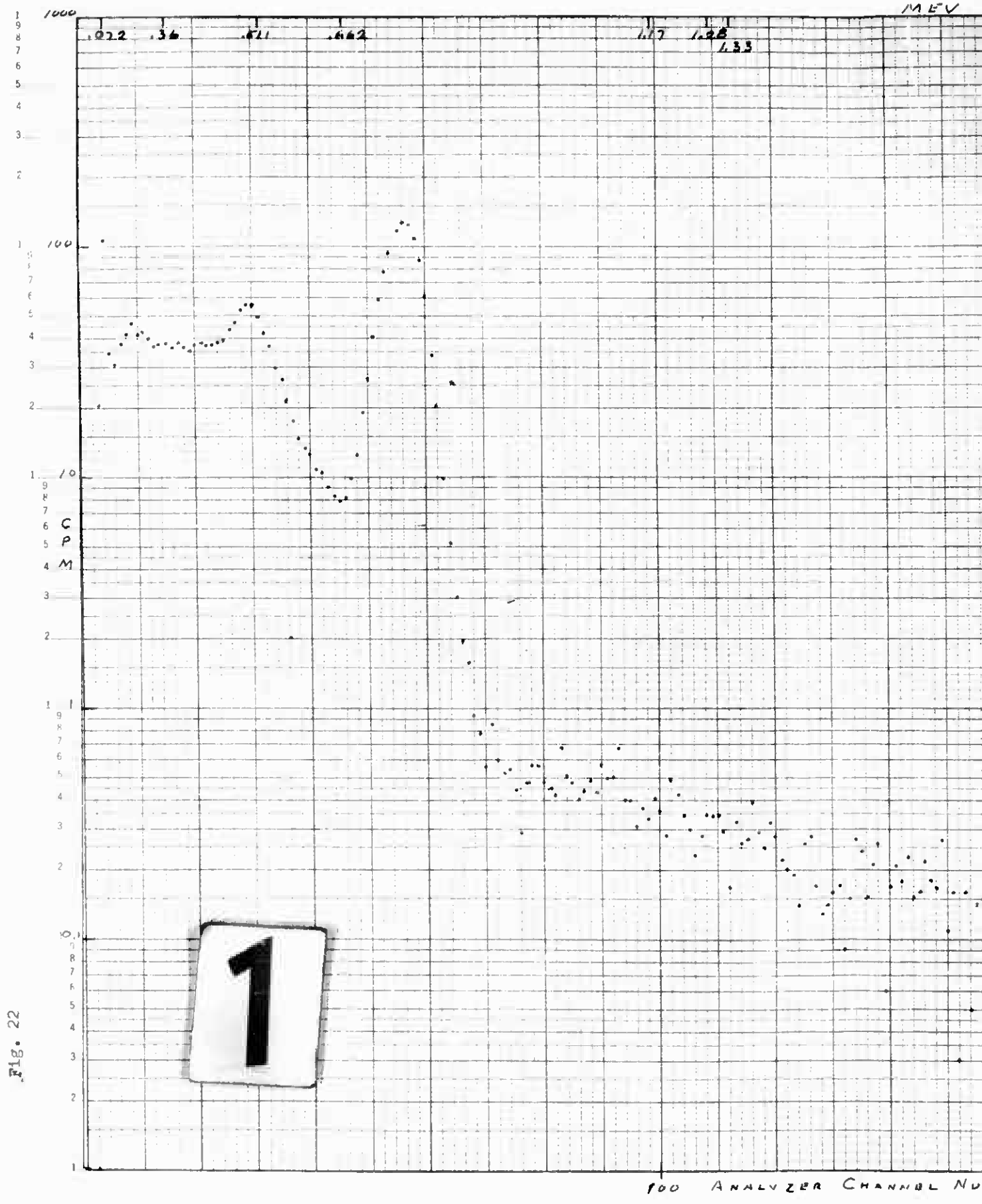
MEV
1000
.022
.34
.511
.662
1.17
1.28
1.33
100
10
1
CPM
100
ANALYZER CHANNEL NU
1

Fig. 22

MEV

28
1.33

1.79

Sample No 3
100 Min. Count

Collected 26 Dec 61

Counted 22 Feb 62

2

ANALYZER CHANNEL NUMBER

200

255

Fig. 22

Sample No. 3
100 Min Count
Collected 26 Dec 61
Counted 22 Feb 62

GNE/Phys/62-2

Sample No. 4

Collection Data:

Sample Collected 1025-1630/2 Jan 62
Weather: Completely overcast; Snowing; Wind=8 knots WSW; Temp=25°F.

Charging Potential	22.0KV
Collection potential	17.5KV
Ionization current	16.0ma*
Volume flow rate of air	47.5 m^3/minute
Collection time	365 minutes
Total air sampled	17,345 m^3

*Decreased ionization current necessitated by arcing due to snow passing through charging section.

Analysis Data:

Date	Integral Count Rate* Counts/min/m^3 of air	Counting Time	Remarks
3/1/62	0.043	10 min	Amp gain=1/4:85
12/1/62	0.075	10 min	Amp gain=1/4:85
26/1/62	0.079	10 min	Amp gain=1/4:85
2/2/62	0.061	100 min	Amp gain=1/4:100
9/2/62	0.075	100 min	Amp gain=1/4:100
17/2/62	0.061	100 min	Amp gain=1/4:100
22/2/62	0.057	100 min	Amp gain=1/4:100

* The integral count rate of this sample is in error by virtue of the solubility fractionation phenomenon. This count rate is also low because of the decreased ionization current required during collection.

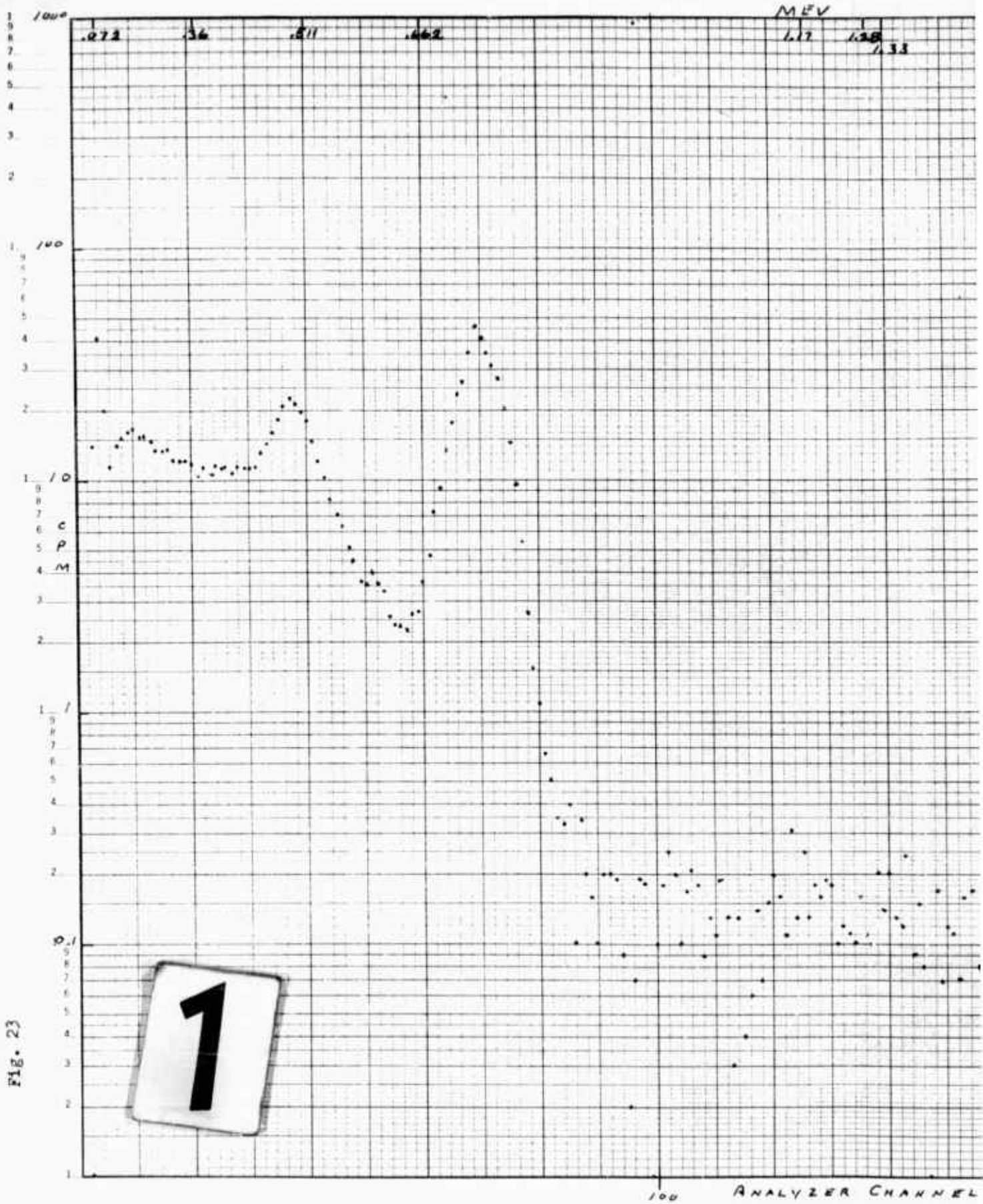
MEV
.272
.36
.511
.662
1.17
1.28
1.33
1000
100
10
1
0.1
CPM
100
ANALYZER CHANNEL

Fig. 23

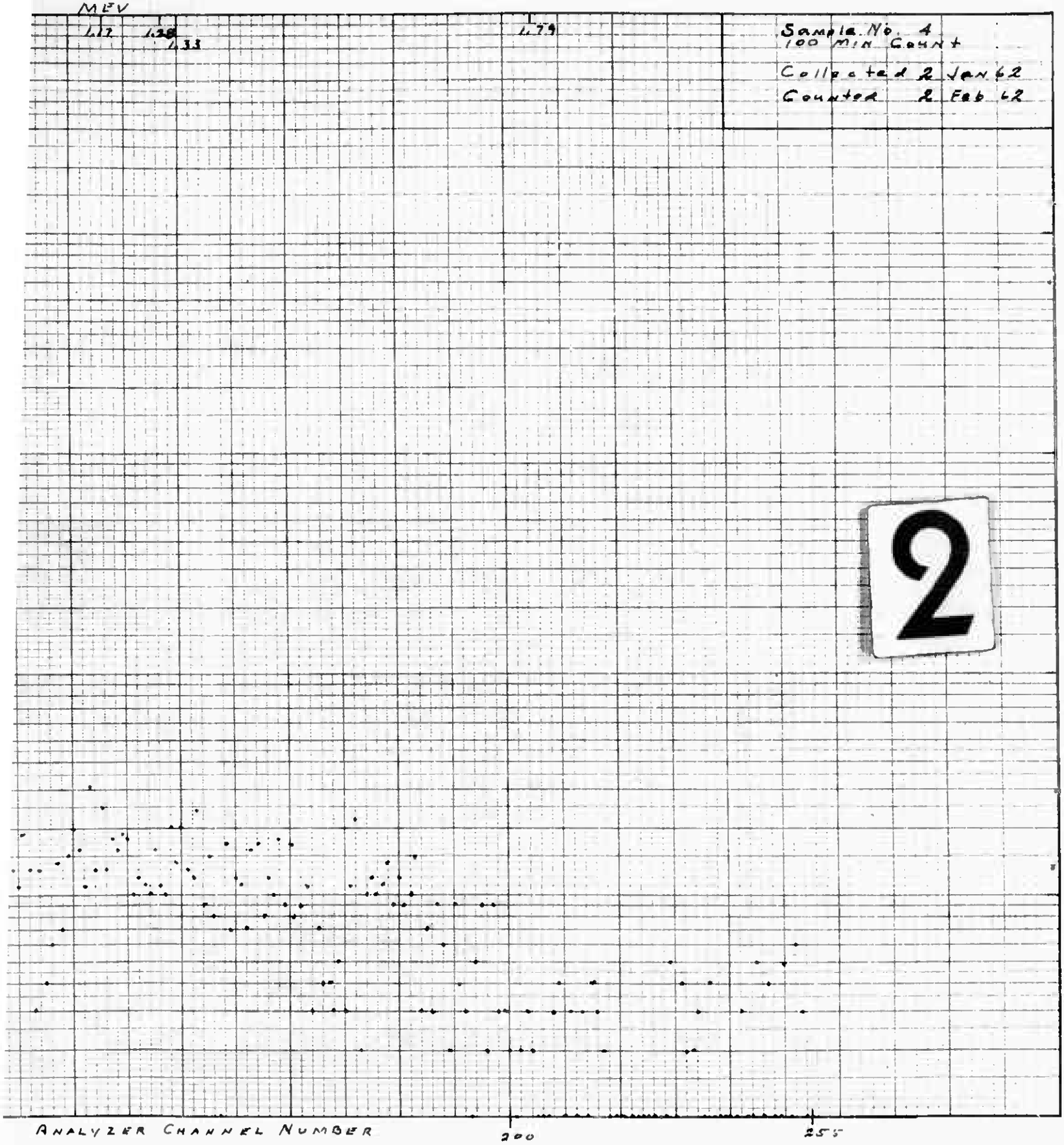
MEV
L17
L28
L33
L79
Sample No. 4
100 MIN Count
Collected 2 Jan 62
Counted 2 Feb 62
2
ANALYZER CHANNEL NUMBER
200
255

Fig. 23

Sample No. 4
100 Min Count
Collected 2 Jan 62
Counted 2 Feb 62

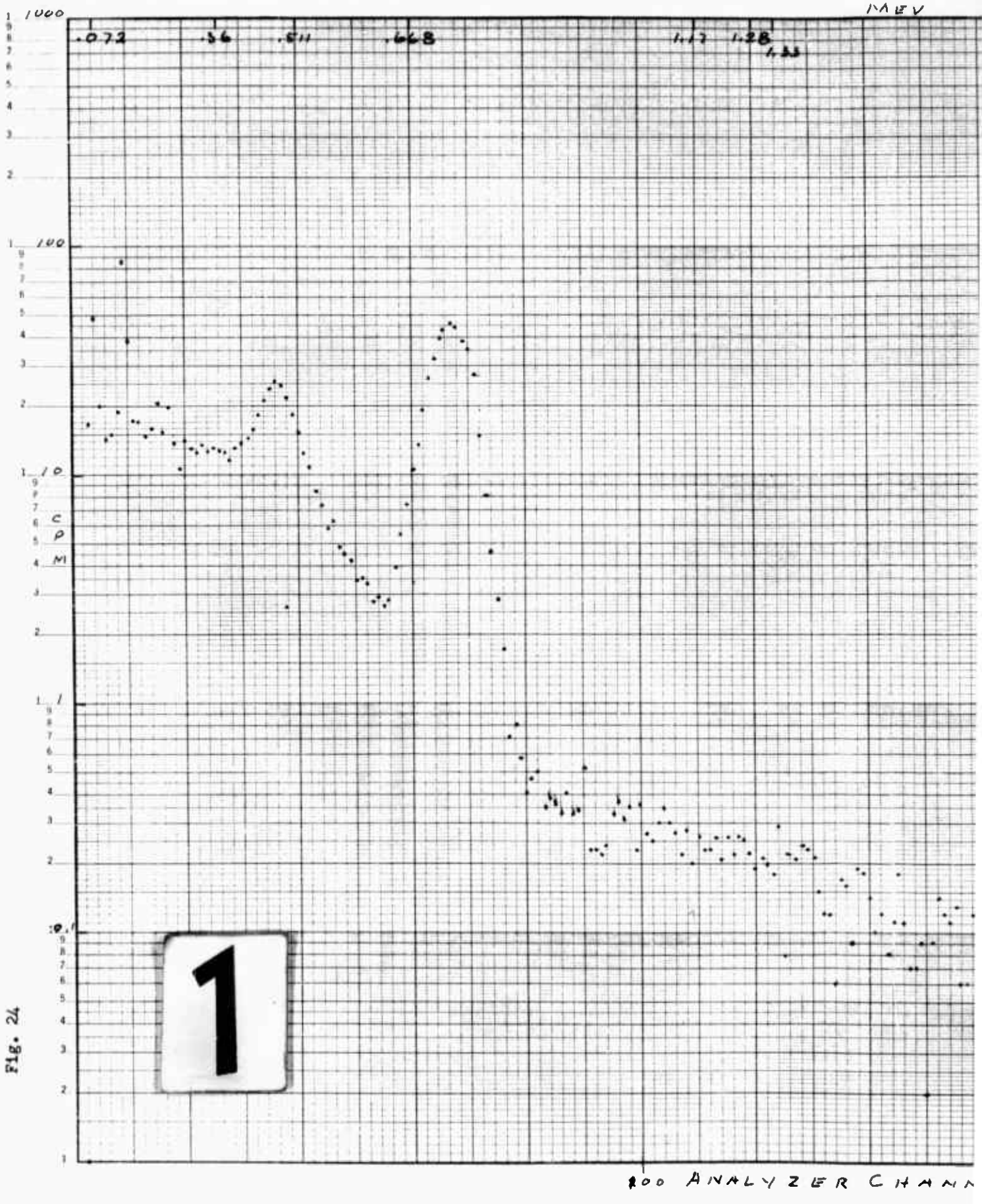
MEV
.072
.56
.611
.668
1.17
1.28
1.33
1000
100
10
1
CPM
1
ANALYZER CHANN

Fig. 24

MEV

1.28 1.33 1.79

Sample No. 4
100 Min Count
Collected 2 JAN 62
Counted 9 Feb 62

2

ANALYZER CHANNEL NUMBER 200 255

MEV

1.28 1.33 1.79

Sample No. 1
100 M.M Count
Collected 2 JAN 62
Counted 9 Feb 62

2

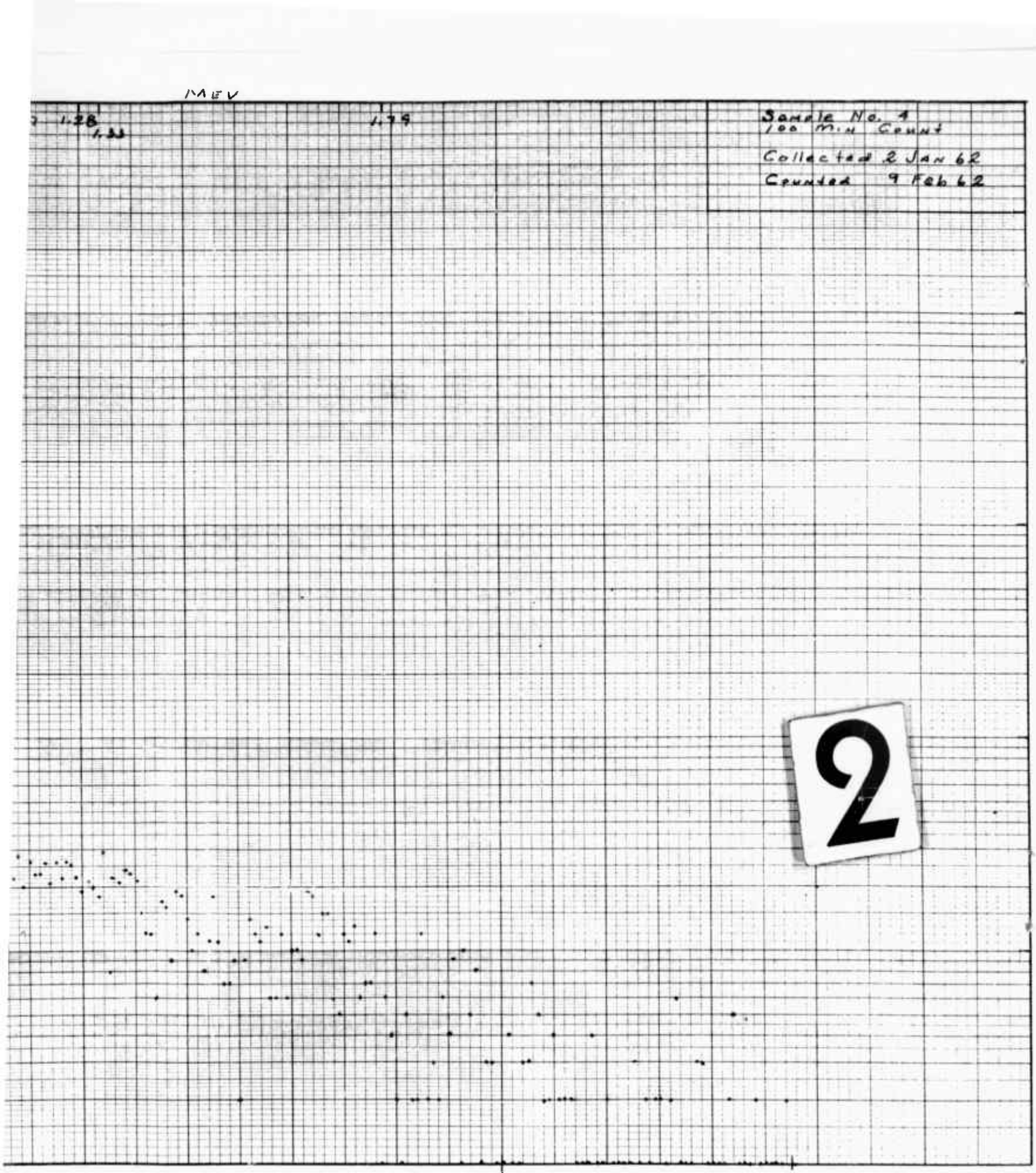

ANALYZER CHANNEL NUMBER 200 255

Fig. 24

Sample No. 4
100 Min Count
Collected 2 Jan 62
Counted 9 Feb 62

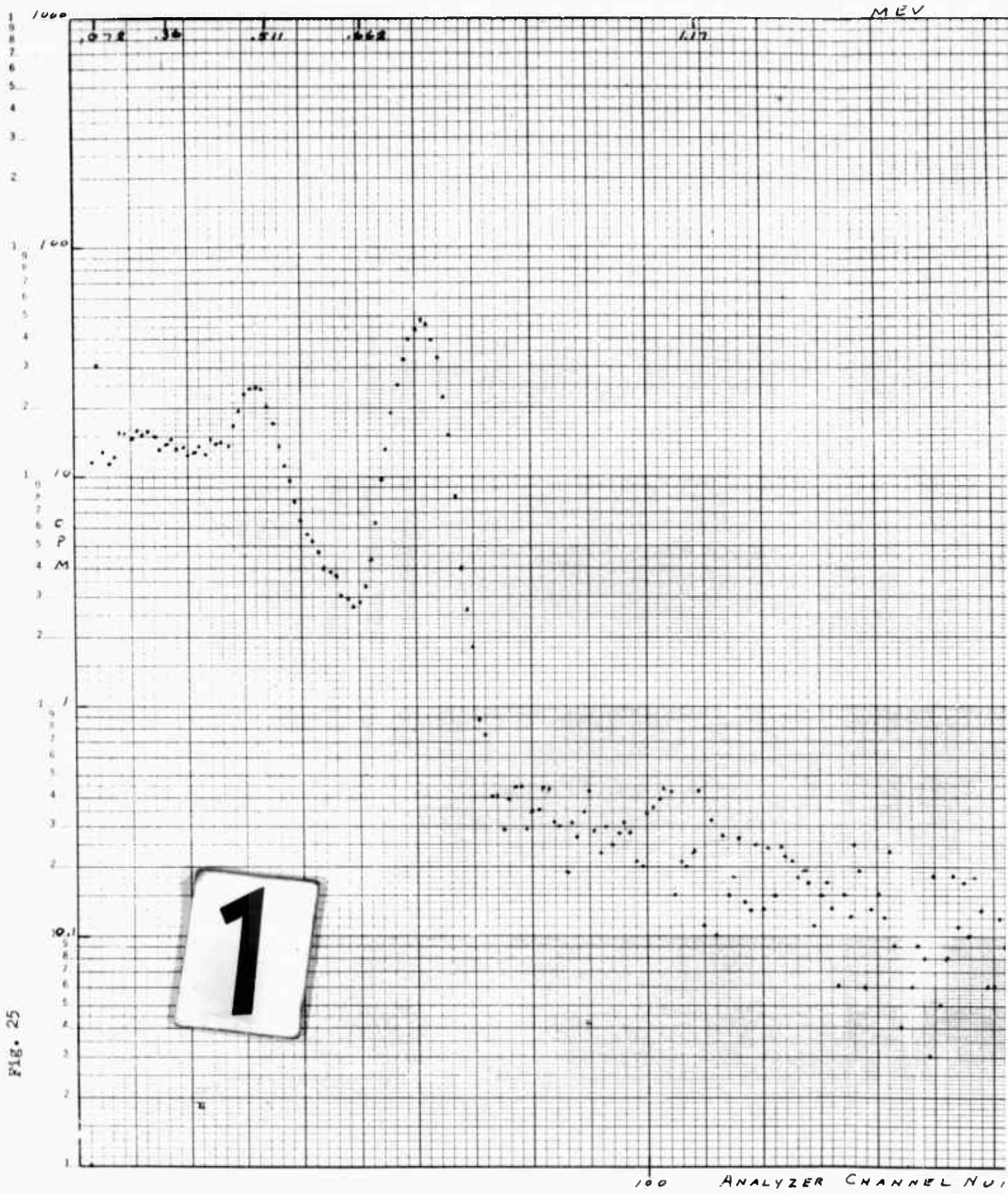
MEV
.072
.36
.511
.662
1.17
1000
100
10
1
0.1
CPM
100
ANALYZER CHANNEL NU

Fig. 25

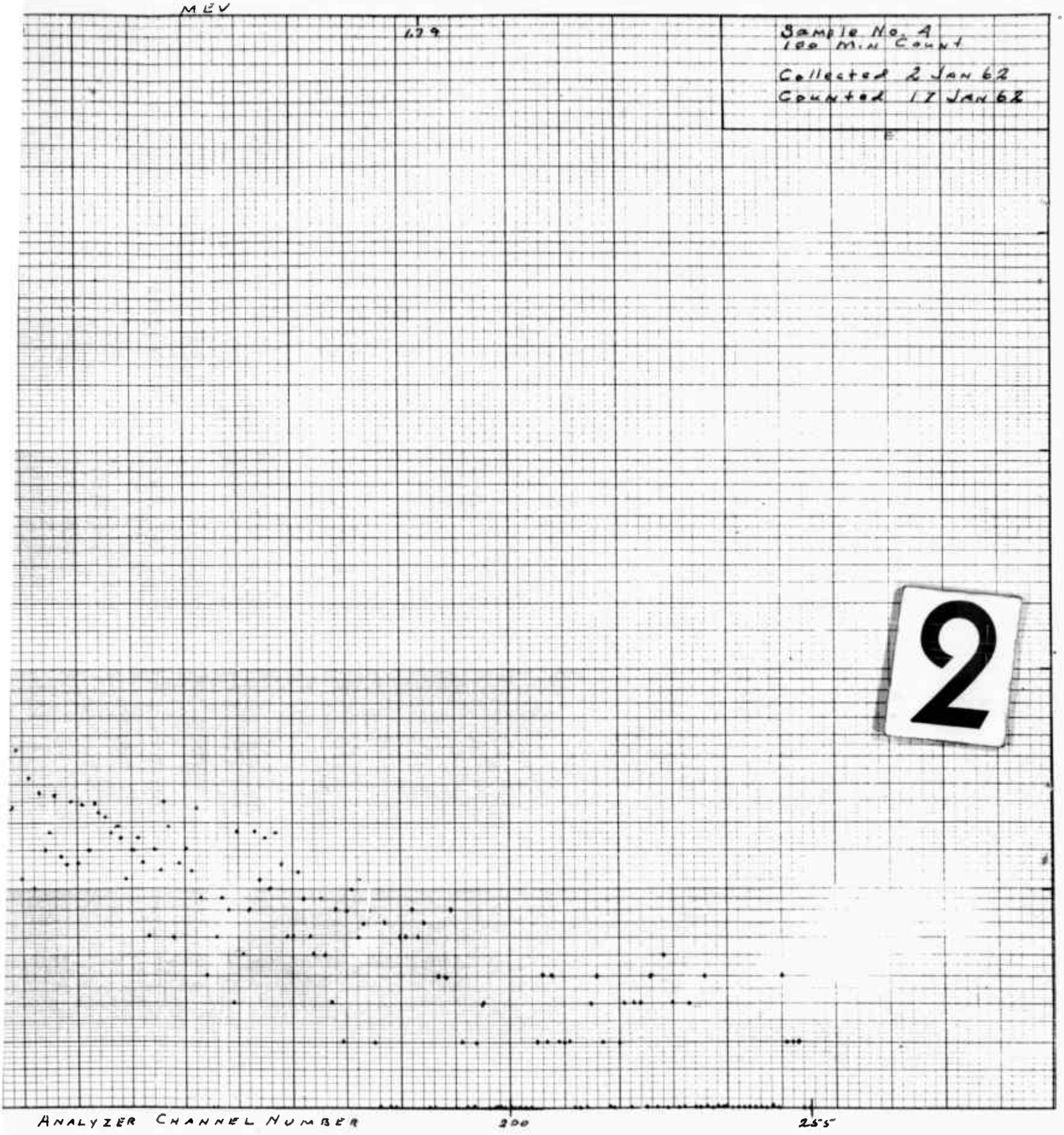
MEV
.179
Sample No. A
100 Min Count
Collected 2 JAN 62
Counted 11 JAN 62
2
ANALYZER CHANNEL NUMBER
200
255

Fig. 25

Sample No. 4
100 Min Count
Collected 2 Jan 62
Counted 17 Jan 62

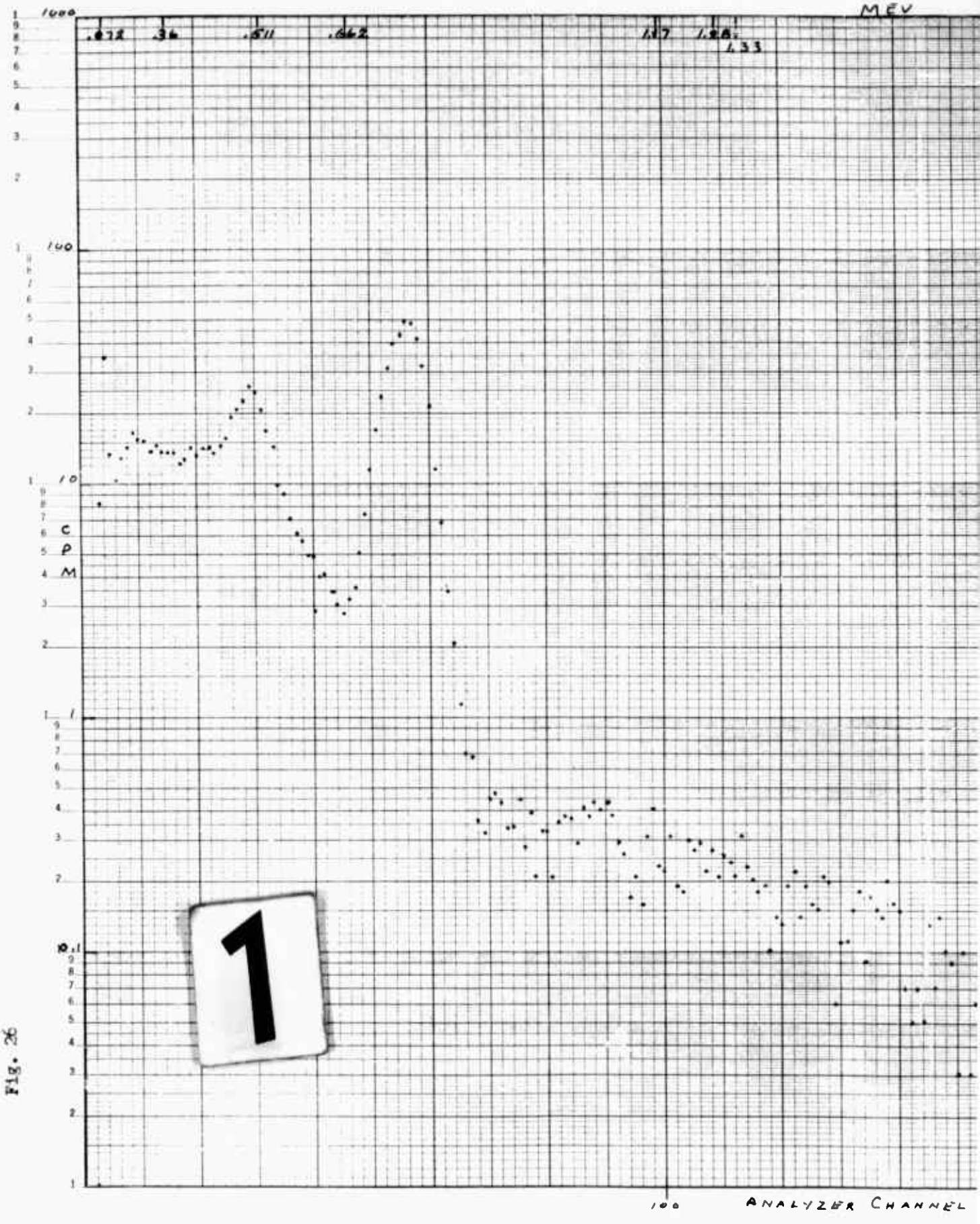
MEV
.072
.36
.511
.662
1.17
1.28
1.33
1000
100
10
1
.1
C
P
M
100
ANALYZER CHANNEL

Fig. 26

MEV

.33

1.09

Sample No. 4
100 Min Count

Collected 2 Jan 62
Counted 22 Feb 62

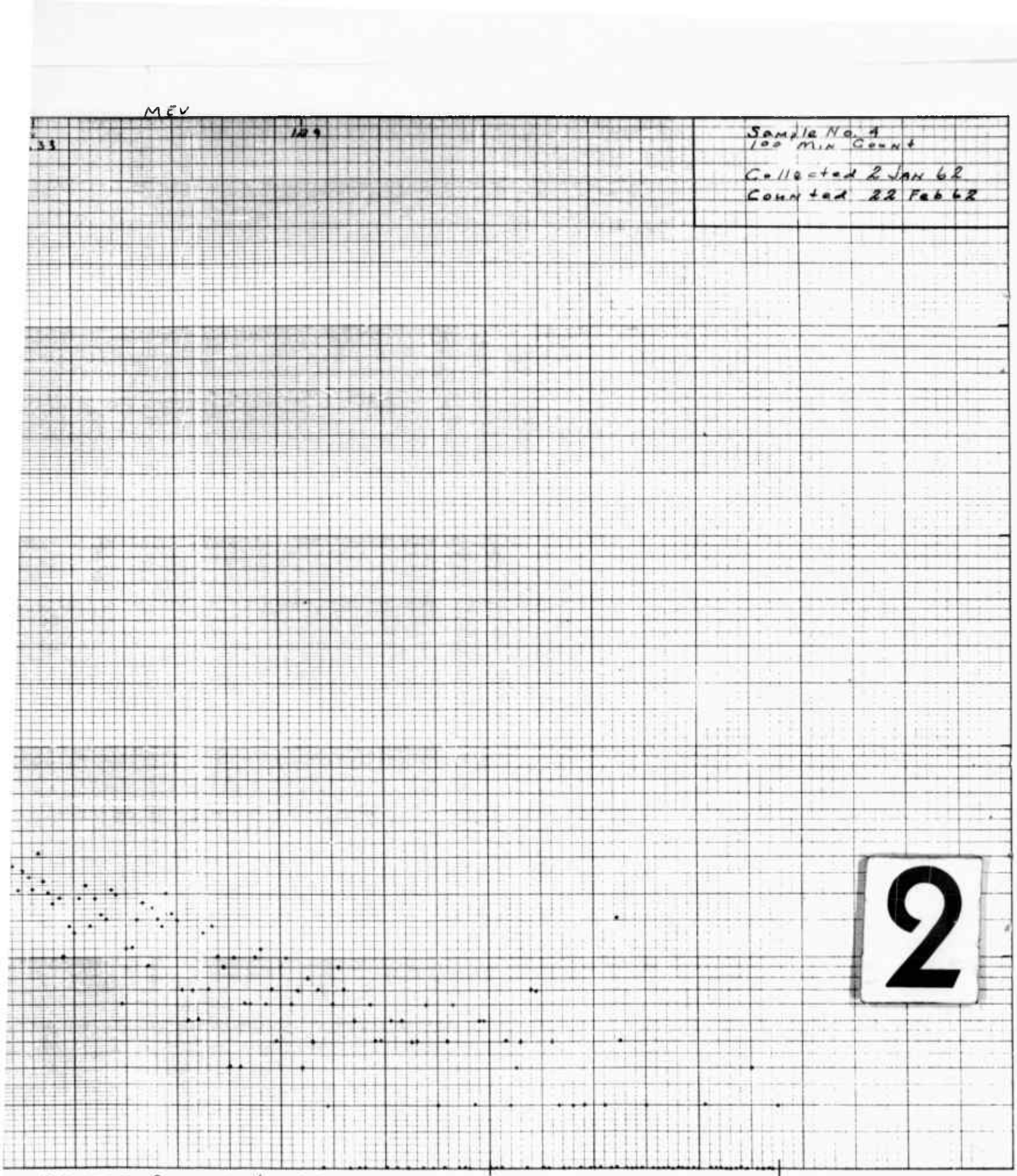

2

ANALYZER CHANNEL NUMBER

200

255

GNE/Phys/62-2

Sample No. 5

Collection Data:

Sample collected 0645-1445/17 Jan 62.
Weather: Clear and cold; Temp=12°F; Wind=3 knots WSW.

Charging Potential	23.5KV
Collection potential	18.5KV
Ionization current	20.0ma
Volume flow rate of air	47.5 m^3/minute
Collection time	480 minutes
Total air sampled	22,810 m^3

As in the other sample collections, the collection system was occasionally shut down by arcing. The collection was monitored and the system restarted immediately after each shut-down.

Analysis Data:

Date	Integral Count Rate Counts/min/m^3 of Air	Counting Time	Remarks
26/1/62	0.275	10 min	Amp gain=1/4:100
2/2/62	0.314	100 min	Amp gain=1/4:100
9/2/62	0.242	100 min	Amp gain=1/4:100
17/2/62	0.269	100 min	Amp gain=1/4:100
22/2/62	0.200	100 min	Amp gain=1/4:100
1/3/62	0.169	500 min*	Amp gain=1/4:100
2/3/62	0.134	1000 min	Amp gain=1/4:100
6/3/62	NA**	200 min	Amp gain=1 :100

* Two extended counts were taken in an attempt to improve counting statistics and accentuate the high-energy low-count-rate peaks for improved spectral peak identification.

** One count was taken with an expanded gain setting to expand the low energy end of the spectrum and permit identification of the adjacent peaka in the low energy spectrum.

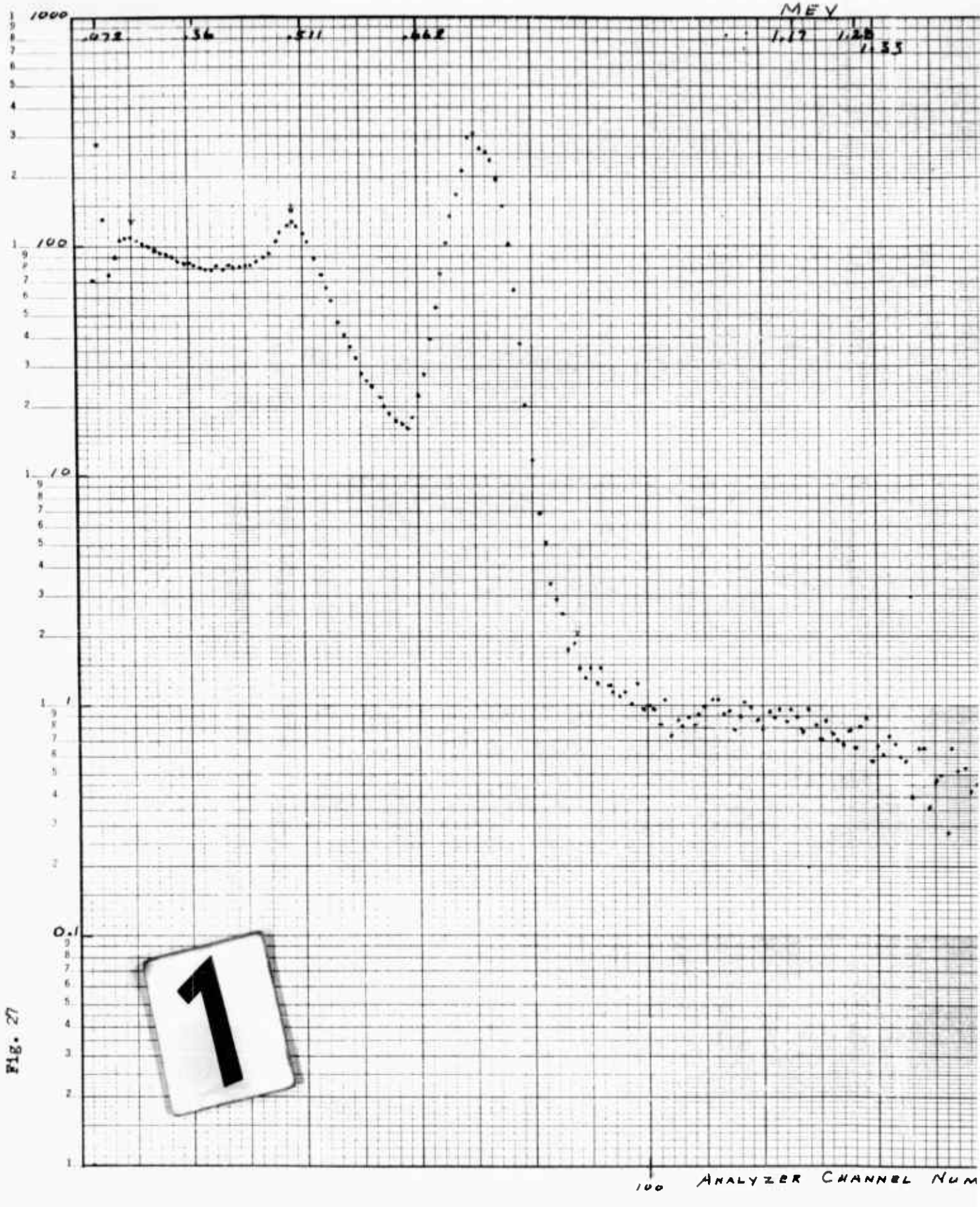
MEV
.072
.36
.511
.662
1.17
1.33
1000
100
10
1
0.1
100
ANALYZER CHANNEL NUM

Fig. 27

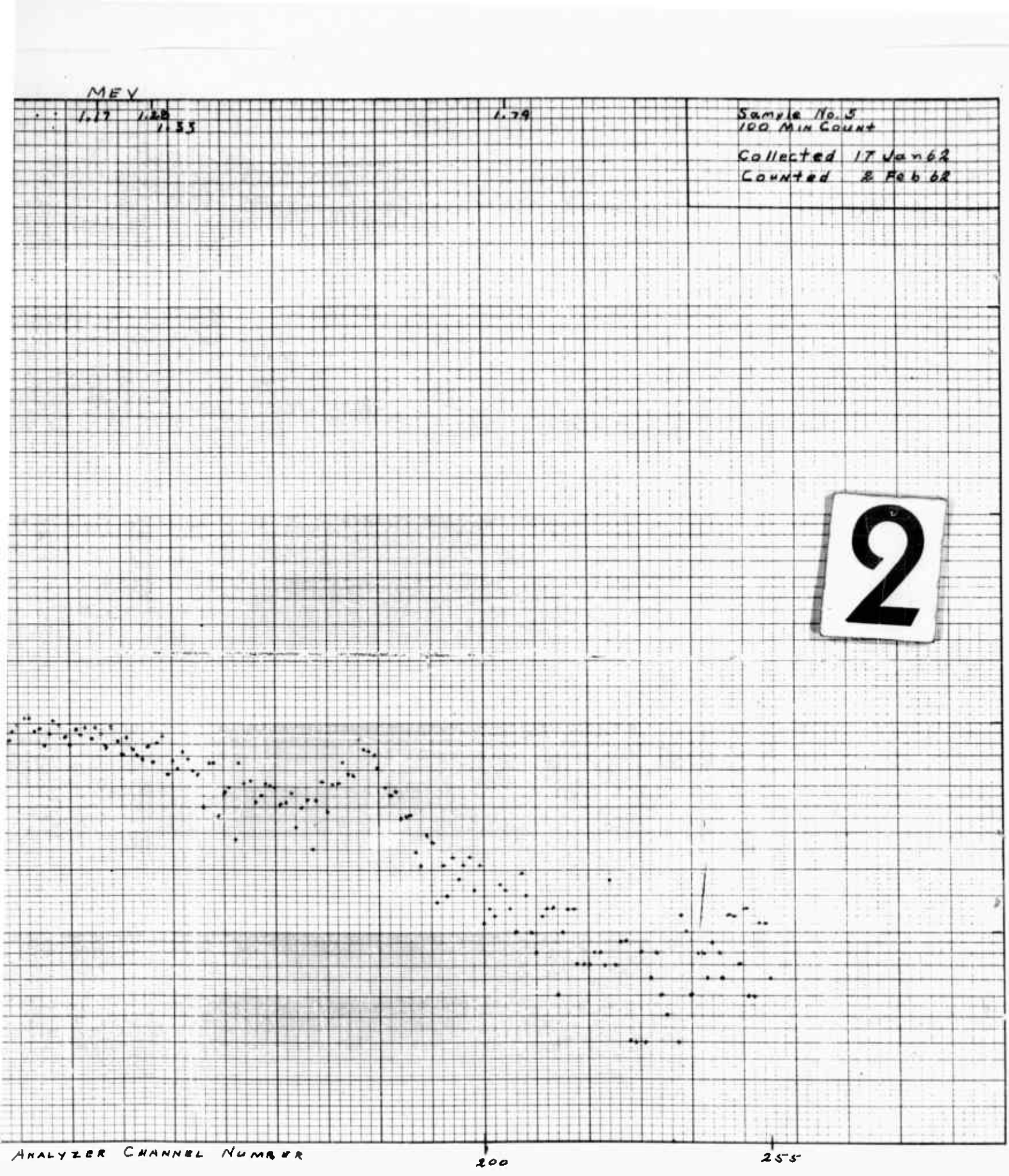
MEV
1.17
1.28
1.33
1.79
Sample No. 5
100 Min Count
Collected 17 Jan 62
Counted 8 Feb 62
2
ANALYZER CHANNEL NUMBER
200
255

Fig. 27

Sample No. 5
100 Min Count
Collected 17 Jan 62
Counted 2 Feb 62

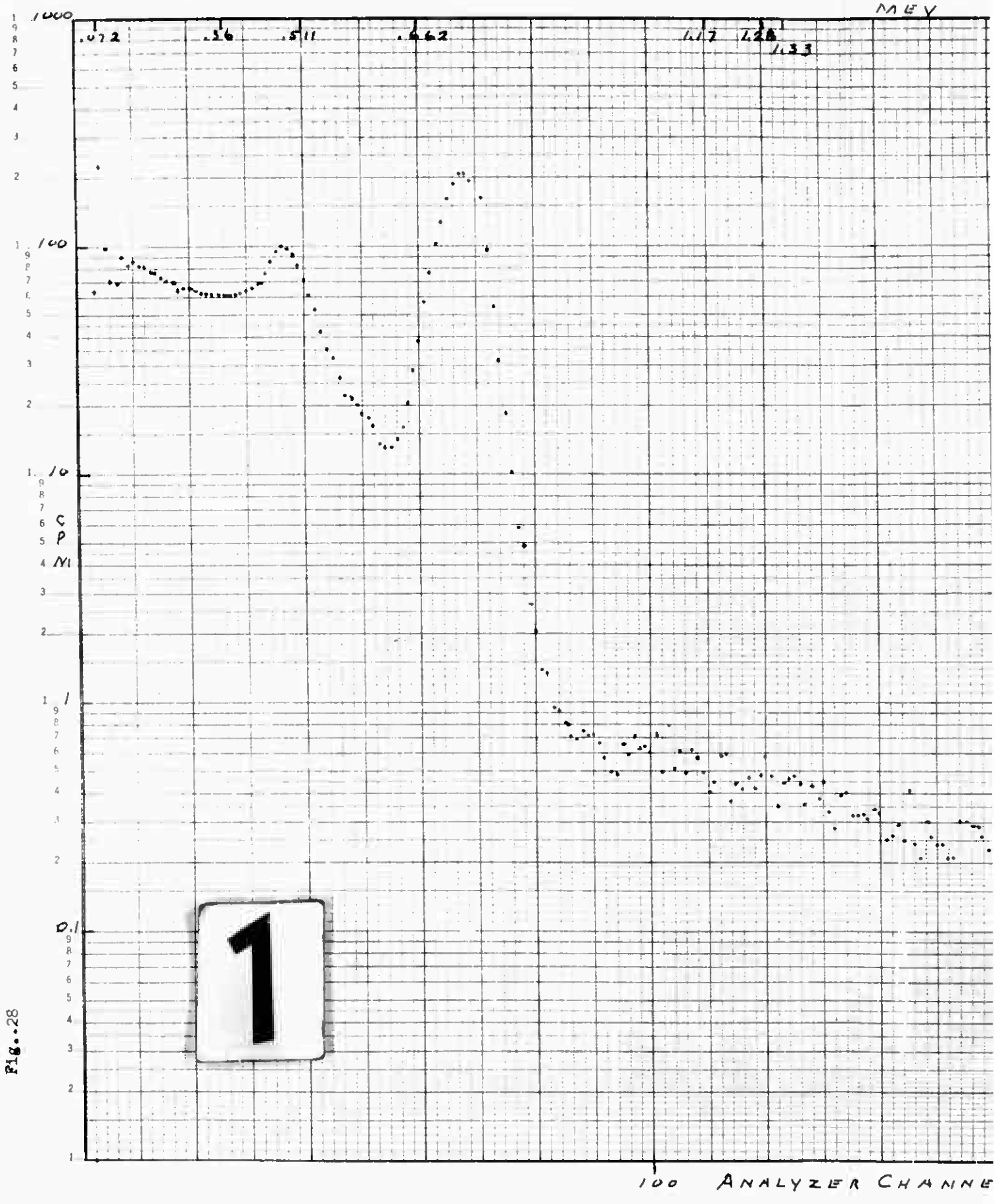
MEV
1000
.072
.256
.511
.662
1.17
1.28
1.33
100
10
CPM
1
0.1
100
ANALYZER CHANNE

Fig. 28

MEV

1.2 1.28 1.33 1.73

Sample No 5
100 Min. Count

Collected 17 Jan 62
Counted 9 Feb 62

2

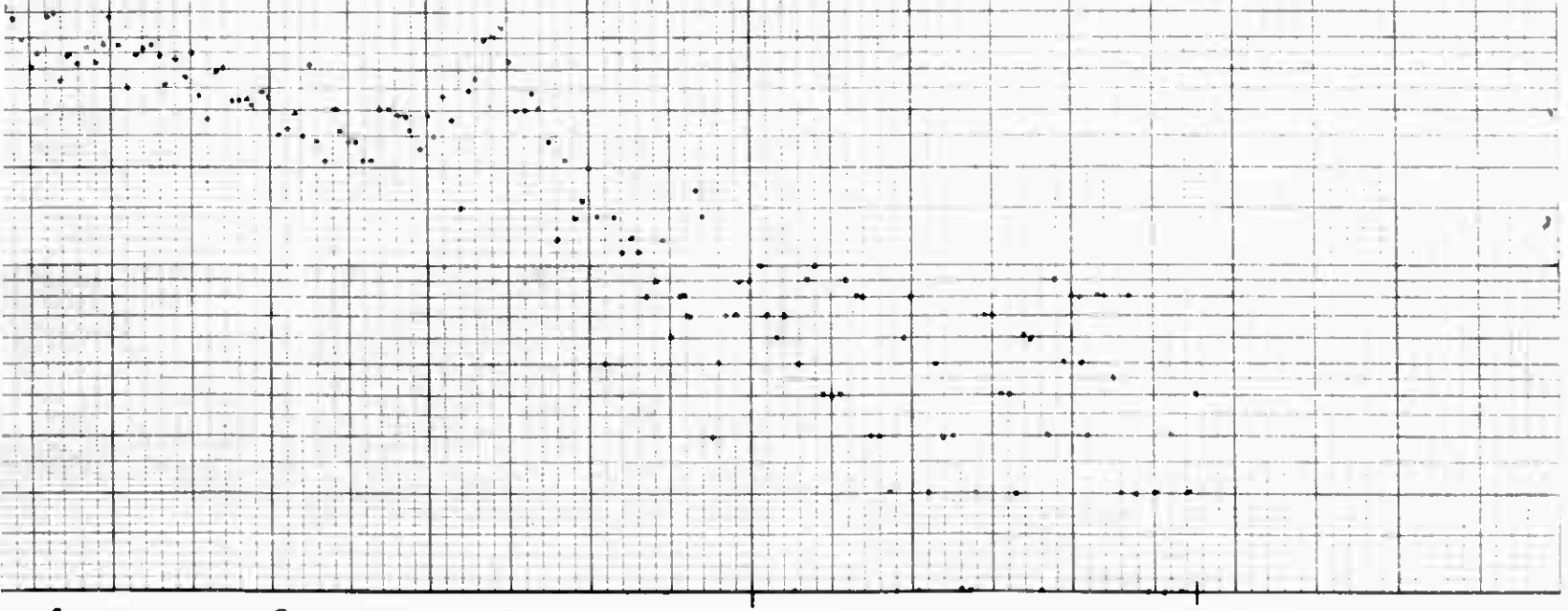

ANALYZER CHANNEL NUMBER 200 255

Fig. 28

Sample No. 5
100 Min Count
Collected 17 Jan 62
Counted 9 Feb 62

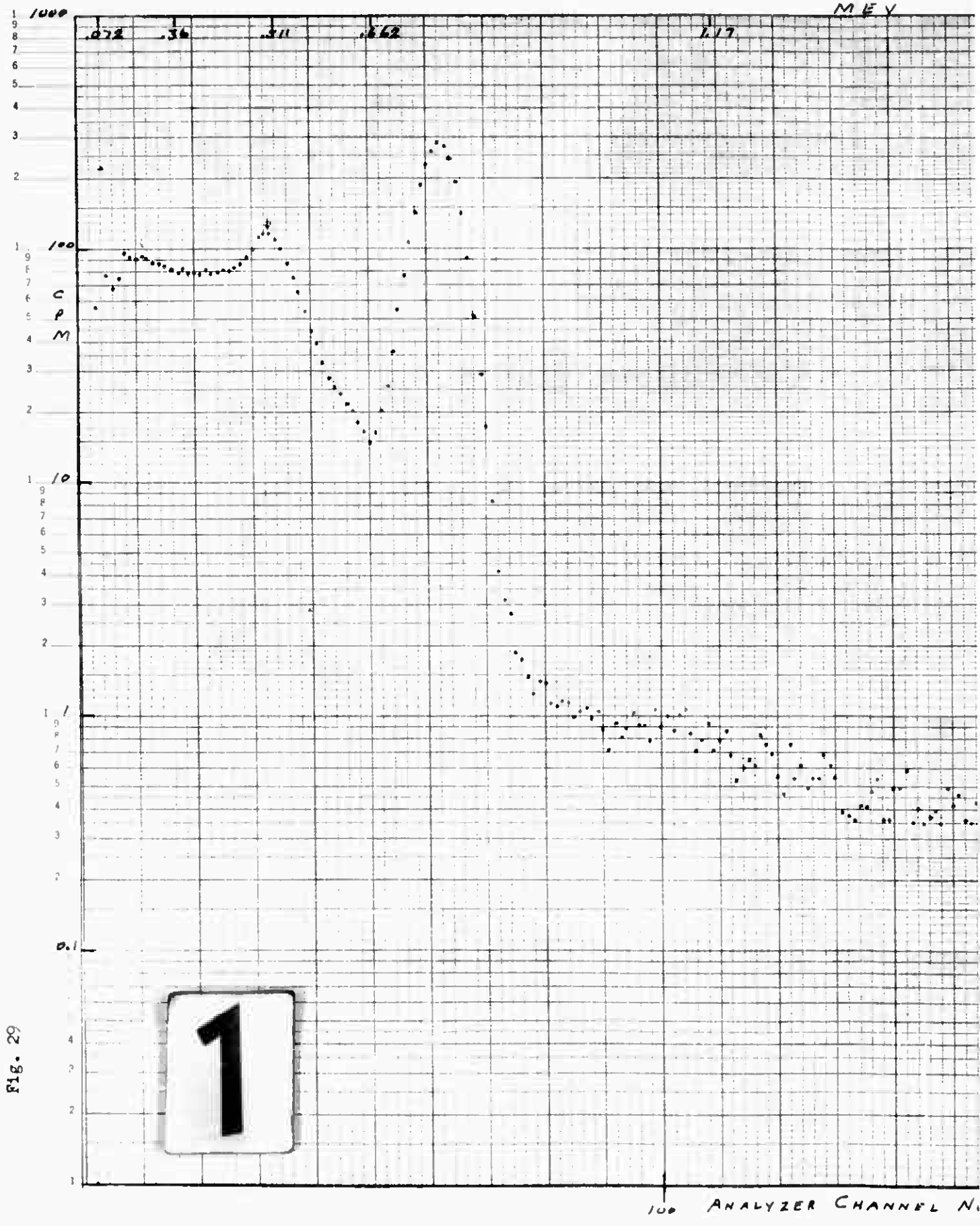
MEV
.072
.36
.511
.662
1.17
1000
100
10
1
0.1
CPM
100
ANALYZER CHANNEL NU

Fig. 29

MEY

17

129

Sample No. 3
100 Min Count

Collected 17 JAN 62
Counted 17 Feb 62

2

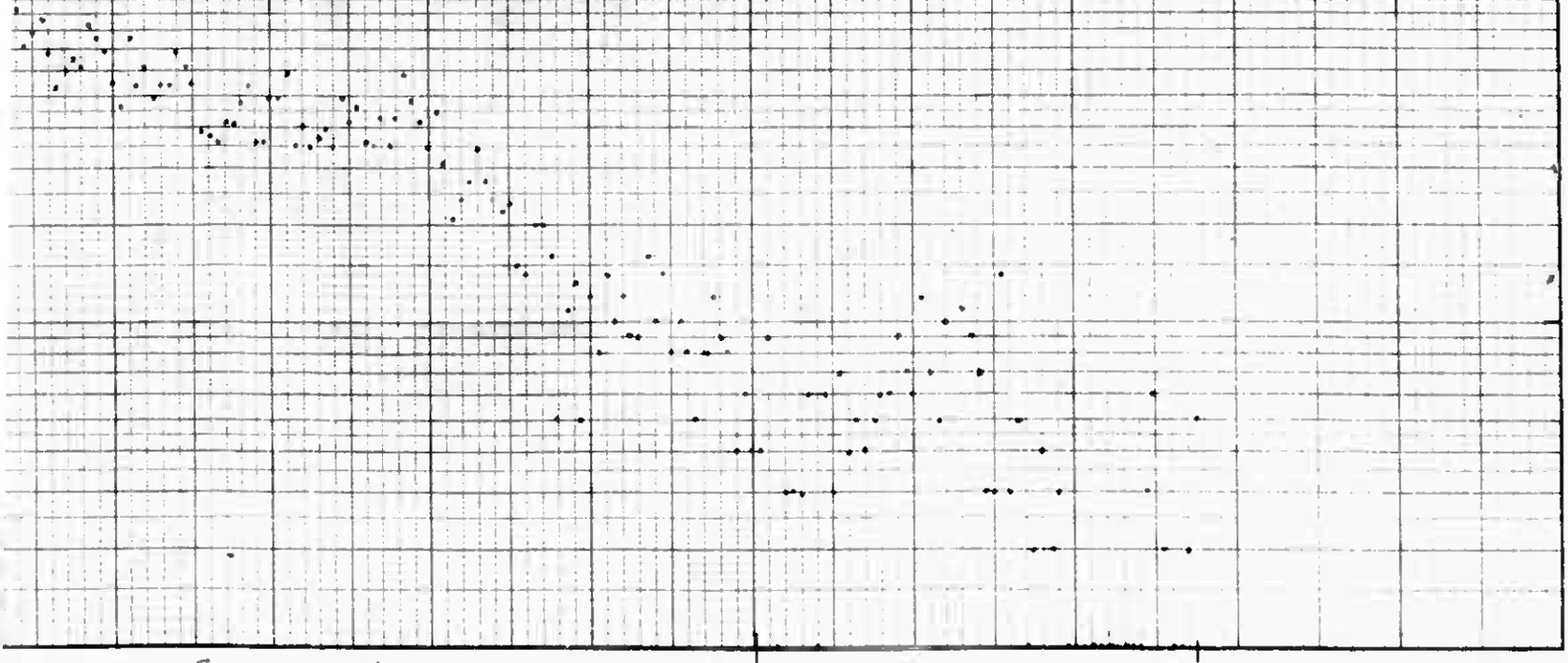

ANALYZER CHANNEL NUMBER

200

255

Fig. 29

Sample No. 5
100 Min Count
Collected 17 Jan 62
Counted 17 Feb 62

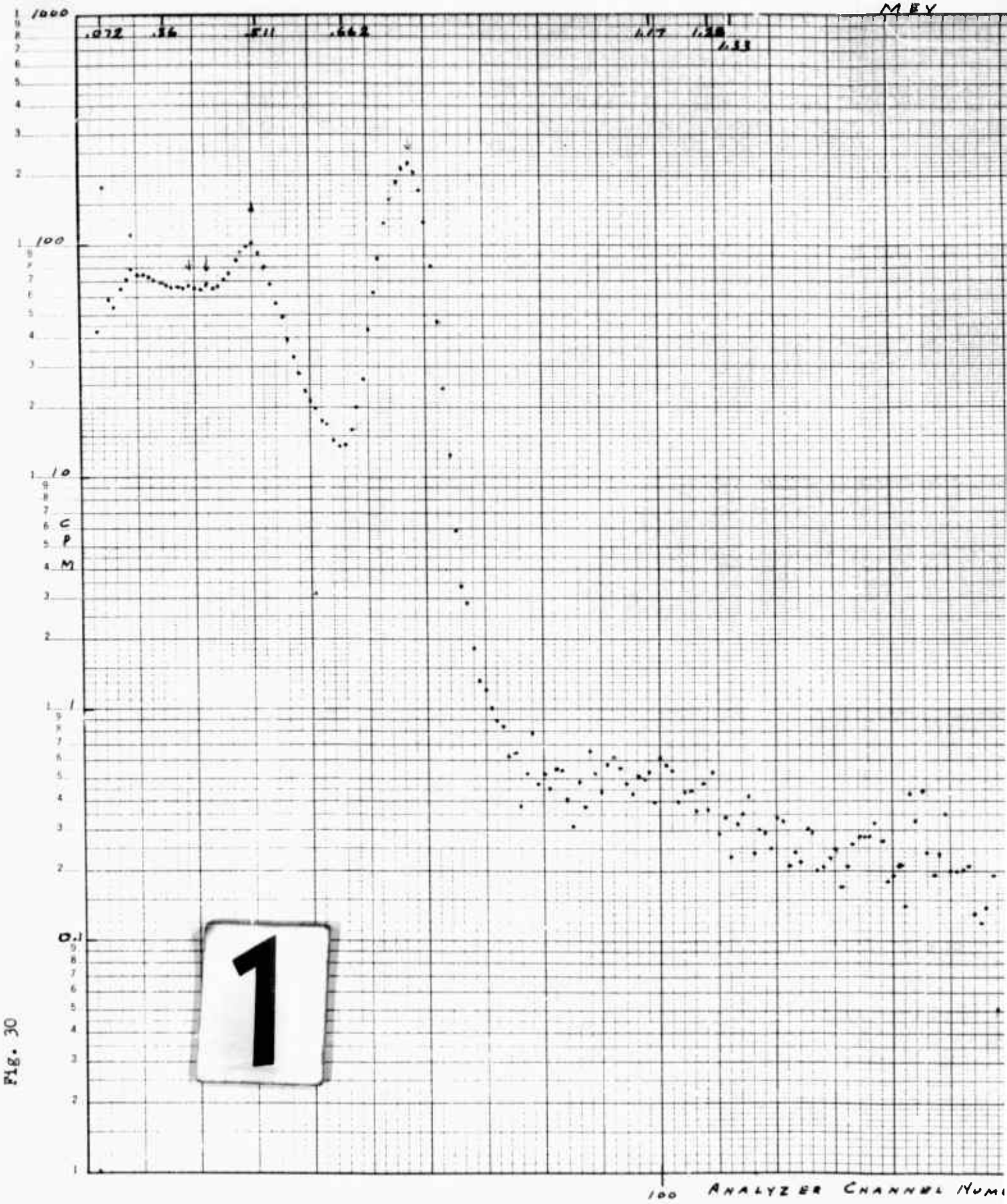
MEV
.072
.36
.511
.662
1.17
1.28
1.33
1000
100
10
1
0.1
CPM
1
100
ANALYZER CHANNEL NUMBER

Fig. 30

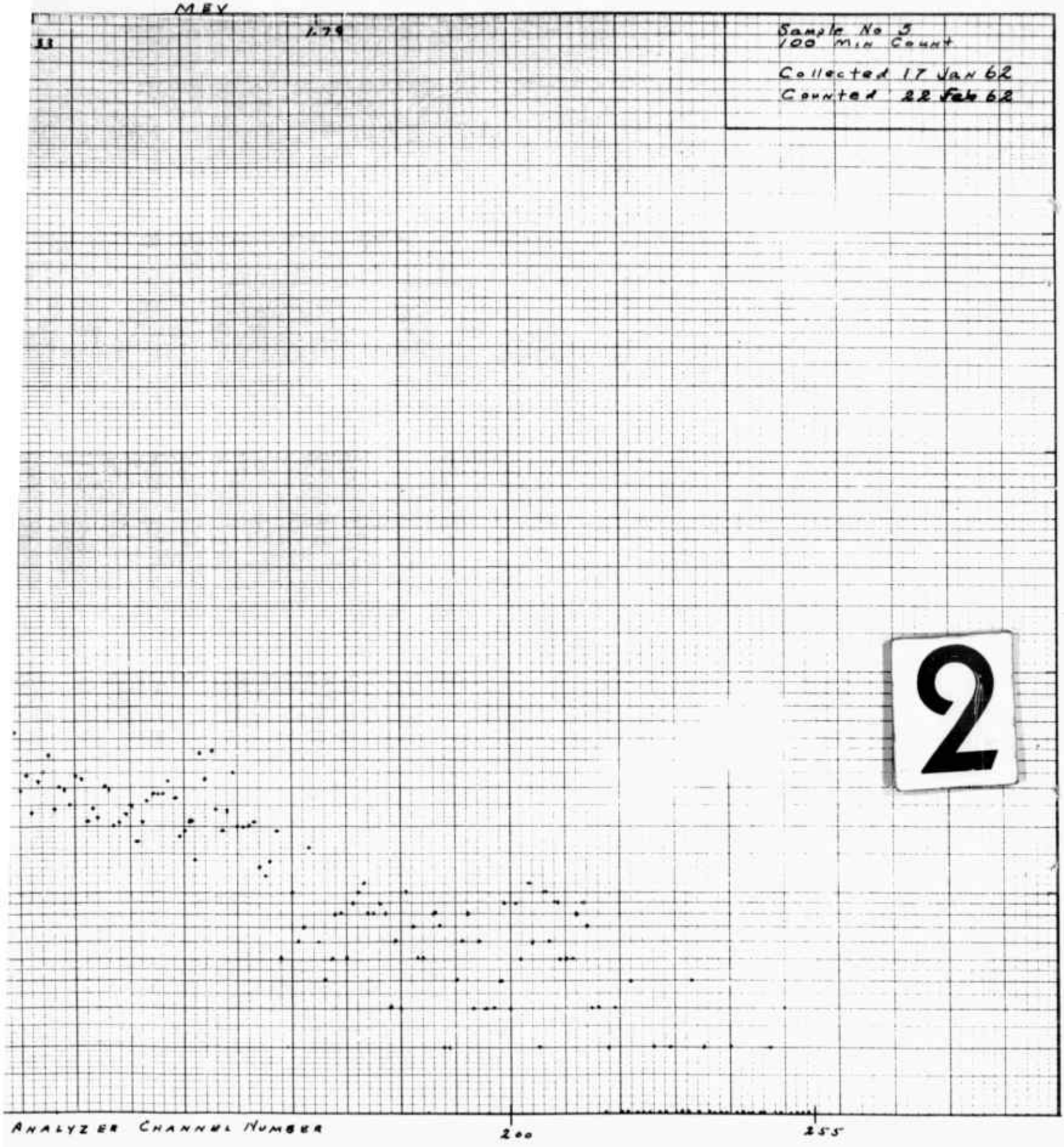
MEV
1.79
33
Sample No 3
100 Min Count
Collected 17 Jan 62
Counted 22 Feb 62
2
ANALYZER CHANNEL NUMBER
200
255

Fig. 30

Sample No. 5
100 Min Count
Collected 17 Jan 62
Counted 22 Feb 62

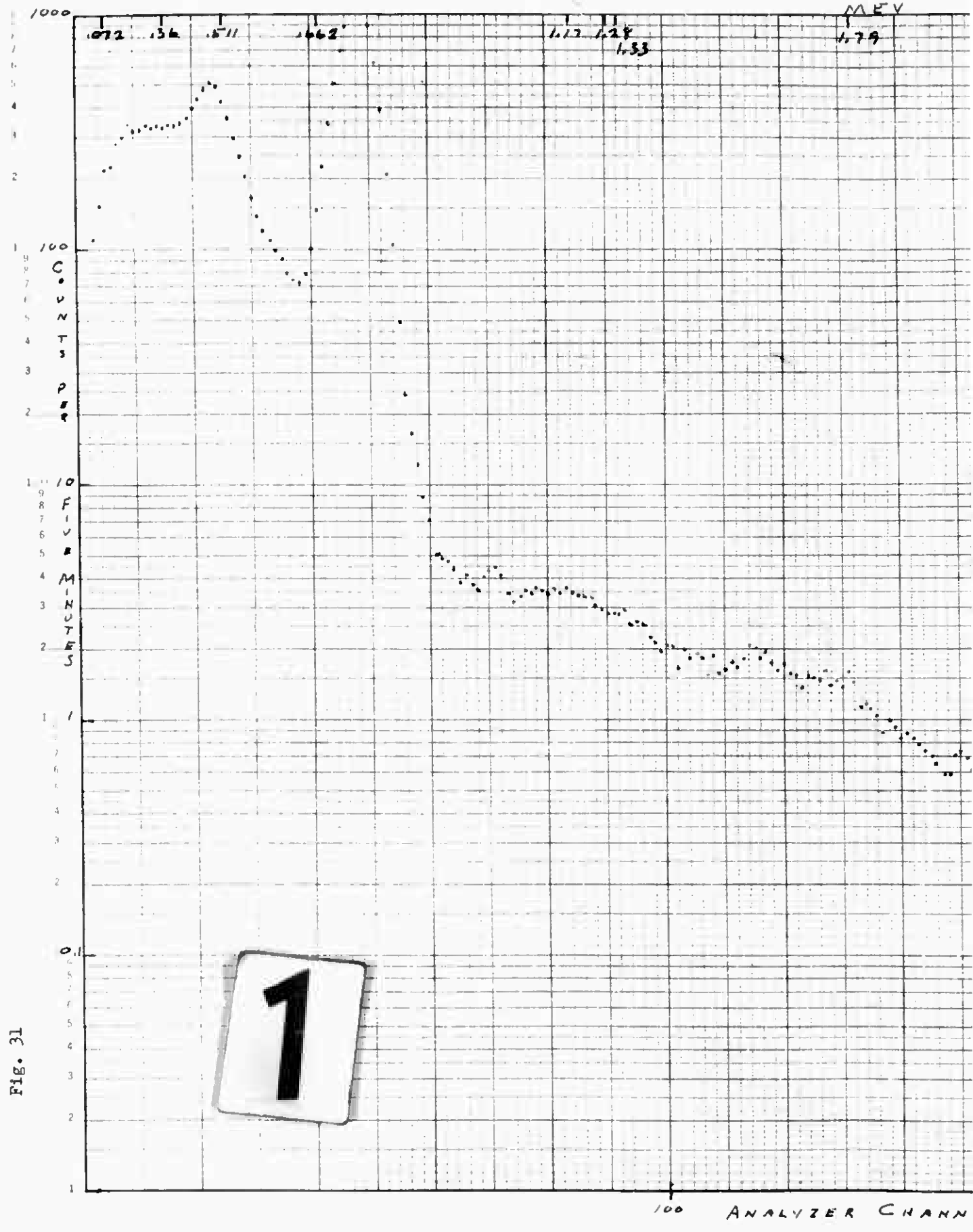
MEV
.072
.136
.511
.662
1.17
1.28
1.33
1.79
1000
100
10
1
0.1
COUNTS PER
CHANNEL
100
ANALYZER CHANN

Fig. 31

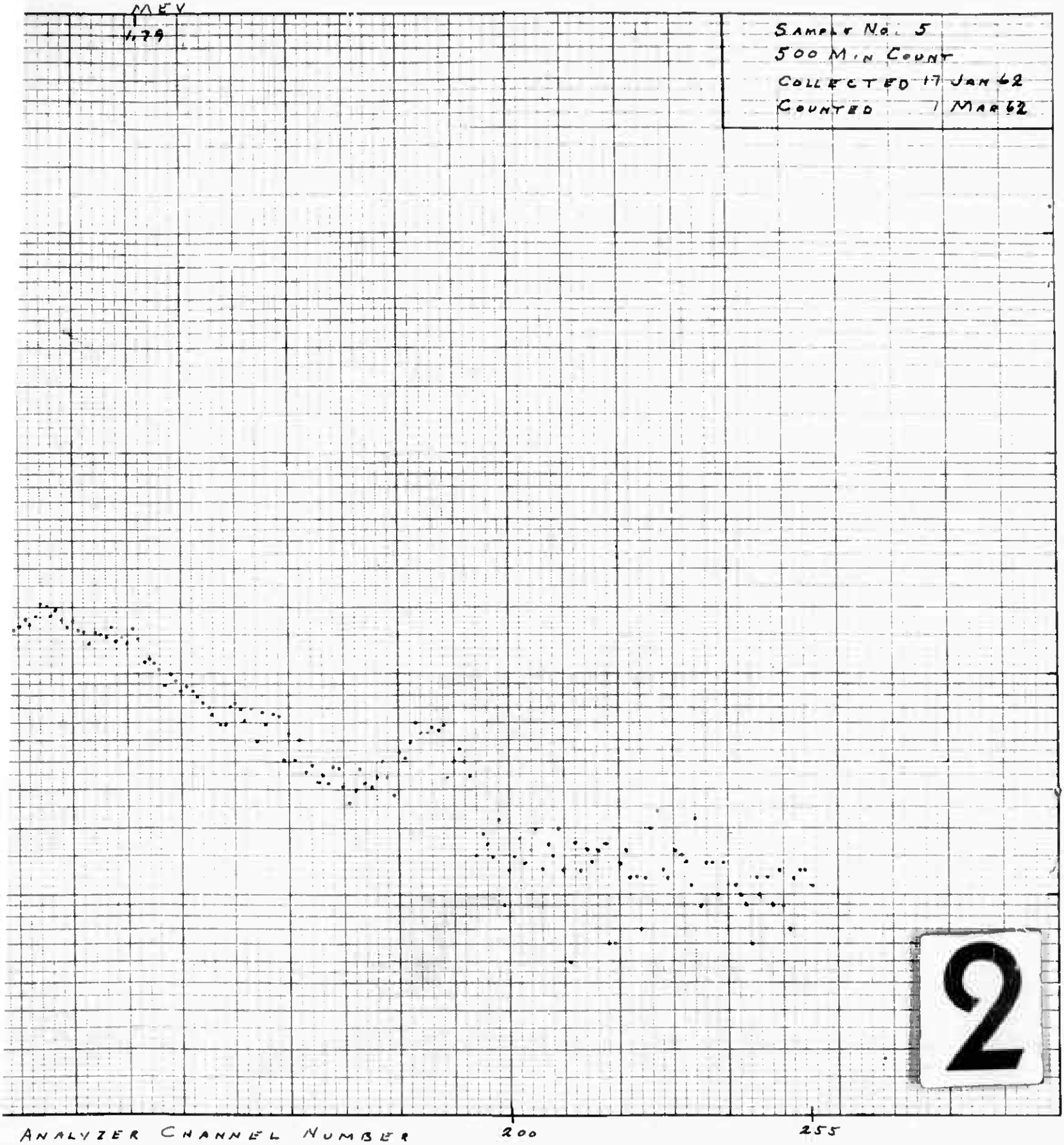
MEV
1.79
SAMPLE NO. 5
500 MIN COUNT
COLLECTED 17 JAN 62
COUNTED 1 MAR 62
2
ANALYZER CHANNEL NUMBER
200
255

Fig. 31

Sample No. 5
500 Min Count
Collected 17 Jan 62
Counted 1 Mar 62

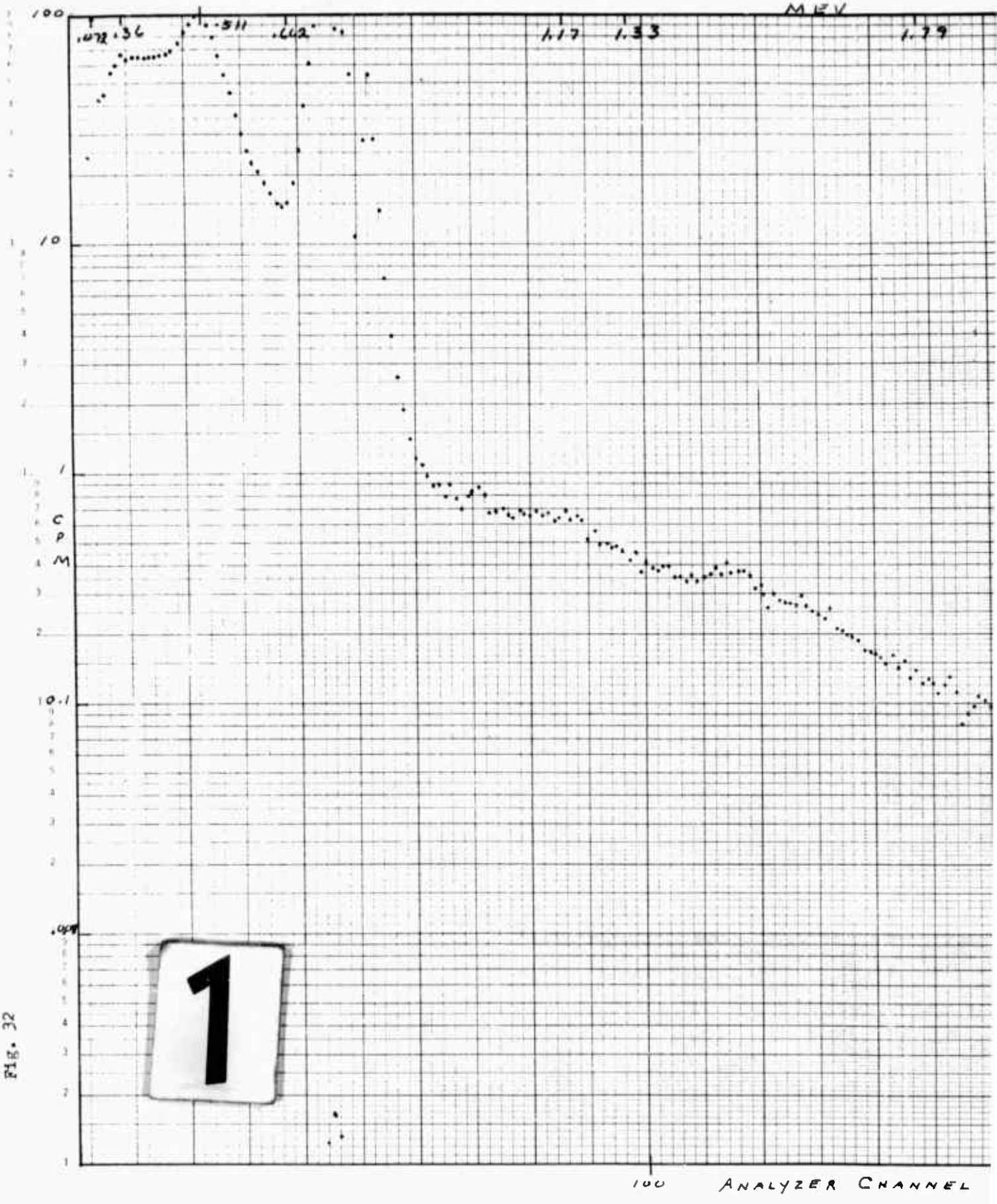
MEV
.072
.36
.511
.662
1.17
1.33
1.79
100
10
1
.1
CPM
100
ANALYZER CHANNEL

FIG. 32

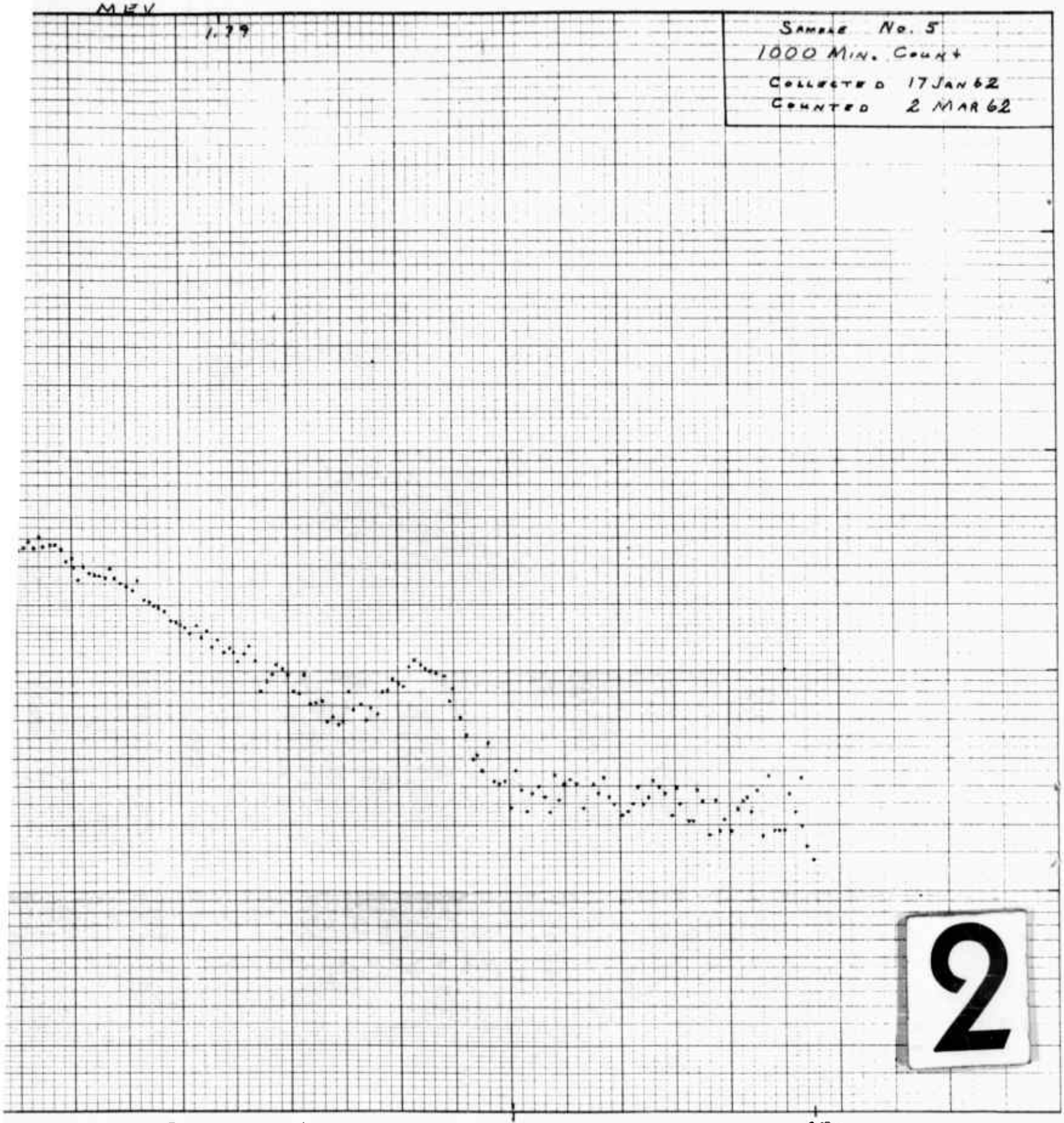
MEV
1.79
SAMPLE No. 5
1000 MIN. COUNT
COLLECTED 17 JAN 62
COUNTED 2 MAR 62
2
ANALYZER CHANNEL NUMBER
200
255

Fig. 32

Sample No. 5
1000 Min Count
Collected 17 Jan 62
Counted 2 Mar 62

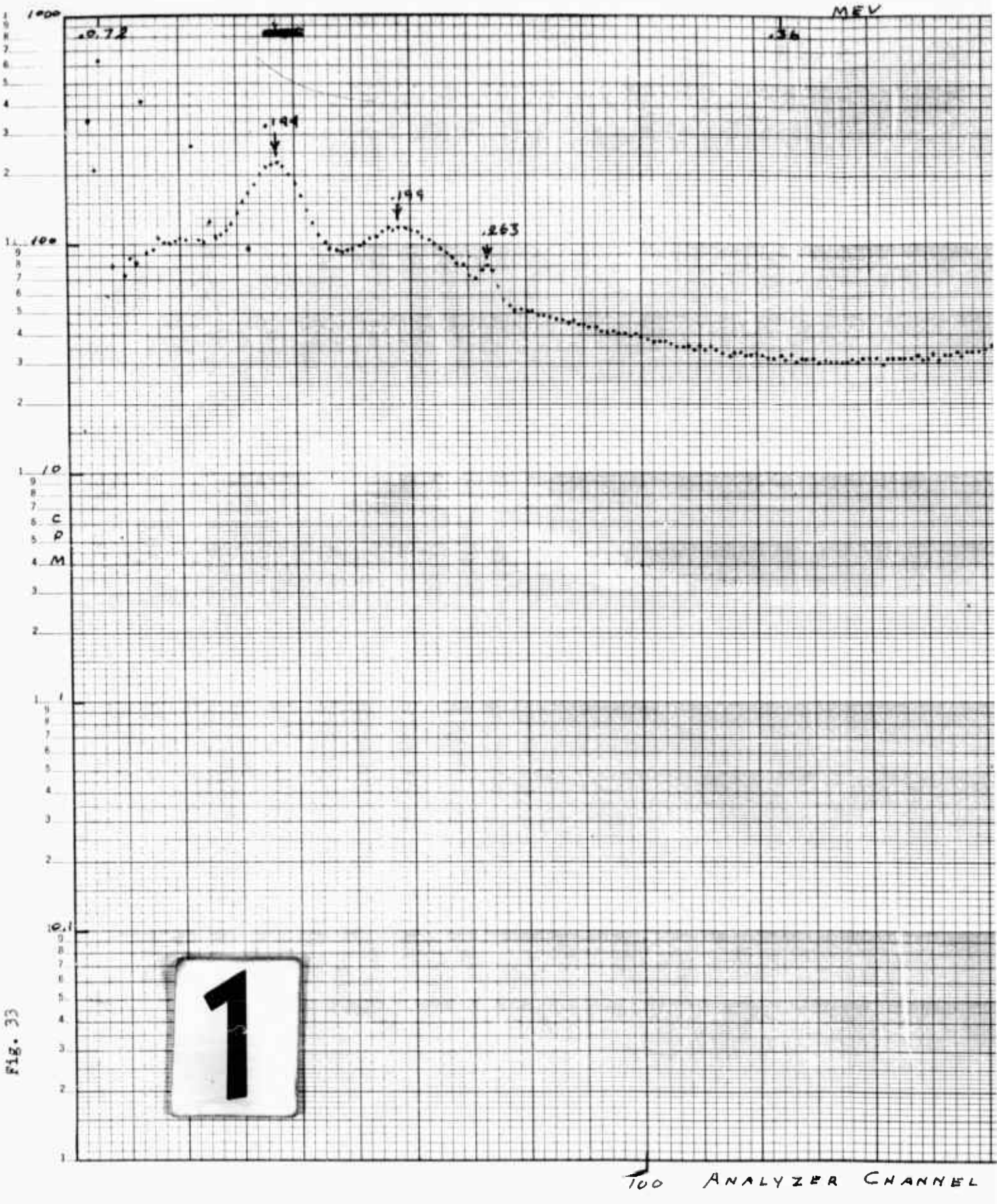
MEV
.072
.36
.194
.199
.263
1000
100
10
1
C
P
M
0.1
100
ANALYZER CHANNEL

Fig. 33

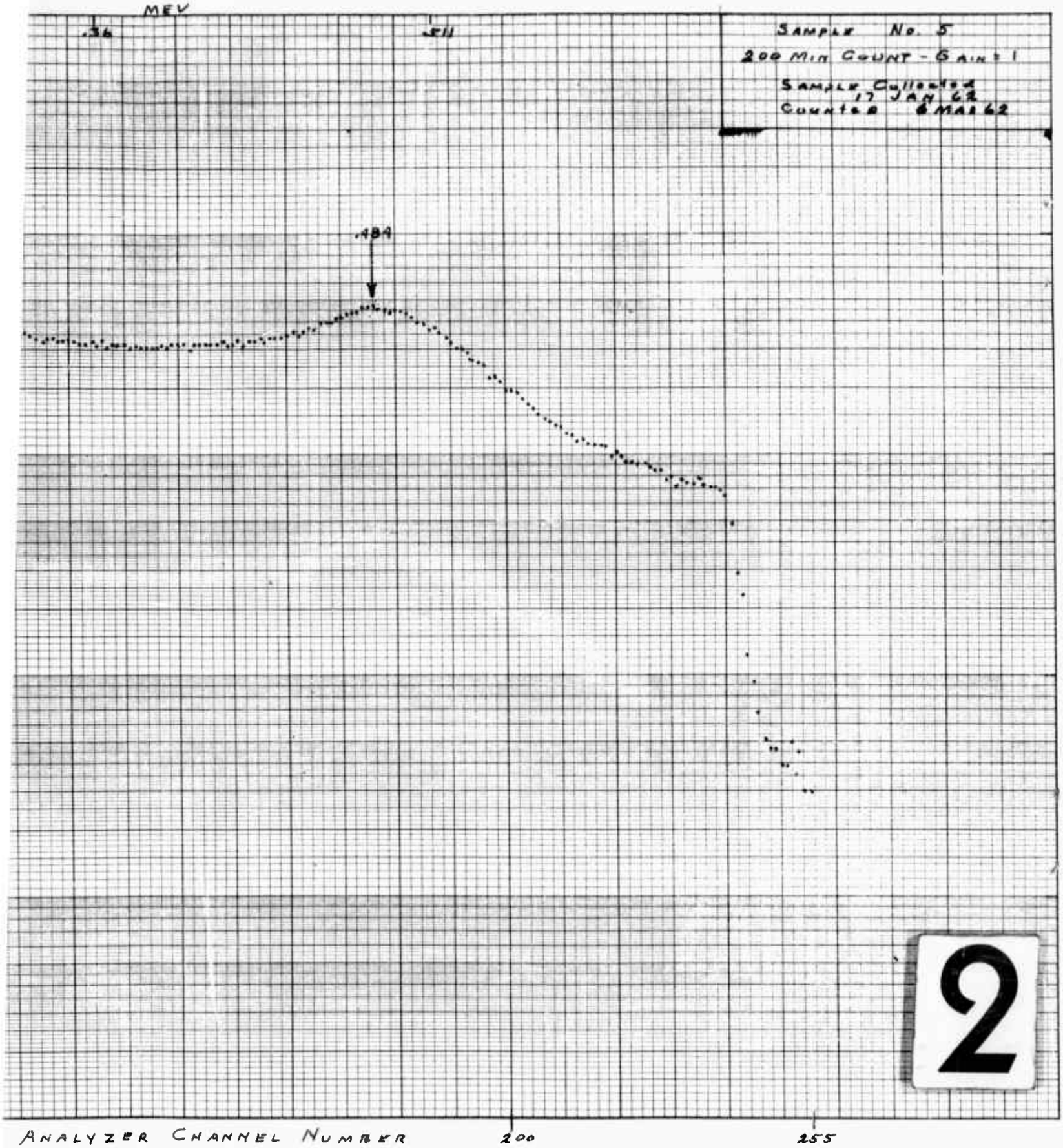
MEV
.36
.511
.484
SAMPLE No. 5
200 MIN COUNT - GAIN 1
SAMPLE COLLECTED
17 JAN 62
COUNTED 8 MAR 62
2
ANALYZER CHANNEL NUMBER
200
255

Fig. 33

Sample No. 5
200 Min Count
Cain = 1
Collected 17 Jan 62
Counted 6 Mar 62

GNE/Phys/62-2

Sample No. 6

Collection Data:

Sample Collected 0822-1130/23 Jan 62.
Weather: Clear and cold; Temp=15°F; Wind=7 knots WSW.

Charging potential	20.3KV
Collection potential	17.3KV
Ionization current	20.0ma
Volume flow rate of air	44.5 m^3/minute
Collection time	188 minutes
Total air sampled	8,357 m^3

This collection was made with the collection plates wrapped with "Handy Wrap." The Gelman Air Sampler filter in the effluent air stream indicated rather heavy collection indicating an inefficient sample collection.

Analysis Data:

Date	Integral Count Rate* Counts/min/m^3 of Air	Counting Time	Remarks
24/1/62	.0096	100 min	Amp gain=1/4:100
26/1/62	.0097	10 min	Amp gain=1/4:100

* Selective solubility fractionation would not have degraded this sample since it was collected directly on the plastic foil and the entire plastic foil sample was counted. The sample loss evidenced by the Gelman post-sampler caused a serious error in the quantitative validity of the sample and the sample was discarded. This analysis portrays the decrease in collection caused by the dielectric foil.

Sample No. 7

Collection Data:

Sample collected 0730-1330/29 Jan 62.
Weather: Cloudy and cold; Temp=27°F; Wind=8 knots SW;
Intermittent snow flurries.

Charging potential	23.2KV
Collection potential	18.3KV
Ionization current	18.8ma
Volume flow rate of air	49.5 m^3/minute
Collection time	360 minutes
Total air sampled	17,820 m^3

The snow flurries caused serious arcing in the charging section. One light bulb was removed from the variable current limiting network. This decreased the maximum power supply output capability to 27.5KV/18.8ma.

Analysis Data:

Date	Integral Count Rate* Counts/min/m^3 of Air	Counting Time	Remarks
30/1/62	0.233	10 min	Amp gain=1/4:100
2/2/62	0.199	100 min	Amp gain=1/4:100
9/2/62	0.205	100 min	Amp gain=1/4:100
17/2/62	0.176	100 min	Amp gain=1/4:100
22/2/62	0.165	100 min	Amp gain=1/4:100

* The integral count rate of this sample is in error by virtue of the fractionation phenomenon.

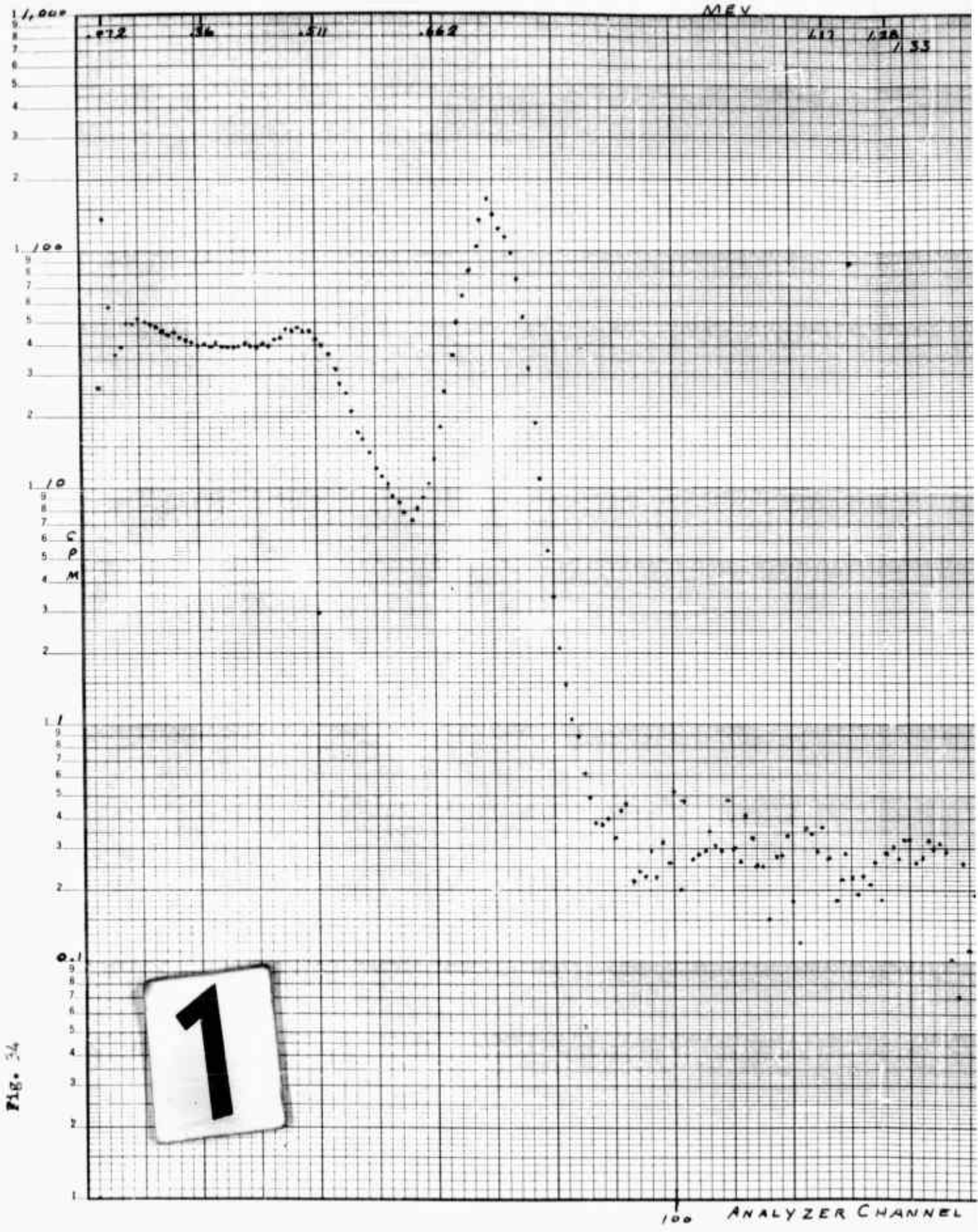
MEV
.272
.36
.511
.662
1.17
1.28
1.33
11,000
1,000
100
10
1
0.1
CPM
100
ANALYZER CHANNEL

Fig. 34

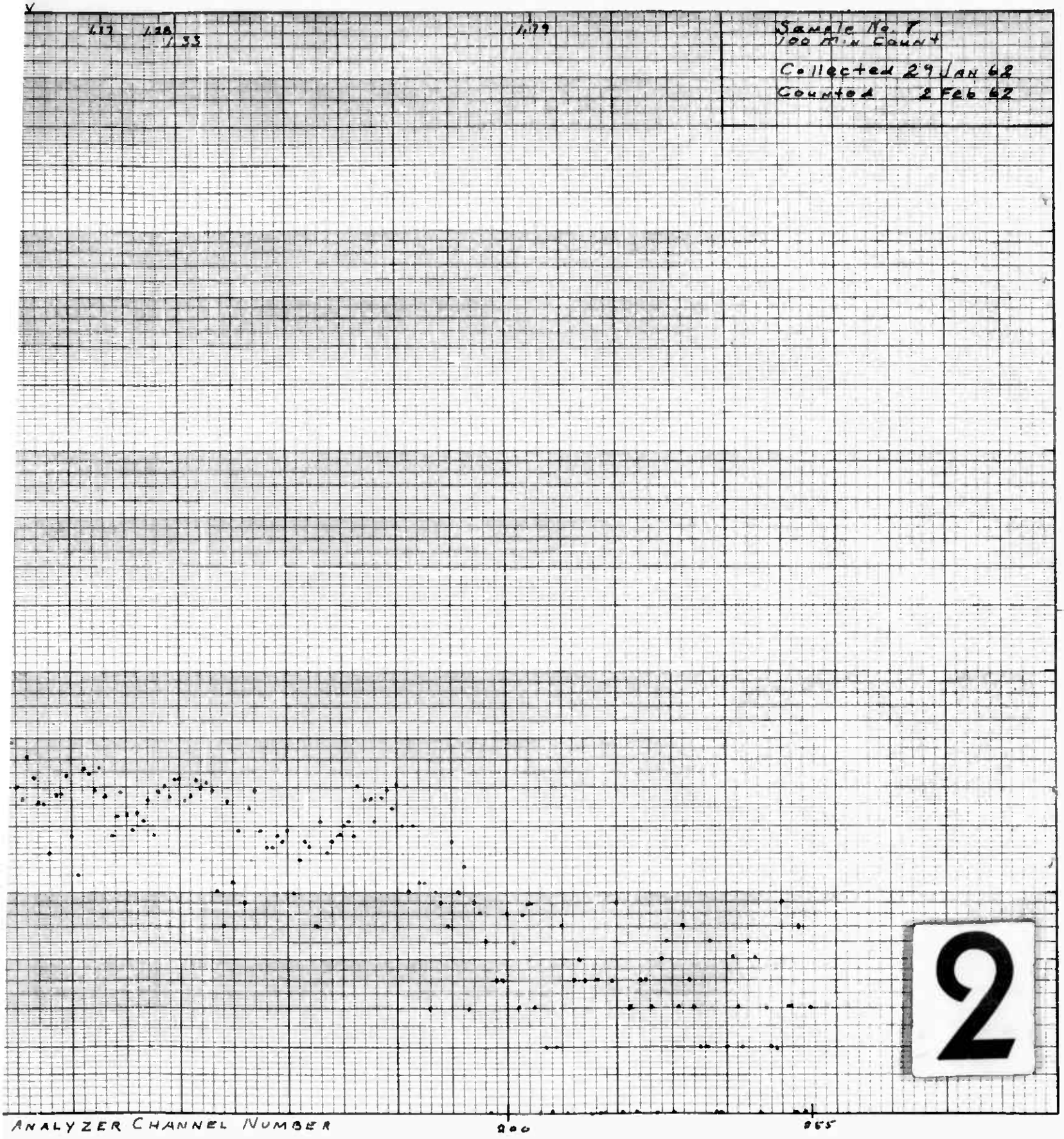
Sample No. 7
100 Min Count
Collected 29 JAN 62
Counted 2 Feb 62
ANALYZER CHANNEL NUMBER
800
865

Fig. 34

Sample No. 7
100 Min Count
Collected 29 Jan 62
Counted 2 Feb 62

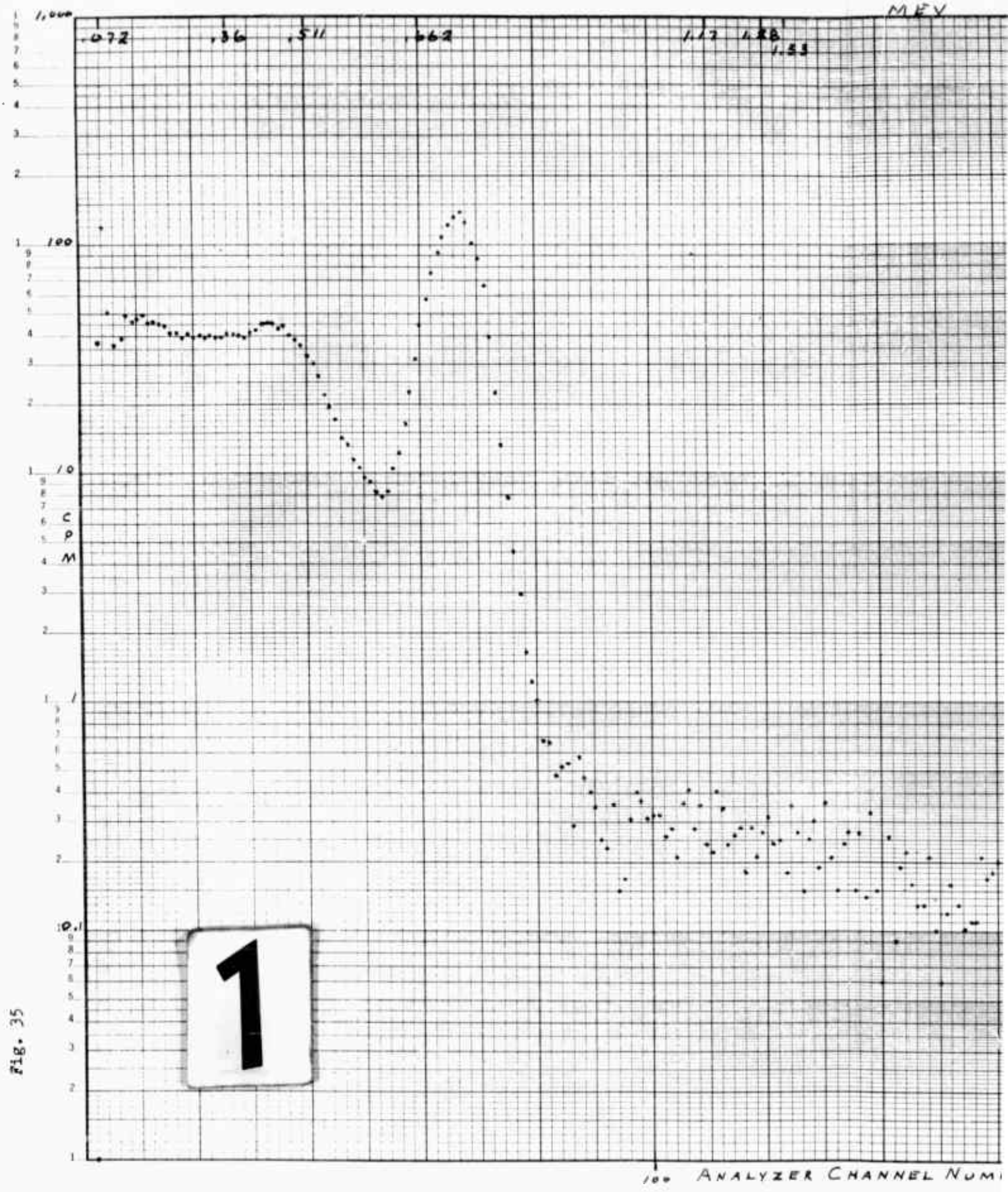
MEV
.072
.36
.511
.662
1.17
1.28
1.53
1,000
100
10
1
0.1
C
P
M
100
ANALYZER CHANNEL NUMB
1

Fig. 35

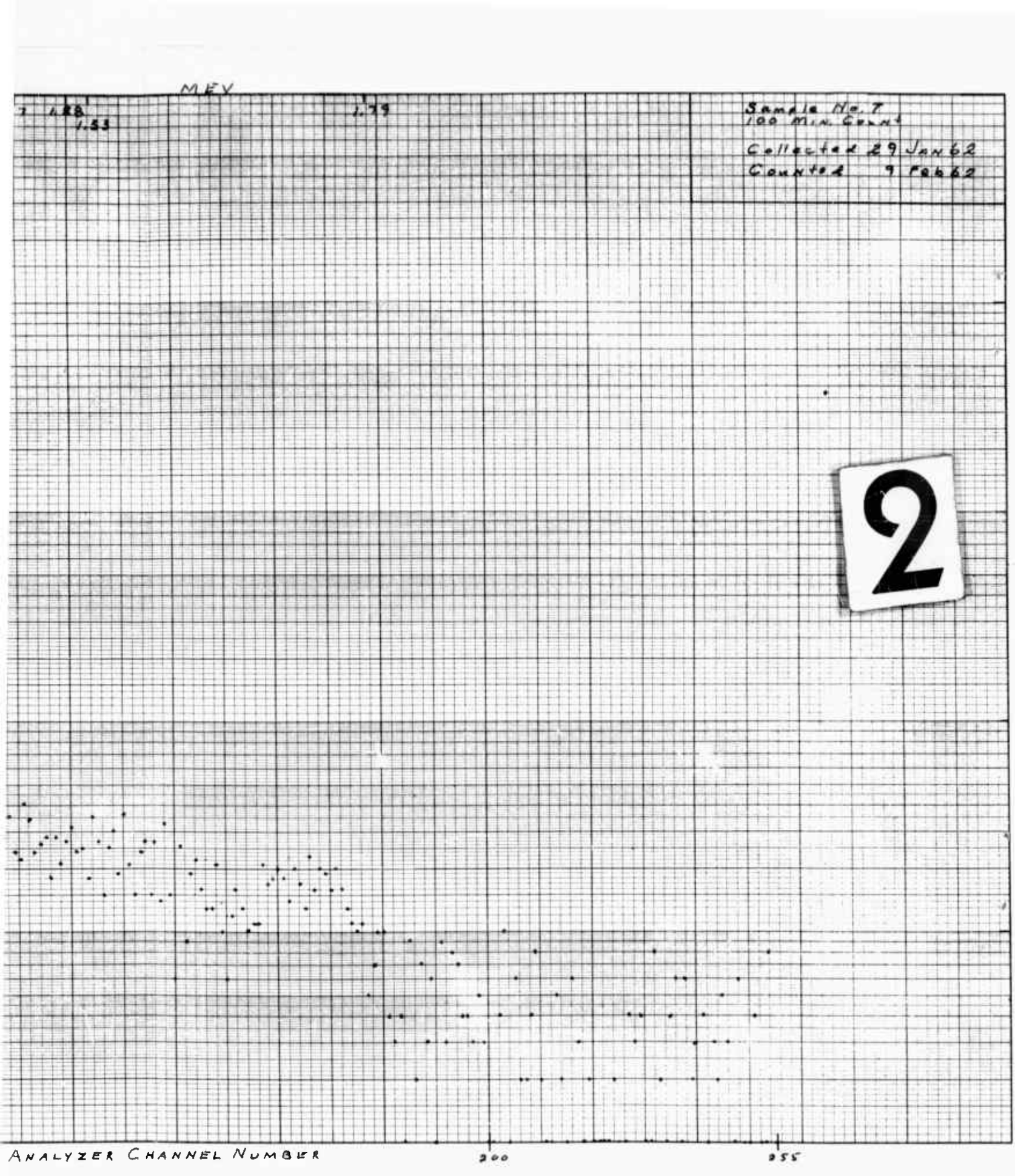
MEV
1.88
1.53
1.79
Sample No. 7
100 MIN. COUNT
Collected 29 JAN 62
Counted 9 FEB 62
2
ANALYZER CHANNEL NUMBER
200
255

Fig. 35

Sample No. 7
100 Min Count
Collected 29 Jan 62
Counted 9 Feb 62

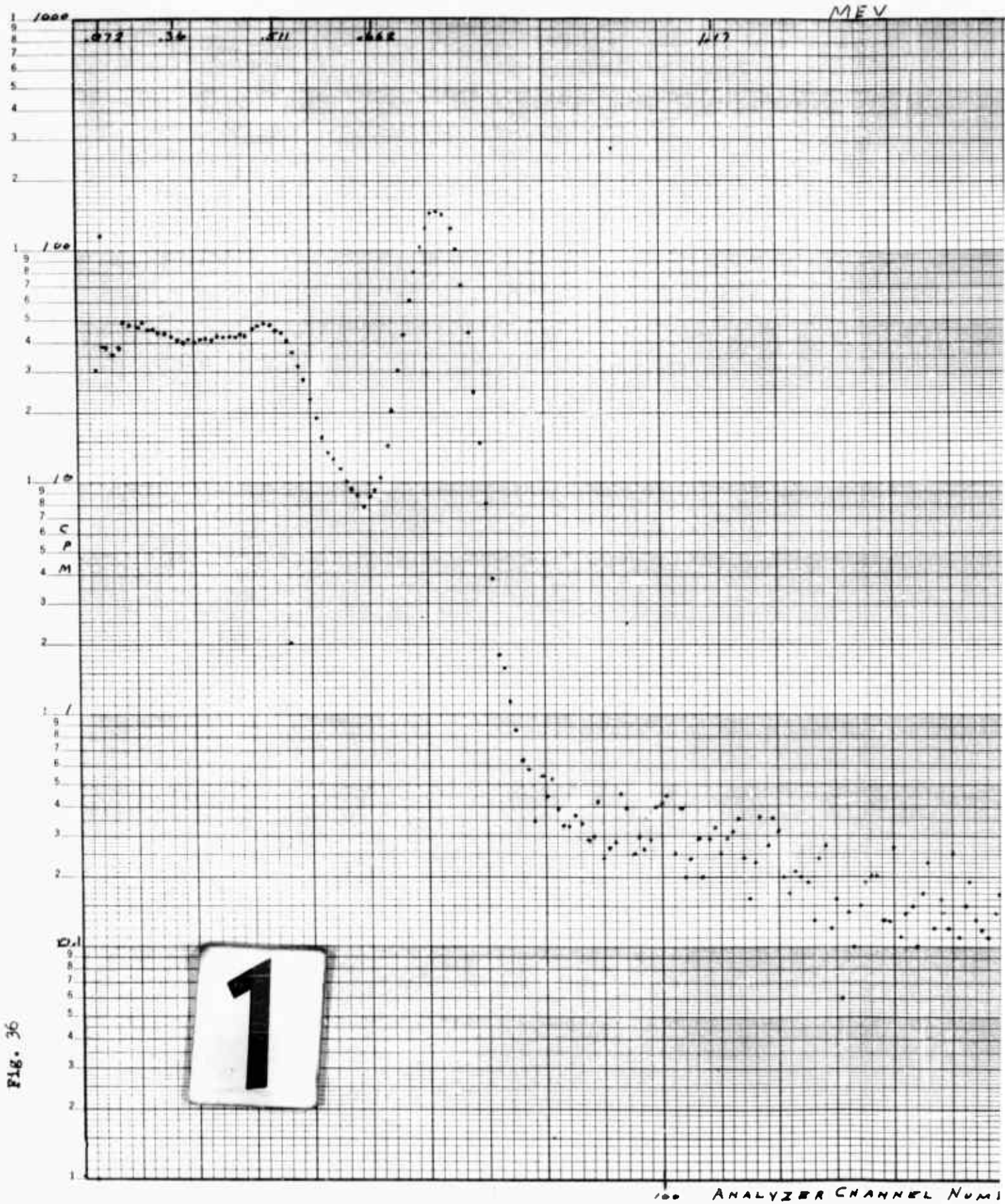

Fig. 36

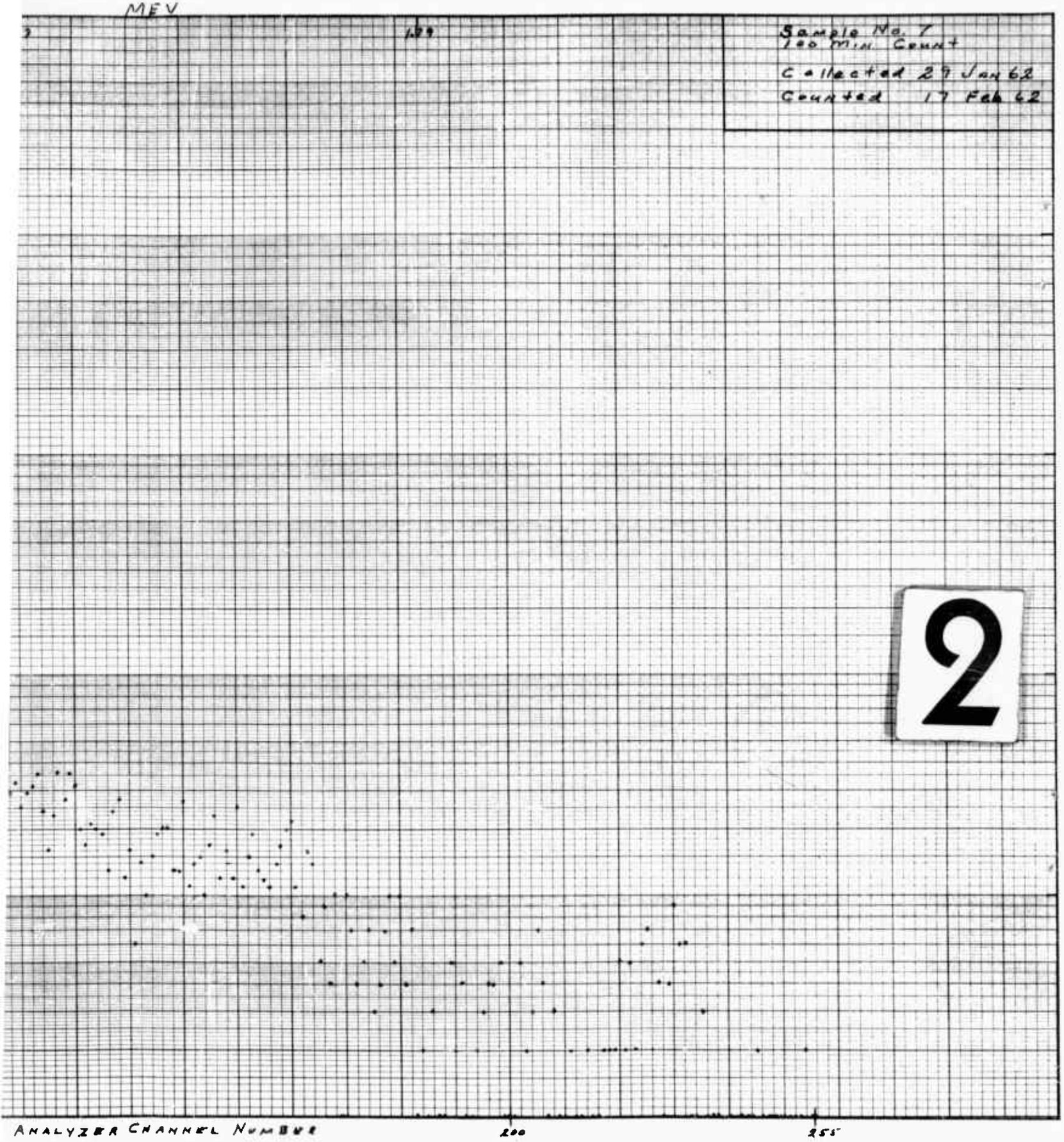
MEV
1.29
Sample No. 7
100 Min. Count
Collected 27 Jan 62
Counted 17 Feb 62
2
ANALYZER CHANNEL NUMBER
200
255

Fig. 36

Sample No. 7
100 Min Count
Collected 29 Jan 62
Counted 17 Feb 62

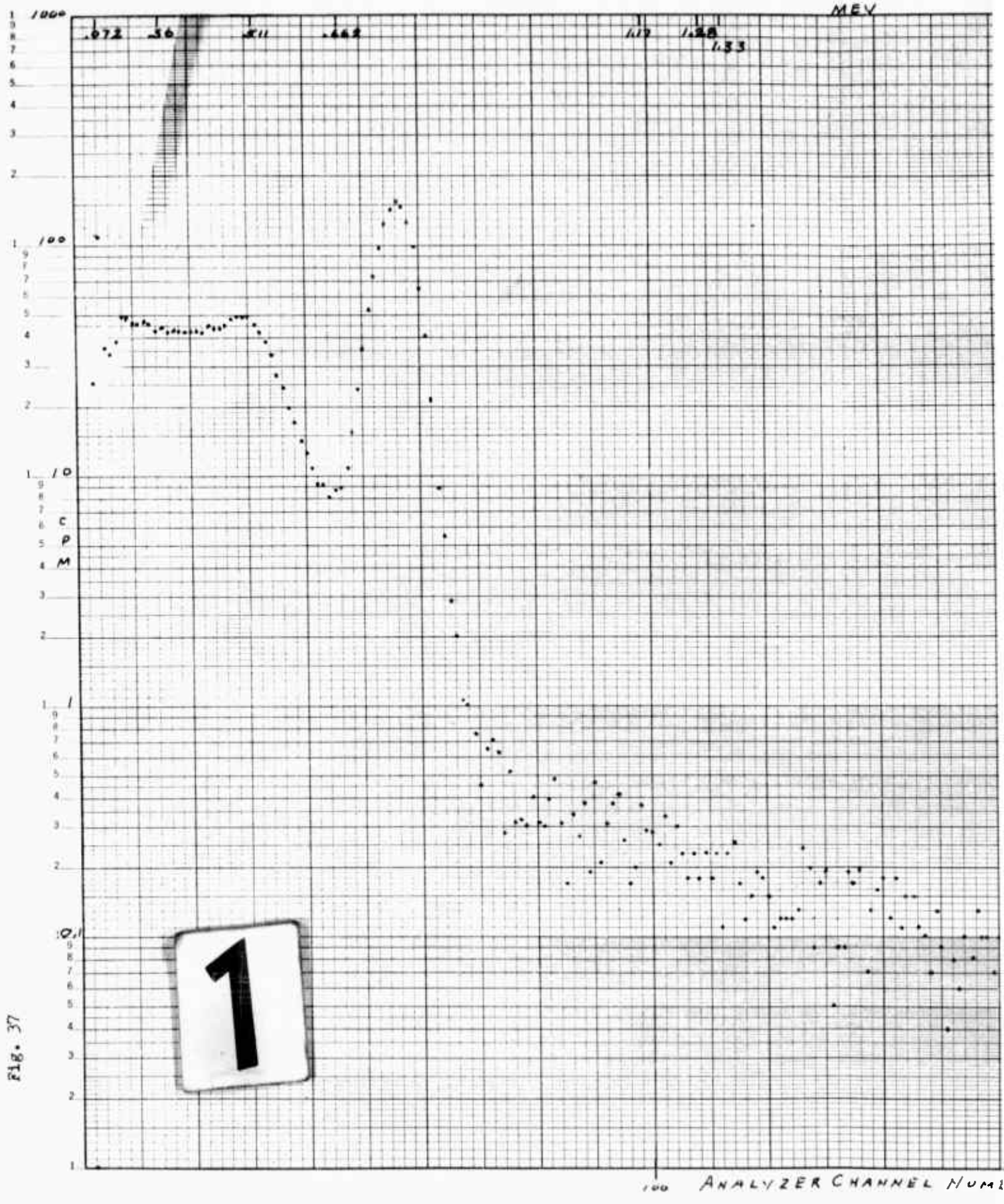
MEV
.072
.36
.511
.662
1.17
1.28
1.33
1000
100
10
CPM
1
0.1
1
100
ANALYZER CHANNEL NUMB

Fig. 37

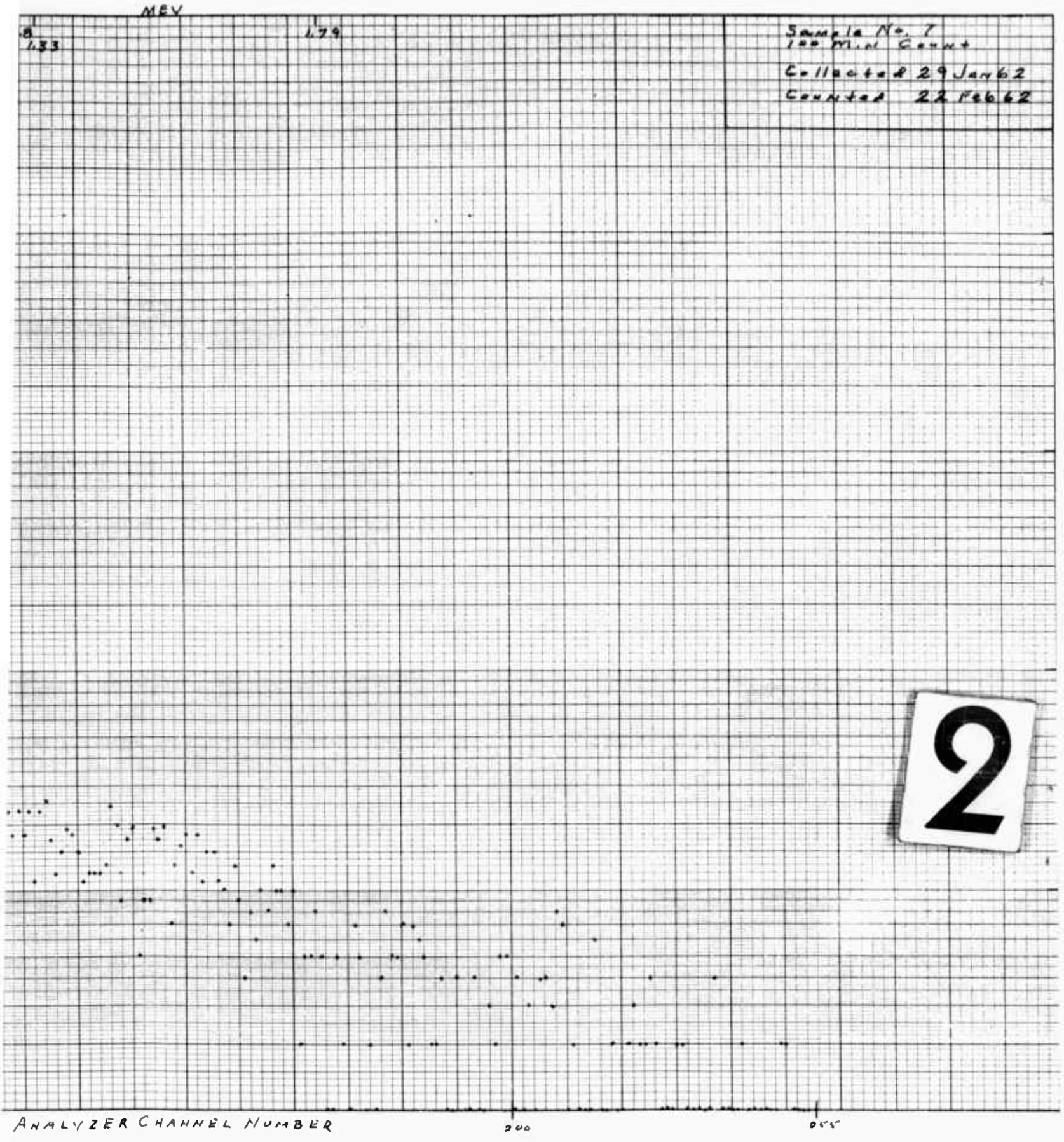
MEV
1.33
1.79
Sample No. 7
100 Min Count
Collected 29 Jan 62
Counted 22 Feb 62
2
ANALYZER CHANNEL NUMBER
200

Fig. 37

Sample No. 7
100 Min Count
Collected 29 Jan 62
Counted 22 Feb 62

Sample No. 8

Collection Data:

Sample collected 0700-1900/6 Feb 62.
Weather: Cloudy and cold; Temp=9°F; Wind=20 knots NE;
Intermittent snow flurries.

Charging potential	24.7KV
Collection potential	20.5KV
Ionization current	19.3ma
Volume flow rate of air	42.6 m^3/minute
Collection time	720 minutes
Total air sampled	30,650 m^3

The snow flurries caused aerious arcing. An examination of the current limiting resistors showed that they were seriously burned and had increased in resistance. This had caused a decrease in the available charging potential and ionization current.

Analysis Data:

Date	Integral Count Rate* Counts/min/m^3 of Air	Counting Time	Remarks
8/2/62	0.157	100 min	above 5μ**
	0.131	100 min	3μ to 5μ**
	0.027	100 min	1.2μ to 3μ**
	0.004	100 min	0.8μ to 1.2μ**
	0.006	100 min	0.45μ to 0.8μ**
	0.017	100 min	0.22μ to 0.45μ**
17/2/62	0.130	100 min	composite sample**
22/2/62	0.144	100 min	composite sample**
26/2/62	0.144	100 min	filtrate residue**
5/3/62	NA***	100 min	Amp gain=1/2:100

* The integral count rate of this sample ia in error by virtue of the fractionation phenomenon.

** The individual filter samples from this collection were counted individually in an attempt to establish a count-rate/particle-size correlation. The results of this analysis are inconclusive since microfilters collect particulates smaller than the filter pore diameter through electrostatic adhesion. The residue from the ten

gallon filtrate was obtained by evaporation and the high count rate of this filtrate residue led to the discovery of the solubility fractionation phenomenon. The composite sample formed from the individual filter samples did not include the filtrate residue.

***The linear amplifier gain was doubled to spread out the spectrum and allow a more detailed examination of the low energy portion of the spectrum.

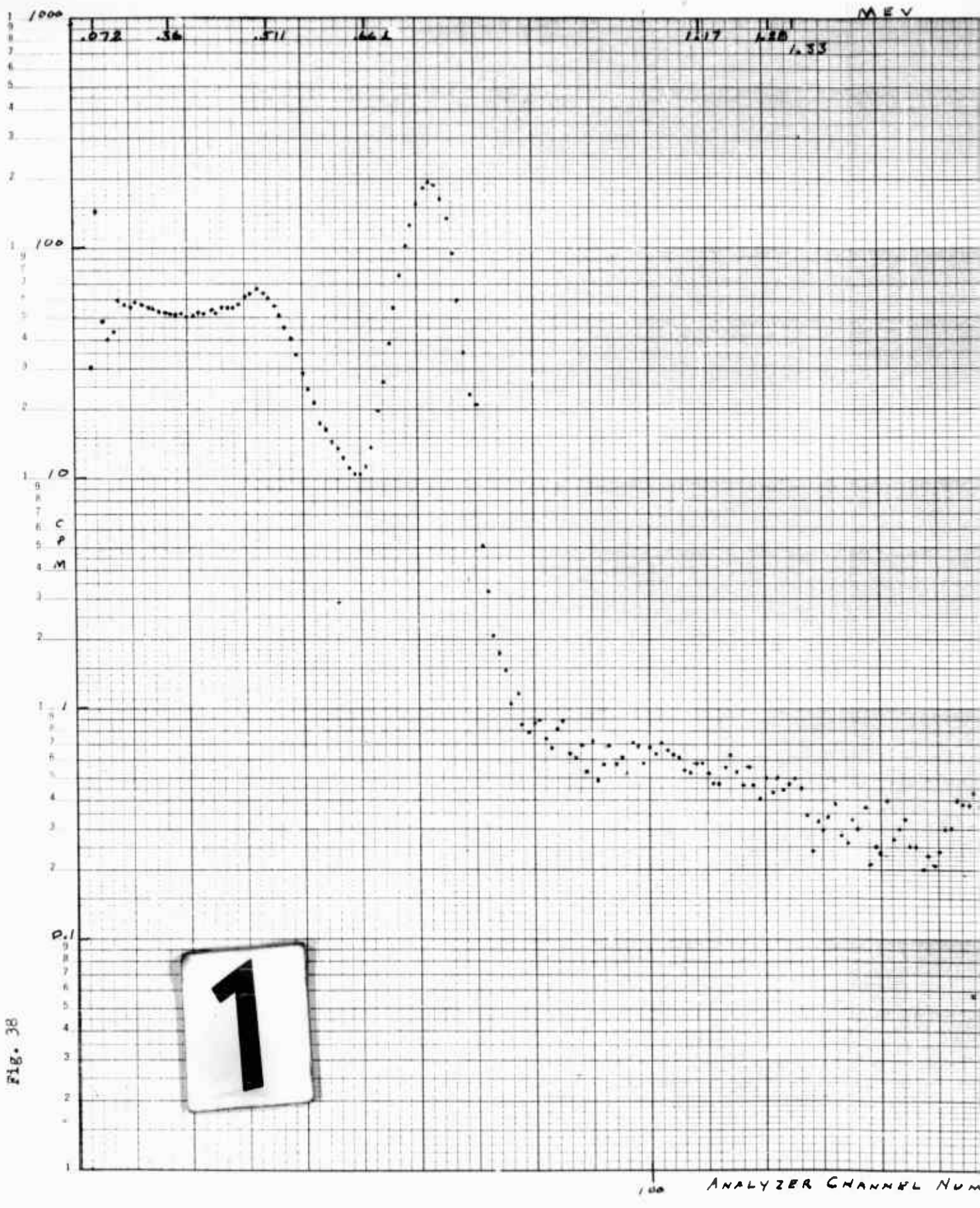
MEV
.072
.36
.511
.662
1.17
1.33
1000
100
10
1
0.1
CPM
ANALYZER CHANNEL NUM

Fig. 38

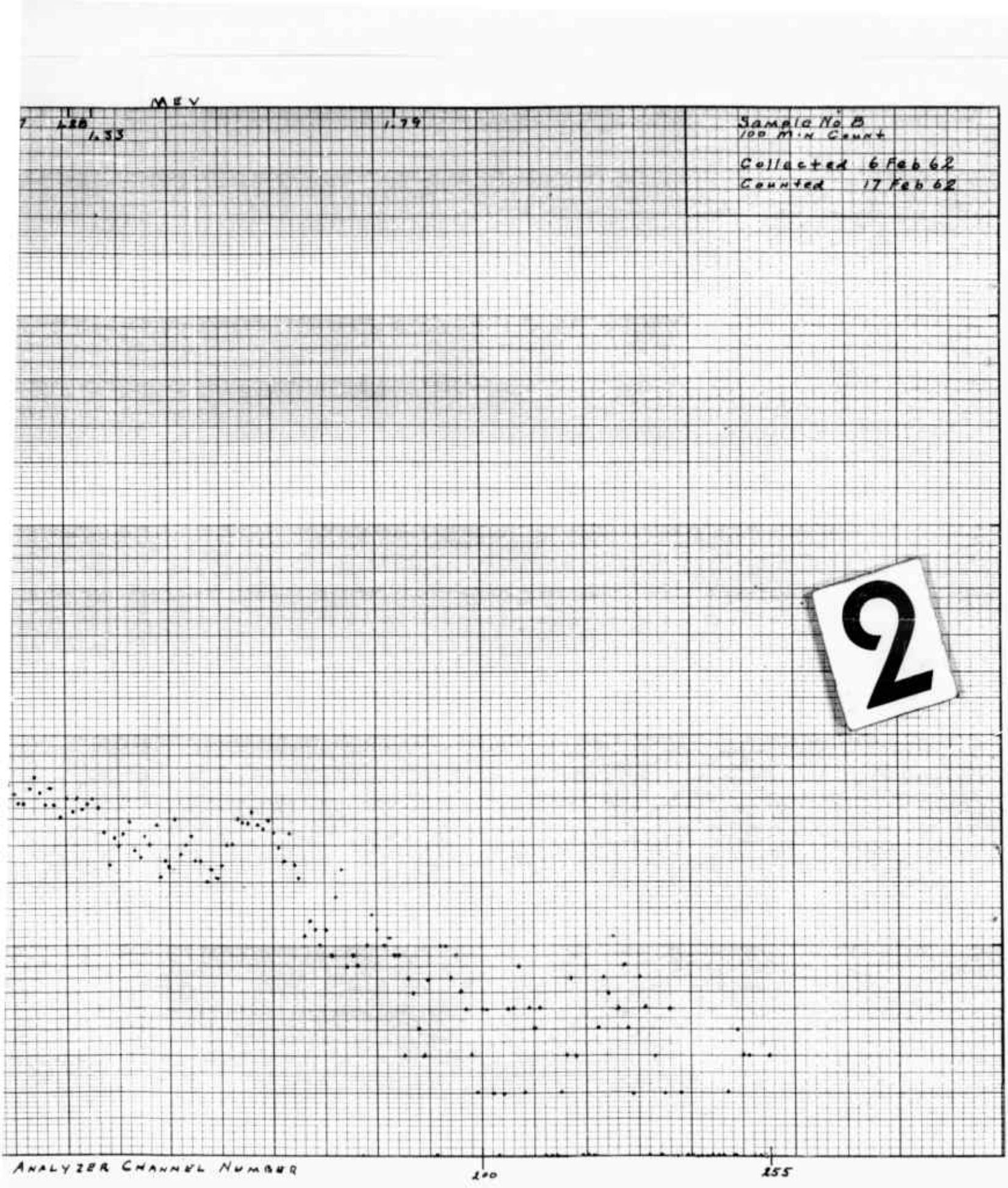
MEV
1.20
1.33
1.79
Sample No B
100 Min Count
Collected 6 Feb 62
Counted 17 Feb 62
2
ANALYZER CHANNEL NUMBER
100
155

Fig. 38

Sample No. 8
100 Min Count
Collected 6 Feb 62
Counted 17 Feb 62

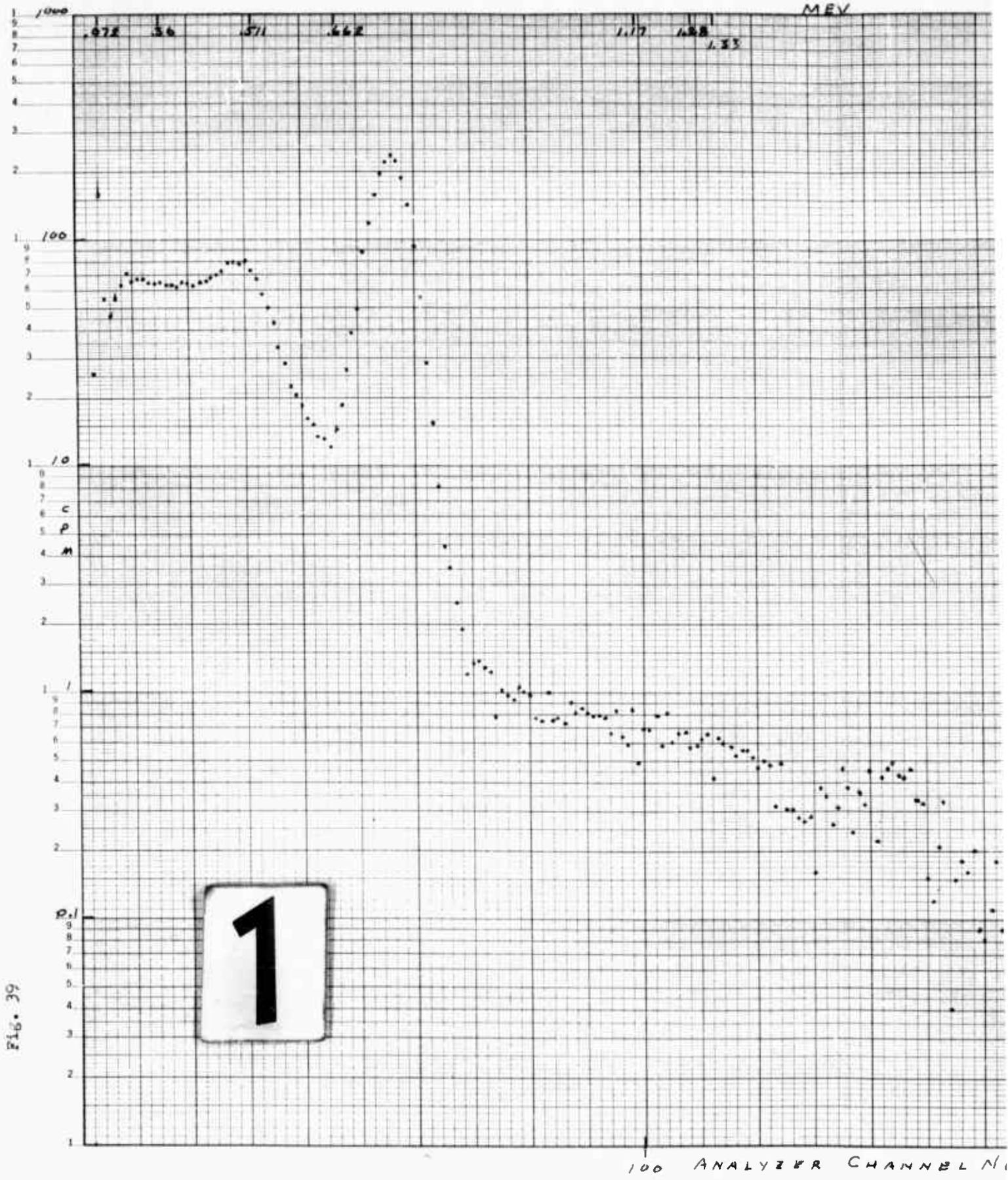
MEV
.072
.36
.511
.662
1.17
1.28
1.33
1,000
100
10
1
0.1
CPM
1
100 ANALYZER CHANNEL N

Fig. 39

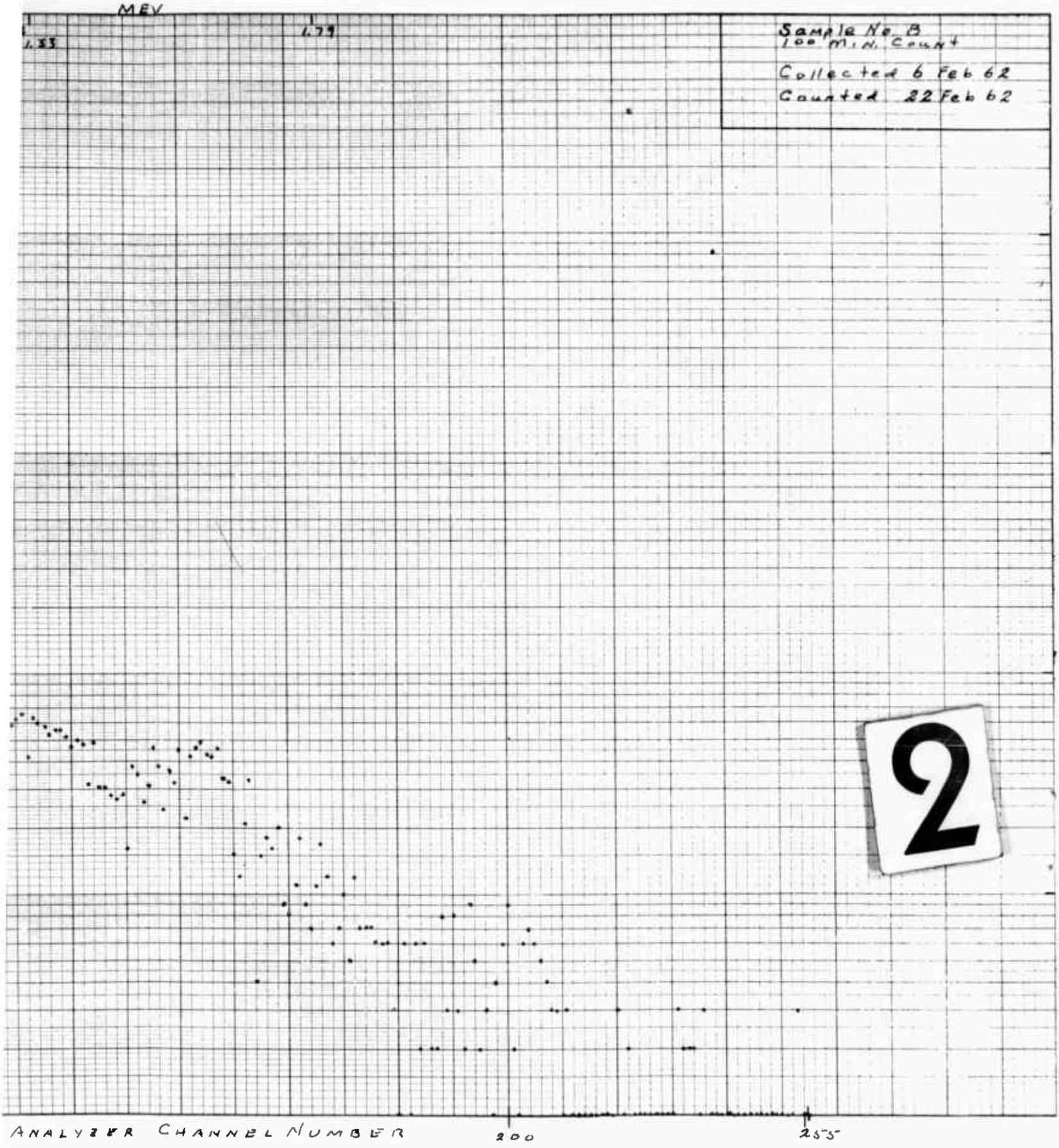
MEV
1.53
1.79
Sample No. B
100 M.N. Count
Collected 6 Feb 62
Counted 22 Feb 62
2
ANALYZER CHANNEL NUMBER
200
255

Fig. 39

Sample No. 8
100 Min Count
Collected 6 Feb 62
Counted 22 Feb 62

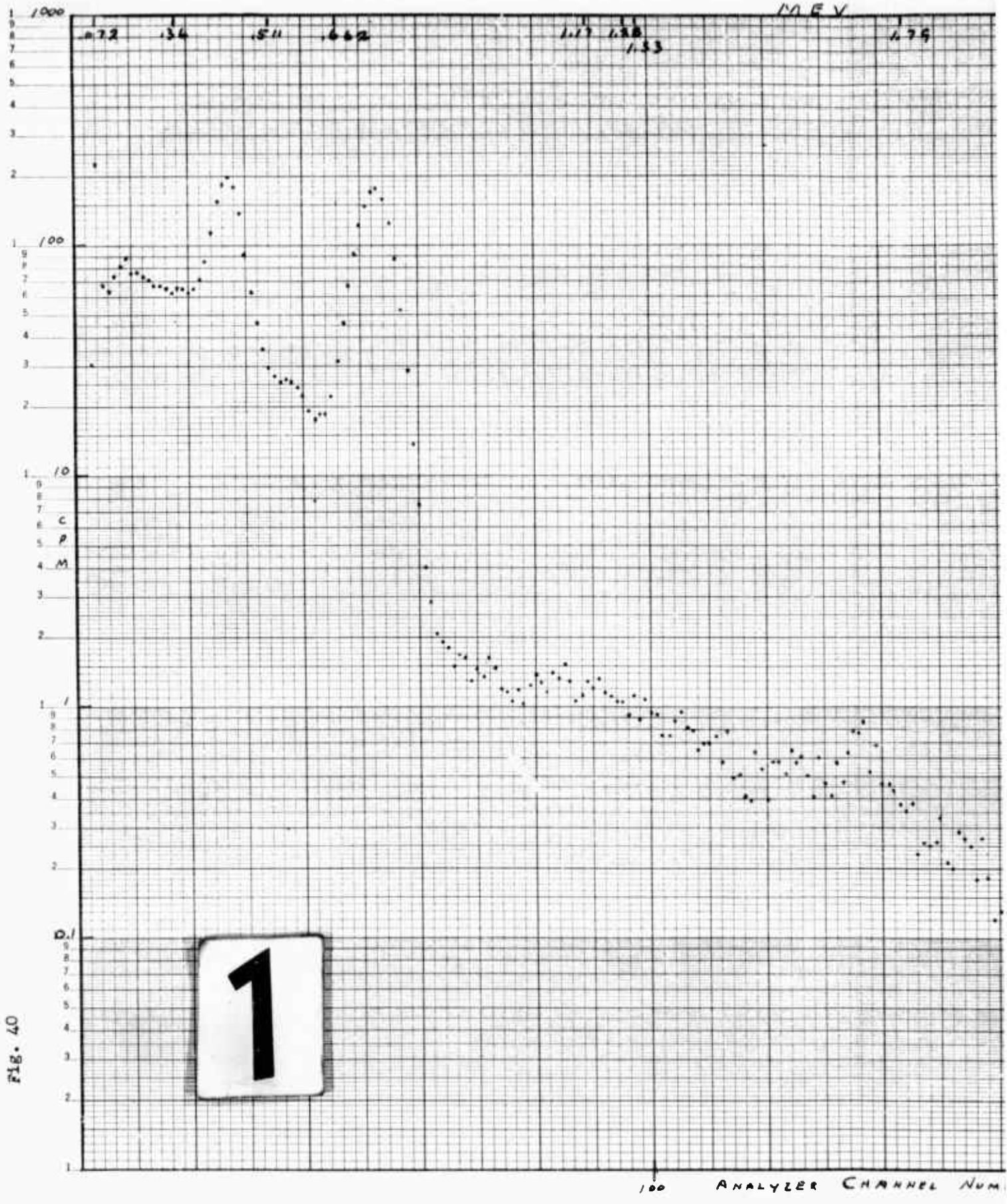
MEV
.72
.84
.511
.662
1.17
1.33
1.76
1000
100
10
1
0.1
C
P
M
100
ANALYZER CHANNEL NUM

Fig. 40

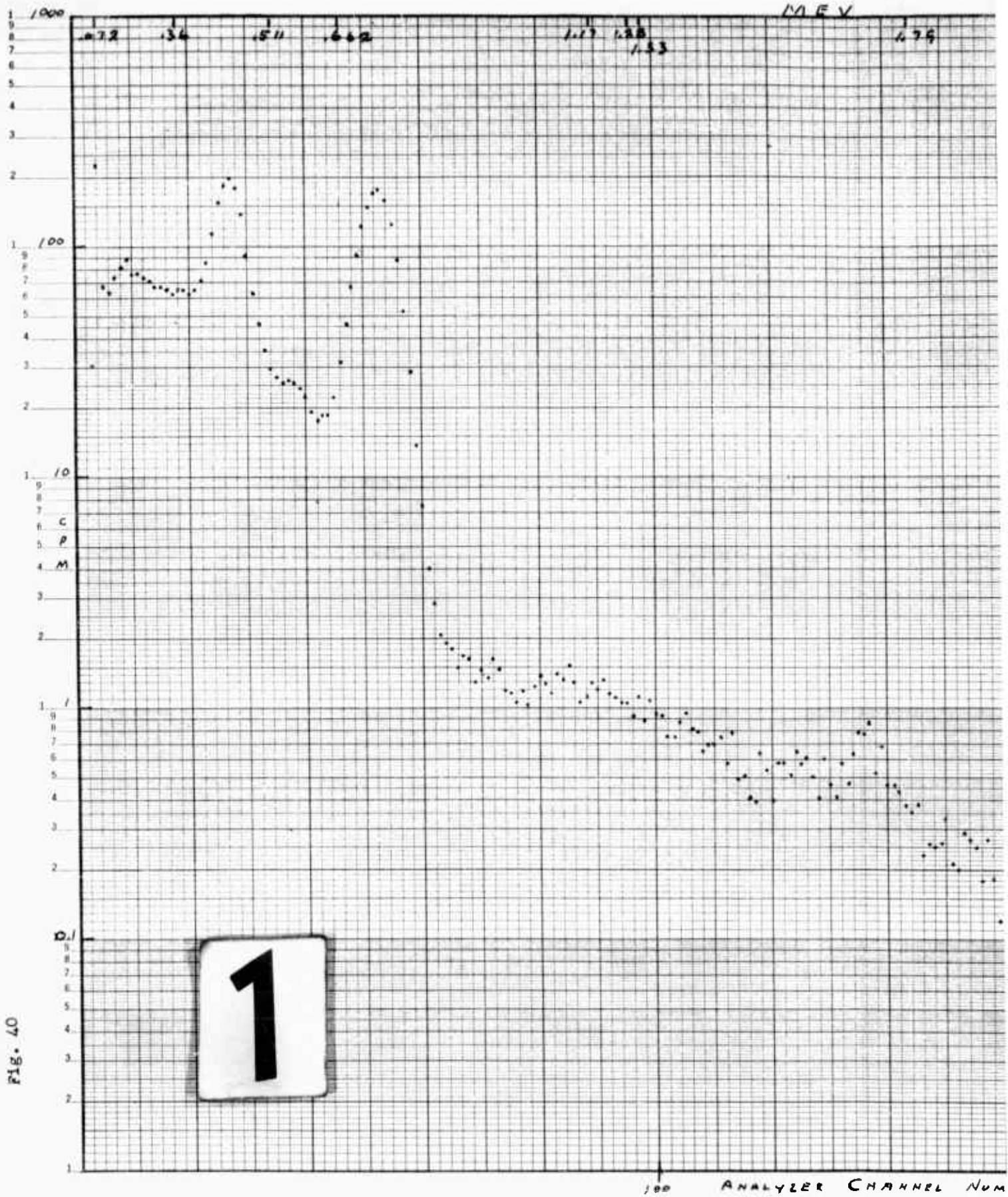
MEV
.172
.34
.511
.662
1.17
1.28
1.33
4.76
1,000
100
10
1
0.1
CPM
100
ANALYZER CHANNEL NUM
1

Fig. 40

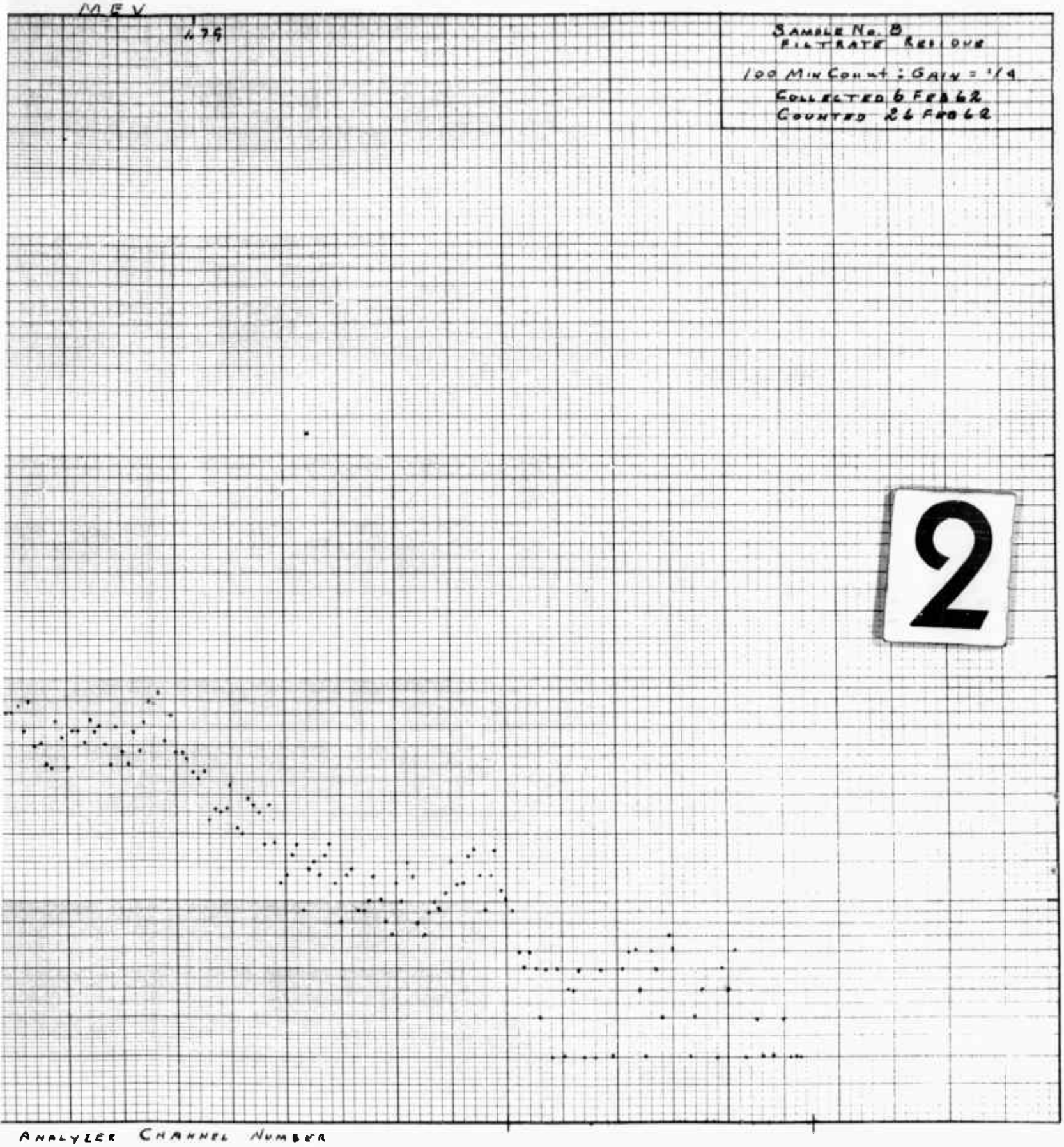
MEV
4.79
SAMPLE No. B
FILTRATE RESIDUE
100 MIN COUNT ; GAIN = 1/4
COLLECTED 6 FEB 62
COUNTED 26 FEB 62
2
ANALYZER CHANNEL NUMBER

Fig. 40

Sample No. 8
Filtrate Residue
100 Min Count
Gain = 1/4
Collected 6 Feb 62
Counted 26 Feb 62

Fig. 41

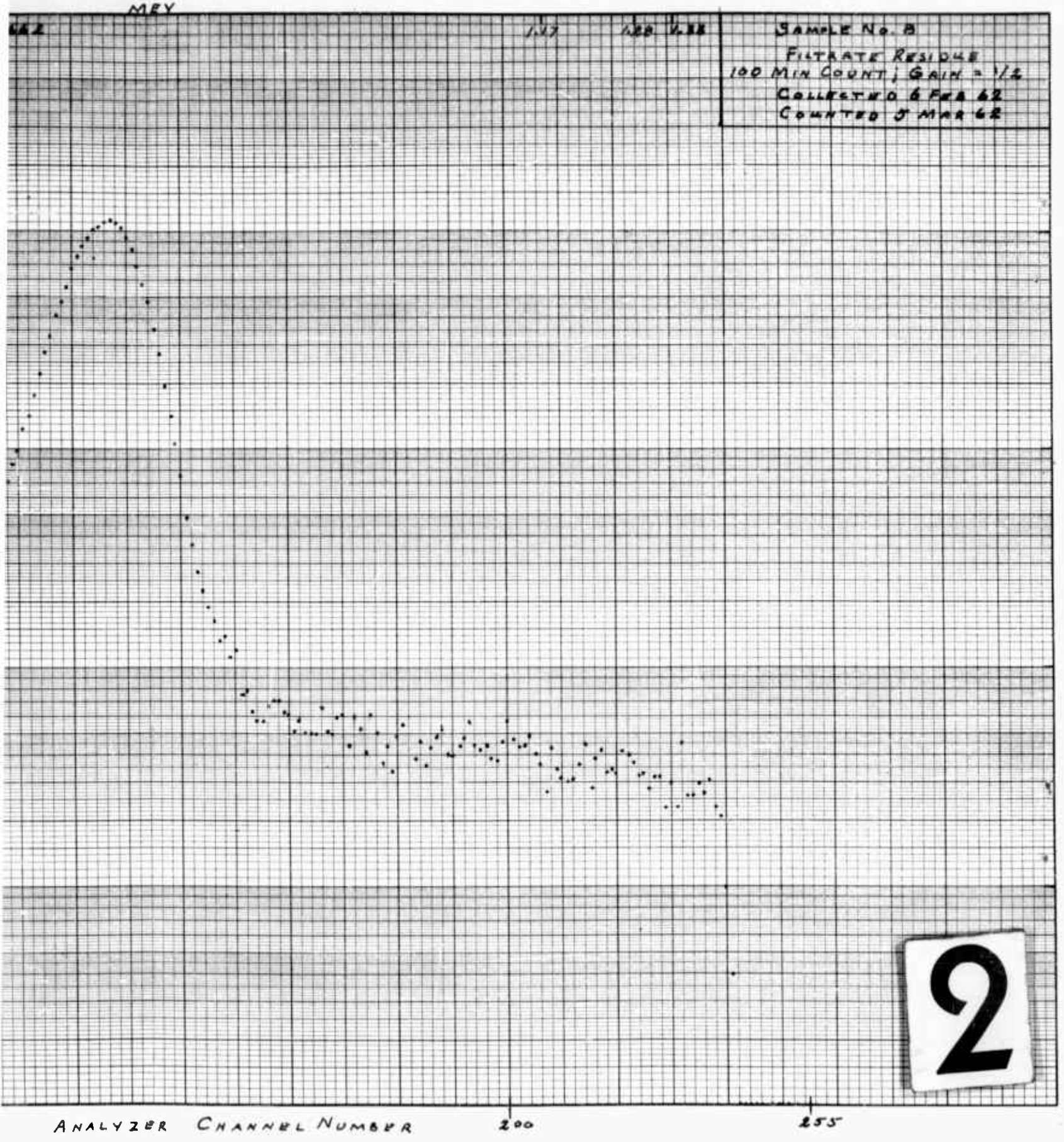
MEY
SAMPLE No. B
FILTRATE RESIDUE
100 MIN COUNT; GAIN = 1/2
COLLECTED 6 FEB 62
COUNTED 7 MAR 62
2
ANALYZER CHANNEL NUMBER
200
255

Fig. 41

Sample No. 8
Filtrate Residue
100 Min Count
Gain = 1/2
Collected 6 Feb 62
Counted 5 Mar 62

Sample No. 9

Collection Data:

Sample collected 0810-1410/19 Feb 62.
Weather: Cloudy and cold; Temp=30°F; Wind=20 knots SW.

Charging potential	22.2KV
Collection potential	16.5KV
Ionization current	20.0ma
Volume flow rate of air	50.5 m^3/minute
Collection time	360 minutes
Total air sampled	18,176 m^3

The current limiting resistor bank was restored to its original value and the charging potential and ionization current capabilities were restored.

Analysis Data:

Date	Integral Count Rate* Counts/min/m^3 of Air	Counting Time	Remarks
20/2/62	0.060	100 min	Amp gain=1/4:100
22/2/62	0.060	100 min	Amp gain=1/4:100

* The integral count rate of this sample is in error by virtue of the fractionation phenomenon.

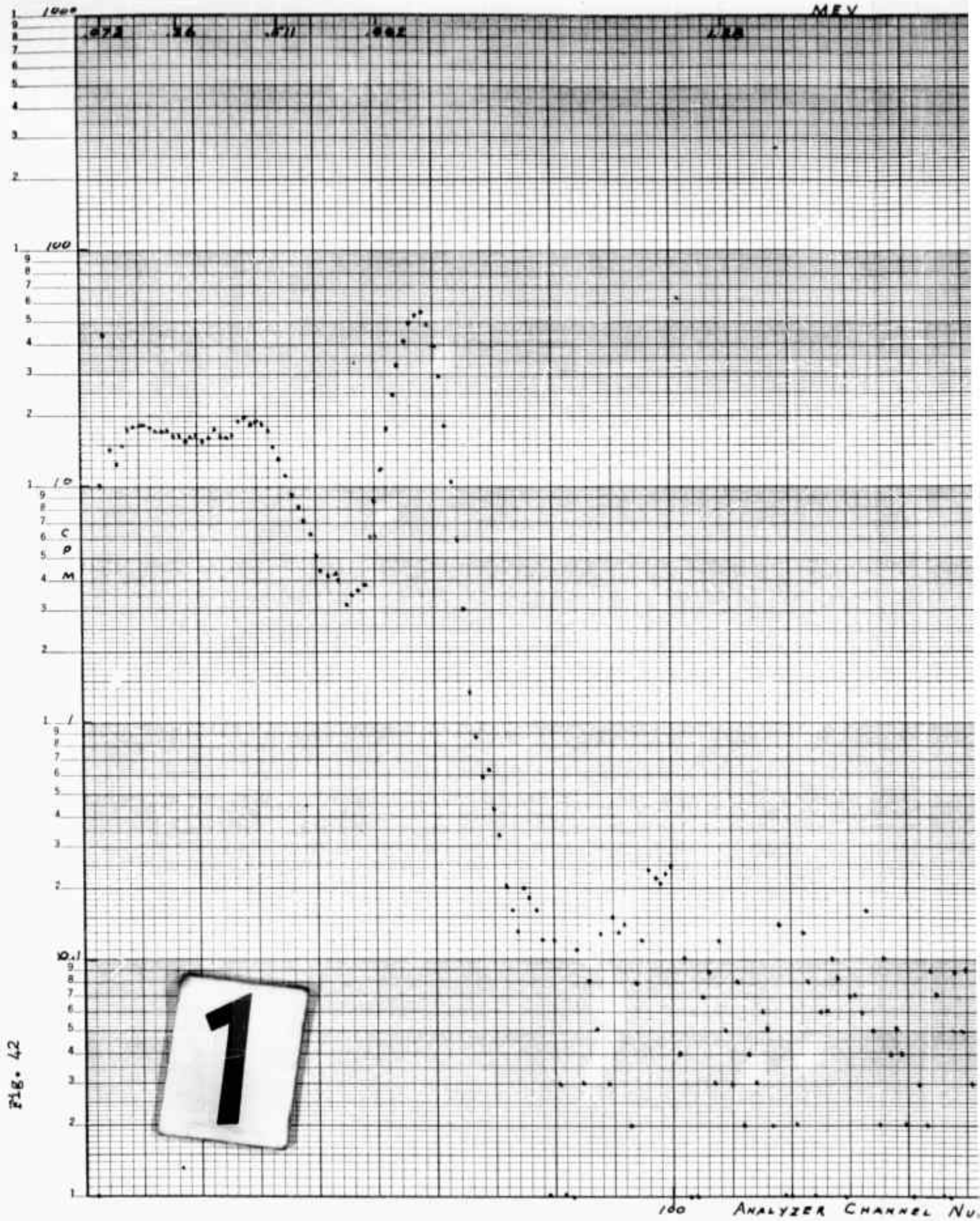
MEV
.078
.36
.811
1.002
1.28
1000
100
10
1
0.1
COUNTS PER MIN
160
ANALYZER CHANNEL NU

Fig. 42

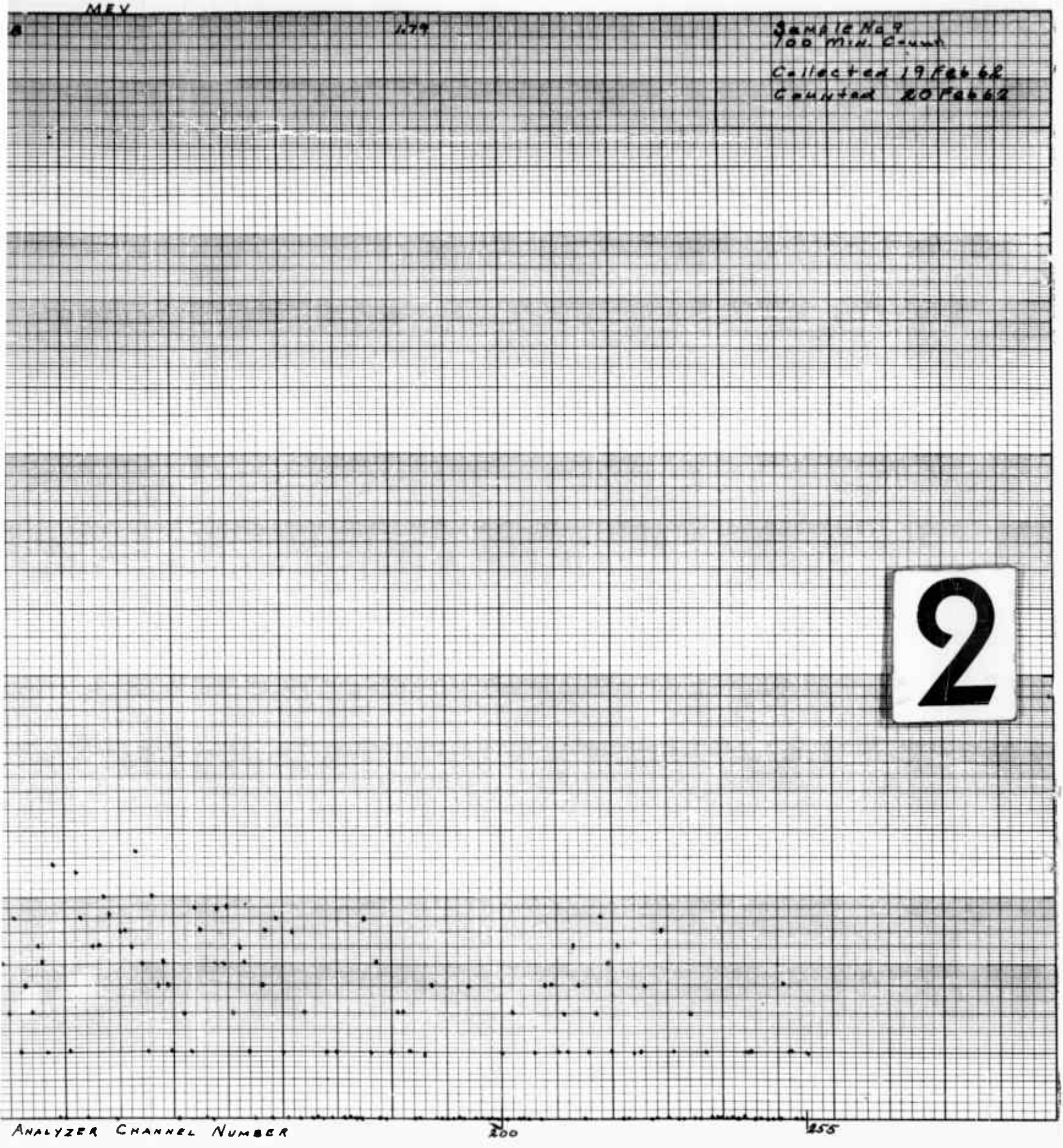
MEV
1.79
Sample No 2
100 min. Count
Collected 19 Feb 62
Counted 20 Feb 62
2
ANALYZER CHANNEL NUMBER
200
255

Fig. 42

Sample No. 9
100 Min Count
Collected 19 Feb 62
Counted 20 Feb 62

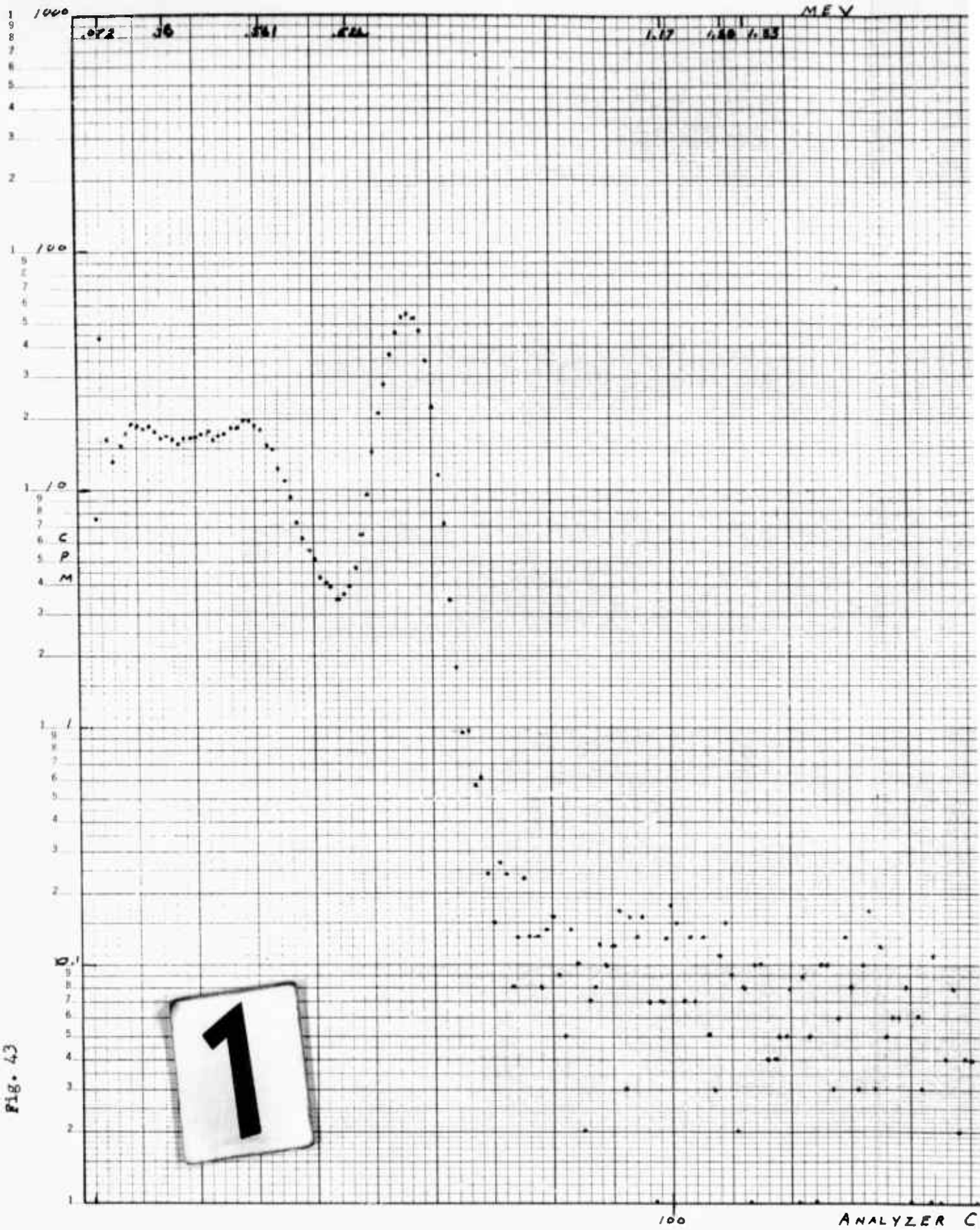

Fig. 43

M. V

1.83

1.74

Sample No. 9
100 Min. Count

Collected 19 Feb 62
Counted 22 Feb 62

2

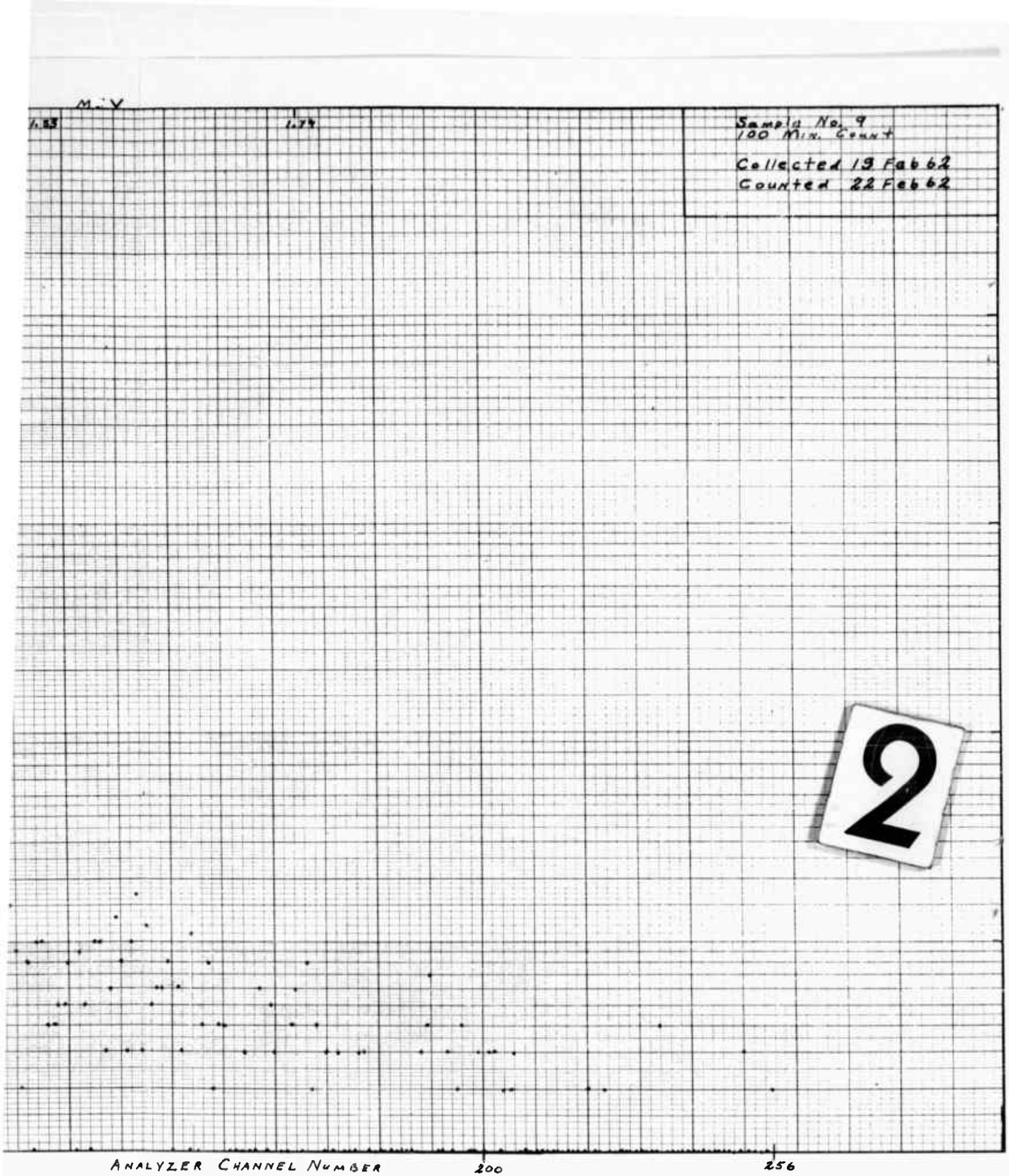

Fig. 43

Sample No. 9
100 Min Count
Collected 19 Feb 62
Counted 22 Feb 62

GNE/Phys/62-2

Sample No. 10

Collection Data:

Sample collected 0930-1730/27 Feb 62.
Weather: Low overcast, Intermittent rain and haze;
Temp=37°F; Wind=12 knots SW.

Charging potential	22.5KV
Collection potential	16.6KV
Ionization current	20.0ma
Volume flow rate of air	49.5 m^3/minute
Collection time	430 minutes
Total air sampled	21,285 m^3

Collection terminated because of excessive arcing in the charging section. This sample was collected to reexamine solubility fractionation phenomenon. The sample was washed by hand with a wet tissue swab to examine possible contribution of ultrasonic energy.

Analysis Data:

Date	Integral Count Rate* Counts/min/m^3 of Air	Counting Time	Remarks
1/3/62	0.034	100 min	composite sample**
	0.037	60 min	above 3.0μ**
	0.001	60 min	1.2μ to 3.0μ**
	0.001	60 min	0.8μ to 1.2μ**
	0.001	60 min	0.45μ to 0.8μ**
	0.001	60 min	0.22μ to 0.45μ**
2/3/62	0.063	100 min	composite sample**
	0.167	100 min	filtrate residue**

* The integral count rate of this sample is in error by virtue of the solubility fractionation phenomenon.

** This analysis confirmed the discovery that an appreciable portion of the sample had been lost in the filtrate. A spectral analysis shows that the energy peaks in the filtrate residue are not due to decay products of natural radioactive decay but are due to the fission products found in the filter sample. This loss of sample could be explained by postulating that an appreciable portion of the radioactive contaminants are associated with aerosols smaller than 0.22μ

in diameter. This postulate would be contrary to many previously reported analyses. An analysis of the solubilities of the nuclides associated with the energy peaks portrayed in these spectra and the fact that there is a variation in relative amplitudes of the peaks in the filter samples with those in the residue sample would suggest that the loss of sample was due to a selective solubility of the radioactive nuclides augmented by a solubility of the contaminant bearing aerosol.

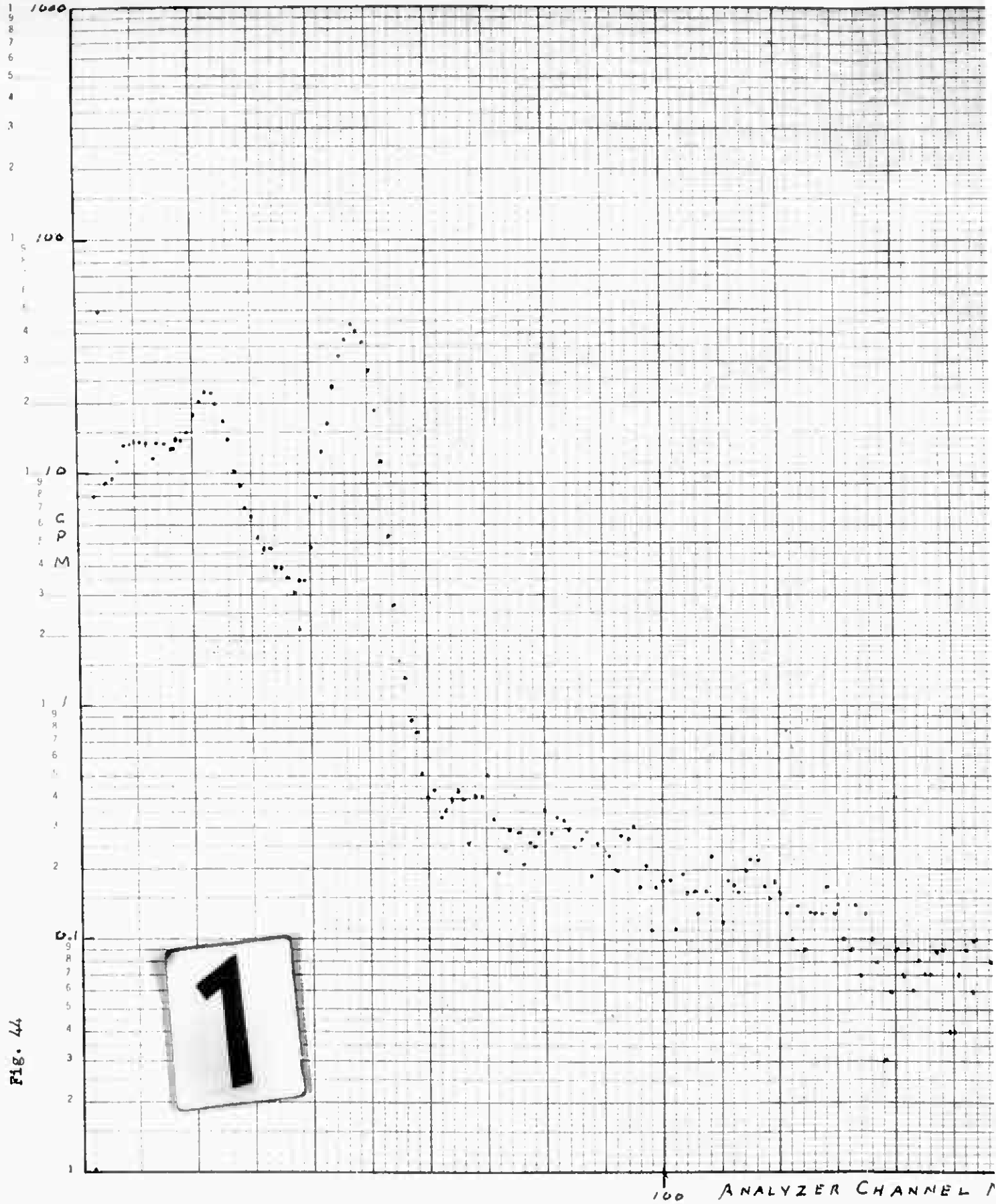

Fig. 44

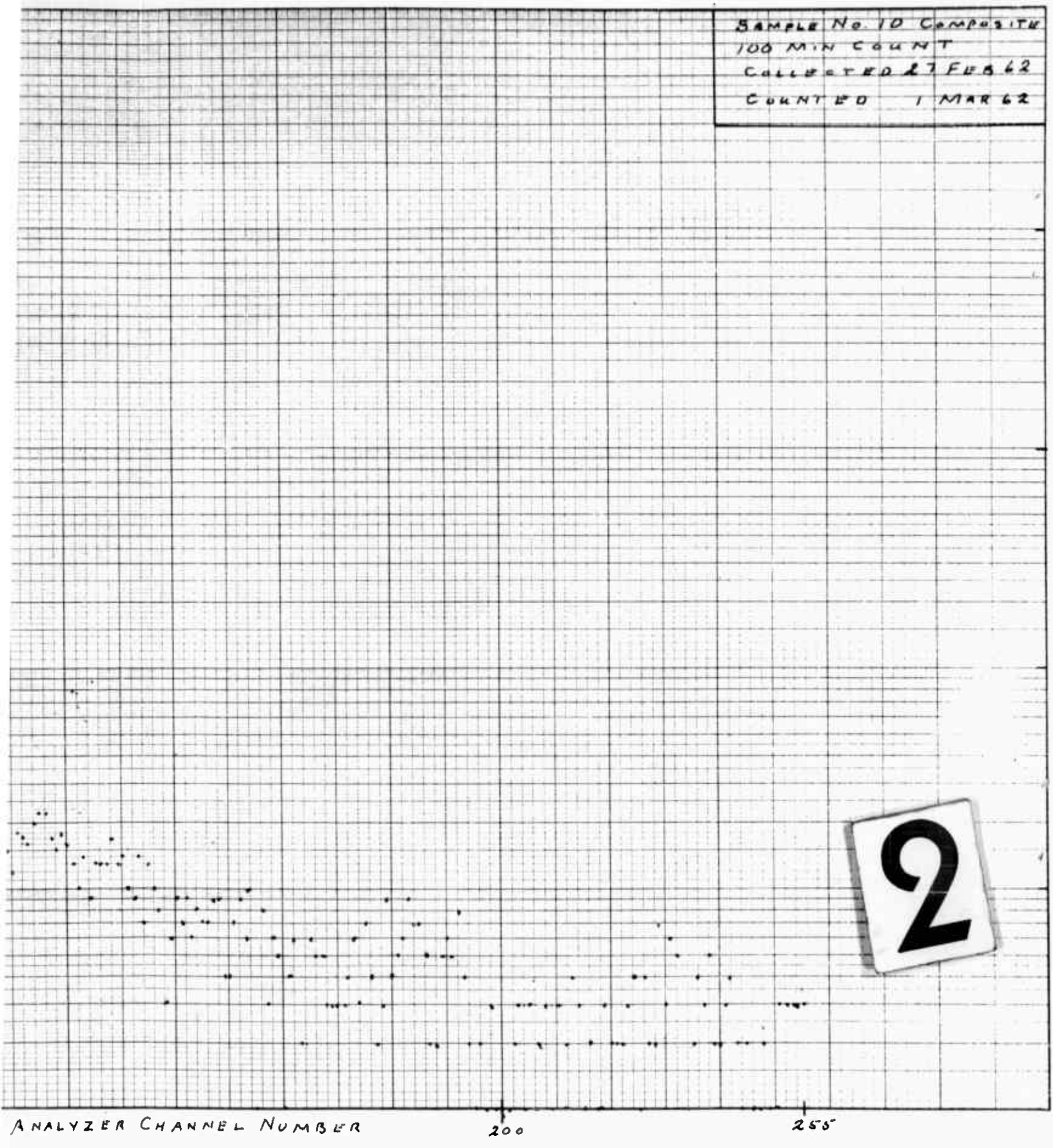
SAMPLE No. 10 COMPOSITE
100 MIN COUNT
COLLECTED 27 FEB 62
COUNTED 1 MAR 62
2
ANALYZER CHANNEL NUMBER
200
255

Fig. 44

Sample No. 10
Composite
100 Min Count
Collected 27 Feb 62
Counted 1 Mar 62

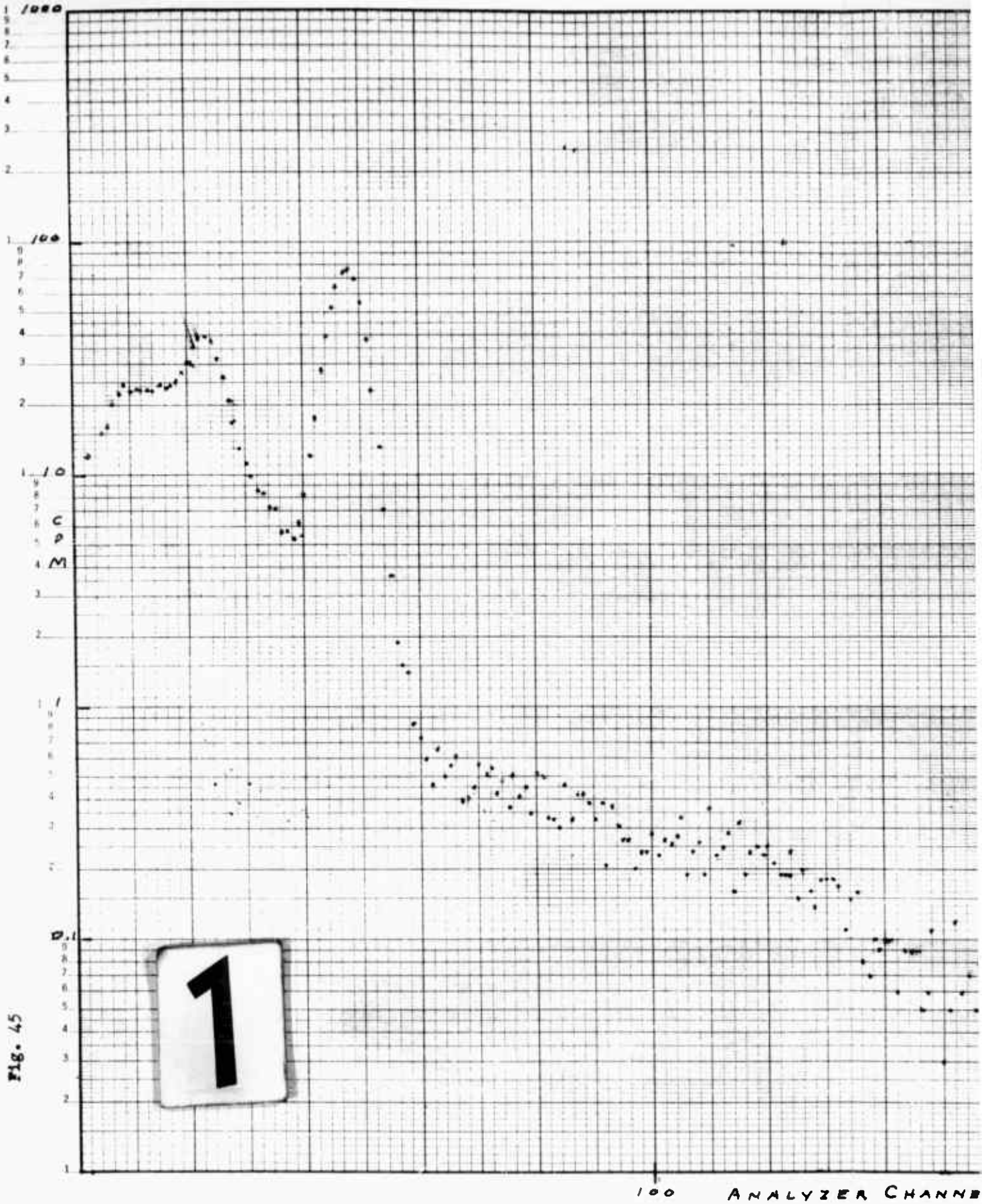

Fig. 45

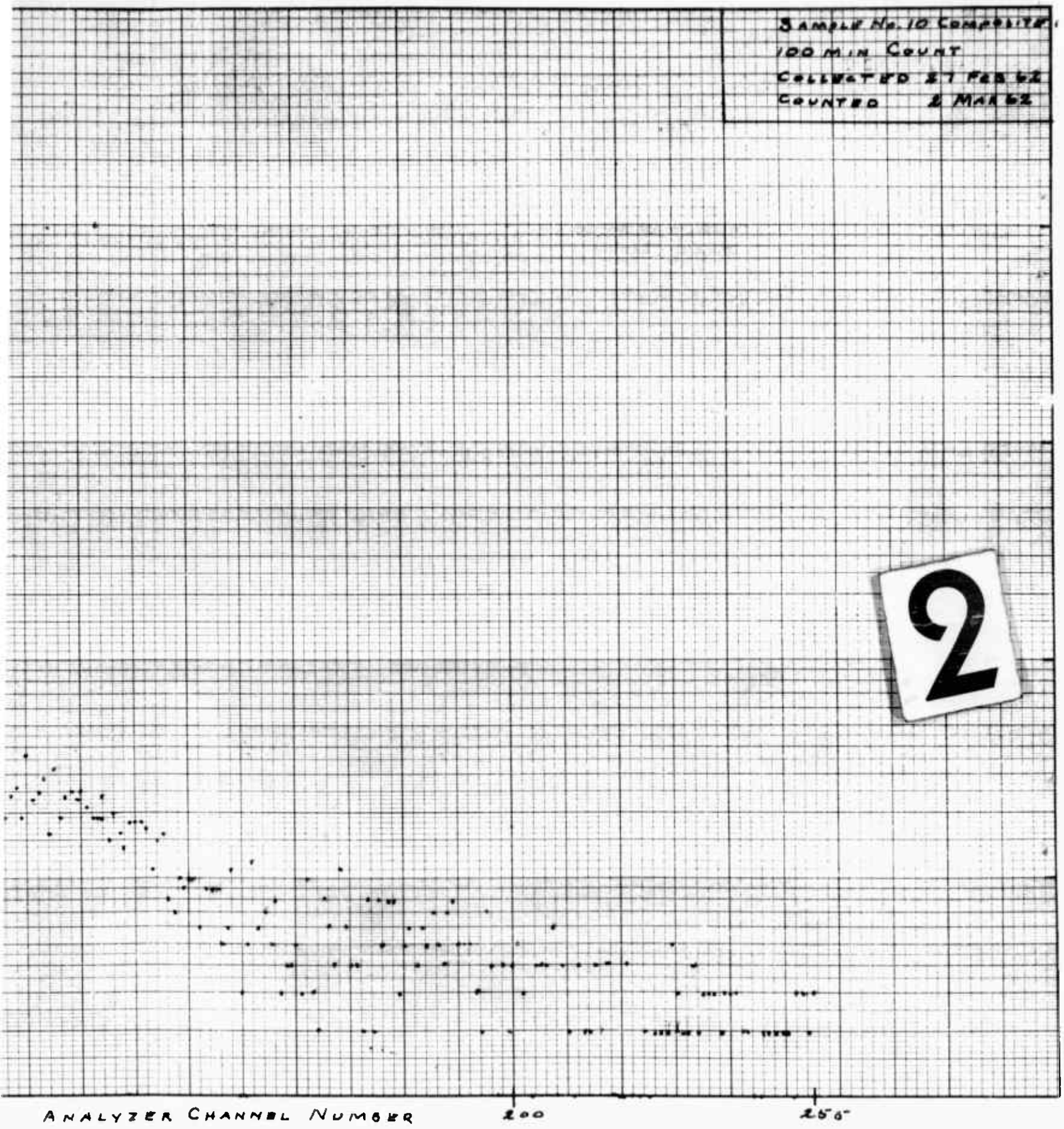
SAMPLE No. 10 COMPOSITE
100 MIN COUNT
COLLECTED 27 FEB 62
COUNTED 2 MAR 62
2
ANALYZER CHANNEL NUMBER
200
250

Fig. 45

Sample No. 10
Composite
100 Min Count
Collected 27 Feb 62
Counted 2 Mar 62

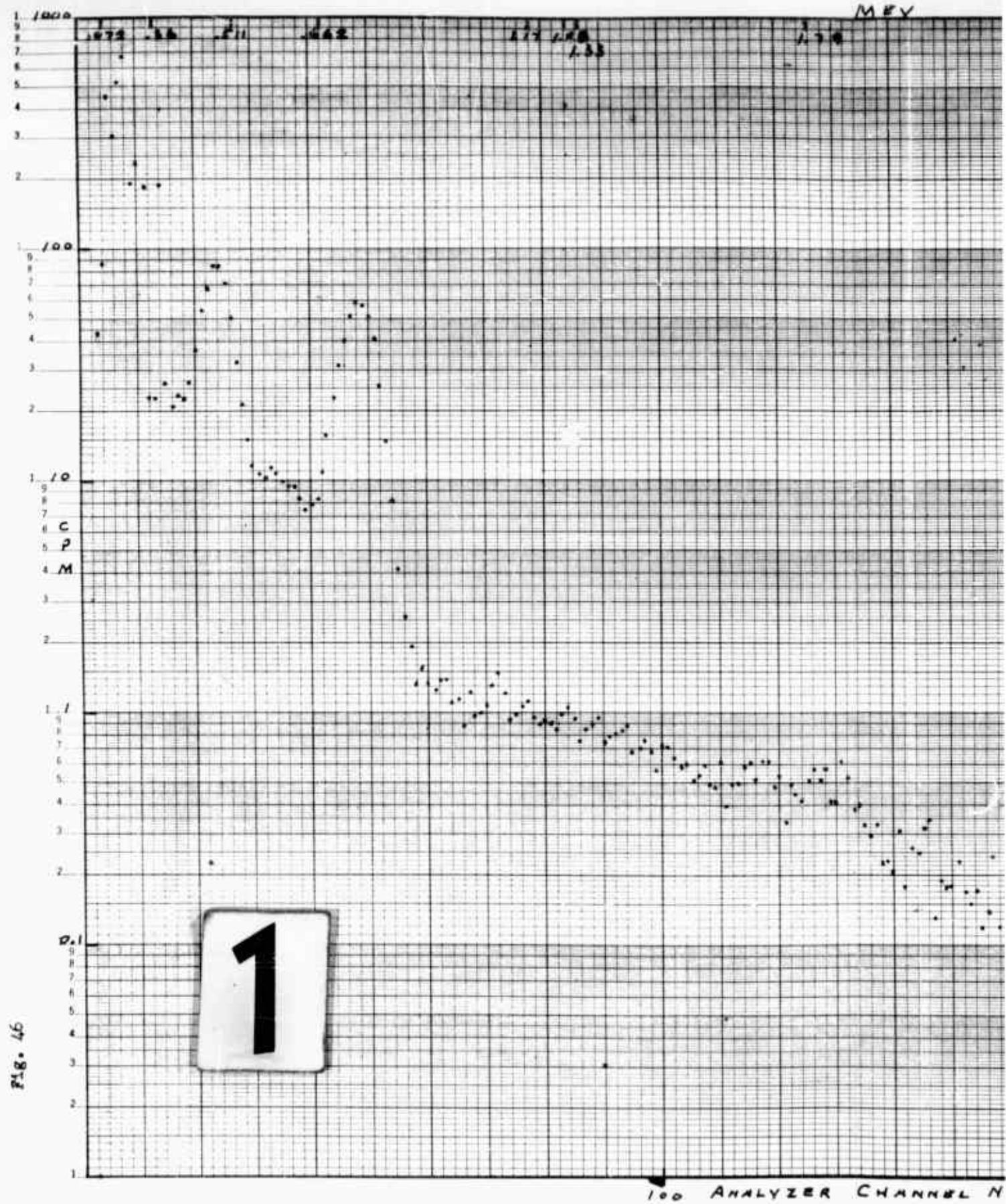
MEV
.672
.86
.911
.662
1.33
1.76
1000
100
10
1
0.1
CPM
100 ANALYZER CHANNEL N

FIG. 46

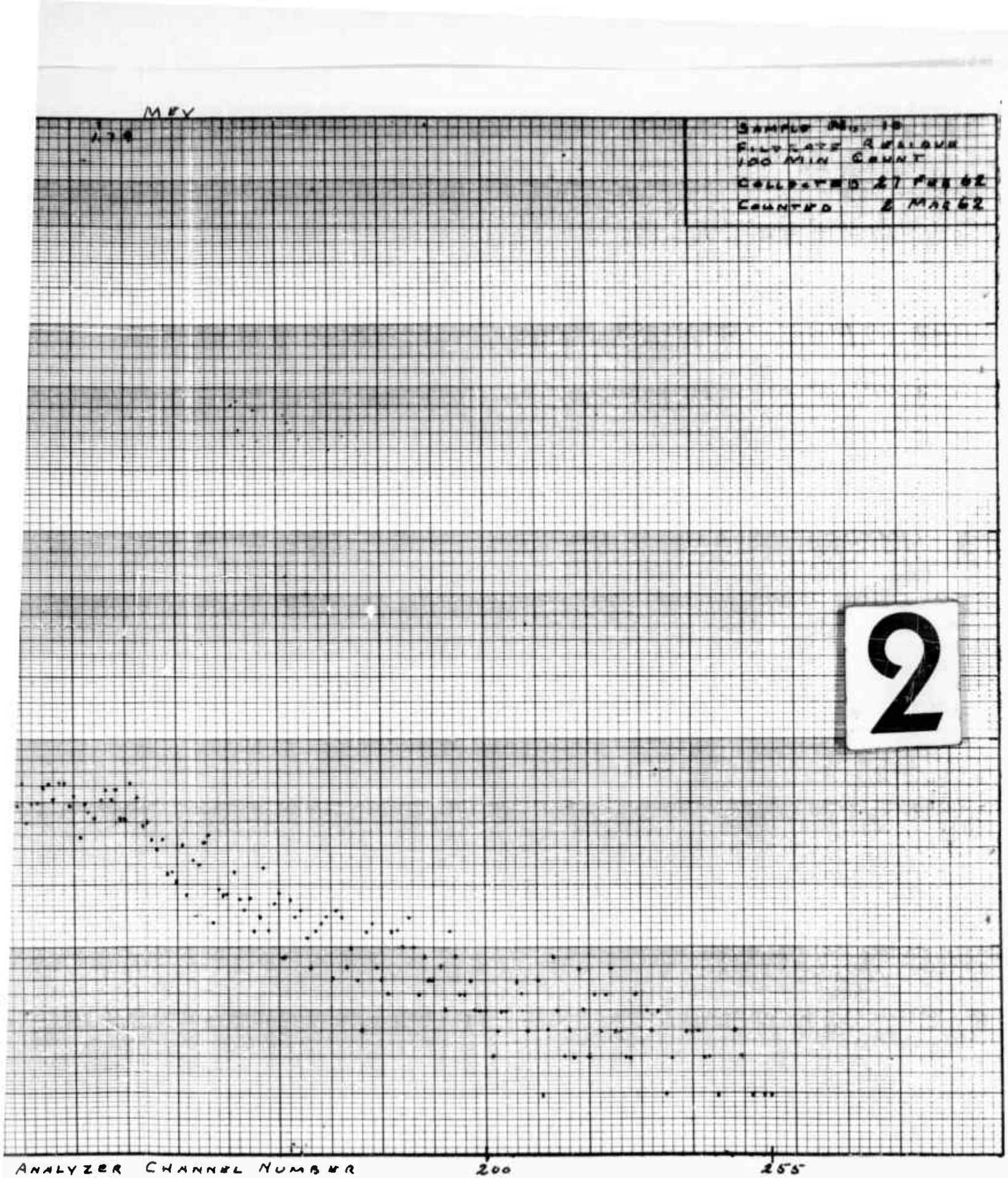
MEV
1.3
SAMPLE NO. 10
FILTER RESIDUE
100 MIN COUNT
COLLECTED 27 FEB 62
COUNTED 2 MAR 62
2
ANALYZER CHANNEL NUMBER
200
255

Fig. 46

Sample No. 10
Filtrate Residue
100 Min Count
Collected 27 Feb 62
Counted 2 Mar 62

GNE/Phys/62-2

Sample No. 11

Collection Data:

Sample collected 0710-1920/7Mar62.
Weather: Partly cloudy; Temp=35°F; Wind=8 knots NW.

Charging potential	21.6KV
Collection potential	17.1KV
Ionization current	20.0ma
Volume flow rate of air	49.5 m^3/minute
Collection time	720 minutes
Total air sampled	35,640 m^3

This sample was collected to continue analysis of solubility phenomenon. The collection plates were washed by hand in isopropyl alcohol, the cleaning fluid was filtered and the individual filter samples retained. The filtrate was evaporated and the residue was analyzed for activity.

Analysis Data:

Date	Integral Count Rate* Counts/min/m^3 of Air	Counting Time	Remarks
8/3/62	0.291	100 min	above 3.0μ**
9/3/62	0.003	100 min	0.45μ to 3.0μ**
	0.002	100 min	0.22μ to 0.45μ**
	0.015	100 min	filtrate residue**
	NA	100 min	filtrate residue*** Amp gain=1/2:100
	NA	100 min	above 3.0μ*** Amp gain=1/2:100
	NA	100 min	above 3.0μ*** Amp gain=1:100
10/3/62	NA	100 min	filtrate residue*** Amp gain=1:100

* The integral count rate of this sample is in error by virtue of the solubility fractionation phenomenon. The sample entitled "above 3.0μ" was filtered through a microfiber glass prefilter with a 3.0μ microfiber filter paper and undoubtedly contained particulates smaller than 3.0μ. This filter sample accounted for 94.2‰ of the

total integral count. The filtrate residue contained 4.57‰ of the total integral count. In the sample collections employing water cleaning, the filtrate residue count rate was as high as or higher than the composite filter sample count rate.

** This analysis shows a decreased sample loss due to solubility fractionation in alcohol. No particle-size/activity correlation can be made from this data.

***The linear amplifier gain was doubled and quadrupled to spread out the spectrum and allow a more detailed examination of the low energy portion of the spectrum of the filtrate residue sample and the filter sample entitled "above 3.0μ".

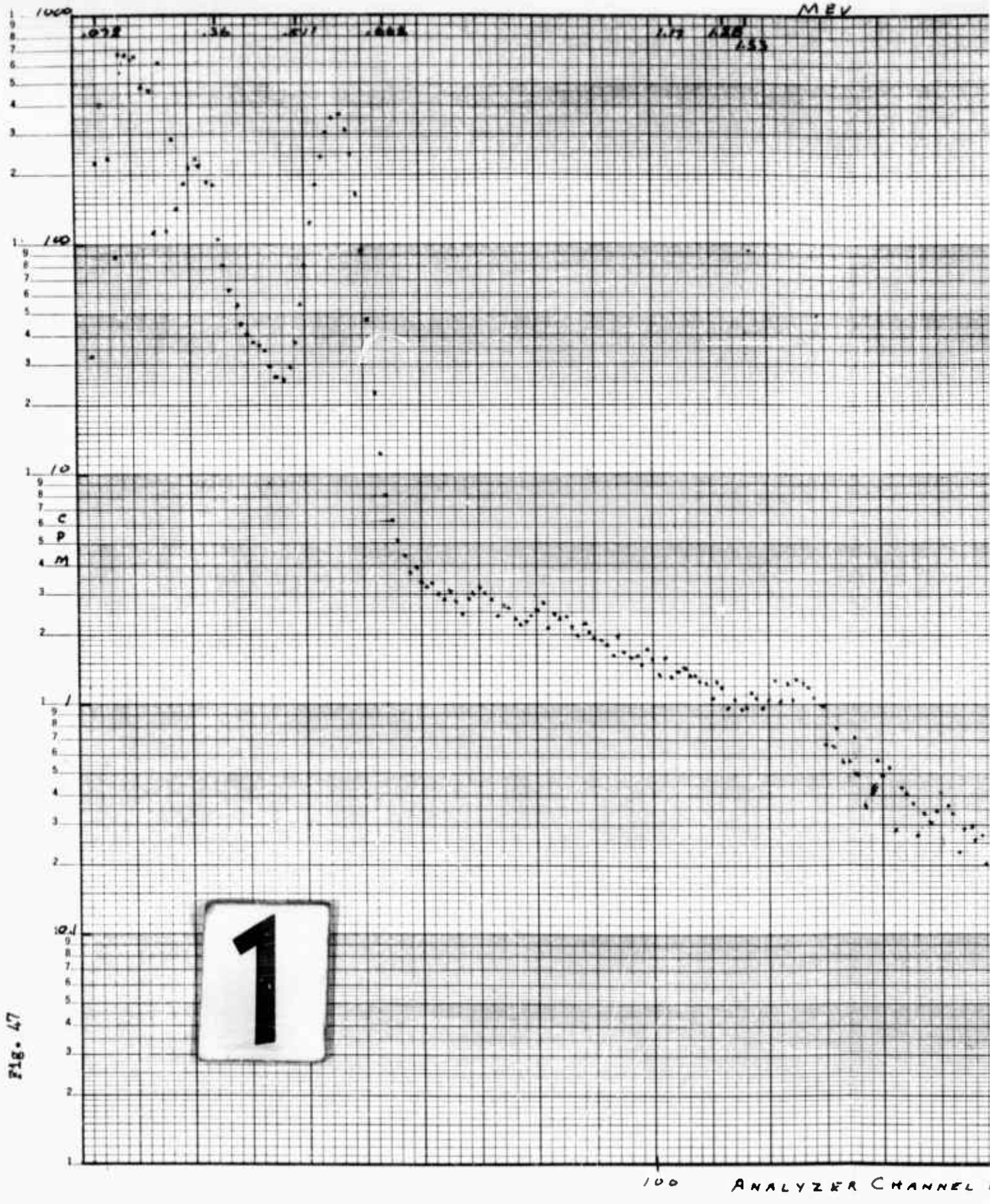

Fig. 47

MEV

1.53

1.29

SAMPLE No. 11 - ABOVE 5.0μ
100 MIN COUNT - GAIN = 1/4
COLLECTED 7 MAR 62
COUNTED 9 MAR 62

2

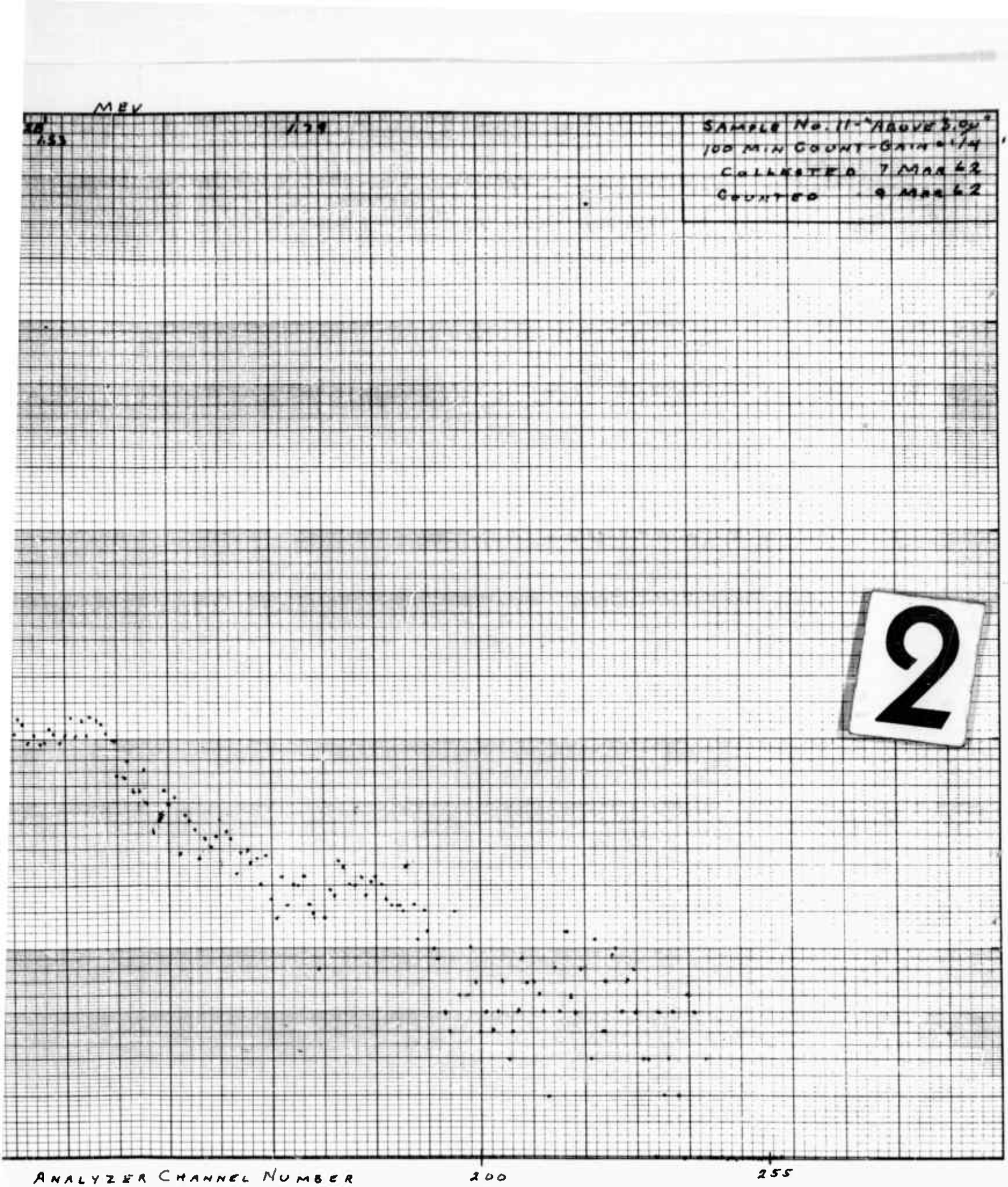

ANALYZER CHANNEL NUMBER

200

255

Fig. 47

Sample No. 11
Above 3μ
100 Min Count
Gain = 1/4
Collected 7 Mar 62
Counted 9 Mar 62

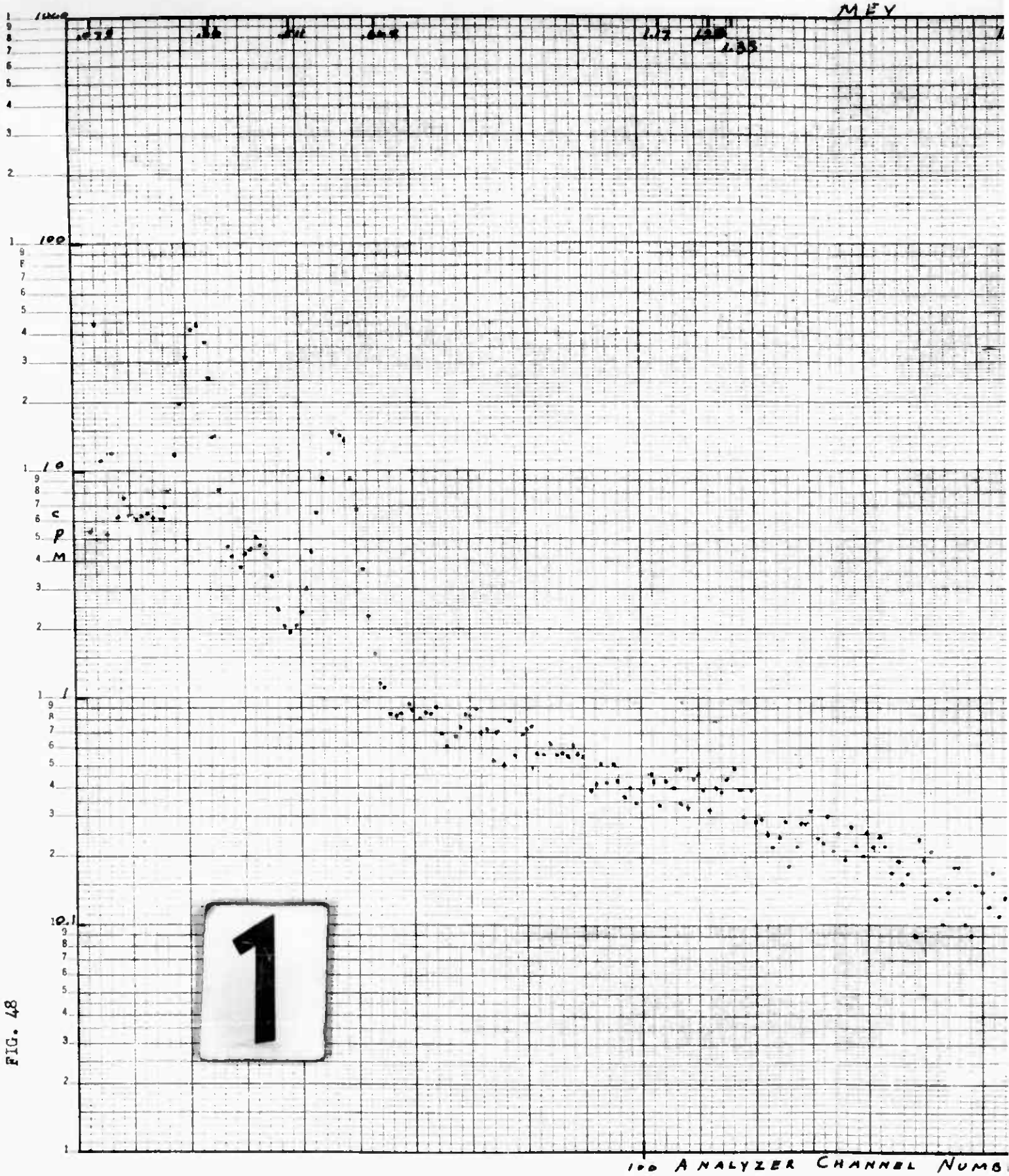

FIG. 48

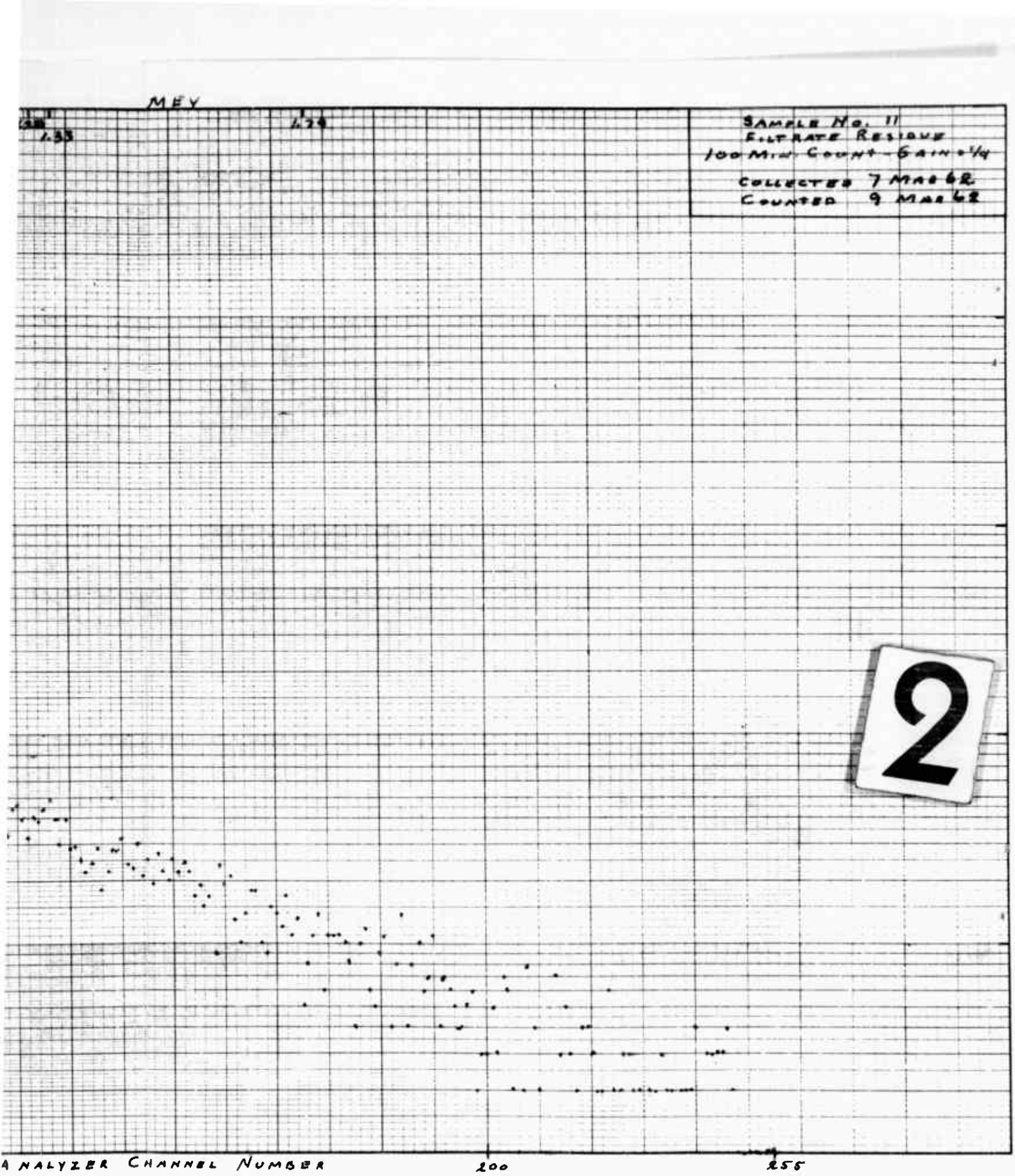
MEV
1.33
1.74
SAMPLE NO. 11
FILTRATE RESIDUE
100 MIN. COUNT - GAIN 1/4
COLLECTED 7 MAR 62
COUNTED 9 MAR 62
2
ANALYZER CHANNEL NUMBER
200
255

Fig. 48

Sample No. 11
Filtrate Residue
100 Min Count
Gain = 1/4
Collected 7 Mar 62
Counted 9 Mar 62

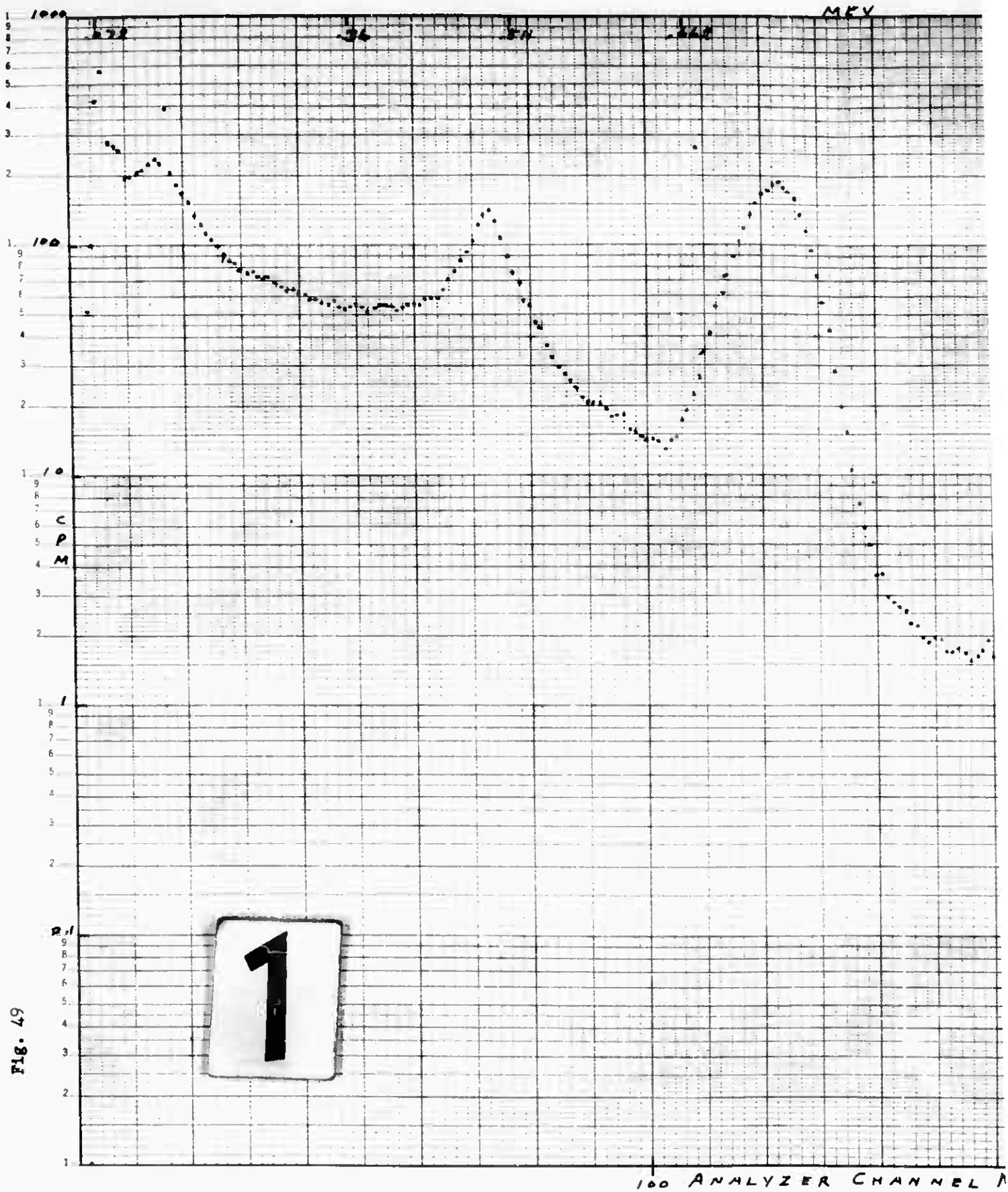

Fig. 49

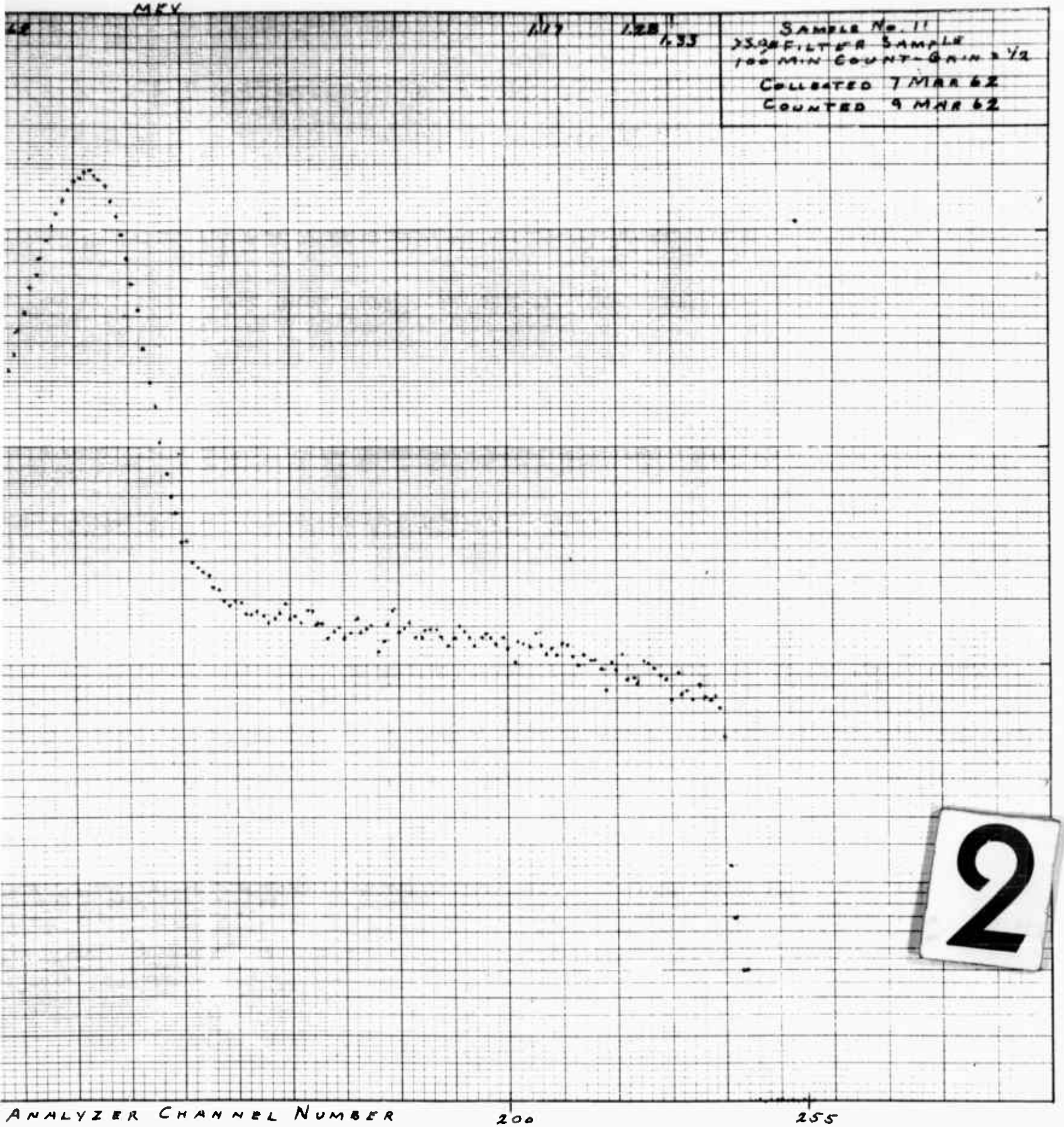
MEV
1.17
1.28
1.33
SAMPLE No. 11
25.9# FILTER SAMPLE
100 MIN COUNT - GAIN = 1/2
COLLECTED 7 MAR 62
COUNTED 9 MAR 62
2
ANALYZER CHANNEL NUMBER
200
255

Fig. 49

Sample No. 11
3μ Filter Sample
100 Min Count
Gain = 1/4
Collected 7 Mar 62
Counted 9 Mar 62

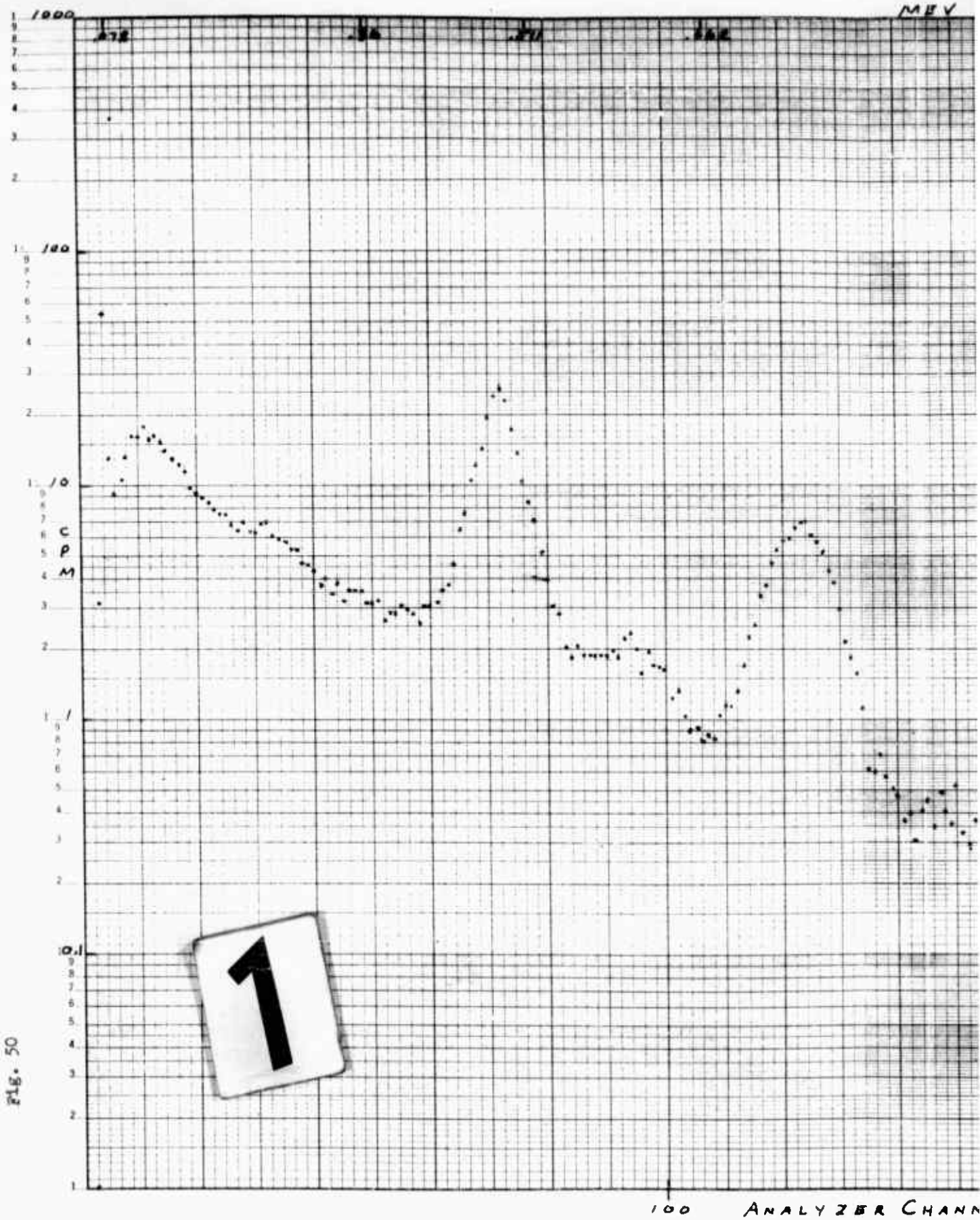

Fig. 50

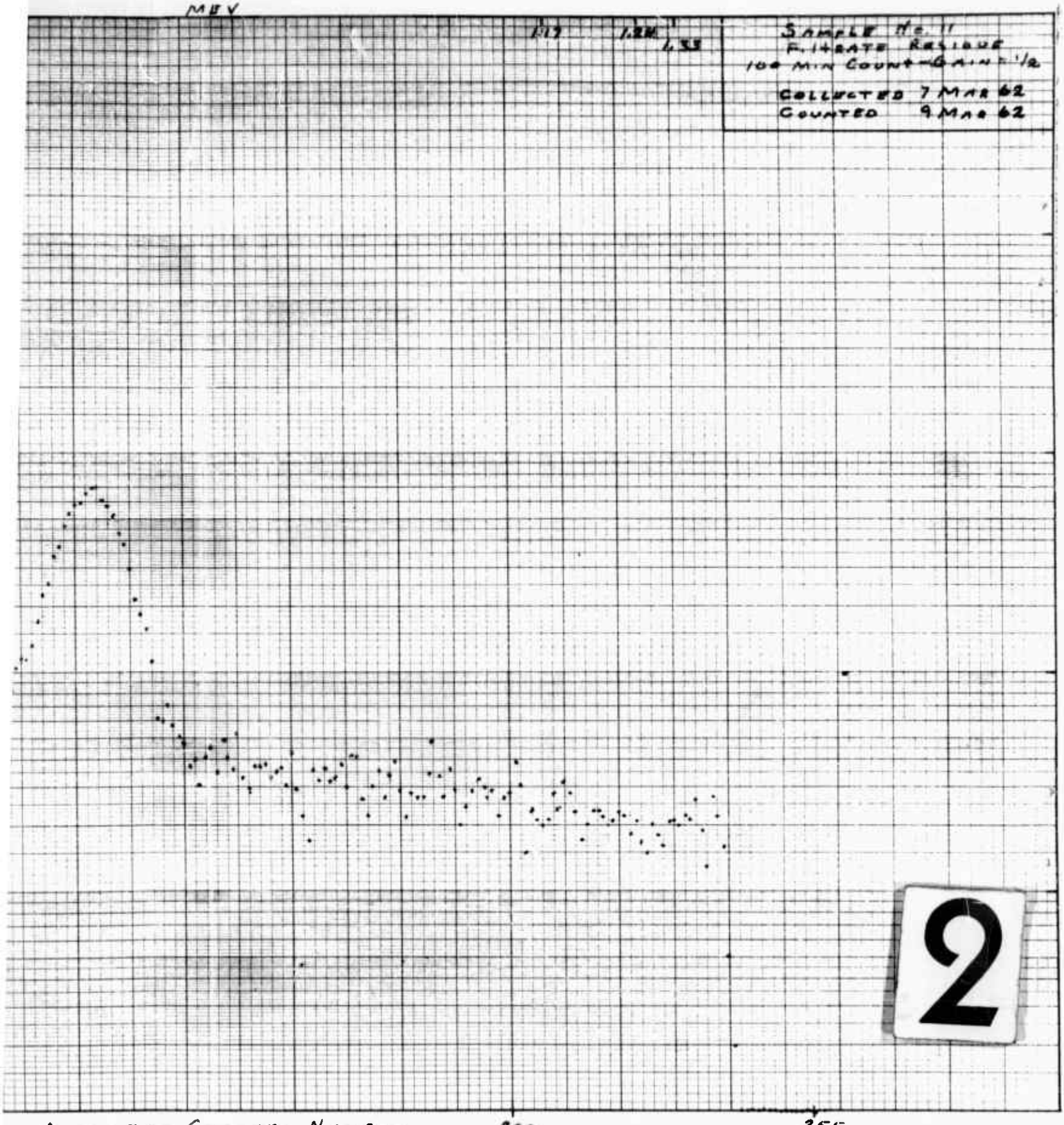
MEV
1.17
1.33
SAMPLE No. 11
F. 14 DATE RESIDUE
100 MIN COUNT - GAIN = 1/2
COLLECTED 7 MAR 62
COUNTED 9 MAR 62
2
ANALYZER CHANNEL NUMBER
200
265

Fig. 50

Sample No. 11
Filtrate Reaidue
100 Min Count
Gain = 1/2
Collected 7 Mar 62
Counted 9 Mar 62

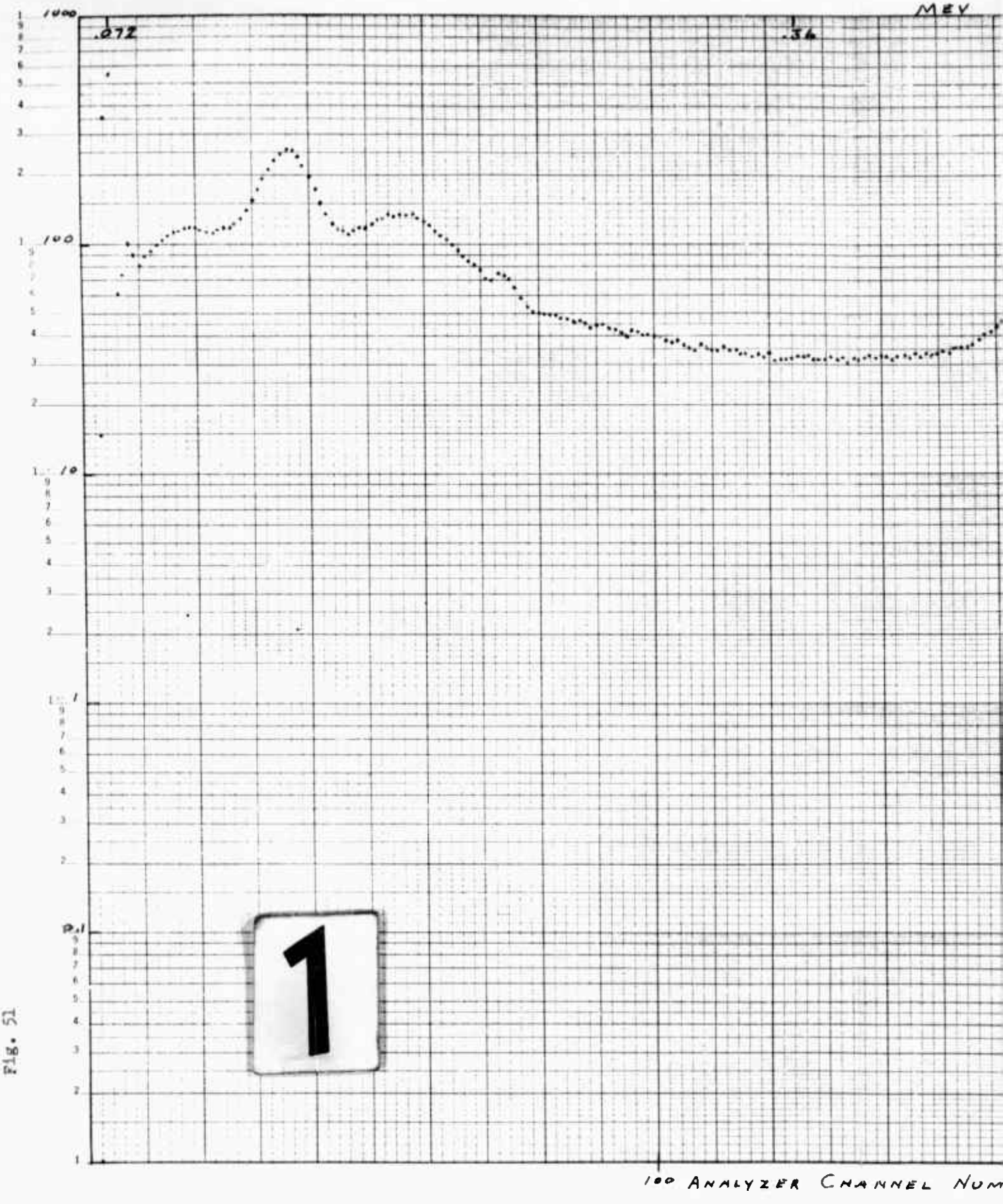

Fig. 51

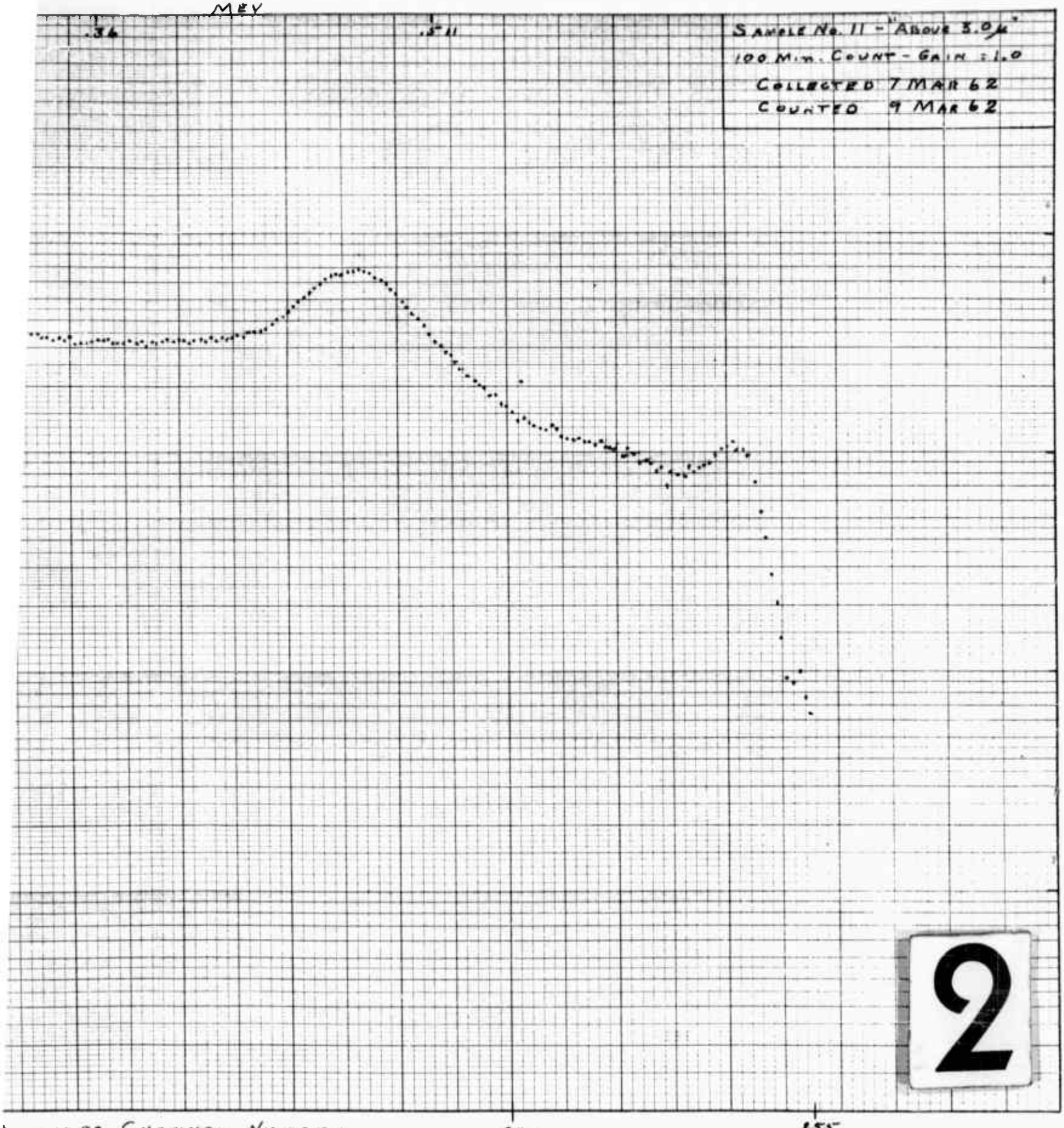
MEV
.36
.5" 11
SAMPLE No. 11 - ABOVE 3.0μ
100 M.m. COUNT - GAIN : 1.0
COLLECTED 7 MAR 62
COUNTED 9 MAR 62
2
ANALYZER CHANNEL NUMBER
200
255

Fig. 51

Sample No. 11
3μ Filter Sample
100 Min Count
Gain = 1
Collected 7 Mar 62
Counted 9 Mar 62

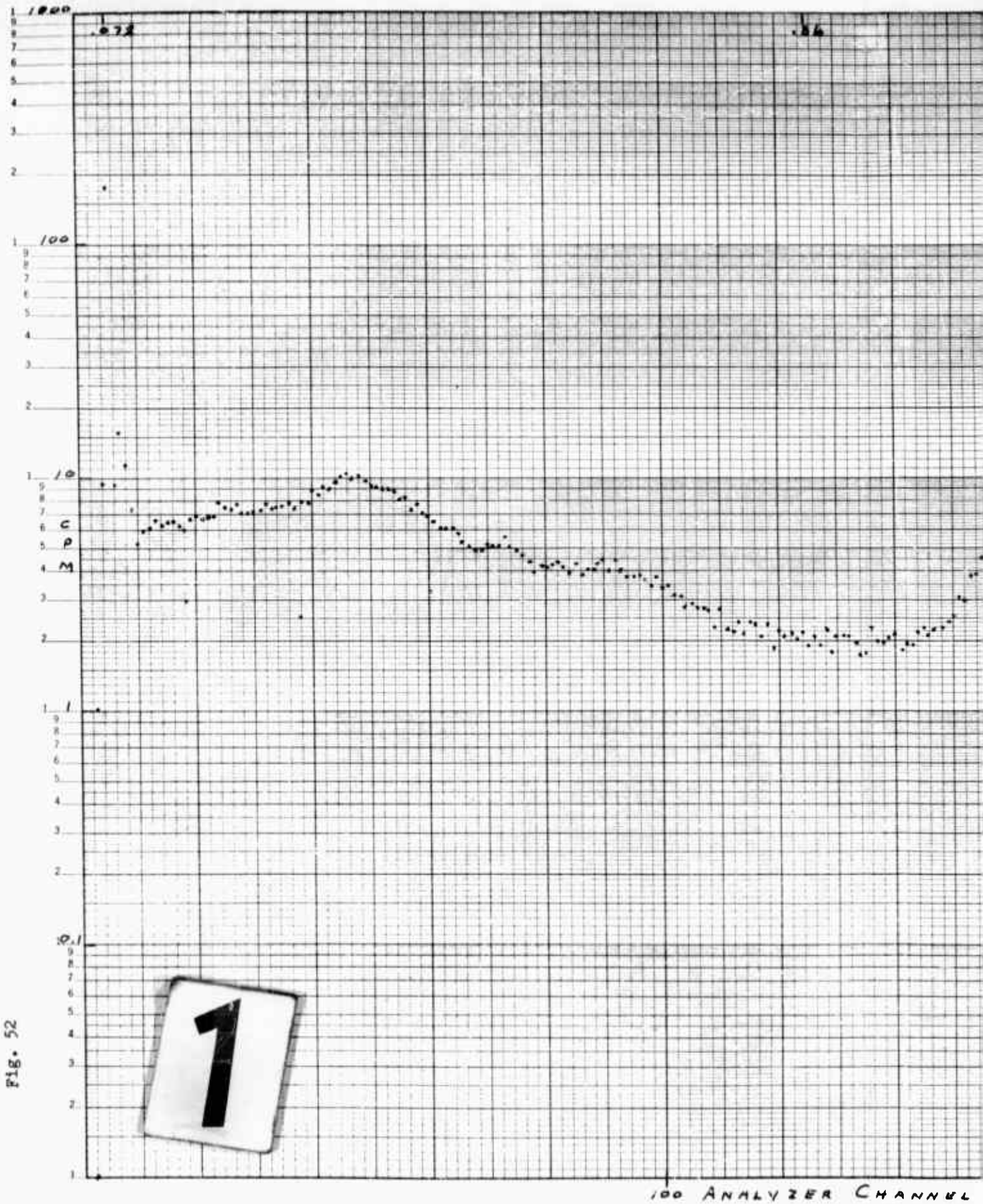

Fig. 52

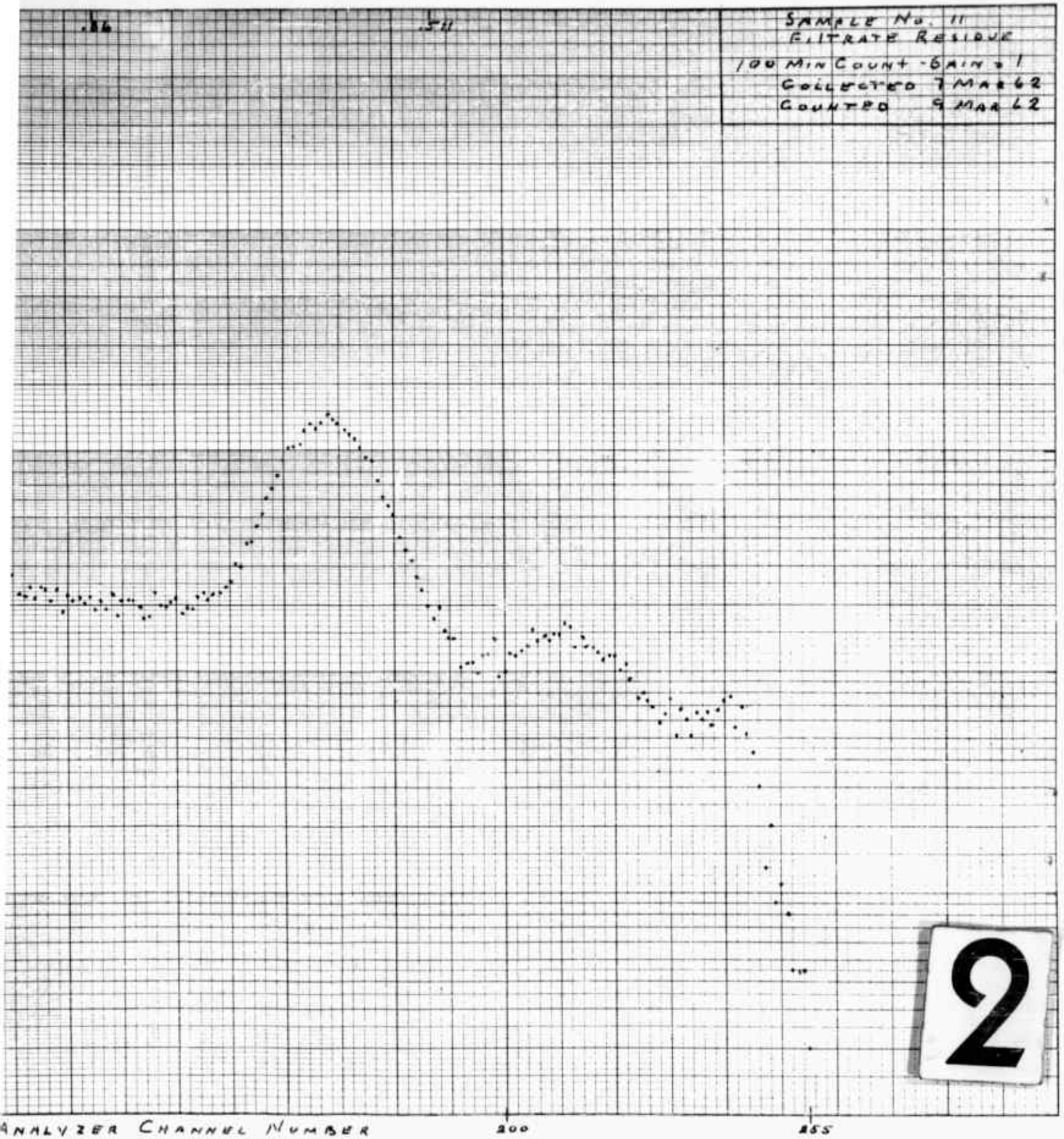
.86
.511
SAMPLE No. 11
FILTRATE RESIDUE
100 MIN COUNT - GAIN = 1
COLLECTED 7 MAR 62
COUNTED 9 MAR 62
2
ANALYZER CHANNEL NUMBER
200
855

Fig. 52

Sample No. 11
Filtrate Residue
100 Min Count
Gain = 1
Collected 7 Mar 62
Counted 9 Mar 62

Sample No. 12

Collection Data:

Sample collected 0755-1435/12 Mar 62.
Weather: Fair and clear.

Charging potential	19.5KV
Collection potential	16.5KV
Ionization current	20.0ma
Volume flow rate of air	59.4 m^3/minute
Collection time	360 minutes
Total air sampled	21,384 m^3

This sample collection was conducted to test the feasibility of collecting on a thin plastic foil -- "Handy Wrap" -- that had been sprayed with an anti-static compound to create a partially conducting surface. Only two of the nine plates were wrapped because of difficulty of assembly. It was postulated that the activity displayed by the two plates might represent one-fourth of the total activity that would be collected by the eight collecting surfaces of the nine collecting plates.

Analysis Data:

Date	Integral Count Rate* Counts/min/m^3 of Air	Counting Time	Remarks
12/3/62	0.0415	100 min	Amp gain=1/4:100

* Assuming a linearity of collection, this would represent a total integral count rate of 4 x 0.0415 = 0.166 counts/min/m^3 of air. Although this collection rate represented a marked improvement over that of the plain plastic foil of Sample No. 6, it would still represent less than one-half of the collection rate of the bare aluminum plates. The increased collection due to the increased conductivity of the foil would indicate, however, that a conducting foil might provide an acceptable collecting surface.

This sample presented the sharpest spectral peaks of any of the samples analyzed despite the relatively low count rate. This increased resolution might be attributed to the thin disc with its improved geometry factor and decreased self-absorption.

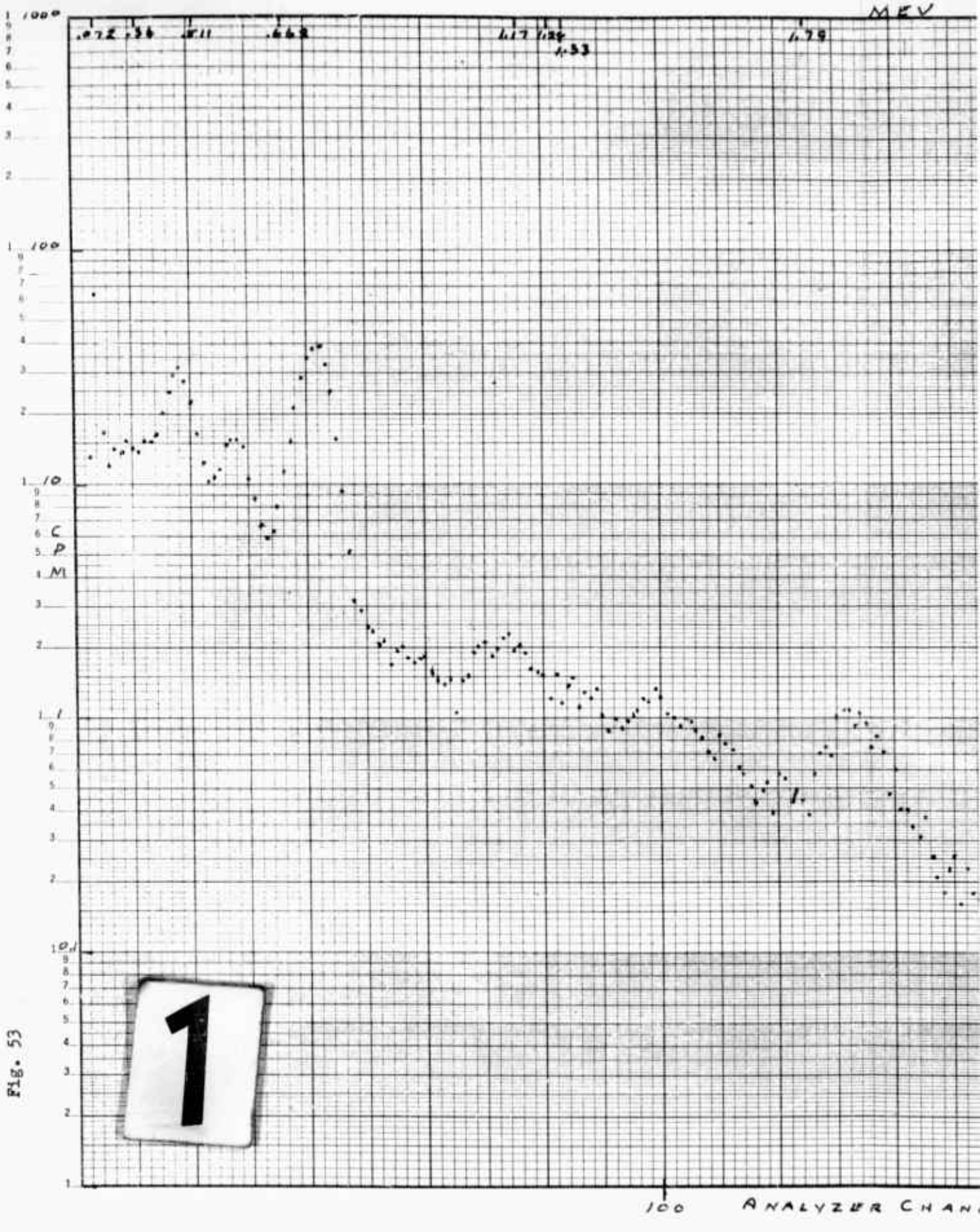
MEV
.072
.56
.811
.662
1.17
1.24
1.33
1.79
1000
100
10
1
C
P
M
I
100
ANALYZER CHAN

Fig. 53

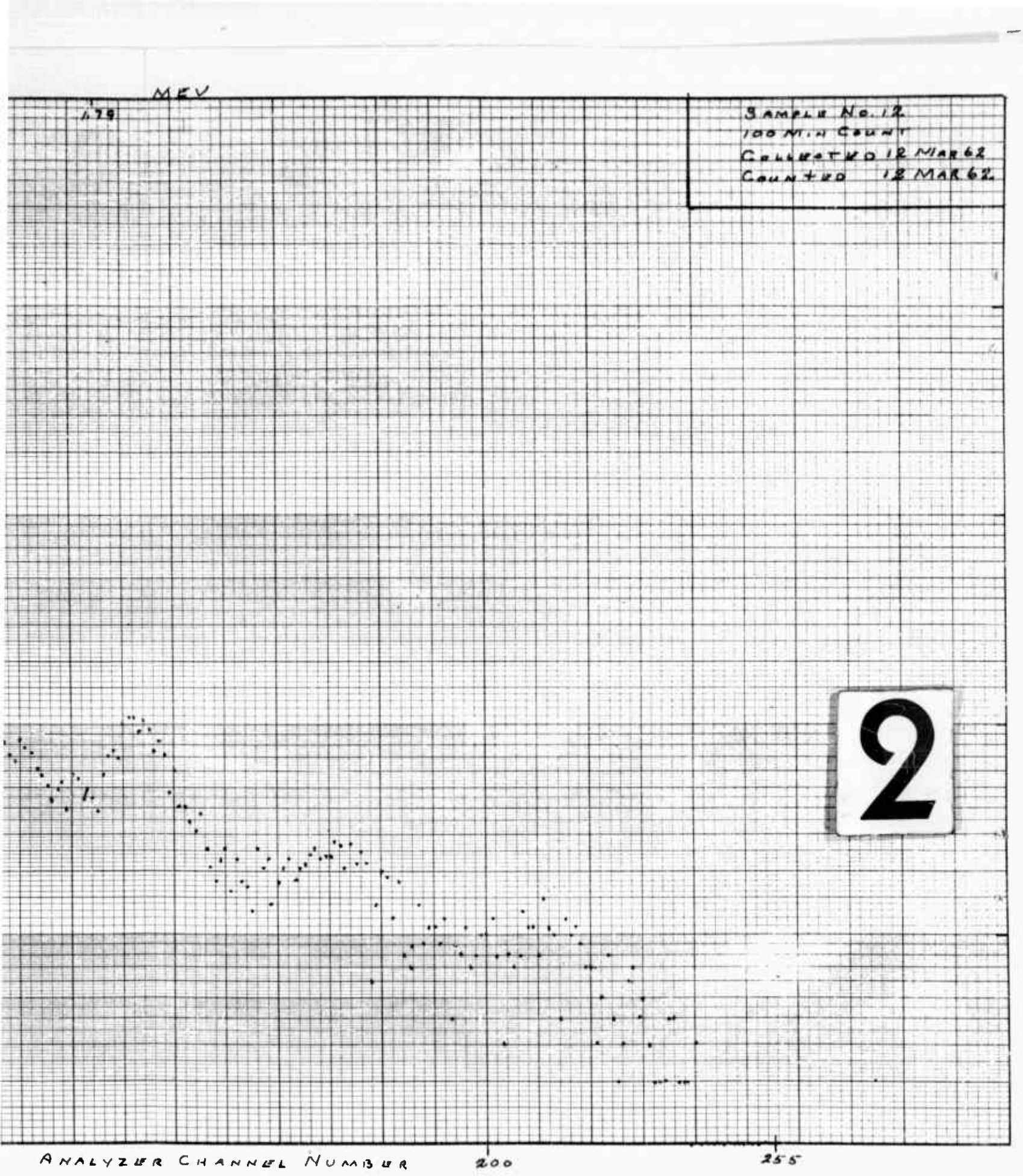
MEV
.479
SAMPLE NO. 12.
100 MIN. COUNT
COLLECTED 12 MAR 62
COUNTED 12 MAR 62.
2
ANALYZER CHANNEL NUMBER
200
255

Fig. 53

Sample No. 12
100 Min Count
Collected 12 Mar 62
Counted 12 Mar 62

Appendix B

Determination of Total Absolute Counting Efficiency

General

This appendix will describe the process by which a cylindrical geometry factor and the ahsolute efficiency of the counting system was determined. This geometry and efficiency factor was needed to transform the observed sample count rate in counts per minute to an airborne activity rate in disintegrations per second per cubic meter of air. Total absolute efficiency values are available for a point source on the axis of and at a measured distance from the face of various size NaI(Tl) scintillation crystals (Ref 10). The collection and secondary concentration processes originally envisioned for this collection technique, however, resulted in a cylindrical sample and absolute efficiency values are not available for this sample configuration. Although subsequent collection studies revealed the inaccuracies of the secondary concentration technique that led to the 2"Dx1" cylindrical sample and the known quantitative errors in the sample analysis precluded definition of a radiological fallout rate with these samples, the methods employed in the definition of a specific counting efficiency would be applicable for a flat disc source or any other configuration and the methodology is included here for guidance in future research efforts.

The process described below will define the sample activity within the limits of error defined by the reliability of the conversion ratio determination and the reproducability of the standard sample configuration. The sample activity, when divided by the measured total volume of air sampled, will define the airborne radioactivity.

Conversion Ratio Determination

A calibrated standard solution of Co^{60} in HCl was available whose activity in disintegrations per second per milliter of solution was known to an accuracy of 3‰. Four point sources were prepared hy pipetting 10λ ($1x10^{-5}$ liters) samples onto .0003" polystyrene films held in aluminum source holders using standard pipetting techniques. This was done to provide point sources required in the subsequent analysis and to define a statistical measure of pipetting variations. A fifth 10λ sample was pipetted into a 70 ml sample of distilled water that had been made strongly basic with NH_4OH. Dilute $FeCl_3$ was added to form a scavenger precipitate that would carry the Co^{60} out of the solution. The mixture was agitated to prevent precipitate settling and 10 ml portions were filtered through filters made up of two Millipore prefilters and one 0.45μ 47mm Millipore filter. The filtrate was reprecipitated and refiltered until the filter sample showed no activity. The filter samples were stacked to form a composite cylinder identical in size and composition to the composite aerosol sample but with a measured known activity.

The prepared point source samples were counted in the counting geometry with the point source positioned adjacent to the crystal canning face and the observed count rates were compared to define a pipetting reliability. The composite cylindrical sample was positioned in the sample holder that was to hold the aerosol sample and a count rate was determined. The average net count rate from the point sources was divided by the net count rate from the cylindrical source to define a point source to cylindrical source count rate ratio. This count rate ratio, when multiplied by the point source absolute efficiency, provided a total absolute efficiency for this counting geometry with a 2"Dx1" high cyndrical sample. This efficiency factor, when applied to the

observed count rate will define the aerosol sample activity. This, in turn, may be used to define the airborne radioactivity in disintegrations per second per cubic meter of air.

Calculations

Background count -- 10 minute counts

	364
	486
	667
	575
Total	2092
Average	523

Point source count -- 10 minute counts

	7230
	7555
	7620
	8755*
Total	22405
Average	7468
Net Point Source Count	6945

Cylindrical source count -- 10 minute count

	3618
Net cylindrical source count	3095

Point source count to cylindrical count ratio

$$\frac{3095}{6945} = 0.4456$$

Total absolute efficiency for a 2"x2" NaI(Tl) scintillation crystal for a point source on the axis .001" from the crystal face for a Co^{60} gamma energy of 1.17/1.33 MEV is equal to 0.28 (Ref 10).

Total absolute efficiency for the counting geometry used for a 2"Dx1" cylindrical sample is equal to

$$(0.4456)x(0.28) = 0.1248$$

Vita

PII Redacted

John Wesley Baker was born [redacted] to John Wesley Baker, Sr. and Bertha Keller Baker. After completing high school at [redacted] in [redacted], he attended Northern Montana College, Havre, Montana for two years. He served in the U.S. Army during World War II and then returned to college at the Montana School of Mines, Butte, Montana. He was commissioned a Second Lieutenant in the United States Air Force concurrently with receiving the degree of Bachelor of Science in Geological Engineering from the Montana School of Mines in 1951. He was trained as a Nuclear Officer at Sandia Base, New Mexico and served in that capacity until 1956. At that time he was enrolled in an Electrical Engineering course at the Air Force Institute of Technology. Upon graduation, he was assigned to a Tactical Missile Wing in Germany where he served as a Launch Flight Commander and Wing Operations Staff Officer until his present reassignment to the Institute of Technology, Air University.

Permanent Address: [redacted]

PII Redacted

This thesis was typed by Miss Joyce E. Smith.